STRENGTH OF MATERIALS I

Doc. Ing. Miroslav Sochor, CSc.

Contents

CONTENTS

CONTENTS

Preface to the 3rd revised edition

This textbook aims to help students taking courses taught in English at CTU, Faculty of Mechanical Engineering, in their studies of one of the most important, and, at the same time, most difficult engineering topics. This course will be taken not only by foreign students (speaking good English and knowing technical and mathematical terms in English), but also by Czech students intending to improve their English while studying a professional subject (perhaps with a view to continuing their studies abroad).

Much of the textbook is devoted to characterizing problems, especially in the first part of each chapter. The book covers the contents of the first introductory course on Strength of Materials. We have had an opportunity to increase the length of the textbook, and we decided to add: i) some important explanatory notes to help the reader to penetrate into the substance of problems; ii) several appropriate examples, showing optimum solutions. (Two kinds of examples are used: a) as integral parts of sections of the textbook – these are not mentioned in the list of contents; b) as explanatory examples – these are introduced in the list of contents).

In accordance with the ISO recommendations, the author (largely) uses [N/mm^2] units, instead of [MPa] (which were formerly also applied for the stresses exerted in solid objects, now used for the pressures in liquids and gases).

In order to accelerate and facilitate the preparation of the manuscript, the notation of figures and equations includes the number of the sections (or subsections), to which is added the serial number of the figure (or equation). For example, in Sec.2.12 the (first) figure will be denoted as Fig.2.12.1, while in subsection 2.12.1, the (first) figure will be denoted as Fig.2.12.1.1.

The author is deeply indebted to his wife, Dr. Ludmila Sochorová, for her patience and understanding while the manuscript was being prepared.

1. <u>Introduction</u>

Engineers study the mechanics of materials mainly in order to have a means of analyzing and designing various machines and load bearing structures.

I should emphasize that the engineer's role is not limited to analysing existing structures and machines subjected to given loading conditions; it is of even greater importance to design new structures and machines, that is, to select the appropriate structural components to perform a given task. Some model examples will help the reader to gain a deeper understanding of the problems explained here.

Both the analysis and the design of a given structure involve determining of *stresses* and *deformations*. To fulfil this task, we apply both theoretical (computational) and experimental approaches; the latter mainly for verification of computed results.

1.1 Basic concepts

1.1.1 <u>External loads (forces)</u>

1.1.1.1 Types of external forces

1) *Surface forces*, i.e. forces exerted on the body surface:
   a) *point (concentrated) forces*, which we consider as spot loadings although they are actually distributed over a certain surface (which is very small in comparison with the whole surface), e.g. concentrated loads on beams, forces in hangers, reactions in supports, etc.
   b) *distributed loads*, which are distributed either over the whole active area of the body surface, or over parts of it, e.g. pressure in a vessel, soil pressure, aerodynamic forces, etc.; distributed load is given per a unit area.

2) *Volume forces* (i.e. forces generated by a field of force), loading the whole body mass, e.g. the dead weight of a body, the force of inertia, centrifugal force, etc.

Types of forces can be subdivided with respect to:

1) *force changes in time:*
   a) *static loading,* which can be either **constant** or **slowly increasing** from a certain value (usually from zero) up to its nominal magnitude, and then remains unchanged. Slow force

application is necessary so that deformation time changes can develop fully and the forces of inertia can be neglected;

    b) *dynamic loading,* which can be for instance:

                i) impact load, characterized by great instantaneous load acceleration;

                ii) cyclic load (periodically changing), which can lead to body *fatigue* fracture;

2) *force site stability:*

    a) *fixed load,* i.e. the load point does not change in time;

    b) *travelling load,* i.e. the load point changes in time, e.g. crane crab, a train loading a bridge, etc.

1.1.1.2 Static equilibrium of external loads

When studying basic problems of the classical *Strength of Materials,* we usually consider the *static* exertion of external loads. This is conditioned by the static equilibrium state of the structure, including reactions, which must be satisfied both for forces and for couples.

1.1.2 Internal forces; stress in general bodies under general loading conditions

Although the introductory lectures will be dealing with simple members (bars, rods, booms) under axial loading, consider first a general body subjected to several loads F_1, F_2, etc. (Fig.1.1.2.1)

To understand the stress condition created by these loads at some point Q, within a body of a general shape, we shall first pass a section through Q, using a plane ξ parallel to the yz plane Fig.1.1.2.1a. The portion of the body to the left of the section, Fig.1.1.2.1b, is subjected to some of the original (*external*) loads, and to normal and shearing forces distributed over the section. We shall denote by ΔR an *internal* force acting on a small area ΔA surrounding point Q and resolving it we shall obtain ΔN_x, ΔV_x, respectively the normal and the shearing (*internal*) forces. Note that the subscript x is used to indicate that the forces ΔN_x, ΔV_x are acting on a surface perpendicular to the x axis. While the normal force ΔN_x has a well defined direction, the shearing force ΔV_x may have any direction in the plane of the section. We shall, therefore, resolve ΔV_x into two component forces, ΔV_{xy} and ΔV_{xz}, in directions parallel to the y and z axes, respectively. Dividing the magnitude of each force by the area ΔA, and letting ΔA approach zero, we define the *force intensities* called **stress(es)** on that section, which are denoted by the Greek letters σ (sigma) and τ (tau).

The three stress components shown in Fig.1.1.2.1:
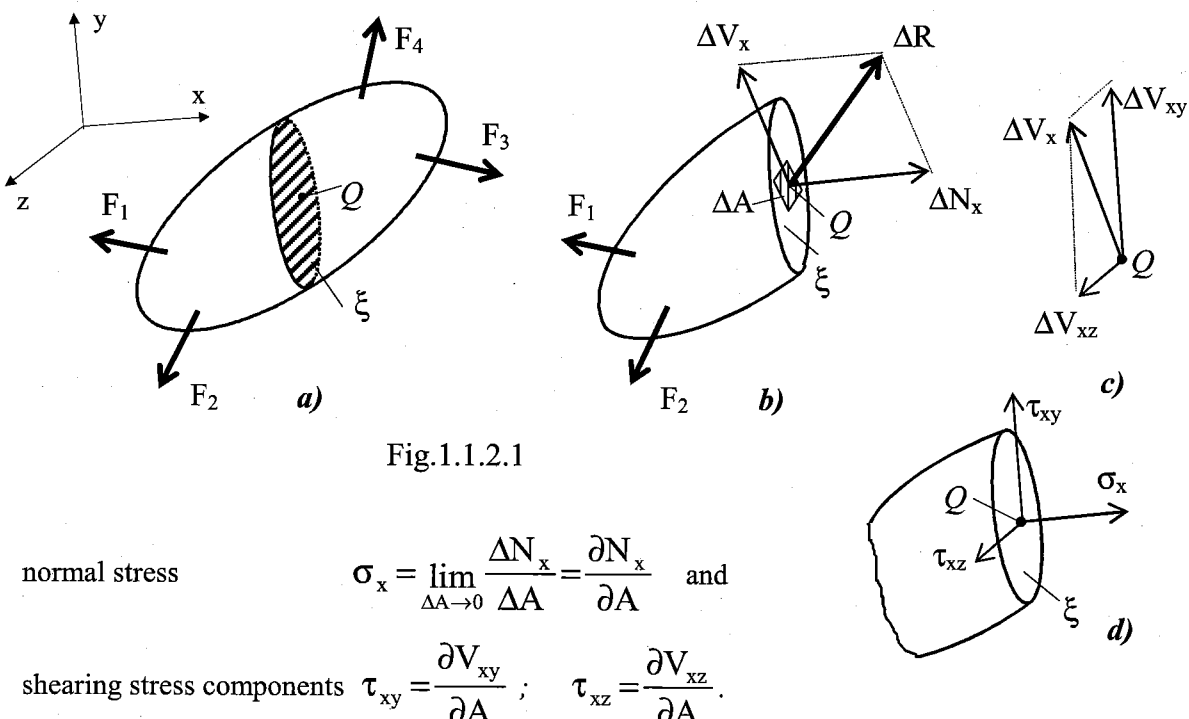
Fig.1.1.2.1

normal stress $\qquad \sigma_x = \lim_{\Delta A \to 0} \dfrac{\Delta N_x}{\Delta A} = \dfrac{\partial N_x}{\partial A}$ and

shearing stress components $\tau_{xy} = \dfrac{\partial V_{xy}}{\partial A}$; $\tau_{xz} = \dfrac{\partial V_{xz}}{\partial A}$.

We note that the first subscript in these stress components is used to indicate that the stresses under consideration are exerted on a surface perpendicular to the x axis. The second subscript in τ_{xy} and τ_{xz} identifies the direction of the component. The normal stress is positive if the corresponding arrow points in the positive x direction, i.e., if the body is in tension, and negative otherwise. Similarly (but here from the mathematical point of view only), the shearing stress components are positive if the corresponding arrows point, respectively, in the positive y and z directions (this has no physical meaning).

The above analysis may also be carried out by considering the portion of the body located to the right of the vertical plane through Q. The same magnitudes, but opposite directions, are obtained for the normal and shearing forces. Therefore, the same values are also obtained for the corresponding stress components, but since the section in the figure now faces the negative x axis, a positive sign for σ_x will indicate that the corresponding arrow points in the negative x direction. We will discuss problems of stress components in detail later.

1.1.3 Assumptions of solution

Right from the beginning I would like to ask you not to be afraid of this course in **Strength of Materials**. Have in mind that it is based on many simplifying assumptions that will be sufficient for a

number of practical applications, and will yield good results. For your information only, there are a number of more complicated problems where it is necessary to turn to comprehensive and highly sophisticated analysis. These problems belong to the scientific study of *theory of elasticity*. Analyses based upon theory of elasticity give much more detailed and more precise information about the state of stress, strain, and deformation at any point within the body than the more simplified type of study that a course in *Strength of Materials* deals with.

One of the most important tools serving the simplified analytical approach is *Saint-Venant's principle*. Let us consider a number of statically equivalent force systems acting over a specified small portion of the surface of an elastic body. Statically equivalent implies that the systems all have the same force and moment resultants. **Saint-Venant's principle** *states that although these various statically equivalent systems may have considerably different localized effects, all have essentially the same effect on stresses at any distance which is large compared to the dimensions of the part of the surface on which these forces are applied.*

The solution of any problem is exact only if the surface forces actually have the distribution indicated by the theory of elasticity solution. However, even if the true forces are not distributed in such a manner, the solution is still of value if one remembers Saint-Venant's principle and does not employ the solution in the immediate vicinity of the points of application of the surface forces.

Compare two axially loaded rubber rods: the first with very rigid plates on both of its ends (transferring the action of the forces) and the second without the plates, Fig.1.1.3.1. Having plotted a raster (grating) on the rods, the nature of *Saint-Venant's principle* can be nicely traced when examining the deformation of these rods.
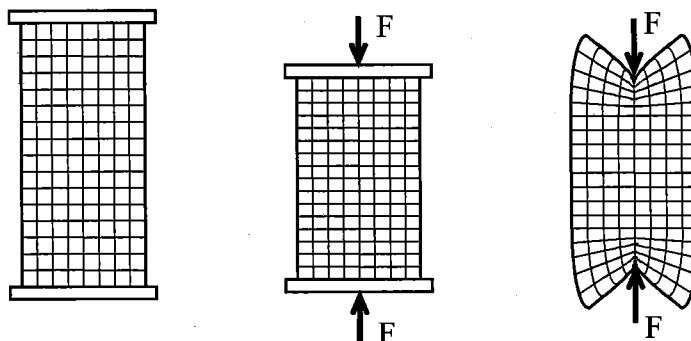
Fig.1.1.3.1

2. Tension and compression

2.1 Assumptions

Straight elements the longitudinal dimension of which is much greater than the other two dimensions are known as rods (or booms and bars, respectively). They have many practical applications. Rods (booms and bars) can have either constant or variable cross-sections. *The line connecting the cross-sectional centroids along a rod is its* **longitudinal axis,** *and if the forces coincide with it there can be only uniaxial loading and no bending in the element.*

2.2 Axially loaded bar

Hence, the simplest case to consider at the start is that of an initially straight metal rod (boom, bar) of constant cross-section, loaded at its ends by a pair of oppositely directed collinear forces F coinciding with the longitudinal axis of the bar (acting through the centroid of each section). For static equilibrium the magnitudes of the forces must be equal. If the (external) forces are directed away from the bar, the bar is said to be in *tension*, Fig.2.2.1*a*; if they are directed toward the bar, a state of *compression* exists, Fig.2.2.1*b*.
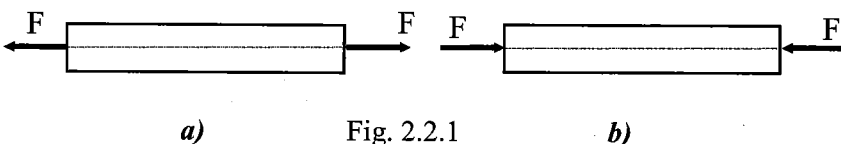
a)   Fig. 2.2.1   *b)*

Under the action of this pair of applied (external) forces, internal resisting forces are set up within the bar and their characteristics may be studied by imagining a plane that is passed through the bar anywhere along its length (x) and oriented perpendicular to the longitudinal axis of the bar, Fig.2.2.2*a*. When we do this we use the *method of sections*. For reasons to be discussed later, this plane should not be „too close" to either end of the bar. If for purposes of analysis the portion of the bar to the right of this plane is considered to be removed,

a)   *b)*   *c)*
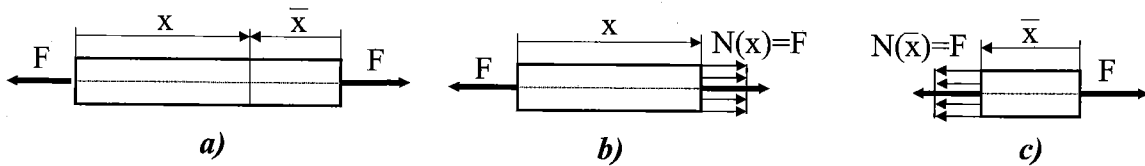
Fig.2.2.2

then it must be replaced by whatever effect it exerts upon the left portion, see the so-called 'free-body diagram' in Fig.2.2.2*b*. By this technique of introducing a cutting plane, the originally internal forces $N(x)$ now become as if external with respect to the remaining portion of the body. For the equilibrium of the portion to the left this effect must be a horizontal force of magnitude $N(x) = F$. However, this force F acting normal to the cross-section is actually the resultant of the distributed forces acting over

this cross-section in a direction normal to it. We can proceed analogously with the right portion when removing the left portion, Fig.2.2.2c.

At this point it is necessary to make some assumptions regarding the manner of variation of these distributed forces, and since the applied force F acts through the centroid it is commonly assumed that they are uniform across the cross-section (Fig.2.2.2b,c). Such a distribution is probably never realized exactly because of the random orientation of the crystalline grains of which the bar is composed. The exact value of the force acting on some very small element of area of the cross-section is a function of the nature and orientation of the crystalline structure at that point. However, over the entire cross-section the variation is described with reasonable engineering accuracy by the assumption of a uniform distribution.

2.3 Normal stress
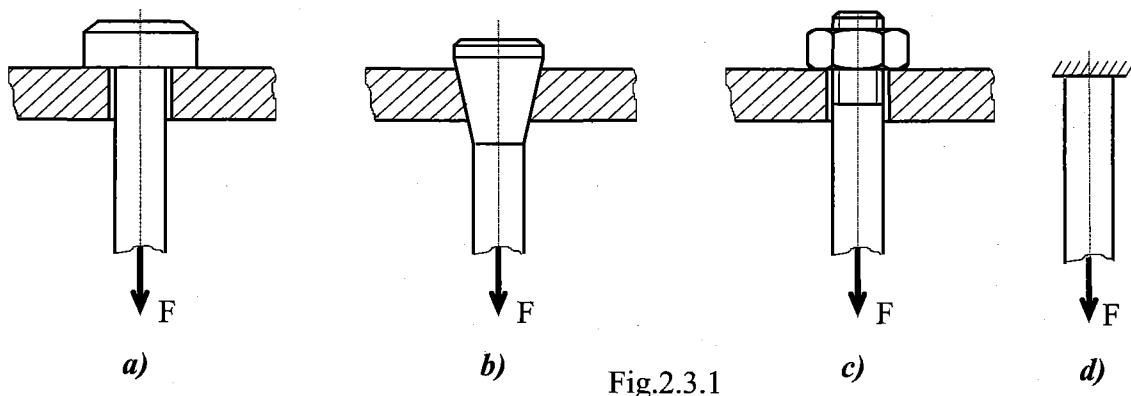
Instead of speaking of the internal force acting on some small element of area, it is better for comparative purposes to treat the normal force acting over a unit area of the cross-section, cf. Sec.1.1.2. The intensity of normal force per unit area is termed the *normal stress* and is expressed in units of force per unit area, i.e. when using SI metric units with F expressed in newtons (N) and A in square meters (m^2), the stress $\sigma = F/A$ will be expressed in N/m^2. This unit is called a *pascal* (Pa) when used with pressure in liquids and gases. In other branches of mechanics, we will use just N/m^2. However, one finds that the unit N/m^2 is an exceedingly small quantity and that, in practice, multiples of this unit must be used, namely, $1\ N/mm^2 = 10^6\ N/m^2$

As was previously stated: if the (external) forces are directed away from the bar, the bar is said to be in tension if they are directed toward the bar, a state of compression exists. To the *tensile internal forces* or *stresses* we attribute *positive signs* (i.e., plus-signs (+)) and the *compressive internal forces* or *stresses* will have *negative signs* (i.e., minus-signs (−)).

(Important: The action of tensile and compressive forces on a bar cannot be considered as being equivalent. At certain values of compressive forces, a phenomenon termed *buckling of columns* can appear, which means a *stability failure* (by lateral deflection of a long slender bar.)

Note: Examples of various types of bar gripping (clamping) are shown in Fig.2.3.1. With respect to *Saint-Venant's principle* (see section 1.1.3), all these cases can be substituted by the computational model presented in Fig.2.3.1d.

a)   b)   Fig.2.3.1   c)   d)
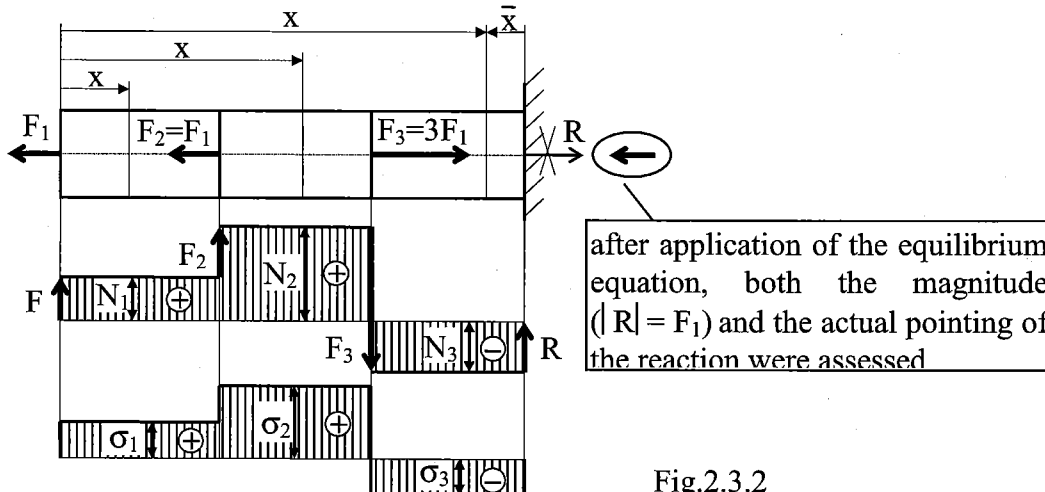
Let us examine another example for the method of sections (Fig.2.3.2):

In this example, we shall explain an easy way in which the method of sections can be applied. Instead of that tedious application of it when one has to draw a free-body diagram of one of the bar portions (with the internal reactive forces), it is sufficient to imagine a section made at a chosen point x along the bar and then add or subtract, respectively, the external forces exerted from one bar end up to cross-section x.

First we shall investigate the value of reaction R *(being an external force)* assuming its action on the right. From unique necessary equilibrium condition, we obtain

$$F_1 + F_2 - F_3 - R = 0 \implies R = F_1 + F_1 - 3F_1 = -F_1 < 0$$

after application of the equilibrium equation, both the magnitude ($|R| = F_1$) and the actual pointing of the reaction were assessed

Fig.2.3.2

Since the result is negative, it means (when concerning *external forces*) that our assumption of the reaction pointing was wrong and we must change it. After have done this, we shall take into our further consideration this new pointing, change the sense in the picture (see Fig.2.3.2, where the crossed arrow of R, which was originally assumed to point to the right, has been replaced with the arrow pointing to the left), and, as far as the magnitude of R is concerned, we will consider only its absolute value

$$R = \left| -F_1 \right| = F_1$$

14

When dealing with *internal forces* and *stresses*, we shall apply the *method of sections*. The rod must be divided into three regions - *I, II, III.*

Going from the left, we sum the external forces in each region, taking into account their respective pointings and thus obtain:

- region *I* ....$N_I(x) = F_1$ $\sigma_I(x) = F_1 / A > 0$ ...tension

- region *II*...$N_{II}(x) = F_1 + F_1 = 2F_1$ $\sigma_{II}(x) = 2 F_1 / A = 2\sigma_I(x) > 0$ ...tension

- region *III*..$N_{III}(x) = F_1 + F_1 - 3 F_1 = -F_1$ $\sigma_{III}(x) = -F_1 / A < 0$ ...compression

We can try to go from the **right,** for instance in region *III*:

- region *III* ...$N_{III}(\bar{x}) = -R = -F_1$ $\sigma_{III}(\bar{x}) = -F_1 / A < 0$ ...compression

2.4 Stress on an oblique plane under axial loading

In the preceding sections, the axial forces exerted on a two-force member (bar) were found to cause normal stresses in that member. The reason was that the stresses were being determined only on planes perpendicular to the longitudinal axis of the bar. As we shall see in this section, axial forces cause both normal and shearing stresses on planes which are not perpendicular to the bar axis.
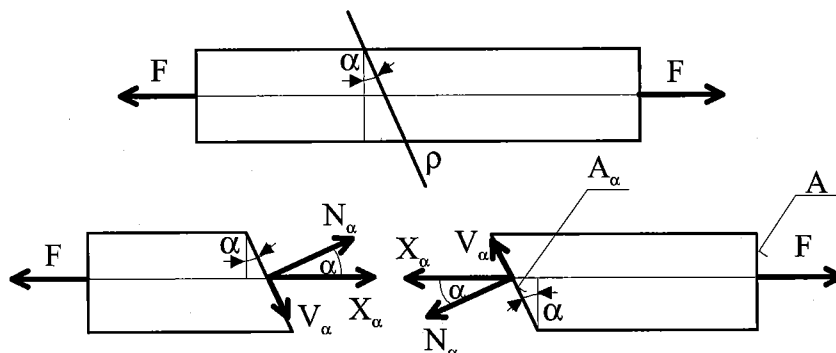
Fig. 2.4.1

Consider now such a two-force member, which is subjected to axial force F (see Fig.2.4.1). If we pass a section ρ forming an angle α with a normal plane and draw the free-body diagrams of the portion of members located to the left and right of that section, respectively, we find from the equilibrium conditions of the free bodies, that the distributed forces acting on the section must be equivalent to force $X_\alpha = F$. Resolving X_α into components N_α and V_α, respectively normal and tangential to the section, we have

$$N_\alpha = F \cdot \cos\alpha \qquad V_\alpha = F \cdot \sin\alpha$$

Force N_α represents the resultant of the normal forces distributed over the section, and force V_α the resultant of the shearing forces. The average values of the corresponding normal and shearing stresses are obtained by dividing, respectively, N_α and V_α by the area $A_\alpha = A/\cos\alpha$ of the section, Fig.2.4.2.

$$\sigma_\alpha = \frac{N_\alpha}{A_\alpha} = \frac{F \cdot \cos\alpha}{\dfrac{A}{\cos\alpha}} = \sigma_x \cdot \cos^2\alpha \ , \quad \tau_\alpha = \frac{V_\alpha}{A_\alpha} = \frac{F \cdot \sin\alpha}{\dfrac{A}{\cos\alpha}} = \sigma_x \cdot \sin\alpha \cdot \cos\alpha \qquad (2.4.1a,b)$$

The stress in the longitudinal direction $\upsilon_\alpha = \dfrac{X_\alpha}{A_\alpha} = \dfrac{F}{\dfrac{A}{\cos\alpha}} = \sigma_x \cdot \cos\alpha \ ;$ (2.4.1c)

It holds $\qquad \upsilon_\alpha{}^2 = \sigma_\alpha{}^2 + \tau_\alpha{}^2$

$\sigma(x) = \dfrac{F}{A}$

$\upsilon_\alpha = \sigma(x) \cdot \cos\alpha \qquad\qquad \sigma_\alpha = \sigma(x) \cdot \cos^2\alpha \qquad\qquad \tau_\alpha = \sigma(x) \cdot \sin\alpha \cdot \cos\alpha$
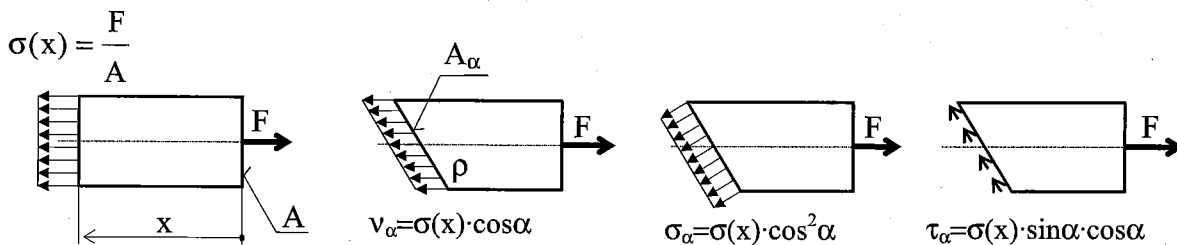
Fig.2.4.2

2.5 Deformation

In the previous sections we analyzed the stress created in various bars when loaded. Another important aspect of the analysis and design of structures relates to the *deformations* caused by loads applied to the structure. Clearly, it is important to avoid deformations so large that they may prevent the structure from fulfilling the purpose for which it was intended. However, the analysis of deformations may also help us in the determination of stresses. Indeed, it is not always possible to determine the forces in the members of a structure by applying only the principles of statics. This is because statics is based on the assumption of undeformable, rigid structures. By considering engineering structures as *deformable* and analyzing the deformations in their various members, it will be possible for us to compute forces which are *statically indeterminate,* i.e., indeterminate in the framework of statics.

Let us consider a suspended rod, of original length L_o and uniform cross-sectional area A_o, Fig.2.5.1. If we apply a load F to its end, the rod - having the uniform stress along its length - will elongate and will have the resulting length $L = L_o + \Delta L$ at its end.
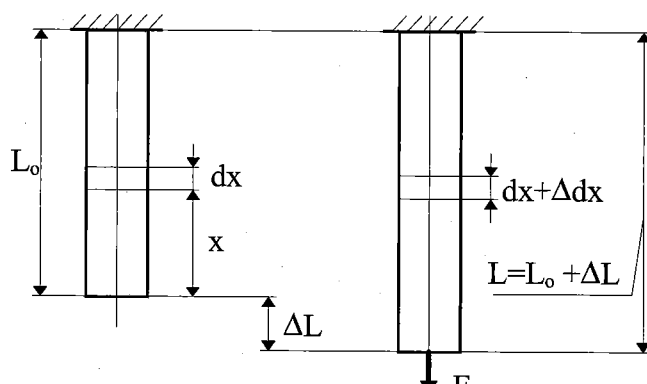
Fig.2.5.1

Increment of its length, i.e. *total deformation* (in this case being elongation)

$$\Delta L = L - L_0 \qquad (2.5.1)$$

expresses the elongation or reduction (shortening) of the rod. We define the *deformation per unit length,* i.e. the ratio of deformation over an original length (on which the stress distribution remains uniform.

- in this case the whole rod length L_o can be applied), called the *(normal) strain* and denoted by the

Greek letter epsilon $$\varepsilon = \frac{L - L_0}{L_0} \qquad (2.5.2)$$

Analogously, an infinitesimal rod element, originally having length dx, will change its length to be $dx + \Delta dx$. The element length dx is changed by the *total deformation* Δdx. The *strain* is then expressed in the following form

$$\varepsilon(x) = \frac{\Delta dx}{dx} \qquad (2.5.3)$$

Formula (2.5.3) can be used in all cases of bars (rods) being under tension or compression (e.g., cases of variable cross-section or variable load having non-uniformly distributed stress) because the stress distribution along (over) an infinitesimal rod element dx is always considered to be uniform!

Strain is usually expressed in units of *m* per *m* (*mm* per *mm*): [*m/m =1*] or [*mm/mm =1*], (and consequently is dimensionless) or can also be expressed as a *percentage [%]*.

The *total deformation* is sometimes used to denote the elongation in [*m*] or [*mm*].

2.6 Stress-strain curve (mechanical properties of materials)

When applying a *tensile test* on a specimen of a material, the *stress-strain curve* is obtained. The *test specimen* is held in the grips of either an electrically driven or a hydraulic testing machine. As the axial load F is gradually increased in increments, the total elongation ΔL over the *gauge length* of the specimen is measured at each increment of load and this is continued until fracture of the specimen takes place. Knowing the original cross-sectional area A_o and the original gauge length L_o of the test specimen, the *normal stress* $\sigma = F/A_o$ and *normal strain* $\varepsilon = \Delta L/L_o$ may be obtained. Having obtained numerous pairs of values of *normal stress* σ and *normal strain* ε, the experimental data may be plotted with these quantities considered as ordinate and abscissa, respectively. This is the *stress-strain diagram* of the material for this type of loading. Stress-strain diagrams assume widely differing forms for various materials: e.g. low-carbon steel; alloy steel (aluminium alloy has similar shape); cast iron
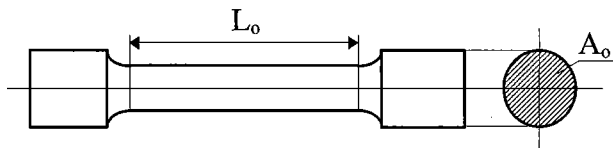
Fig.2.6.1

(glass, stone).

Metallic engineering materials are commonly classed as either *ductile* or *brittle*. A ductile material (e.g., structural steel or aluminium) is characterized by its ability to yield at normal temperatures and

by having a relatively large tensile strain up to the point of rupture, whereas a brittle material (e.g., cast iron or concrete) has relatively low strain up to the same point. A standard measure of ductility is its *percent elongation*, which is defined a

$$Percent\ elongation = 100.(L_B - L_o)/L_o$$

where L_B denotes the final length of the tensile test specimen at rupture. An arbitrary strain of 0.05 *mm/mm* (or percent elongation of 5%) is frequently taken as the dividing line between these two classes. For ductile materials, the percent elongation reaches up to 20%. (Another measure of ductility is the *percent reduction in area*, defined as
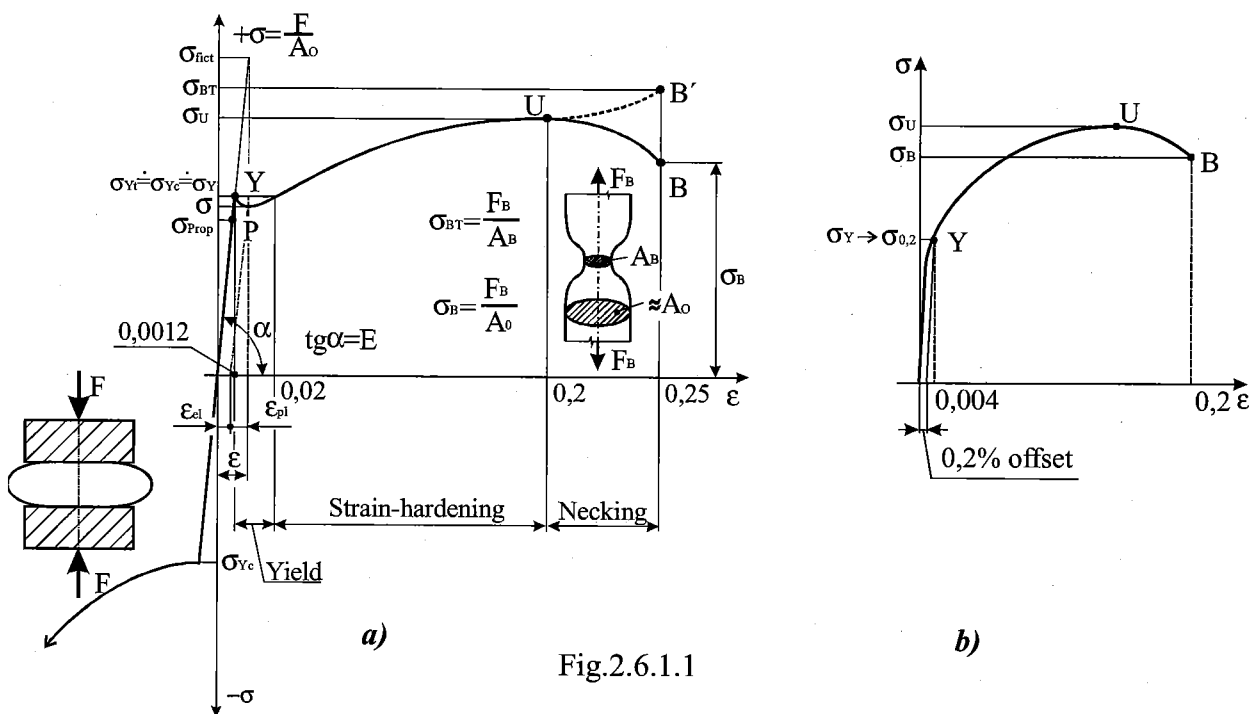
$$Percent\ reduction\ in\ area = 100(A_o - A_B)/A_o,$$

where A_B denotes the minimum cross-sectional area of the specimen at rupture. For structural steel, a 60 to 70% reduction in area is common.)

2.6.1 Hooke's law

For any material having a stress-strain curve of the form shown in Fig.2.6.1.1, which is typical for: a) low-carbon steel; b) aluminium alloy or alloy steel,

Fig.2.6.1.1

it is evident that the relation between stress and strain is linear for comparatively small values of strain. This linear relation between elongation and the axial force causing it (since these quantities

respectively differ from the strain and stress only by a constant factor) was first noticed by Sir Robert Hooke in 1678 and is called *Hooke's law*. To describe this initial linear range of action of the material we may consequently write

$$\sigma = E \cdot \varepsilon \, , \qquad\qquad (2.6.1.1)$$

where E denotes the (steep) slope of the straight-line portion of the curves in Fig.2.6.1.1*a,b*. The quantity E, i.e., the ratio of the unit stress to the unit strain, is *the modulus of elasticity* of the material in tension, or, as it is often called, *Young's modulus*. Values of E for various engineering materials are tabulated in handbooks (E for the most common materials is listed in the Table 2.6.7.1, cf. Sec. 2.7). Since the unit strain ε is a pure number (being a ratio of two lengths) it is evident that E has the same units as does stress, i.e., MPa. For many common engineering materials the modulus of elasticity in compression is very nearly equal to that found in tension. It should be carefully noted that the behaviour of materials under load as discussed in this textbook is restricted (unless otherwise stated) to the linear region of the stress-strain curve.

(Brittle materials, e.g., cast iron, have the stress-strain diagram curved in its whole region - Fig.2.6.2.1*a,b*. With such materials, we cannot strictly speak about the modulus of elasticity. To simplify computation, we even here approximate - with respect to the required accuracy - the necessary part of the diagram by a straight line - Fig.2.6.2.1*b* - and the value of the respective modulus of elasticity is then given in certain limits.)

2.6.2 Mechanical characteristics of materials

The stress-strain curve shown in Fig.2.6.1.1*a* may be used to characterize several strength properties of a *ductile material*:

The initial portion of the stress-strain curve, being a straight line with a steep slope, ends with the ordinate of point P, known as the *proportional limit*. (For a brittle material, which has a stress-strain curve as shown in Fig.2.6.2.1*a,b*, there is no proportional limit). The ordinate of a point almost coincident with (slightly larger than) P is known as the *elastic limit*, i.e., such a maximum stress that there is no permanent or residual deformation when the load is entirely removed. (That region of the stress-strain curve extending from the origin to the proportional limit P is called the *elastic range*; that stress-strain curve region extending from P - more precisely from the elastic limit - to the point of rupture B is called the *plastic range*. This problem will be discussed in the next course in the textbook Strength of Materials II). After a critical value σ_Y (point Y) of the stress has been reached, the specimen undergoes a large deformation with a relatively small increase in the applied load. This deformation is caused by slippage of the material along oblique surfaces and is due, therefore, primarily to shearing stresses. (The stress σ_{fict} is only imaginary, i.e., such a stress as if the material maintains its elastic property even after it has exceeded σ_Y). As we may note from the stress-strain diagrams of two typical ductile materials (Fig.2.6.1.1*a,b*), the

elongation of the specimen after it has started to yield may be 200 times as large as its deformation before yield. After a certain maximum value of the load (corresponding to point U) has been reached, the diameter of the portion of the specimen begins to decrease, due to local *plastic instability*. This phenomenon is known as *necking*. After necking has begun, somewhat lower loads are sufficient to keep the specimen elongating further, until it ruptures (point B). We note that the rupture occurs along a cone-shaped surface which forms an angle of approximately 45° with the original surface of the specimen. This indicates that shear is primarily responsible for the failure of ductile materials, and confirms the fact that, under an axial load, shearing stresses are largest on surfaces forming an angle of 45° with the load (cf. Sec.2.4 and Sec.5.2). The stress σ_Y at which yield is initiated is called the *yield strength* of the material, the stress σ_U corresponding to the maximum load applied to the specimen is known as the *ultimate strength*, and the stress σ_B corresponding to rupture is called the *breaking strength*.

If a specimen made of a ductile material were loaded in compression instead of tension, the stress-strain curve obtained would be essentially the same through its initial straight-line portion and through the beginning of the portion corresponding to yield and strain hardening. Particularly noteworthy is the fact that for a given steel, the yield strength is the same in both tension and compression. For larger values of strain, the tension and compression stress-strain curves diverge, and it should be noted that necking cannot occur in compression.

The stress-strain diagrams of Fig.2.6.1.1*a,b* show that structural steel and aluminium, while both ductile, have different yield characteristics. In the case of structural steel (Fig.2.6.1.1*a*), the stress remains constant over a large range of values of the strain after the onset of yield. Later the stress must be increased to keep elongating the specimen, until the maximum value σ_U has been reached. This is due to a property of the material known as *strain-hardening*.

(The yield strength of structural steel may be determined during the tensile test by watching the load dial. After increasing steadily, the load is observed to suddenly drop to a slightly lower value which is maintained for a certain period while specimen keeps elongating. In a very carefully conducted test, one may be able to distinguish between the *upper yield point,* which corresponds to the load reached just before yield starts, and the *lower yield point,* which corresponds to the load required to maintain yield. Since the former is transient, the latter, i.e., lower yield point, should be used to determine the yield strength of the material.)

In the case of aluminium (Fig.2.6.1.1*b*) and of many other ductile materials, the onset of yield is not characterized by a horizontal portion of the stress-strain curve. Instead the stress keeps increasing - although not linearly - until the ultimate strength is reached. Necking then begins, leading eventually to

rupture. For such materials, one may define the yield strength by the offset method. The yield strength at 0.2% offset ($\sigma_{0.2}$) - which is the most common - is obtained by drawing through the point of the horizontal axis of abscissa $\varepsilon = 0.2\%$ (or $\varepsilon = 0.002$), a line parallel to the initial straight-line portion of the stress-strain diagram. The stress σ_Y corresponding to the point Y obtained in this fashion is defined as the yield strength at 0.2% offset.

a)   *b)*
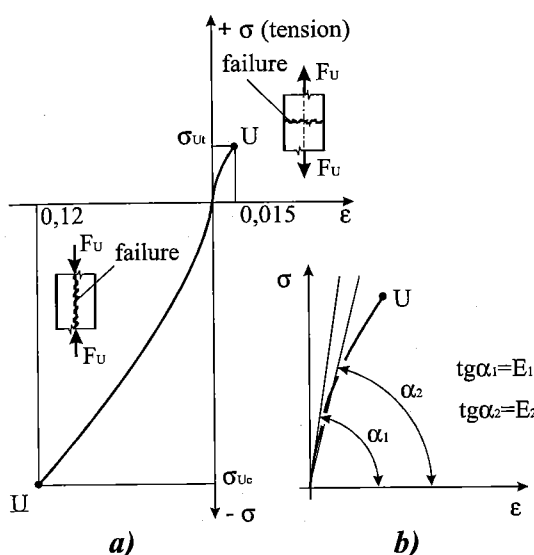
Fig.2.6.2.1

Brittle materials (e.g., cast iron, glass, and stone) are characterized by the fact that rupture occurs without any noticeable prior change in the rate of elongation (Fig.2.6.2.1*a,b*).

Thus, for brittle materials, there is no difference between the ultimate strength and the breaking strength. Also, the strain at the time of rupture is much smaller for brittle than for ductile materials. When a brittle material is loaded in tension, rupture occurs along a surface perpendicular to the load; while at compression, rupture occurs in a surface parallel to the load. From Fig.2.6.2.1*a*, we note the absence of any necking of the specimen. We conclude from this observation that normal stresses are primarily responsible for the failure of brittle materials.

For most brittle materials, one finds that the ultimate strength in compression is much larger than that in tension (Fig.2.6.2.1a). This is due to the presence of flaws, such as microscopic cracks or cavities, which tend to weaken the material in tension, while not appreciably affecting its resistance to compressive failure.

We recall that the stress plotted in the diagrams of Figs.2.6.1.1*a,b* and 2.6.2.1*a* was obtained by dividing the load F by the cross-sectional area A_o of the specimen measured before any deformation had taken place. Since the cross-sectional area of the specimen decreases as F increases, the stress plotted in our diagrams does not represent the actual stress in the specimen. The difference between the *engineering stress* $\sigma = F/A_o$ that we computed and the *true stress* $\sigma_t = F/A$ (dashed line) obtained by dividing F by the cross-sectional area A of the deformed specimen becomes apparent in ductile materials mainly after necking has started. While the engineering stress σ, which is directly proportional to the load F, decreases with F during the necking phase, the true stress σ_t, which is proportional to F but also inversely proportional to A, is observed to keep increasing until rupture of the specimen occurs (Fig.2.6.1.1*a*).

2.6.3 Factor of safety; strength criterion; allowable stress; limit analysis

A structural member or a machine component must be designed so that its ultimate load is considerably larger than the load the member or component will be allowed to carry under normal conditions of utilization. This smaller load is generally referred to as the *working load,* whose maximum value is denoted as the *allowable (working) load.* In many applications a linear relationship exists between a load and the stress caused by the load. Thus, we can apply the terms: the *working stress* and the *allowable (working) stress,* respectively. The ratio of the *limit stress* σ_{lim} to the *working stress* σ is defined as the *factor of safety k* :

$$k_Y = \frac{\sigma_Y}{\sigma} > 1 \text{ (related to the yield strength);} \qquad (2.6.3.1a)$$

$$k_U = \frac{\sigma_U}{\sigma} > 1 \text{ (related to the ultimate strength);} \qquad (2.6.3.1b)$$

The *allowable stress* is then defined when a chosen *minimum factor of safety* k_{min} is applied to the respective limit stress, which depends on the type of material:

a/ ductile material... $\sigma_{all} = \dfrac{\sigma_Y}{k_{Y\,min}}$, which holds for both tension and compression ; $\qquad (2.6.3.2)$

b/ brittle material... $\sigma_{all;t} = \dfrac{\sigma_{Ut}}{k_{U\,min}}$, which holds for tension $\qquad (2.6.3.3a)$

$\sigma_{all;c} = \dfrac{\sigma_{Uc}}{k_{U\,min}}$, which holds for compression $\qquad (2.6.3.3b)$

Based on the respective allowable stress we define the *strength criterion* for the respective type of material (the criteria defined in this chapter are restricted to uniaxial loading only):

a) ductile material ... $|\sigma| \leq \sigma_{all}$ ... tension and compression $\qquad (2.6.3.4)$

(sometimes the working stress for ductile materials is also checked by ... $|\sigma| \leq \sigma_U / k_{U\,min}$)

b) brittle material ... $\sigma \leq \sigma_{all;t}$ ... tension $\qquad (2.6.3.5a)$

$|\sigma| \leq \sigma_{all;c}$ ... compression $\qquad (2.6.3.5b)$

The values of the factors of safety depend on the type of structures and their operating application. For normal design we recommend $k_{Ymin} \approx 2$ and $k_{Umin} \approx 4$.

Note: A *limit analysis* of a structure can be carried out (cf.Chap.5), taking the factor of safety (k_Y or k_U) to be equal to unity :

a/ with a *ductile material,* this refers to the *yield criterion* ... $|\sigma| = \sigma_Y$; $\qquad (2.6.3.6)$

b/ with a *brittle material,* this refers to the *brittle fracture criterion* having two parts:

for tension ...$\sigma = \sigma_{Ut}$;   for compression ...$|\sigma| = \sigma_{Uc}$;   (2.6.3.7a,b)

2.7 Application of Hooke's law to deformation computation

a) Consider a homogeneous rod of length L and uniform cross-sectional area A subjected to a centric axial load F at its end (Fig.2.5.1). In such a rod, normal stress (at an arbitrary point x)

$$\sigma(x) = \frac{N(x)}{A_0} = \frac{F}{A_0} = \sigma \quad \text{is constant}$$

and normal strain, being constant as well, can be expressed for the rod whole length L (cf. Sec.2.5) as

$$\varepsilon = \frac{\Delta L}{L_0}$$

If the stress σ does not exceed the proportional limit of the material, we may apply Hooke's law and write

$$\varepsilon = \frac{\Delta L}{L_o} = \frac{\sigma}{E} = \frac{F}{A_o \cdot E} \tag{2.7.1a}$$

Then, the total deformation is $\Delta L = \dfrac{\sigma \cdot L_0}{E} = \dfrac{F \cdot L_0}{A_0 \cdot E}$ (2.7.1b)

b) If a rod is loaded at various points, or if it consists of several portions of various cross-sections and possibly of various materials, we must divide it into component parts which individually satisfy the required conditions for the application of the formulae (2.7.1a,b). Denoting respectively by N_i ,L_i, A_i , and E_i the internal force, length, cross-sectional area, and modulus of elasticity corresponding to part i, we express the deformation of the entire rod as

$$\Delta L = \sum_i \Delta L_i = \sum_i \frac{N_i \cdot L_i}{A_i \cdot E_i} \tag{2.7.2}$$

c) We recall from Sec. 2.5 that, in the case of a rod of variable cross-section, the strain ε depends upon the position x where it is computed and is defined as $\varepsilon = \Delta dx/dx$ (Fig.2.5.1). Solving for Δdx and substituting for ε from Eq.(2.7.1a), we express the deformation of an element of length dx as

$$\frac{\Delta dx}{dx} = \varepsilon(x) = \frac{\sigma(x)}{E} \Rightarrow \quad \Delta dx = \frac{\sigma(x)}{E} dx \tag{2.7.3a}$$

The total deformation of the rod is obtained by integrating this expression over the length L of the rod, i.e.,

$$\Delta L = \int_{(L)} \Delta dx = \int_{(L)} \frac{\sigma(x)}{E} dx \tag{2.7.3b}$$

Formula (2.7.3*b*) should be used in place of (2.7.1*b*), not only when the cross-sectional area *A* is a function of *x*, but also when the internal force *N(x)* depends upon *x*, as is the case for a rod hanging under its own weight, or a rotating arm, etc.

Introduction of the concepts of *stiffness* and *flexibility*

Eq.(2.7.1.b) can be rewritten as

$$\Delta L = \frac{FL_0}{EA_0} = \frac{F}{k} = F \cdot \delta \qquad \Rightarrow$$

$$\delta = \frac{1}{k} = \frac{L_0}{EA_0} \quad \left[mm \cdot N^{-1}\right]; \quad k = \frac{1}{\delta} = \frac{EA_0}{L_0} \quad \left[N \cdot mm^{-1}\right]$$

which define: *flexibility* δ, which is a deformation (elongation or shortening) whose magnitude is produced by a unit force;

on the other hand *stiffness* **k** numerically equals the force magnitude being necessary to produce a unit deformation (elongation or shortening).

Note: Because the initial length L_0 and cross-sectional area A_0 of a rod do not differ greatly numerically (when the rod is stressed in the range of Hooke's law) from their final magnitudes *L*, *A*, respectively, after the rod deformation, we do not in practice use the subscript, i.e., we put in the above formulae $L_0 \to L$ and $A_0 \to A$.

2.8 Poisson's ratio μ

In all engineering materials, the elongation *ΔL* produced by an axial tensile force *F* in the direction *x* of the force is accompanied by a contraction in any transverse direction (for the parallelepiped in Fig.2.8.1 the lateral total strains are *Δa*, *Δb*, in the direction of the corresponding coordinates *y, z*). In order to find out more easily all total strains, we have shifted the deformed configuration into one parallelepiped corner.
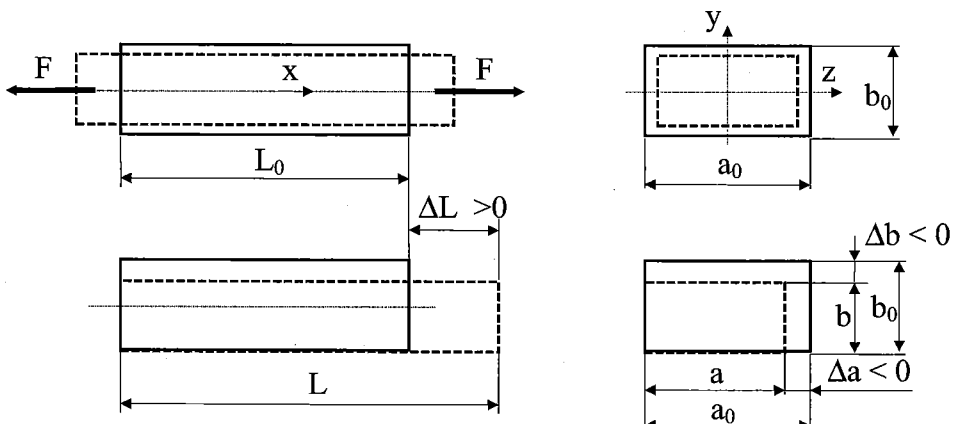
Fig.2.8.1

The strains in the respective directions are (the total strains *Δa*, *Δb* being negative, cf. Fig.2.8.1, the strains ε_y, ε_z are negative as well)

$$\varepsilon_x = \frac{\Delta L}{L_0} \geq 0; \qquad \varepsilon_y = \frac{\Delta b}{b_0} \leq 0; \qquad \varepsilon_z = \frac{\Delta a}{a_0} \leq 0$$

Assuming the rod material to be both *homogeneous* and *isotropic,* the *lateral strains* are equal, i.e.,

$$\varepsilon_y = \varepsilon_z$$

The absolute value of the ratio of the lateral strain over the axial strain is called *Poisson's ratio* and is denoted by the Greek letter μ. There hold the expressions:

$$\mu = -\frac{\varepsilon_y}{\varepsilon_x} = -\frac{\varepsilon_z}{\varepsilon_x}; \quad \text{or} \quad \mu = \left|\frac{\varepsilon_y}{\varepsilon_x}\right| = \left|\frac{\varepsilon_z}{\varepsilon_x}\right|$$

After applying Hooke's law, we obtain the lateral strains as a function of the load F

$$\varepsilon_y = \varepsilon_z = -\mu \cdot \varepsilon_x = -\frac{\mu \sigma_x}{E} = -\frac{\mu F}{EA_0},$$

from which we can express the respective total strains

$$\Delta a = a_0 \cdot \varepsilon_z = -a_0 \cdot \mu \cdot \frac{F}{EA_0}; \quad \Delta b = b_0 \cdot \varepsilon_y = -b_0 \cdot \mu \cdot \frac{F}{EA_0}$$

The range of *Poisson's ratio* values for engineering materials can be obtained readily by examining the *relative change in volume* of a piece of material, cf. Sec.2.9.

2.9 Relative change in volume

Let us study the change in volume of the parallelepiped from Fig.2.8.1. Its volume, being before loading $$V_0 = L_0 \cdot a_0 \cdot b_0,$$

will change after deformation as follows,

$$V = L \cdot a \cdot b = L_0 \cdot a_0 \cdot b_0 \cdot (1+\varepsilon_x) \cdot (1+\varepsilon_y) \cdot (1+\varepsilon_z) =$$

$$= V_0 \cdot \left(1 + \varepsilon_x + \varepsilon_y + \varepsilon_z + \varepsilon_x \cdot \varepsilon_y + \varepsilon_y \varepsilon_z + \varepsilon_z \cdot \varepsilon_x + \varepsilon_x \cdot \varepsilon_y \cdot \varepsilon_z\right)$$

when taking into account the change in the parallelepiped dimensions:

$$L = L_0 + \Delta L = L_0 \cdot \left(1 + \frac{\Delta L}{L_0}\right) = L_0 \cdot (1+\varepsilon_x); \quad a = a_0 \cdot (1+\varepsilon_z); \quad b = b_0 \cdot (1+\varepsilon_y).$$

Since the strains ε_x, ε_y, ε_z, have small magnitudes, when within the range of Hooke's law, their mutual products can be cancelled, considering them as small quantities of higher orders. Thus, the volume expression can be simplified into the shape

$$V \approx V_0 \cdot \left(1 + \varepsilon_x + \varepsilon_y + \varepsilon_z\right).$$

The relative change in volume can then be expressed as

$$\Theta = \frac{V - V_0}{V_0} = \frac{\Delta V}{V_0} \approx \varepsilon_x + \varepsilon_y + \varepsilon_z \qquad (2.9.1)$$

For uniaxial <u>tension</u> (where it holds $\varepsilon_y = \varepsilon_z = -\mu \cdot \varepsilon_x$), the expression (2.9.1) can be rewritten in the following form and must, logically, be <u>positive</u>

$$\Theta = \frac{\Delta V}{V_0} = \varepsilon_x \cdot (1 - 2\mu) = \sigma_x \cdot \frac{(1 - 2\mu)}{E} \geq 0 \qquad (2.9.2)$$

In order to ensure that the *relative change in volume* is positive, *Poisson's ratio* must range

$$0 \leq \mu \leq \frac{1}{2} \qquad (2.9.3)$$

We may note that an ideal material having a value $\mu = 0$ could be stretched in one direction <u>without any lateral contraction</u>. On the other hand, an ideal material for which $\mu = 1/2$ would be *perfectly incompressible* $(\Theta = 0)$. What may be surprising is that for rubber $\mu \rightarrow 1/2$.

Introducing the constant

$$K = \frac{E}{3(1 - 2\mu)} \qquad (2.9.4)$$

we write Eq. (2.9.2) in the form $\qquad \Theta = \frac{\sigma_x}{3K} \qquad (2.9.5)$

The constant K is known as the *bulk modulus* of the material.

(A case of special interest is that of a body subjected to a uniform hydrostatic pressure p. Each of the stress components is then equal to $-p$ and Eq. (2.9.1) yields $\Theta = -p \cdot [\, 3(1-2\mu) \,/\, E\,] = -p\,/\,K$. In this case the *bulk modulus K* is called the *modulus of compression* of the material.)

Table of the *modulus of elasticity E* (cf. Sec.2.6), *Poisson's ratio μ* and the *coefficient of thermal expansion α* (cf. Sec.3.6) for <u>common materials</u>:

Table 2.9.1

Material	$E \cdot 10^5$ [N/mm^2]	μ [$-$]	$\alpha \cdot 10^{-6}$ [K^{-1}]
Steel	2.1	0.3	12
Nickel	2.1	0.3	13
Copper	1.15	0.36	14
Aluminium	0.72	0.35	23
Cast iron	0.7 - 1.2	0.25 - 0.27	9

2.10 Principle of superposition of stresses and displacements

Let us assume that two forces load the bar in Fig.2.10.1. Consider first that only the load F_1 is applied to the rod. Then, at an arbitrary point (cross-section) x, produced are internal force $N(x) = F_1$ and stress

$$\sigma_1(x) = \frac{F_1}{A_0} .$$

If, on the contrary, the load F_2 acts separately we obtain stress

$$\sigma_2(x) = \frac{F_2}{A_0} .$$
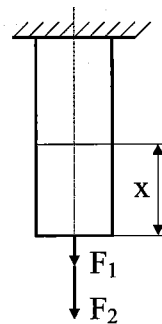
Fig. 2.10.1

If both loads exert simultaneously, the internal force is given as the sum of all the external forces acting from one rod end up to the cross-section x, thus $N(x) = F_1 + F_2$. The resulting stress is then

$$\sigma(x) = \frac{N(x)}{A_0} = \frac{F_1 + F_2}{A_0} = \frac{F_1}{A_0} + \frac{F_2}{A_0} = \sigma_1(x) + \sigma_2(x) \tag{2.10.1}$$
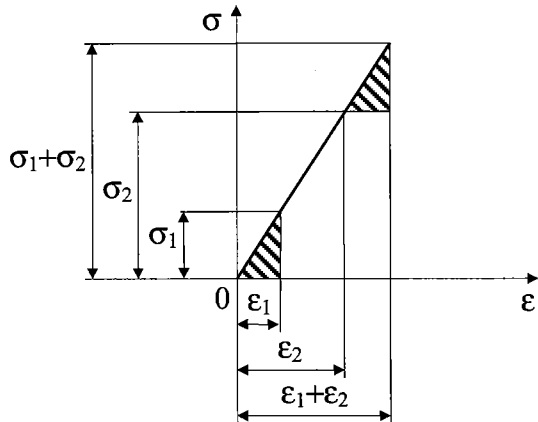
The resulting stress, in the considered cross-section x, is then equal to the sum - *superposition* - of the separated stresses. This statement represents a formulation of the *principle of the superposition of stresses*. It holds under the following conditions:

- the exerting forces, and, consequently, the corresponding stresses act on the same axis;
- the force actions upon the body do not change substantially owing to the body deformation.

Fig. 2.10.2

If the σ-ε relation is linear, i.e., if it obeys Hooke's law, the *principle of the superposition of strains* also hold. This can easily be proved from Fig.2.10.2:

ε_1 corresponds to the separately exerting σ_1;

ε_2 corresponds to the separately exerting σ_2 ;

and the sum of strains $\varepsilon_1 + \varepsilon_2$ corresponds to the sum of stresses $\sigma_1 + \sigma_2$.

Note: It should be taken into account that the stress and strain state in a body may be influenced by the prior history of the body loading, i.e., by the manufacturing technology, changes of surrounding temperature, mounting influences, etc.

2.11 Various effects influencing the stress and strain assessment in an axially loaded bar

2.11.1 Variable load

Variable loading of a bar can be produced for instance by the *bar's own weight effect* when suspended, or by the *bar's own centrifugal force* when revolving.

A) A suspended bar of a uniform cross-sectional area A and length L, made of material having the allowable strength σ_{all} (Fig.2.11.1.1), is subjected to load F (at its free end) and its own weight (represented by the specific weight $\gamma = \rho.g$ obtained as a product of the specific mass ρ and the acceleration of gravity g).

Fig.2.11.1.1

Solution:
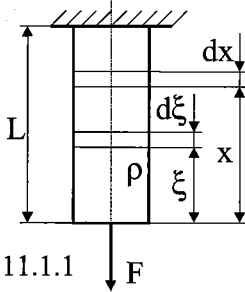
By applying the method of sections on the bar, and starting from the bottom free end, the internal force, at an arbitrary point x of the bar, is found to be

$$N(x) = F + \int_0^x g \cdot \rho \cdot A \cdot d\xi = F + \gamma \cdot A \cdot x$$

where the integral represents the sum of the elemental gravity forces obtained as the product of the specific weight $\gamma = \rho.g$ and the elemental volume $A.d\xi$ at an arbitrary bar point given by the auxiliary coordinate ξ. The second force member in the previous relation can also be obtained when taking the bar volume $V(x) = A.x$ from the free end up to x and multiplying it by $\gamma = \rho.g$. Dividing the internal force by the cross-sectional area A we obtain the stress distribution along the bar (note that the second member representing the stress contributed by the bar weight does not depend on the bar cross-sectional area A) in the form

$$\sigma(x) = \frac{N(x)}{A} = \frac{F}{A} + \gamma \cdot x,$$

which we shall utilize for two important purposes:

a) the strength condition (where $\sigma_{max} = \sigma(x=L)$ is applied):

$$\sigma_{max} = \frac{F}{A} + \gamma \cdot L \leq \sigma_{all}$$

b) the bar deformation can be obtained by applying Eq.(2.5.3) (since the stress is variable along the bar length)

$$\Delta L = \int\limits_0^L \Delta dx = \int\limits_0^L \varepsilon(x)dx = \int\limits_0^L \frac{\sigma(x)}{E}dx = \frac{1}{E}\int\limits_0^L \left(\frac{F}{A}+\gamma\cdot x\right)dx =$$

$$= \frac{FL}{EA} + \frac{\gamma\cdot L^2}{2E} = \frac{FL}{EA} + \frac{GL}{2EA} = \Delta L_F + \Delta L_\gamma$$

(The part of the bar elongation expressed by the second member can be interpreted as $\Delta L_\gamma = (GL)/2EA$ when placing the total weight $G = \gamma.A.L$ in the bar centroid situated at the bar half length).

B) An arm (the dimensions of which are given in Fig.2.11.1.2) rotates with an angle velocity ω
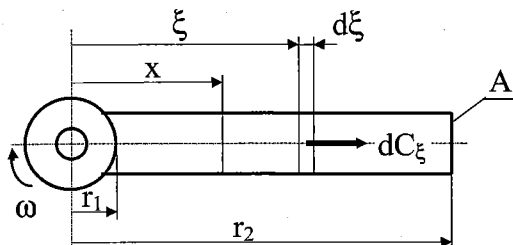
Fig.2.11.1.2

Approach the solution similarly as in the previous case with the main difference that, instead of the arm's own weight, it is the centrifugal force ($C = m.r.\omega^2$) which stresses the member. This is a problem of *centrifugal force* which belongs among problems of *forces of inertia*. Applying *d'Alembert's principle*, we consider forces of inertia as being external forces and then apply the *method of sections*.

Another problem involving centrifugal force is a *revolving ring*:

Assess the stress state arising in a ring revolving (rotating) with an angular velocity ω, Fig.2.11.1.3. The ring is made of material having the specific mass ρ, and its thickness a is much smaller than its radius r. The ring depth is

Fig. 2.11.1.3

denoted b and it cannot be very large, otherwise the ring would pass into a rotating cylinder and axial stress would arise (parallel with the axis of revolution).
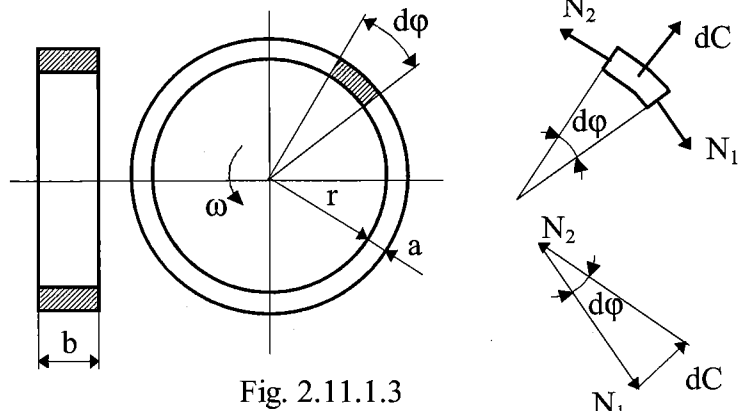
Solution:

Using two radial sections mutually declined about an infinitesimal angle $d\varphi$ we shall obtain a segment, in cross-sections of which internal forces

N_1, N_2 will arise due to the action of centrifugal force

$$dC = dm\cdot r\cdot\omega^2 = r\cdot d\varphi\cdot a\cdot b\cdot\rho\cdot r\cdot\omega^2$$

It follows from the symmetry of the ring that $N_1 = N_2 = N$.

From the element equilibrium we obtain

29

$$dC - 2N \sin\frac{d\varphi}{2} = 0 \qquad \Rightarrow \qquad dC = N \cdot d\varphi$$

(considering that for infinitesimally small angles holds $\sin [(d\varphi)/2] \approx d\varphi/2$)

Thus, in the ring cross-sections, the forces

$$N = \frac{dC}{d\varphi} = a \cdot b \cdot \rho \cdot \left(r^2 \cdot \omega^2\right) = a \cdot b \cdot \rho \cdot v^2$$

are acting, where $v \, [m{\cdot}s^{-1}]$ ... circumferential velocity.

Supposing that there is a uniformly distributed stress in the cross-sections, the circumferential stress is expressed as

$$\sigma = \frac{N}{a \cdot b} = \rho \cdot v^2$$

Denoting the original length of the ring circumference as $c = 2.\pi r,$ the ring circumference will increase, while rotating, to

$$c_\omega = c + \Delta c = 2\pi(r + \Delta r)$$

Expressing the circumferential (or tangent) strain, we obtain

$$\varepsilon_t = \frac{\left(c_\omega - c\right)}{c} = \frac{2\pi(r + \Delta r) - 2\pi r}{2\pi r} = \frac{\Delta r}{r}$$

Thus, we can express the radius increment, caused by the rotation, as

$$\Delta r = \varepsilon_t \cdot r = \frac{\sigma_t}{E} = \frac{\rho v^2}{E}$$

Note that the radius change is computed from the circumferential strain.

2.11.2 Variable cross-section
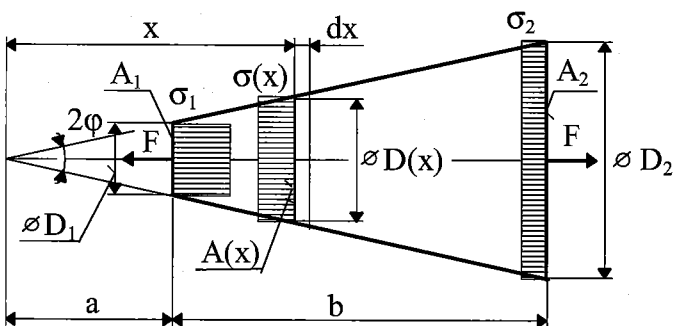
Fig.2.11.2.1

Assess the stress state and deformation of a rod with a variable cross-section (tapered rod) loaded with a constant force F, Fig.2.11.2.1. (If the change in the cross-sectional area is not abrupt (the conicity is moderate), the stress distribution over an arbitrary cross-section x can be considered constant (Fig.2.11.2.1)).

Applying the method of sections we have:

Internal force $\quad N(x) = F$

Stress $\quad \sigma(x) = \dfrac{N(x)}{A(x)} = \dfrac{F \cdot a^2}{A_1 \cdot x^2}$

which was obtained after substitution of the relation for the cross-sectional area *A(x)*, based on the squared ratio of two similar triangles (Fig.2.11.2.1):

$$\left(\frac{D_1}{D(x)}\right)^2 = \left(\frac{a}{x}\right)^2 = \frac{A_1}{A(x)} \quad ; \quad \left(\frac{D_1}{D_2}\right)^2 = \left(\frac{a}{a+b}\right)^2 = \frac{A_1}{A_2}$$

Strength criterion

Deformation $\quad \Delta L = \displaystyle\int_{a}^{a+b} \frac{F \cdot a^2}{E \cdot A_1} \cdot \frac{dx}{x^2} = \frac{F \cdot b}{E \cdot A_1} \cdot \frac{a}{(a+b)} = \frac{F \cdot b}{E \cdot A_1} \cdot \sqrt{\frac{A_1}{A_2}} = \frac{F \cdot b}{E \cdot \sqrt{A_1 \cdot A_2}}$

(With respect to the stress variability along the rod axis, we have applied formula 2.5.3).

Note: The last example summarizes an engineering procedure leading to the results needed when solving statically determinate (SD) structures. This procedure can be written by means of a part of flow diagram, which is explained in Chapter 3. That flow diagram contains 10 items for solving a general structure, both SD and SI (statically indeterminate), from which the last items from 6 to 10 contain:

Item 6) *Assessing internal forces.*

Item 7) *Assessing stresses*

Item 8) *Dimensioning (using a respective **strength criterion**)*

Item 9) *Checking the actual stress distribution (when computing numerical examples)*

Item 10) *Assessing deformation (displacement, stiffness, flexibility)*

2.11.3 Bars (cables) of uniform strength

First consider a long suspended bar, or cable, of uniform cross-sectional area. Such a cable can be, for instance, used as a bearing component for a mine lift (having weight *Q*). Considering the cable alone, loaded due to its own gravity, we shall find a linear stress distribution along its length, with the maximum stress being at the top. It is evident that, for most of the length, the cable carrying capacity is not utilized, and, which is worse, for a very long cable, with the uniform cross-sectional area, it might be impossible to carry any lift cabin at all! A solution can be found in the construction of a so called *cable of uniform strength* having a variable cross-sectional area, Fig.2.11.3.1!
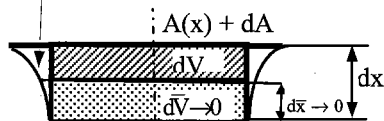
In solving this problem, we shall not use the method of sections, but we shall write the equilibrium equation for a cable element being cut at an arbitrary site x. Drawing the cut-out element, we attach to both cross-sections the allowable stress σ_{all}, and write

$$\sigma_{all} \cdot A(x) - \sigma_{all} \cdot [A(x) + dA(x)] + dG = 0$$

where $dG = A(x) \cdot dx \cdot \rho \cdot g$...own cable element gravity

(ρ...specific mass)

This **superfluous** volume part converges to zero more quickly than $d\overline{V} \to 0$

Then we will find successively the expression for the cross-sectional area change $A(x)$ along the cable length

$$\frac{dA(x)}{A(x)} = \frac{\rho \cdot g}{\sigma_{all}} \cdot dx \Rightarrow$$

$$A(x) = C \cdot e^{[\rho g/\sigma_{all}] \cdot x}$$

Applying the boundary condition for $x = 0$, where $A(x=0) = A_o = Q / \sigma_{all}$, we obtain

$$A(x) = A_o \cdot e^{[\rho g/\sigma_{all}] \cdot x} = \frac{Q}{\sigma_{all}} \cdot e^{[\rho g/\sigma_{all}] \cdot x}$$
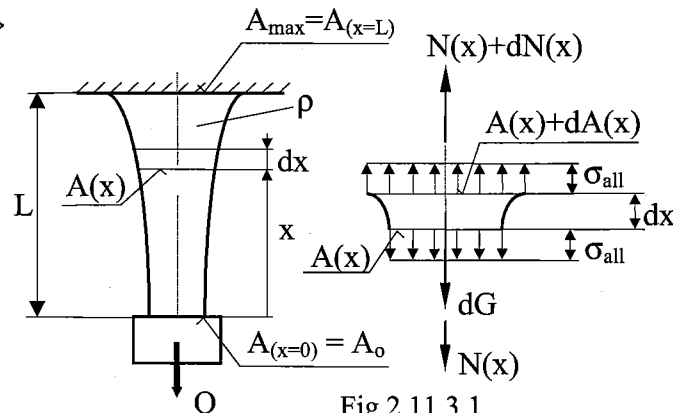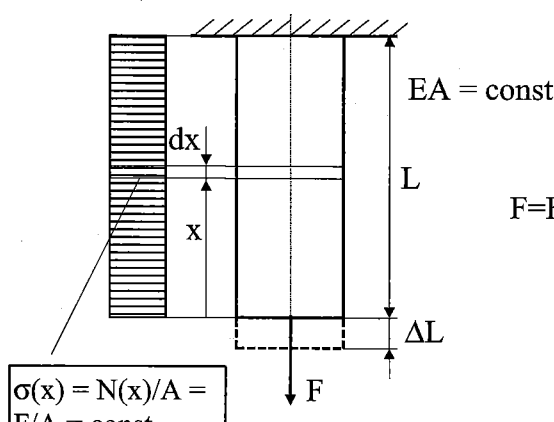
Fig.2.11.3.1
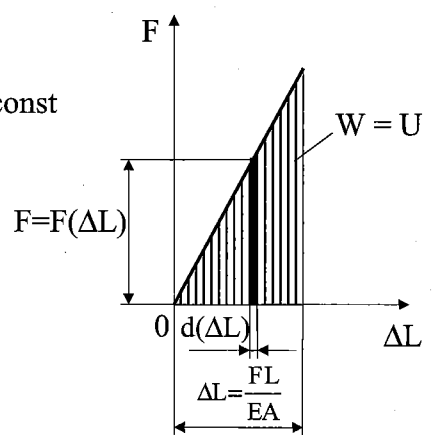
In order to define maximum cross-sectional area A_{max} of the cable, we substitute in this formula $x = L$.

2.12 Strain energy
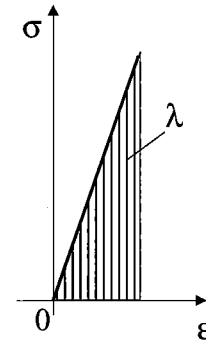
When a slowly increasing axial load F acts upon an elastic body (stressed within the range of Hooke's law) and, subsequently, deforms it, the work W executed by load F is stored within the body (because the kinetic energy can be neglected) in the form of *strain energy* U, i.e., $W = U$. The strain energy is always a scalar quantity.

$\sigma(x) = N(x)/A = F/A = const$

a)

Fig.2.12.1

b)
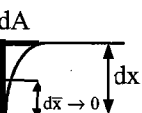
c)

First we will deal with a simple problem in Fig.2.12.1, where the stress is *uniformly* distributed along the rod length. In this case it holds

write the equilibriu
element, we attach
ne part
quickly

dA

dx
$d\bar{x} \to 0$

ange $A(x)$ along t

$N(x)+dN(x)$

$A(x)+dA(x)$

σ_{all}

d
σ_{all}

dG

$N(x)$

.3.1

this formula $x = L$

n the range of Hooke

the body (because t

in energy is always

σ

λ

0

ε

c)

tress is *uniform*

$$\Delta L = \frac{FL}{EA} \Rightarrow F = \frac{EA}{L} \cdot \Delta L \qquad (2.12.1)$$

Let us now consider the work dW done by the load F as the rod elongates by a small amount $d(\Delta L)$. This *elementary work* is equal to the product of the current magnitude F of the load and the corresponding small elongation $d(\Delta L)$. We write

$$dW = F \cdot d(\Delta L)$$

and note that the expression obtained is equal to the element of area of width $d(\Delta L)$ under the load-deformation diagram. The *total work W*, done by the nominal value F of the load as the rod undergoes the total deformation ΔL, is (when substituting for F and ΔL from Eq.2.12.1) thus

$$W = \int_{(L)} F \cdot d(\Delta L) = \int_0^{\Delta L} \frac{EA}{L} \cdot \Delta L \cdot d(\Delta L) = \frac{EA}{L} \cdot \frac{\Delta L^2}{2} = \frac{1}{2} \cdot F \cdot \Delta L \quad \left(= \frac{F^2 \cdot L}{2 \cdot EA} \right) \qquad (2.12.2)$$

and is equal to the area under the load-deformation diagram in Fig.2.12.1, see the vertically hatched area. Since it holds $W = U$, the *total strain energy,* when the stress is uniformly distributed along the bar length (where internal force $N(x) = const, i.e., N = F$), is expressed in the shape

$$U = \frac{F^2 \cdot L}{2 \cdot EA} \left(= \frac{N^2 \cdot L}{2 \cdot EA} \right) , \quad \text{or} \quad U = \frac{\sigma^2}{2E} \cdot AL = \lambda \cdot V \qquad (2.12.3a,b)$$

In Eq. (2.12.3b) we introduced the *strain energy density*
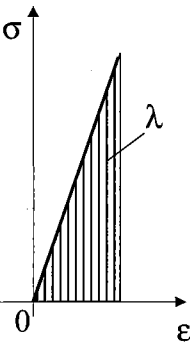
$$\lambda = \frac{U}{V} = \frac{1}{2} \cdot \sigma \cdot \varepsilon = \frac{\sigma^2}{2E} \quad \textbf{per unit volume,} \qquad (2.12.4)$$

which is equal to the area under stress-strain diagram of the material, see Fig.2.12.1c. Eq.(2.12.4), which holds for $\sigma = const,$ can be modified into the form

$$\lambda = \frac{dU}{dV} = \frac{1}{2} \cdot \sigma(x) \cdot \varepsilon(x) = \frac{\sigma^2(x)}{2E} \qquad (2.12.5)$$

in the case of variable stress $\sigma(x)$.

The general formula used for the *total strain energy* expression for an arbitrary axial loading of a bar (resulting in an arbitrary stress distribution along the bar length) can be readily obtained in a similar way (see Eq. 2.12.2), by introducing the corresponding internal force $N(x)$ and finding the strain energy accumulated in an elementary bar length dx as

$$dU = \frac{1}{2} N(x) \cdot \Delta dx , \qquad (2.12.6a)$$

or, based on Eq.(2.12.5), $\quad dU = \lambda \cdot dV = \frac{\sigma^2(x)}{2E} \cdot dV \qquad (2.12.6b)$

After substituting for Δdx from Eq.(2.7.3a) into Eq.(2.12.6a) and integrating along the bar length we have the general formula for the *total strain energy* produced by uniaxial loading as follows

$$U = \frac{1}{2} \int_{(L)} \frac{N^2(x)}{E(x) \cdot A(x)} \cdot dx \qquad (2.12.7a)$$

or we can integrate Eq.(2.12.6b) and obtain (for uniaxial loading)
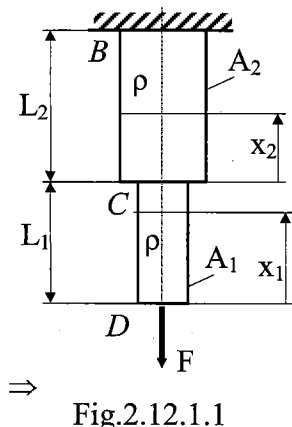
$$U = \int_{(L)} \lambda \cdot dV = \int_{(L)} \frac{\sigma^2(x)}{2E} \cdot A(x) \cdot dx \qquad (2.12.7b)$$

2.12.1 Strain energy stored in rods stressed by various type of loading.

The suspended rod in Fig 2.12.1.1 consists of two portions BC and CD made of the same material, but of different lengths and cross sections. Determine the strain energy of the rod when it is subjected to a centric load F, while also taking into account its own gravity influence (specific mass $\rho \Rightarrow$ specific gravity $\gamma = g\rho$). (We can express the resulting weight of each portion: $G_1 = g\rho.A_1L_1$ and $G_2 = g\rho.A_2L_2$, respectively.)

Solution:

Applying the *method of sections* we have

$$N(x_1) = F + g\rho A_1 x_1$$

$$N(x_2) = F + g\rho A_1 L_1 + g\rho A_2 x_2 = F + G_1 + g\rho A_2 x_2$$

Applying Eq.(2.12.7a), we have the strain energies U_1, U_2 successively for the two portions:

$$U_1 = \frac{1}{2} \int_{(L_1)} \frac{N^2(x_1)}{E \cdot A_1} \cdot dx = \frac{1}{2EA_1} \cdot \int_0^{L_1} (F + g\rho A_1 x_1)^2 dx_1$$

$\Rightarrow$

Fig.2.12.1.1

$$U_1 = \frac{1}{2} \cdot \frac{F^2 L_1}{EA_1} + F \cdot \frac{G_1 L_1}{2EA_1} + \frac{G_1^2 \cdot L_1}{6EA_1} = U_{1F} + F \cdot \Delta L_{1\gamma} + U_{1\gamma} \neq U_{1F} + U_{1\gamma} \qquad *)$$

Analogously

$$U_2 = \frac{1}{2EA_2} \cdot \int_0^{L_2} (F + g\rho A_1 L_1 + g\rho A_2 x_2)^2 dx_2 = \frac{1}{2} \cdot \frac{F^2 L_2}{EA_2} + (F + G_1) \cdot \frac{G_2 L_2}{2EA_2} + \frac{G_2^2 \cdot L_2}{6EA_2}$$

$\Rightarrow$

$$U_2 = U_{2F} + (F + G_1) \cdot \Delta L_{2\gamma} + U_{2\gamma} \neq U_{2F} + U_{2\gamma} \qquad **)$$

where: U_{1F}, U_{2F}, $U_{1\gamma}$, $U_{2\gamma}$ ... the strain energy produced in each portion by singular action of F and the portion's own gravity, respectively;

$\Delta L_{1\gamma}, \Delta L_{2\gamma}$ ... the elongation of each portion caused by the respective own gravity only (cf. Sec.2.11.1).

The total strain energy for the whole rod is

$$U = U_1 + U_2$$

Note: The strain energy formula, Eq.(2.12.4), being a <u>quadratic function with respect to forces</u>, does not allow us to apply the *superposition principle* (cf. Sec.2.10), therefore we cannot obtain the total strain energy of a member by simply adding the partial strain energies produced by single exerted loads, see *) and **) expressions.

2.12.2 <u>Bars stressed by *impact* loading</u>

Another case of strain energy application is when we assess the stress state of a bar hit by a moving object (Fig.2.12.2.1).
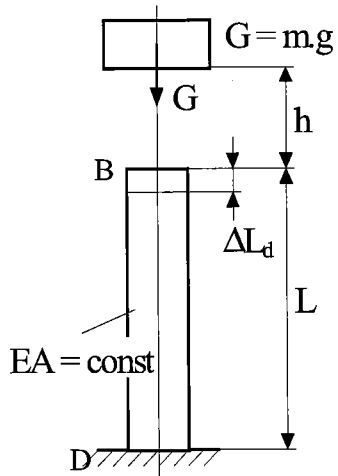
Fig.2.12.2.1

Consider a rod *BD* of uniform cross section which is hit at its end *B* by a body of mass *m*, Fig.2.12.2.1. The mass (a pile driver) being suspended at height *h* above the rod *BC*, has the **potential** *energy*

$$\Delta W_p = mg \cdot (h + \Delta L_d)$$

with respect to the rod end *B*.

As the rod deforms under the impact by ΔL_d, *dynamic stress* develops within the rod and reaches the maximum value σ_d. In the case of uniform rod, the stress σ_d has the same value throughout the rod and we can write the *elongation* (contraction) of the bar *due to dynamic loading* in the form (see Eq.2.7.1*b*)

$$\Delta L_d = \frac{\sigma_d}{E} \cdot L$$

After vibrating for a while, the rod will come to rest and then the *static elongation*

$$\Delta L_{st} = \frac{mg \cdot L}{EA} = \frac{G}{A} \cdot \frac{L}{E} = \sigma_{st} \cdot \frac{L}{E}$$

remains in the rod due to the weight $G = mg$ acting now statically which produces the *static stress* $\sigma_{st} = (G/A)$ in the pile driver. Such sequence of events is referred to as an *impact loading*.

In order to determine the maximum value σ_d of the stress occurring at a given point of a structure subjected to an impact load, we shall make several simplifying assumptions:

First, we shall assume that the *potential* (or *kinetic*) *energy* of the striking body *is transferred entirely to the structure* and, thus, that the strain energy U_d corresponding to the maximum deformation ΔL_d is

$$U_d = \Delta W_p \Rightarrow \frac{1}{2} \cdot \frac{\sigma_d^2}{E} \cdot A \cdot L = mg(h + \Delta L_d) = G\left(h + \frac{\sigma_d \cdot L}{E}\right)$$

This assumption leads to the following two specific requirements:

1. No energy should be dissipated during the impact.

2. The striking body should not bounce off the structure and retain parts of the respective kinetic, or potential, energy. This, in turn, necessitates that the inertia of the structure is negligible, compared to the inertia of the striking body.

Returning to the pile driver and modifying the above obtained quadratic equation, we obtain

$$\sigma_d{}^2 - \sigma_d \cdot 2 \cdot \sigma_{st} - 2 \cdot \sigma_{st} \cdot \frac{E \cdot h}{L} = 0 \, ;$$

and after extracting the roots we shall find that the physically valid root is

$$\sigma_d = \sigma_{st} \left\{ 1 \pm \sqrt{1 + \frac{2EA}{GL} \cdot h} \right\} = \sigma_{st} \cdot k_d \; *)$$

For $h \rightarrow 0$, we obtain an interesting result stating that

$$\sigma_d = 2\sigma_{st}$$

And for $h >> \Delta L_d$, the expression *) can be simplified into the form

$$\sigma_d = \sigma_{st} \sqrt{\frac{2EA}{GL} \cdot h} = \sigma_{st} \cdot k_d \; **)$$

In both expressions *) and **), k_d means the so-called *structure impact coefficient.*

Note: Analogously we can solve a problem of *a mine lift,* which, *after a certain time Δt [s]*

of descending at a constant velocity v, is suddenly stopped.

Given: v = 1 [m/s]... velocity of the cabin

$\Delta t = 1$ [min]... time to the stoppage

$m = 10^3$ [kg]...cabin mass (G = mg [N]...cabin weight);   g = 9.81 [m/s²] ... gravitational acceleration

$\sigma_{all} = 10^8 \left[N / m^2 \right] = 10^2 \left[N / mm^2 \right]$ ... allowable stress of the cable

$E = 2 \cdot 10^{11}$ [N/m² = Pa] = $2 \cdot 10^5$ [N/mm² = MPa] ... Young's modulus of the cable

Additional terms to be considered:
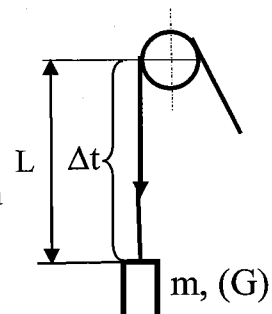
L [m] ... length of the cable, from the wheel to the cabin, when it stopped

A [m²]... cross-sectional area of the cable

U_d [J=kgm²/s²] ... dynamic strain energy stored in the cable just after it has stopped

K [J] ... kinetic energy in the descending (v = const) cabin

k_d [1] ... structure impact coefficient

Solution:

The **lift kinetic energy** is transferred into the strain energy of the cable holding the cabin:

$$U_d = \Delta K \Rightarrow \frac{1}{2} \cdot \frac{\sigma_d^2}{E} \cdot A \cdot L = \frac{mv^2}{2}$$

Modifying the quadratic equation obtained above, we have

$$\sigma_d^2 = \frac{mv^2}{A \cdot L} \cdot E \Rightarrow \sigma_d = v \cdot \sqrt{\frac{m}{A} \cdot \frac{E}{L}} = v \cdot \sqrt{\frac{G}{A \cdot g} \cdot \frac{G}{G} \cdot \frac{A}{A} \cdot \frac{E}{v \cdot \Delta t}} = \sigma_{st} \cdot \sqrt{\frac{v \cdot A \cdot E}{g \cdot G \cdot \Delta t}} = \sigma_{st} \cdot k_d \quad [N/m^2]$$

where $\sigma_{st} = (G/A)$ is the *static stress* and $L = v \cdot \Delta t$ is the *cable length* which, in time Δt, is just unwound and has to absorb the *kinetic energy* ΔK

Static dimensioning

$$\sigma_{st} = \frac{G}{A} = \sigma_{all} \Rightarrow \frac{10^3 \cdot 9.81}{A} \le 10^8 \Rightarrow A \ge 9.81 \cdot 10^{-5} [m^2]$$

$$\left(d = \sqrt{\frac{4A}{\pi}} \ge 0.0112[m] = 11.2[mm] \right)$$

Dynamic dimensioning, where first the dynamic coefficient k_d is to be assessed:

$$k_d = \sqrt{\frac{v \cdot A \cdot E}{g \cdot G \cdot \Delta t}} = \sqrt{\frac{1 \cdot 9.81 \cdot 10^{-5} \cdot 2 \cdot 10^{11}}{9.81 \cdot 9.81 \cdot 10^3 \cdot 60}} = 1.84 \Rightarrow$$

$$\sigma_d = \sigma_{st} \cdot k_d = 1.84 \cdot \sigma_{st}$$

We see that such a lift (having the cabin connected directly with the cable) cannot be operated. What can be done? This machinery needs a flexible element to be installed between the cable and the cabin to absorb the kinetic energy:

$$\Delta K = \frac{m \cdot v^2}{2} = \frac{10^3 \cdot 1}{2} = 5 \cdot 10^2 \left[\frac{kg \cdot m^2}{s^2} = \frac{kg \cdot m}{s^2} \cdot m = N \cdot m = J \right].$$

In **Chapter 8** (Sec. 8.5.2), the deflection of helical springs is discussed. When coming there, we shall design **a helical spring** which can serve for that purpose, i.e., accumulate the lift kinetic energy.

2.13 Castigliano's theorem

Let us consider a general three-dimensional (3D) elastic body loaded by forces $F_1, F_2,..., F_i, ..., F_n$, being in static equilibrium, Fig.2.13.1. We denote with u_i the displacement under force F_i in the direction of F_i, produced by the force system. If we assume that all forces are applied simultaneously and gradually increase from zero to their nominal values, then the work done by the force system is

$$U = \frac{F_1 u_1}{2} + \cdots + \frac{F_i u_i}{2} + \cdots \frac{F_n u_n}{2} = U(F_1 \dots F_i \dots F_n) \quad (2.13.1)$$

(This work is stored within the body as elastic strain energy.)
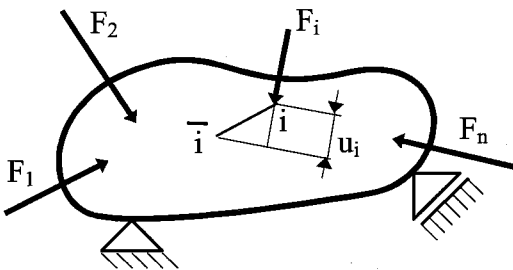
Fig.2.13.1
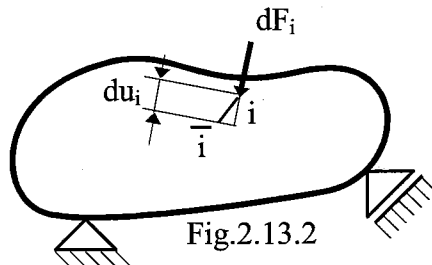
Fig.2.13.2

Let us now increase the *i-th* force by an amount dF_i . This slightly changes both the state of deformation and also the internal strain energy. The increase in the latter is given by

$$dU = \left(\frac{\partial U}{\partial F_i}\right) dF_i$$

Thus the total strain energy after the increase in the *i-th* force is

$$U_1 = U + dU = U + \left(\frac{\partial U}{\partial F_i}\right) dF_i \tag{2.13.2}$$

Let us reconsider this problem by first applying a very small force dF_i alone to the elastic body. Then, we apply the same forces as before, namely, $F_1 ...F_i ...F_n$. Due to the application of dF_i there is a displacement in the direction of dF_i, which is infinitesimal and may be denoted by du_i, producing an infinitesimal strain energy *(1/2) dF_i du_i* , Fig.2.13.2. Now, when $F_1...F_i ...F_n$ are applied their effect on the body will not be changed by the presence of dF_i and the internal strain energy arising from application of $F_1....F_i ...F_n$, will be that indicated in (2.13.1). But as these forces are being applied the small force dF_i goes through the additional displacement u_i caused by the forces $F_1....F_i ...F_n$. Thus, it gives rise to additional work *dF_i u_i* which is stored as internal energy (note that the coefficient 1/2 is now missing since dF_i had already obtained its nominal value) and hence the total strain energy in this case is

$$U_2 = U + dF_i u_i + \frac{dF_i du_i}{2} \tag{2.13.3}$$

Since the final strain energy must be independent of the order in which the forces are applied, we may

equate (2.13.2) and (2.13.3), i.e., $U + \left(\frac{\partial U}{\partial F_i}\right) dF_i = U + dF_i u_i + \underbrace{\frac{dF_i du_i}{2}}_{0}$ resulting in

$$u_i = \frac{\partial U}{\partial F_i} \tag{2.13.4}$$

This is *Castigliano's theorem*, named after the Italian engineer Alberto Castigliano (1847 - 1884) who first stated that *the partial derivative of the total internal strain energy with respect to any external applied force yields the displacement of an elastic body under the point of application of that force in the direction of that force.*

(The term **force** here is used in its most general sense and implies either a true force or a couple. For the case of a *couple*, Castigliano's theorem yields *angular movements* under the point of application of the couple tending in the sense of rotation of the couple (cf. Sec. **bending**))

Note: When solving *statically indeterminate* structures, the so called *Second Castigliano's theorem* can be used, i.e., $u_i = \dfrac{\partial U}{\partial F_i} = 0$, expressing that *the statically indeterminate force makes the structure strain energy to be minimum*. This holds only for non-prestressed structures, cf. Chapter 3, Sec.3.3.

It is important to observe that the above derivation required that we be able to vary the *i-th* force F_i independently of the other forces. Thus, F_i must be statically independent of the other external forces, implying that the energy U must always be expressed in terms of statically independent forces. (Obviously, reactions that can be determined by statics cannot be considered as independent force.)

The simplest application of this theorem is for an axially loaded (by F) prismatic rod (dimensions $A, L;$ material E). Based on the strain energy formula (see Eq.2.12.3) that we assessed for such a rod in Sec.2.12 and applying Eq.(2.13.4), we obtain

$$u_F = \Delta L_F = \frac{\partial U}{\partial F} = \frac{\partial}{\partial F}\left(\frac{F^2 \cdot L}{2 \cdot EA}\right) = \frac{FL}{EA}$$

We will find out that this is the rod elongation ΔL we have already assessed.

Applying the above indicated partial derivative formally to the general expression for strain energy accumulated in a member that is uniaxially loaded (see Eq.2.12.7a), we can write

$$u_i = \frac{\partial U}{\partial F_i} = \frac{\partial}{\partial F_i}\left[\int_{(L)} \frac{N^2(x)}{2 \cdot E(x) \cdot A(x)} dx\right] \qquad (2.13.5)$$

Executing the proposed derivation inside the integral (because the force F - with respect to which we shall differentiate - does not depend on the coordinate x - with respect to which we are to integrate), we obtain

$$u_i = \int_{(L)} \frac{N(x)}{E(x) \cdot A(x)} \cdot \frac{\partial N(x)}{\partial F_i} dx \qquad (2.13.6)$$

The expression (2.13.6), called *Mohr's integral,* will also be applied, in various modifications, to the computations of deformations when other loading types (e.g., torsion, bending) are concerned. (It is highlighted, in formulae (2.13.5) and (2.13.6), that all the quantities might be variables. Subsequently we will not usually do this, with the exception of forces).

Taking into account that the internal force $N(x)$ is a linear function of the external force F_i, then F_i will not appear in the derivative $(\partial N(x)/\partial F_i)$, which is dimensionless. The expression (2.13.6) can be rewritten into the form

$$u_i = \int_{(L)} \frac{N(x)}{EA} \cdot n_i(x) dx \qquad (2.13.7)$$

where: $N(x)$... the internal force acting in the site x, produced by external loading;
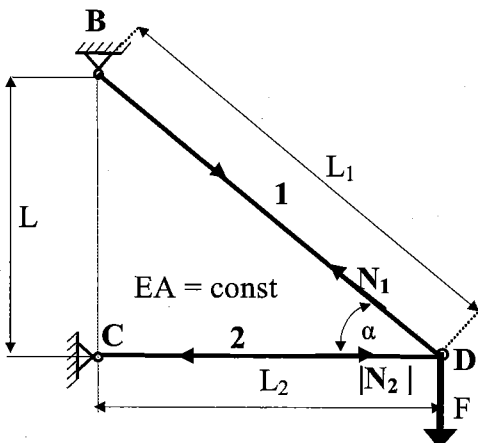
$n_i(x) = (\partial N / \partial F_i)$ ... the internal (dimensionless) force acting in the rod site x, produced by a unit (dimensionless) load applied both in the point and direction of the looked-for displacement

(If the computed displacement has a negative sign, its pointing will be opposite to that of the unitary force.)

Note: The presented *Mohr's integral* (also called "*Unit-load*" method) enables an easy <u>displacement computation</u> even in such cases where <u>no concentrated external force acts. We shall simply put the unit load into the point and direction of the required (computed) displacement</u>. This statement can easily be proved, when, by applying Castigliano's theorem, an imaginative force F is exerted in such a place and, thus, the internal force is expressed as $N = f(F_i, F)$: first executing the derivation $(\partial U / \partial F)$ and then setting $F \to 0$ in the result, it can be found that $(\partial N / \partial F) = n(x)$ also holds, and has the same meaning as stated above.
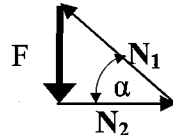
2.14 Complement

Example 2.14.1: The application of the <u>procedure described in the **note** under Sec. 2.11.2</u> when solving a truss.

Solution :

Item 6: Internal forces: $N_1 = F/\sin\alpha$; $|N_2| = F/\tan\alpha$

Int. forces assumption: $N_1 > 0$, $N_2 < 0$, is satisfied
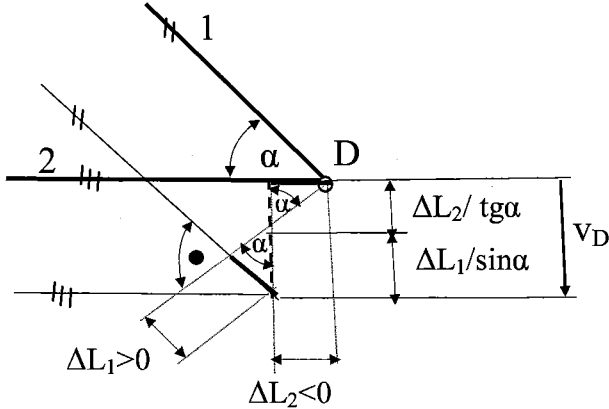
Item 7: Stresses $\sigma_1 = \dfrac{N_1}{A}$; $\sigma_2 = \dfrac{N_2}{A}$

Item 8: Dimensioning $\sigma_1 = \dfrac{N_1}{A} = \dfrac{F}{A \cdot \sin\alpha} \leq \sigma_{all}$ $\quad |\sigma_2| = \dfrac{|N_2|}{A} = \dfrac{F}{A \cdot \tan\alpha} \leq \sigma_{all}$

Item 9: Non-numerical example, i.e., no checking of the resulting stresses values

Item 10: Displacement of the pin D:

    a) **Geometric** approach where a change in angle α is neglected, see the figure below:

$$v_D = \frac{\Delta L_1}{\sin\alpha} + \frac{|\Delta L_2|}{\tan\alpha} = \frac{N_1 \cdot L_1}{EA \cdot \sin\alpha} + \frac{|N_2| \cdot L_2}{EA \cdot \tan\alpha} = \frac{F \cdot L}{EA}\left[\frac{1}{\sin^3\alpha} + \frac{1}{\tan^3\alpha}\right] = \frac{F \cdot L}{EA \cdot \sin^3\alpha}\left[1 + \cos^3\alpha\right] \text{ *)}$$

    b) **Castigliano's theorem** application: (*no figure is necessary*)
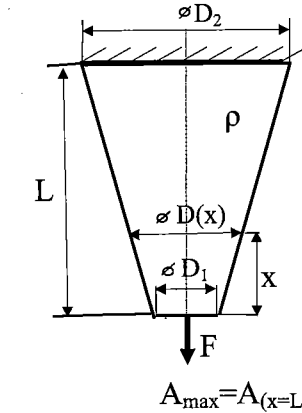
Strain energy for tension-compression $U = \dfrac{1}{2}\sum_i \dfrac{N^2_i \cdot L_i}{E_i \cdot A_i}$ is derived by the vertical concentrated load F exerted at the pin D downwards, which results in the vertical displacement v_D:

$$v_D = \frac{\partial U}{\partial F} = \frac{1}{EA}\sum_{i=1}^{5} N_i \cdot \frac{\partial N_i}{\partial F} \cdot L_i = \frac{1}{EA}\left[\frac{F}{\sin\alpha} \cdot \frac{1}{\sin\alpha} \cdot \frac{L}{\sin\alpha} + \left(-\frac{F}{\tan\alpha}\right)\left(-\frac{1}{\tan\alpha}\right)\frac{L}{\tan\alpha}\right] = \frac{F \cdot L}{EA \cdot \sin^3\alpha}\left[1+\cos^3\alpha\right] > 0$$
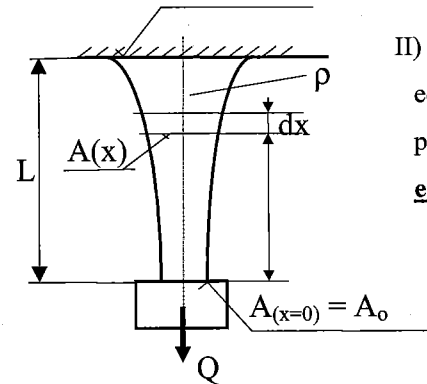
Notice that the vertical displacement v_D is positive, i.e., it has the same sense as the load F and is equal to the result *) above.

Helping remarks:

There are several tasks in Chapter 2 (e.g., 2.11.1 and 2.11.2 compared with 2.11.3) **looking to be solvable by the same approach, but, in reality, they are basically different problems.**
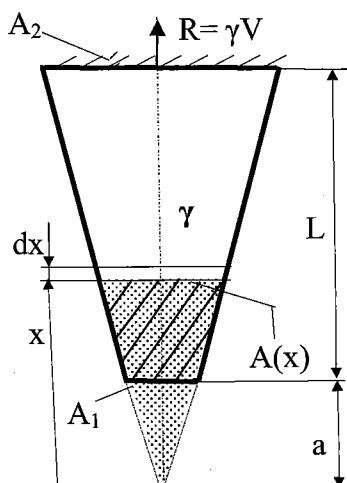
I) When combining a _variable load_ (e.g., own weight) and a _variable cross-section_ (e.g., that of a conical shape) with a rod bearing a load F the solution of such a SD structure is based also on the **method of sections** and the 6 – 10 items of the flow diagram can be applied.

II) _Bars (cables) of uniform strength_ (Sec. 2.11.3), which are based on the equilibrium equation of an element, see Fig.2.11.3.1. When solving this problem, **we shall not use the method of sections, but we shall write the equilibrium equation for a cable element** being cut at an arbitrary site x.

Example 2.14.2: Truncated cone subjected to its own weight

Given: Specific weight ($\gamma = \rho.g$); geometry ($A_2/A_1 = k$, L); material (E, σ_{all}).

Fig.2.14.2.1

Task: The structure solution by using the flow diagram.

Solution:

When using _the similar triangles_ method, we can assess the cross-sectional areas in arbitrary sections (x-position):

$$\left(\frac{D_1}{D(x)}\right)^2 = \left(\frac{a}{x}\right)^2 = \frac{A_1}{A(x)} \Rightarrow \frac{1}{A(x)} = \frac{1}{A_1}\cdot\left(\frac{a}{x}\right)^2;$$

The parameter a depends on the conical bar dimensions:

$$\frac{A_2}{A_1} = \left(\frac{D_2}{D_1}\right)^2 = \left(\frac{a+L}{a}\right)^2,$$

As the rod is SD, we start with *Item 6*:

Item 6: Internal forces are obtained when subtracting the weights of the cone parts graphically denoted in Fig.2.14.2.1:

$$N(x) = G(x) = \gamma \cdot V(x) - \gamma \cdot V(a) = \frac{\gamma}{3}\left[A(x) \cdot x - A_1 \cdot a\right] \Rightarrow$$

Item 7: Normal stress

$$\sigma(x) = \frac{N(x)}{A(x)} = \frac{\gamma}{3} \cdot \left[\frac{A(x)}{A(x)} \cdot x - \overbrace{\frac{1}{A_1} \cdot \left(\frac{a}{x}\right)^2}^{1/A(x)} \cdot A_1 \cdot a\right] = \frac{\gamma}{3}\left[x - \frac{a^3}{x^2}\right],$$

A simple checking: for $x = a$: $\sigma_1 = \frac{\gamma}{3}\left[a - \frac{a^3}{a^2}\right] = 0 \dots$this is correct;

$$\sigma_2 = \frac{\gamma}{3}\left[L + a - \frac{a^3}{(L+a)^2}\right] = \frac{\gamma}{3}\left[\frac{(L+a)^3 - a^3}{(L+a)^2}\right] = \frac{\gamma}{3}\left[\frac{L^3 + 3aL^2 + 3a^2L + a^3 - a^3}{(L+a)^2}\right] =$$

for $x = L+a$:

$$= \frac{\gamma}{3}\left[\frac{L^3 + 3aL^2 + 3a^2L}{(L+a)^2}\right]$$

Item 8: Dimensioning, i.e., $\sigma_{max} = \frac{\gamma}{3}\left[\frac{L^3 + 3aL^2 + 3a^2L}{(L+a)^2}\right] \le \sigma_{all}$

This *strength criterion* can be used for assessing either *the rod material ($\gamma = \rho \cdot g$)*, or *its size*

Item 9: Checking (when solved numerically)

Item10: Deformation

$$\Delta L = \int\limits_a^{L+a} \Delta dx = \int\limits_a^{L+a} \varepsilon(x)dx = \int\limits_a^{L+a} \frac{\sigma(x)}{E}dx = \frac{\gamma}{3E}\int\limits_a^{L+a}\left[x - \frac{a^3}{x^2}\right] \cdot dx =$$

$$= \frac{\gamma}{3E}\left[\frac{x^2}{2} + a^3 \cdot \left(\frac{1}{x}\right)\right]_a^{L+a} = \frac{\gamma}{3E}\left[\frac{(L+a)^2}{2} - \frac{a^2}{2} + a^3\left(\frac{1}{L+a} - \frac{1}{a}\right)\right]$$

Note: Mind that the rod conicity must be moderate (cf. Sec.2.11.2, p.30). When this assumption is not obeyed then this approximate method does not yield suitable results.

3. Statically indeterminate uniaxial problems

3.1 Definition of statically indeterminate structures

In the problems considered in the preceding chapter, we could always use *equilibrium equations* and the *method of sections* to determine the internal forces produced in the various portions of a member under given loading conditions. Such problems are denoted as *statically determinate.*

There are many problems, however, in which the internal forces cannot be determined from statics alone because there are more unknown forces (their number being *n*) acting on a body than there are equations of equilibrium (their number being *r*). Therefore, such cases are known as statically indeterminate problems. The *degree* of the *static indeterminateness* (denoted by *s*) is then given by

$$s = n - r$$

For their solution we shall utilize an advantage of the study of Strength of Materials over the study of Statics, when taking into account the *elasticity* and *deformability* of members, i.e., *the equilibrium equations must be completed by relations involving deformation (*called **deformation conditions** or **compatibility equations**) obtained by considering the geometry of the problem.*

Some examples of SI structures will be undertaken in this chapter.

3.2 General procedure applied when solving statically indeterminate problems

When solving a **statically indeterminate** problem, we can generally proceed as follows:

1) *Find out* whether the structure under consideration is *statically determinate* (SD) or *indeterminate* (SI). For this purpose, we can either use an exact static analysis or a tentative approach. When the structure has been proved to be SI to a certain degree (*s*), the solution procedure will pass to item 2.

2) *Release the structure to the SD state*, i.e., all the superfluous static parameters (supports or members) are to be removed (in the number *s*) and substituted by so-called *SI forces* (or *SI couples* - cf. Secs.8.4 and 12.1), evidently in the number *s*.

3) *Write r equations of static equilibrium* (sometimes this is not necessary in order to determine the internal forces of the undertaken structure, but it serves for the determination of all the reactions in question).
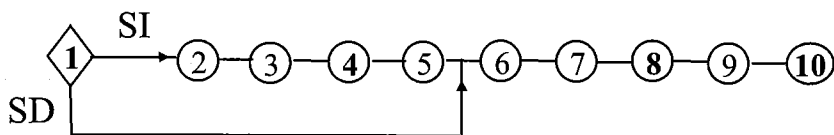
4) *Write s relevant equations of compatibility (or geometric equations, or deformation relations)* which must correspond to the relevant structure localities, i.e., those where the superfluous static parameters have been removed.

5) A*pply constitutive relations (or force-displacement relations)*, i.e., modifications of *Hooke's law*, in order to transform geometric quantities (displacements) into static quantities (forces).

Item *1* is decisive:

a) If the structure is <u>statically indeterminate</u> we proceed through all the following items (*2 ↔ 5*) as long as we assess all unknown (external) forces (including SI forces). <u>Since engineering tasks consist in dimension and deformation assessment of structures</u>, the items applied when solving SD members (cf. Sec.14, where they are denoted as $x + 1$, $x + 2$ ....$x + 5$), are to be added to the above presented procedure (while being denoted by numbers from *6* to *10*, since we have substituted $x = 5$, which expresses the number of the above presented items for the solution of SI forces). It follows from this that altogether <u>ten steps are to be applied when designing a SI structure</u>.

b) If the structure is <u>statically determinate</u> we just jump from the (decisive) step *1* immediately to step *6* and proceed as far as step *10*.

Then, all problems, SD and SI, can be solved by applying the following *flow diagram (chart):*

The most important items (*1, 4, 8* and *10*) are highlighted.

Later examples will show how to handle SI problems.

3.3 Bar attached to rigid supports

A bar *BC* of uniform cross-sectional area A and length L is attached to rigid supports. An axial load F is applied to the bar at a distance L_1 from the left support, Fig.3.3.1. What are the reactions R_B and R_C in the supports?

Proceeding according to Sec.3.2, we have:

ad 1) The case is *statically indeterminate to the first degree* (1° SI) because there are two unknown reactions R_B , R_C and only one equilibrium equation can be written (uniaxial force system).
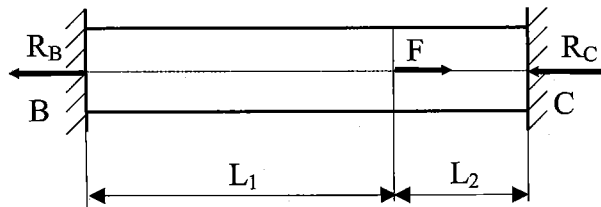
Fig.3.3.1

ad 2) Consider that the bar is cut just to the left of the supporting wall C, the static influence of which is substituted by the *SI force* R_C , Fig.3.3.2 (R_C is now temporarily considered as an *action* while R_B remains all along as a *reaction*).
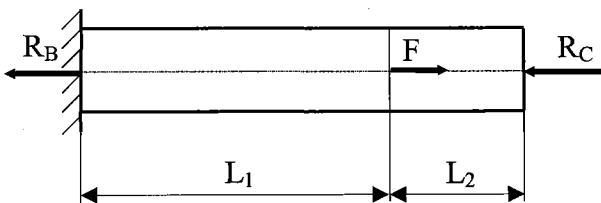
Fig.3.3.2

ad 3)   Equilibrium equation

$$F - R_B - R_C = 0$$

ad 4) The relevant **deformation relation** (*compatibility equation*) is obtained when comparing Fig.3.3.1 and Fig.3.3.2, which results in the requirement for zero displacement of the bar at the released point C, i.e.,

$$\Delta L_C = 0 \ ,$$

where ΔL_C can be decomposed in two ways:

a) **either** as the sum of the elongations (or contractions) of the separate bar fields, which are subjected to their respective internal forces, i.e.,

$$\Delta L_C = \Delta L_1 + \Delta L_2 \ ;$$

b) **or** as the sum of the elongations (or contractions) of the whole bar when applying the *principle of superposition* of the actions exerted separately in their turn on the bar, i.e.,

$$\Delta L_C = \Delta L_F - \left| \Delta L_{R_C} \right| \ ;$$

ad 5) The constitutive equations, i.e., Hooke's law, can be expressed:

ad a) **either**

Fig.3.3.3

45
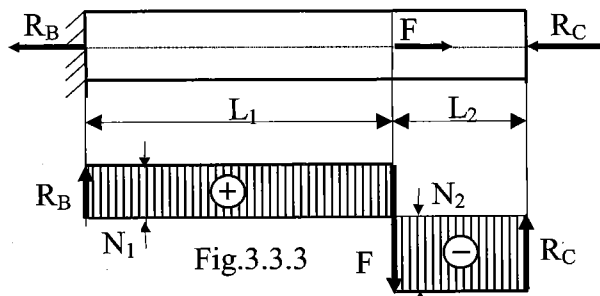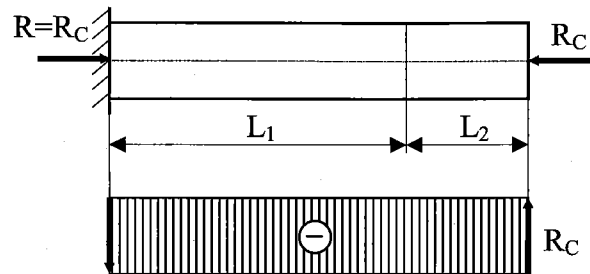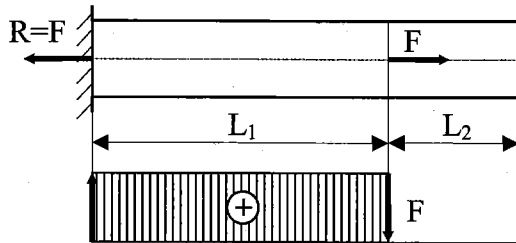
ad b) **or**

$$\Delta L_F = \frac{F \cdot L_1}{EA}$$

$$\left|\Delta L_{R_C}\right| = \frac{R_C \cdot (L_1 + L_2)}{EA}$$

When substituting item 5) into 4), we obtain:

a) **either**
$$\Delta L_1 + \Delta L_2 = \frac{(F - R_C) \cdot L_1}{EA} + \frac{(-R_C) \cdot L_2}{EA}$$

b) **or**
$$\Delta L_F - \left|\Delta L_{R_C}\right| = \frac{F \cdot L_1}{EA} - \frac{R_C \cdot (L_1 + L_2)}{EA}$$

Both presented approaches (ad a/; ad b/) yield the same <u>SI force</u>

$$R_C = F \cdot \frac{L_1}{(L_1 + L_2)}$$

which, after executing the foregoing procedure (resulting in finding one of the two originally unknown reactions R_B , R_C), can finally again be considered as a reaction.

After substituting R_C into item 3) (equilibrium eq.) we obtain the other reaction

$$R_B = F \cdot \frac{L_2}{(L_1 + L_2)}$$

Note: In order to assess the reactions R_B, R_C, it is also possible to apply:
   i) Castigliano's Theorem:
   Based on Fig.3.3.3, we express the strain energy accumulated in the rod

$$U = \frac{1}{2EA}\sum_i N_i^2 \cdot L_i = \frac{1}{2EA}\left[N_1^2 \cdot L_1 + N_2^2 \cdot L_2\right],$$

Second Castigliano's Theorem for SI systems (non-prestressed), cf. p.38, yields
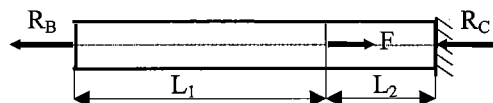
$$\frac{\partial U}{\partial R_C} = 0 \Rightarrow \frac{1}{EA}\left[N_1 \cdot \frac{\partial N_1}{\partial R_C} \cdot L_1 + N_2 \cdot \frac{\partial N_2}{\partial R_C} \cdot L_2\right] =$$

$$= \frac{1}{EA}\left[(F - R_C) \cdot (-1) \cdot L_1 + (-R_C) \cdot (-1) \cdot L_2\right] = 0 \Rightarrow R_C = F \cdot \frac{L_1}{(L_1 + L_2)}$$

   ii) The concept of *flexibility*: $\delta = \frac{\Delta L}{F} \Rightarrow F = \frac{\Delta L}{\delta}$, cf. p.23.

   Based on Fig.3.3.2, where the bar was released at the point *C*, the *compatibility equation* can be expressed as $\Delta L_C = 0 = F \cdot \delta_1 - R_C \cdot (\delta_1 + \delta_2)$ and the SI force R_C is then

$$R_C = F \cdot \frac{\delta_1}{\delta_1 + \delta_2} = F \cdot \frac{\delta_1}{\delta_{total}} = F \cdot \frac{\dfrac{L_1}{EA}}{\dfrac{L_1}{EA} + \dfrac{L_2}{EA}} = F \cdot \frac{L_1}{(L_1 + L_2)}$$, while the reaction R_B can be assessed,

using the same concept, when the bar is released at the other support B, we have

the *compatibility equation* $\Delta L_B = 0 = R_C \cdot (\delta_1 + \delta_2) - F \cdot \delta_2$ and R_C (now the SI force, due to releasing

the support B) is $\quad R_B = F \cdot \dfrac{\delta_2}{\delta_1 + \delta_2} = F \cdot \dfrac{\delta_2}{\delta_{total}} = F \cdot \dfrac{\dfrac{L_2}{EA}}{\dfrac{L_1}{EA} + \dfrac{L_2}{EA}} = F \cdot \dfrac{L_2}{(L_1 + L_2)}$

Summary: This concept of *flexibility* is suitable for structures with *loads in series*, while for structures with *loads in parallel* (e.g., cf. Sec 3.4) the concept of *stiffness* is to apply.

Now we have answered the question asked above: **we know the reactions.**

Items from 6-10 can be executed as follows:

ad 6+7) *Assessment of internal forces + stresses.* (Using the *method of sections*).

- field 1: $\quad N_1(x) = F - R_C = R_B$; $\qquad \sigma_1(x) = \dfrac{N_1(x)}{A} = \dfrac{R_B}{A} = \dfrac{F \cdot L_2}{A \cdot (L_1 + L_2)}$ ...*tension*

- field 2: $\quad N_2(x) = -R_C$; $\qquad \sigma_2(x) = \dfrac{N_2(x)}{A} = -\dfrac{R_C}{A} = -\dfrac{F \cdot L_1}{A \cdot (L_1 + L_2)}$ ...*compression*

Considering $L_1 > L_2$, we shall determine $\quad |\sigma|_{max} = |\sigma|_2 = \dfrac{F \cdot L_1}{A \cdot (L_1 + L_2)}$

ad 8) *Dimensioning* (using the **strength criterion**)

$$|\sigma|_{max} = |\sigma|_2 = \frac{F \cdot L_1}{A \cdot (L_1 + L_2)} \leq \sigma_{all}$$

Knowing, for instance, the cross-sectional area *A* we can assess the allowable load

$$F \leq F_{all} = A \cdot \sigma_{all} \cdot \frac{L_1 + L_2}{L_1}$$

ad 9) *Checking the actual stress distribution*

If we had carried out the computation numerically, we should have checked the actual stress distribution along the bar axis.

Ad 10) *Displacement (deformation, stiffness, flexibility) assessment*

Let us assess the displacement of the bar site where load F is applied with respect to clamping B (i.e., the deformation ΔL_{BF} of the left part of the bar).

To solve this task we shall take into consideration only the *BF* part of the bar being subjected to the tensile load $F - R_C = R_B$. From this follows the displacement

$$\Delta L_{BF} = \frac{F \cdot L_1 \cdot L_2}{EA \cdot (L_1 + L_2)} > 0 \quad ...elongation.$$

The same result (numerically) - but with the opposite sign - will be obtained if we consider the right *FC* part of the bar

$$\Delta L_{FC} = -\frac{F \cdot L_1 \cdot L_2}{EA \cdot (L_1 + L_2)} < 0 ...contraction \Rightarrow |\Delta L_{FC}| = \Delta L_{BF} = \Delta L_F$$

From the displacement ΔL_F we can obtain, for instance, the *flexibility* of this structure with respect to the site of the application of load *F*

$$\delta_F = \frac{\Delta L_F}{F} = \frac{L_1 \cdot L_2}{EA \cdot (L_1 + L_2)} \quad [mm \cdot N^{-1}] ;$$
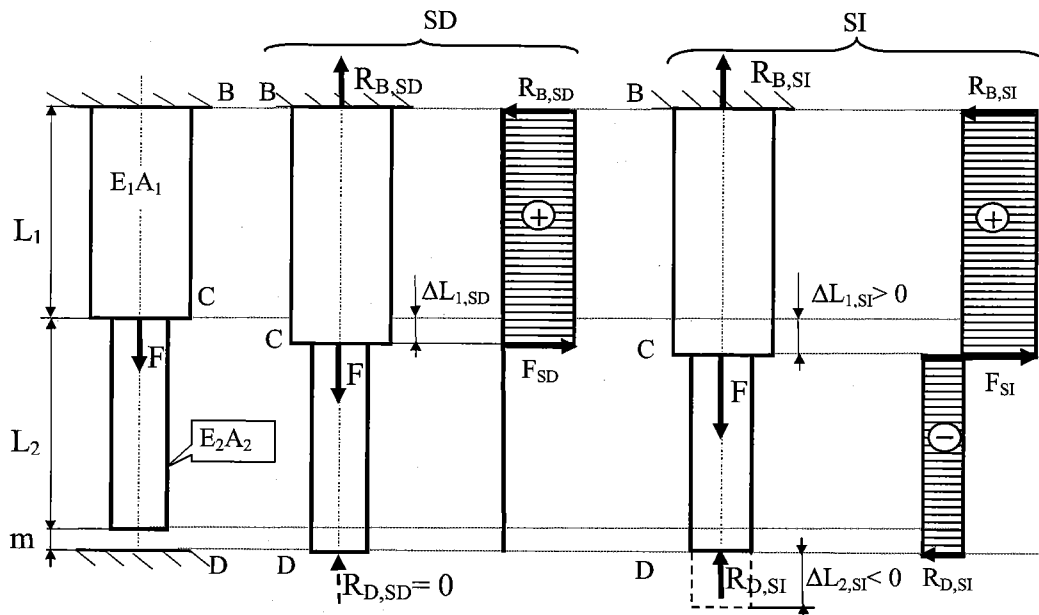
and the *stiffness* with respect to the same point

$$k_F = \frac{1}{\delta_F} = \frac{F}{\Delta L_F} = \frac{EA \cdot (L_1 + L_2)}{L_1 \cdot L_2} \quad [N \cdot mm^{-1}]$$

Example 3.3.1: A bar of two parts *BC* and *CB*, having different cross-sections and materials, is attached to the rigid support *B* and have the gap $m << L_1, L_2$ to the rigid support *D*.

Execute a discussion about the load *F* values causing the bar to be:

i) SD, i.e., $F \le F_{SD}$; ii) SI i.e., $F \ge F_{SD}$, while obeying the *strength criterion* $|\sigma|_{max} \le \sigma_{all}$

Solution: (we will apply the concept of *flexibility,* cf. Sec. 3.3)

ad i) <u>SD force assessing</u>: $\Delta L_D = m = F \cdot \delta_1 \Rightarrow F_{SD} = \dfrac{m}{\delta_1} = \dfrac{m \cdot E_1 \cdot A_1}{L_1}$

ad ii) <u>SI force assessing</u>:

compatibility eq. . $\Delta L_D = m = F \cdot \delta_1 - R_D \cdot (\delta_1 + \delta_2)$, equilibrium eq... $F - R_B - R_D = 0$

Reactions:... $R_C = F \cdot \dfrac{\delta_1}{\delta_1 + \delta_2} - \dfrac{m}{\delta_1 + \delta_2} = F \cdot \dfrac{\dfrac{L_1}{E_1 A_1}}{\dfrac{L_1}{E_1 A_1} + \dfrac{L_2}{E_2 A_2}} - \dfrac{m}{\dfrac{L_1}{E_1 A_1} + \dfrac{L_2}{E_2 A_2}}$; $R_B = F \cdot \dfrac{\delta_2}{\delta_1 + \delta_2} + \dfrac{m}{\delta_1 + \delta_2}$

Strength criterion: $|\sigma|_{max} = \max\left(\dfrac{R_B}{A_1}; \left|\dfrac{R_D}{A_2}\right|\right) \le \sigma_{all}$

3.4 Parallel members connected with a rigid plate

Consider a steel tube surrounding a solid aluminum cylinder, the assembly being compressed between infinitely rigid cover plates by centrally applied forces, as shown in Fig.3.4.1. Assess the stresses σ_{St}, σ_{Al}, in the two members, respectively.
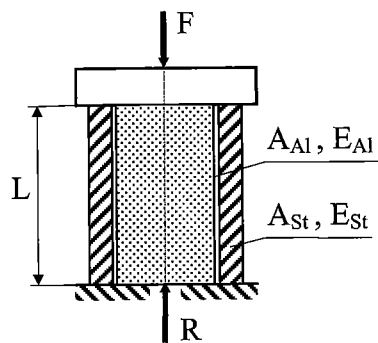
Fig.3.4.1

Solution: We can proceed according to the items given in Sec.3.1:
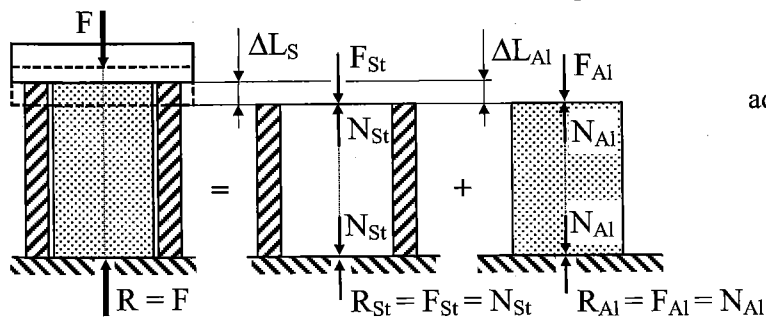
ad 1) In order to answer the problem, we must assess the decomposition of load F into <u>two portions</u> F_{St} , F_{Al} , which stress the steel and aluminum members with the internal forces N_{St} , N_{Al} , respectively (see Fig.3.4.2). As all forces exerting in this structure are collinear, only <u>one equilibrium equation</u> ($F - R = 0$) can be written, confirming that the case is *SI to the first degree.*

ad 2) Since this structure has no redundant support parameters, it is not necessary to release the structure to the SD state (and then introduce the respective SI force), according to item 2 (cf. Sec.3.1).

ad 3) The static equation can be written in the form

$$F - N_{St} - N_{Al} = 0$$

ad 4) The necessary relation between the displacements of the members is based on a kinematically admissible deformation of the structure, Fig.3.4.2. Thus, the deformation condition is

$$\left|\Delta L_{St}\right| = \left|\Delta L_{Al}\right|$$

ad 5) Applying Hooke's law we have

$$\left|\Delta L_{St}\right| = \frac{N_{St} \cdot L}{E_{St} \cdot A_{St}}$$

$$\left|\Delta L_{Al}\right| = \frac{N_{Al} \cdot L}{E_{Al} \cdot A_{Al}}$$

Fig.3.4.2

Substituting item 5) into item 4) we obtain $\quad N_{St} = N_{Al} \cdot \dfrac{E_{St} \cdot A_{St}}{E_{Al} \cdot A_{Al}} \quad *)$

The relation *), when combined with item 3), yields

$$N_{Al} = F \cdot \frac{E_{Al} \cdot A_{Al}}{E_{Al} \cdot A_{Al} + E_{St} \cdot A_{St}} > 0 \quad \text{and analogously} \quad N_{St} = F \cdot \frac{E_{St} \cdot A_{St}}{E_{Al} \cdot A_{Al} + E_{St} \cdot A_{St}} > 0$$

The positive signs confirm that the internal forces were correctly assumed as compressive. After dividing the internal forces obtained in this way by the respective cross-sectional areas we will have stresses in both portions, respectively, as follows:

$$\sigma_{Al} = -\frac{N_{Al}}{A_{Al}} = -\frac{F}{A_{Al}} \cdot \frac{E_{Al} \cdot A_{Al}}{E_{Al} \cdot A_{Al} + E_{St} \cdot A_{St}} ; \; \sigma_{St} = -\frac{N_{St}}{A_{St}} = -\frac{F}{A_{St}} \cdot \frac{E_{St} \cdot A_{St}}{E_{Al} \cdot A_{Al} + E_{St} \cdot A_{St}}$$

We have had to add negative signs to the resulting <u>compressive</u> stresses in accordance with the sign convention (cf. Sec.2.3).

Important note:

Using the concept of **_stiffness_** for expressing internal forces we have, after rearranging them and simplified subscripts (Al = 1, St = 2)

$$N_1 = F \cdot \frac{\dfrac{E_1 \cdot A_1}{L_1}}{\dfrac{E_1 \cdot A_1}{L_1} + \dfrac{E_2 \cdot A_2}{L_2}} = F \frac{k_1}{k_1 + k_2} > 0 \; ; \; N_2 = F \cdot \frac{\dfrac{E_2 \cdot A_2}{L_2}}{\dfrac{E_1 \cdot A_1}{L_1} + \dfrac{E_2 \cdot A_2}{L_2}} = F \frac{k_2}{k_1 + k_2} > 0$$

When expressing the internal forces of structure members by using these stiffness symbols for a generalized structure of **_n_** parallel members, i.e.,

$$N_1 = F \frac{k_1}{k_1 + k_2 + ...k_n} > 0, \;......\; N_n = F \frac{k_n}{k_1 + k_2 + ...k_n} > 0, \text{ etc.}$$

Now, when looking at the compatibility eq., (i.e., item 4), and Fig.3.4.2, we estimate that also a structure of **_n_** parallel members deforms about the same value as each of its components themselves, i.e.,

$$\Delta L = \Delta L_1 = \Delta L_2 = ...\Delta L_n$$

When expressing

$$\Delta L = \frac{F}{k_{total}} = \frac{N_1 + N_2 + ...N_n}{k_{total}} ; \quad \Delta L_1 = \frac{N_1}{k_1}; \quad \Delta L_2 = \frac{N_2}{k_2}; ...\Delta L_n = \frac{N_n}{k_n} ,$$

we have

$$\frac{N_1 + N_2 + ...N_n}{k_{total}} = \frac{N_1}{k_1} + \frac{N_2}{k_2}...\frac{N_n}{k_n} \Rightarrow k_{total} = k_1 + k_2 + ... + k_n .$$

We see that **the total stiffness** of a structure with parallel members **equals to the <u>sum</u> of its components stiffnesses** (i.e., an analogy with **_parallel capacities in electricity_**).

Conclusion:
Utilizing this characteristic, **we can solve internal forces and deformations of other structures having parallel members of different type of design and loading**, e.g., torsion of parallel shafts or loading parallel springs of various designs. (See Chapter 5: <u>Torsion of Circular Shafts</u> where two parallel problems will be solved: _Example 8.4.2 Shaft of two material_ and _8.5.4 Springs in parallel_)

3.5 Pin-connected framework

A vertical load F is supported by a statically indeterminate pin-connected framework (Fig.3.5.1). All bars are made of the same material (modulus of elasticity E) and have the same cross-sectional area A. Determine the internal forces in the bars of the framework. Determine the displacement v_M.
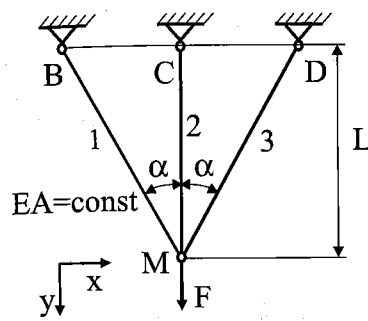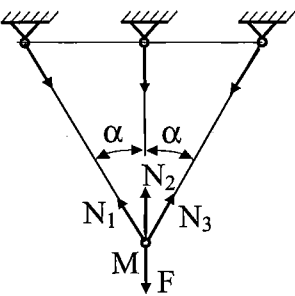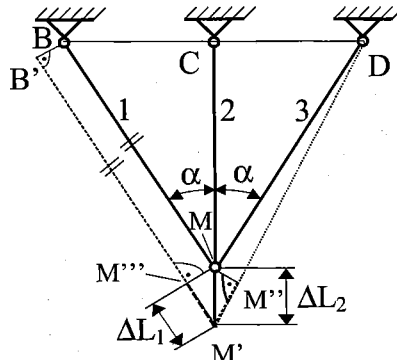
Fig.3.5.1   Fig.3.5.2   Fig.3.5.3

Observing the SI procedure items (cf. Sec.3.2), we will proceed freely without marking them numerically. Assuming that the <u>tensile</u> (arrows facing each other) internal forces N_1, N_2, N_3 (**which are not in series as in Sec.3.3**) exerting in the framework rods in the pin M balance the load F, Fig.3.5.2, we can write two component equations of static equilibrium in the horizontal and vertical directions, respectively, as follows:

$$N_1 \cdot \sin\alpha - N_3 \cdot \sin\alpha = 0 ; \qquad F - N_1 \cdot \cos\alpha - N_2 - N_3 \cdot \cos\alpha = 0 \qquad (3.5.1a)$$

The former equation states that $N_1 = N_3 = N$ which could be obtained immediately as a consequence of the vertical symmetry of the framework. Substituting this equality into the latter expression we have

$$F - 2 \cdot (N \cdot \cos\alpha) - N_2 = 0 \qquad (3.5.1b)$$

Consulting these two sets of static relations (in set (3.5.1a) we have three unknown internal forces and only two equilibrium equations; in Eq.(3.5.1b) there are two unknown internal forces and only one equilibrium equation) it is evident that in each case always one equation is missing, i.e., the framework is *SI to the first degree.*

A *supplementary equation,* i.e., *deformation relation,* **is established from consideration of the kinematically possible deformation** (Fig.**3.5.3**), which is used **instead of releasing the SI structure,** as applied in Sec.3.3 - i.e., see item 2 of the flow diagram in Sec.3.2 and its application in Sec.3.3.. The deformed structure is shown in Fig.3.5.3 either by the dashed line $B'M'''$ or by the dotted line DM''. The dotted line to the right shows an actual deformation of a lateral rod (3 or 1). Because of the smallness of the deformations being considered, the arc MM'' with the center at D can be replaced by

a normal to $B'M''$ and the change in the angle α can be neglected, i.e., it holds $MM'M'' \approx \alpha$. It follows from that the elongation of the bar 3 (or 1) is $M'M'' = \Delta L_3 \, (= \Delta L_1)$.

(The same effect can be obtained when, neglecting the change in the angle α, a parallel line is drawn with a lateral rod (see the dashed line $B'M'$ to the left in Fig.3.5.3) and its original length BM is compared with the parallel line $B'M'$ (representing the deformed state)).

Thus, outgoing from the right-angled triangle $MM'M''$,Fig.3.5.3, the compatibility of the displacements (*deformation relation*) is then expressed in the form

$$\Delta L_1 = \Delta L_2 \cdot \cos\alpha \tag{3.5.2}$$

The respective constitutive equations are

$$\Delta L_1 = \frac{N_1 \cdot L}{EA \cdot \cos\alpha} ; \qquad \Delta L_2 = \frac{N_2 \cdot L}{EA} \tag{3.5.3}$$

Combining the last three expressions we have

$$\frac{N_1 \cdot L}{EA \cdot \cos\alpha} = \frac{N_2 \cdot L}{EA} \cdot \cos\alpha \quad \Rightarrow \quad N_1 = N_2 \cdot \cos^2\alpha = N_3 = N \tag{3.5.4}$$

Substituting Eq.(3.5.4) into Eq.(3.5.1a) or Eq. (3.5.1b) we obtain the internal forces in the rods as follows:

$$N_1 = F \cdot \frac{\cos^2\alpha}{1 + 2\cos^3\alpha} = N_3 = N ; \qquad N_2 = F \cdot \frac{1}{1 + 2\cos^3\alpha} \tag{3.5.5}$$

The forces have positive signs, which confirms that our assumption was correct and the framework members are stressed in tension.

The displacement v_M of the pin M in the vertical direction y can be obtained from the central bar CM elongation, i.e.,

$$v_M = \Delta L_2 = \frac{N_2 \cdot L}{EA} = \frac{F \cdot L}{EA} \cdot \frac{1}{1 + 2\cos^3\alpha}$$

3.6 Problems involving temperature changes

All of the members and structures that we have considered so far were assumed to remain at the same temperature while they were being loaded. We shall now consider various situations involving changes in temperature.

Let us first consider a homogeneous rod of uniform cross-section and length L, which rests freely on a smooth horizontal surface. If the temperature of the rod is raised by Δt, we observe that the rod

elongates by an amount ΔL_t , which is proportional to both the temperature change Δt and length L of the rod. We have

$$\Delta L_t = \alpha \cdot \Delta t \cdot L \qquad (3.6.1)$$

where α is a constant characteristic of the material, called the *coefficient of thermal expansion*. Since ΔL_t and L are both expressed in units of length, α represents a quantity *per degree C (Celsius or Centigrade)*. With the elongation ΔL_t there must be an associated strain

$$\varepsilon_t = \frac{\Delta L_t}{L} = \alpha \cdot \Delta t \qquad (3.6.2)$$

This strain is referred to as a *thermal strain* because it is caused by the change in temperature of the rod. In the **SD** case there is no stress associated with the strain ε_t.

Let us consider a bar being clamped at a temperature t_o between two rigid walls, Fig.3.6.1. At temperature t_o the rod is stress free in the configuration shown. Determine the stress in the rod when the temperature has dropped to t_l. We know from Sec.3.3 that such a case is *SI to the first degree* .

Fig.3.6.1

$$\Delta L_{R_C} = |\Delta L_t|$$
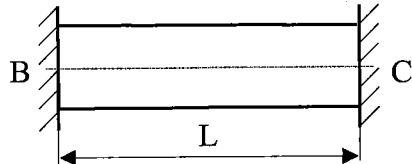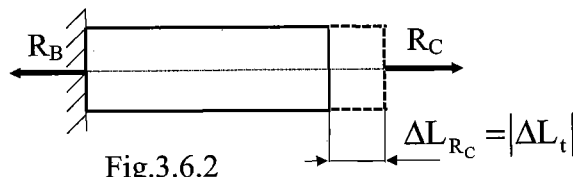
Fig.3.6.2

One approach to this problem is to assume that the bar is cut free from the wall at the right end, Fig.3.6.2. In that event it is free to contract when the temperature falls by about

$$|\Delta t| = t_0 - t_1$$

and the bar shortens by an amount ΔL_t.

It is next necessary to find the statically indeterminate axial force R_C that must be applied to the bar to stretch it ΔL_{R_C} to restore the right end to its original position. Shortly, after carrying out

- static equilibrium equation $\qquad R_B - R_C = 0 \Rightarrow R_B = R_C = R$

- deformation condition $\qquad \Delta L_C = 0 \Rightarrow \Delta L_{R_C} = |\Delta L_t|$

- constitutive and physical relations $\quad \Delta L_{R_C} = \dfrac{R_C \cdot L}{EA}$ and Eq.(3.6.1), i.e., $|\Delta L_t| = \alpha \cdot |\Delta t| \cdot L$

and combining these expressions we have thermal stress

$$\sigma = \frac{R_C}{A} = E \cdot \alpha \cdot |\Delta t|$$

which depends neither on the cross-sectional area A nor on the length L of the bar, and thus can be influenced only by the temperature difference Δt .

3.7 Various types of statically indeterminate structures composed of uniaxially stressed members

3.7.1 Structures having geometric defects due to manufacturing inaccuracy
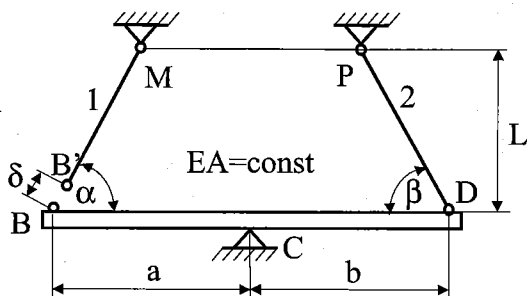
Fig.3.7.1.1

A swinging horizontal rigid bar BD is pinned at point C and is intended to be supported by two wires (1 and 2) at points B and D (Fig.3.7.1.1). However, wire 1 was manufactured a bit shorter (having the length $B'M$) than it should have been. Thus, when mounting (assembling) the structure, a small gap δ appeared between the hinges B and B'.

Determine the stress arising in the two wires after a forced junction of the hinges B and B'.
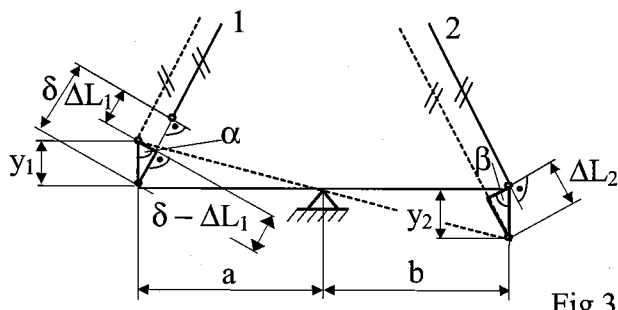
Solution:

When the structure is assembled, two tensile forces, N_1 and N_2 respectively, arise in the wires. If we are not interested in the reaction produced at support C, there is only one static equilibrium equation - moments taken about point C, i.e.,

$$N_1 \cdot \sin\alpha \cdot a - N_2 \cdot \sin\beta \cdot b = 0 \qquad (3.7.1.1)$$

from which it follows that the structure is *SI to the first degree.*

To obtain the required deformation condition, a relevant, kinematically admissible, deformation of the structure has to be assessed (cf. Sec.3.5), as shown in Fig.3.7.1.2. Based on this picture, we can successively find out

$$y_1 = \frac{\delta - \Delta L_1}{\sin\alpha}; \ y_2 = \frac{\Delta L_2}{\sin\beta}; \ \frac{y_1}{a} = \frac{y_2}{b}$$

Fig.3.7.1.2

from which the deformation (compatibility) relation can be expressed in the form

$$\frac{\delta - \Delta L_1}{a \cdot \sin\alpha} = \frac{\Delta L_2}{b \cdot \sin\beta} \qquad (3.7.1.2)$$

Constitutive relations are easy to assess by applying Hooke's law as follows

$$\Delta L_1 = \frac{N_1 \cdot L/\sin\alpha}{EA} \quad (3.7.1.3a) \qquad \Delta L_2 = \frac{N_2 \cdot L/\sin\beta}{EA} \quad (3.7.1.3b)$$

Note that the gap $\delta \ll L_1$, and therefore it does not appear in Eq.(3.7.1.3a), which expresses the elongation of the wire 1, since in engineering practice, it is neglected with respect to the bar length in algebraic sums, i.e. $L_1 + \delta \approx L_1$. Combining all the presented relations, we finally have:

$$N_1 = \delta EA \cdot \frac{b^2 \cdot \sin\alpha \cdot \sin^3\beta}{a^2 L \cdot \sin^3\alpha + b^2 L \cdot \sin^3\beta} ; \quad N_2 = \delta EA \cdot \frac{ab \cdot \sin^2\alpha \cdot \sin^2\beta}{a^2 L \cdot \sin^3\alpha + b^2 L \cdot \sin^3\beta}$$

3.7.2 <u>Statically indeterminate structure to the *second* degree with a *temperature* influence</u>

A bar BC is considered to be absolutely rigid and is horizontal before load F is applied at C as shown in Fig.3.7.2.1. The connection at B is a pin, and BC is supported by two vertical rods MN and KD of length L and an inclined rod ND. All the rods have the same cross-sectional area A and are made of the same material (modulus of elasticity E). The rod KD has been heated, i.e. $\Delta t_3 > 0$, after the assembly of the structure. Find the resulting internal forces in the bars.
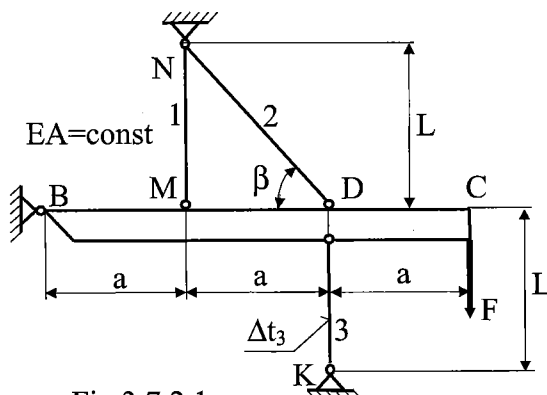
Fig.3.7.2.1
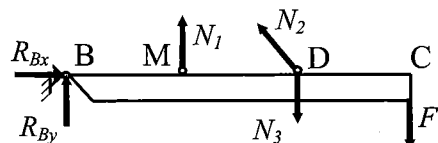
Fig.3.7.2.2
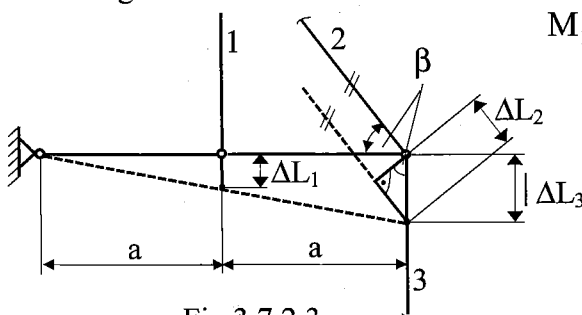
Fig.3.7.2.3

Solution:

From the free-body diagram in Fig.3.7.2.2 it is evident that there are <u>five unknown forces</u> N_1, N_2, N_3, R_{bx}, R_{by} while only <u>three static equilibrium equations</u> are available, i.e., the structure is <u>SI to the second degree</u> (or, taking into account that the task is to determine the internal forces in the bars, we can <u>only sum the moments about B</u>, while having <u>three unknown forces N_1, N_2, N_3</u>).

Choosing the latter possibility and assuming tensile forces being exerted in the rods we have

$$M_B = F \cdot 3a + N_3 \cdot 2a - N_2 \cdot \sin\beta \cdot 2a - N_1 \cdot a = 0$$

The structure being SI to the second degree we have to write two compatibility relations (see Fig.3.7.2.3):

a) $\Delta L_2 = |\Delta L_3| \cdot \sin\beta \quad (= -\Delta L_3 \cdot \sin\beta)$
b) $\dfrac{\Delta L_1}{a} = \dfrac{|\Delta L_3|}{2a} \quad \left(= -\dfrac{\Delta L_3}{2a}\right)$

Constitutive equations:

$$\Delta L_1 = \frac{N_1 \cdot L}{EA} \quad ; \quad \Delta L_2 = \frac{N_2 \cdot L / \sin\beta}{EA} \quad ; \quad \Delta L_3 = \frac{N_3 \cdot L}{EA} + \alpha \cdot \Delta t_3 \cdot L < 0$$

(The latter deformation ΔL_3 is negative according to the kinematically possible deformation of the structure shown in Fig.3.7.2.3, where we assume a shortening of the rod KD).

After executing all necessary algebraic operations we obtain the internal forces in the rods as follows:

$$N_1 = \frac{3F - 2\alpha \cdot \Delta t_3 \cdot EA}{5 + 4 \cdot \sin^3\beta}; \qquad N_2 = \frac{3F - 2\alpha \cdot \Delta t_3 \cdot EA}{5 + 4 \cdot \sin^3\beta} \cdot 2 \cdot \sin^2\beta$$

$$N_3 = -\frac{6F + \alpha \cdot \Delta t_3 \cdot EA(1 + 4 \cdot \sin^3\beta)}{5 + 4 \cdot \sin^3\beta}$$

The forces N_1, N_2 are positive (i.e., tensile) only when the following relation between the load F and the heating Δt_3 holds:

$$F \geq \frac{2}{3} \cdot \alpha \cdot EA \cdot \Delta t_3 .$$

The force N_3 was determined as negative, i.e., compressive, always when $\Delta t_3 > 0$ (i.e., the rod 3 is heated).

3.7.3 Additional examples:

Example 3.7.3.1 Statically indeterminate structure to the *second* degree with a *temperature* influence (cf. Sec. 3.7.2 , p.48) solved by *Castigliano's Theorem*

A complete *(slightly modified)* **flow diagram** *(cf. p.43)* is applied: i.e., all the necessary parameters of a structure are obtained: i) dimensions and ii) allowable load.

Solution:
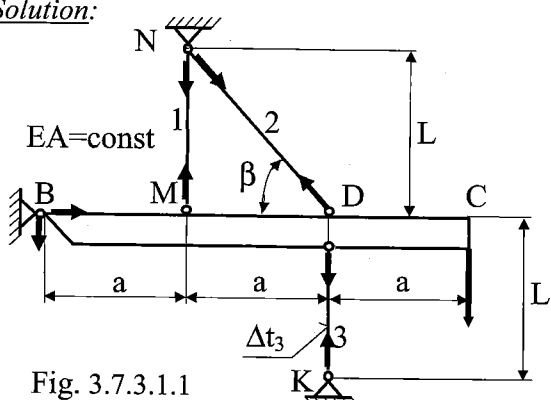
Fig. 3.7.3.1.1

Item 1: SI assessment:

As being interested only in internal forces N_1, N_2, N_3, we have:

3 unknowns and

1 equilibrium equation available (the moment about point B),

i.e., the structure is **SI 2°**

Item **2: The structure is to be released to obtain a SD basic system:**

Two of the three rods shall be chosen to be cut:

As there is a prestressed structure— due to the rod 3 heating —one of the cut rods has to be rod 3, the other cut rod can be either rod 1 or rod 2. Their internal forces N_2 and N_3 will be substituted by statically indeterminate forces N_2, N_3 (usually denoted X_2, X_3), respectively.
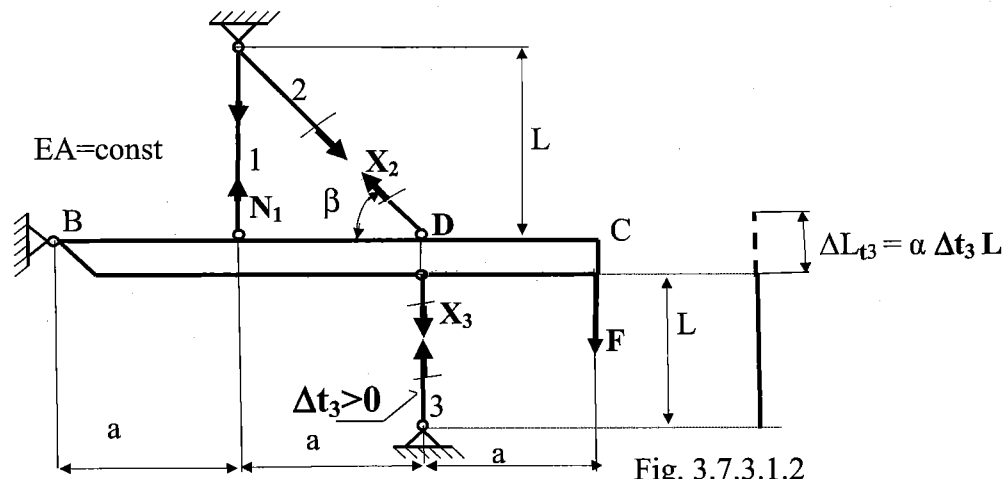
Fig. 3.7.3.1.2

Item **3: Equilibrium equations**

If the values of reactions in the pin B are not requested, only *the moment equilibrium equation about B is necessary*:

$$M_B = F \cdot 3a + X_3 \cdot 2a - X_2 \cdot \sin\beta \cdot 2a - N_1 \cdot a = 0 \Rightarrow$$

$$N_1 = 3F + 2X_3 - 2X_2 \cdot \sin\beta$$

*)

Item **4: Compatibility equations** (*CE 1, 2*) will be expressed by means of *Castigliano's Theorem*:

1) $\dfrac{\partial U}{\partial X_2} = 0$
2) $\dfrac{\partial U}{\partial X_3} = -\alpha \cdot \Delta t_3 \cdot L$

Note: Here we apply:
- **zero** in *CE1*, because the member 2 is deformed together with the absolutely rigid bar (BC) all the time, i.e., they are not disconnected. (here is applied so called *Second Castigliano's Theorem*, cf. Sec.2.13)

- $\Delta L_{t3} = \alpha \; \Delta t_3 \; L$ in *CE2*, i.e., the difference between the original length of rod 3 ($L_3 = L$) before heating and that of $L_3 = L + \alpha \; \Delta t_3 \; L$ after heating. A negative sign is applied in *CE2* because there the compressive force N_{3t} is produced in rod 3, which is opposite to the tension force N_3 assumed.

Such structures are called: **prestressed structures, here influenced by changes in temperature.**

Item **5: Instead of constitution eqs. we express the structure strain energy:**

$$U = \frac{1}{2EA} \sum_i N_i^2 \cdot L_i = \frac{L}{2EA}\left[N_1^2 + X_2^2 \cdot \frac{1}{\sin\beta} + X_3^2 \right]$$

When applying the compatibility equations, we have:

$$\frac{\partial U}{\partial X_2} = \frac{L}{EA}\left[N_1 \cdot \frac{\partial N_1}{\partial X_2} + \frac{X_2}{\sin\beta} \cdot \frac{\partial X_2}{\partial X_2} + X_3 \cdot \frac{\partial X_3}{\partial X_2}\right] = 0$$

$$\frac{\partial U}{\partial X_3} = \frac{L}{EA}\left[N_1 \cdot \frac{\partial N_1}{\partial X_3} + \frac{X_2}{\sin\beta} \cdot \frac{\partial X_2}{\partial X_3} + X_3 \cdot \frac{\partial X_3}{\partial X_3}\right] = -\alpha \cdot \Delta t_3 \cdot L$$

and using eq. *), we have, respectively,

$$\frac{\partial U}{\partial X_2} = \frac{L}{EA}\left[N_1 \cdot (-2\sin\beta) + \frac{X_2}{\sin\beta} \cdot 1 + X_3 \cdot 0\right] = 0 \longrightarrow X_2 = N_1 \cdot 2\sin^2\beta \quad **)$$

$$\frac{\partial U}{\partial X_3} = \frac{L}{EA}\left[N_1 \cdot 2 + \frac{X_2}{\sin\beta} \cdot 0 + X_3 \cdot 1\right] = -\alpha \cdot \Delta t_3 \cdot L \longrightarrow X_3 = -2N_1 - EA\alpha \cdot \Delta t_3 \quad ***)$$

And when returning back to the Eqs. *), **) and ***), we obtain stepwise:

$$N_1 = 3F + 2(-2N_1 - EA\alpha \cdot \Delta t_3) - 2\sin\beta \cdot (N_1 \cdot 2\sin^2\beta) \Rightarrow$$
$$N_1 \cdot (1 + 4 + 4\sin^3\beta) = 3F - 2 \cdot EA\alpha \cdot \Delta t_3 \Rightarrow$$

$$N_1 = \frac{3F - 2 \cdot EA\alpha \cdot \Delta t_3}{5 + 4\sin^3\beta} \geq 0 \quad \text{or} < 0;$$

$$N_2 = X_2 = \frac{6F - 4 \cdot EA\alpha \cdot \Delta t_3}{5 + 4\sin^3\beta} \cdot \sin^2\beta \geq 0 \quad \text{or} < 0;$$

$$N_3 = X_3 = -\frac{6F + EA\alpha \cdot \Delta t_3 \cdot (1 + 4\sin^3\beta)}{5 + 4\sin^3\beta} < 0;$$

i.e., we do not still know if the **supposition was correct or wasn't,** it means that there could be either **tension** or **compression** or $N_{1/2} = 0$

i.e., the **supposition** was **incorrect** and, at the same time, it means **compression**

@

These @) results coincide with those solved by using the common method for SI structures (cf., p.55)

Further, there is to continue according the flow diagram:

Item **6: Internal forces** N_i (in this case, those have been already obtained in the Item **5**)

Item **7: Stress distribution**

$$\sigma_1 = \frac{N_1}{A} = \frac{3F - 2 \cdot EA\alpha \cdot \Delta t_3}{A \cdot (5 + 4\sin^3\beta)};$$

$$\sigma_2 = \frac{N_2}{A} = \frac{6F - 4 \cdot EA\alpha \cdot \Delta t_3}{A \cdot (5 + 4\sin^3\beta)} \cdot \sin^2\beta;$$

$$\sigma_3 = \frac{N_3}{A} = -\frac{6F + EA\alpha \cdot \Delta t_3 \cdot (1 + 4\sin^3\beta)}{A \cdot (5 + 4\sin^3\beta)} < 0;$$

In order to assess $|\sigma|_{max}$, we will look for the mutual influence of the two types of loading, i.e., *F* and *Δt_3> 0*.

From the shapes of σ_1 and σ_2, it is clear that **they could be equal zero** if $F = \dfrac{2}{3} \cdot \alpha \cdot EA \cdot \Delta t_3$.

From this follows that for load $F > \dfrac{2}{3} \cdot \alpha \cdot EA \cdot \Delta t_3$, there is **tension** and for load $F < \dfrac{2}{3} \cdot \alpha \cdot EA \cdot \Delta t_3$, there is **compression**, respectively.

At the same time, it is necessary to assess the influence of the rod 2 tilt magnitude, given by angle β, i.e., we will study the rod 2 extreme tilts:

a/ $\beta = 0$
$$\sigma_1 = \frac{N_1}{A} = \frac{3F - 2 \cdot EA\alpha \cdot \Delta t_3}{A \cdot 5};$$
$$\sigma_2 = \frac{N_2}{A} = \frac{6F - 4 \cdot EA\alpha \cdot \Delta t_3}{A \cdot 5} \cdot 0 = 0;$$
$$\sigma_3 = \frac{N_3}{A} = -\frac{6F + EA\alpha \cdot \Delta t_3}{A \cdot 5};$$

b/ $\beta = 90^o$
$$\sigma_1 = \frac{N_1}{A} = \frac{3F - 2 \cdot EA\alpha \cdot \Delta t_3}{A \cdot 9};$$
$$\sigma_2 = \frac{N_2}{A} = \frac{6F - 4 \cdot EA\alpha \cdot \Delta t_3}{A \cdot 9};$$
$$\sigma_3 = \frac{N_3}{A} = -\frac{6F + 5 \cdot EA\alpha \cdot \Delta t_3}{A \cdot 9};$$

The maximum stress is then $|\sigma|_{max} = |\sigma_3|$ holding for all the angles β.

Item 8: Dimensioning

Strength criterion for a ductile material: $|\sigma|_{max} = |\sigma_3| = \dfrac{6F + EA\alpha \cdot \Delta t_3 \cdot (1 + 4\sin^3 \beta)}{A \cdot (5 + 4\sin^3 \beta)} \le \sigma_{all} = \dfrac{\sigma_Y}{k_{Y\,min}}$,

from which we can compute:

e.g., the **cross-section A** based on F and $\Delta t_3 > 0$: $A \ge \dfrac{6F + EA\alpha \cdot \Delta t_3 \cdot (1 + 4\sin^3 \beta)}{\sigma_{all} \cdot (5 + 4\sin^3 \beta)}$, etc.

Item 9: Checking (it is to be applied for examples solved numerically).

Item 10: The **vertical displacement at the bar position C** (v_C) can be obtained very simply from the kinematically possible deformation, Fig.3.7.2.3, part 3.7.2, pp.48-49, where, substituting

$$N_1 = \frac{3F - 2 \cdot EA\alpha \cdot \Delta t_3}{5 + 4\sin^3 \beta} \text{ into } \Delta L_1 = \frac{N_1 \cdot L}{EA} \Rightarrow \Delta L_1 = \frac{L}{EA} \cdot \frac{3F - 2 \cdot EA\alpha \cdot \Delta t_3}{5 + 4\sin^3 \beta}.$$

As the bar BC is absolutely stiff, we obtain $\quad \dfrac{v_C}{3a} = \dfrac{\Delta L_1}{a} \Rightarrow y_C = 3 \cdot \Delta L_1.$

Then we assess $\quad v_C = \dfrac{L}{EA} \cdot \dfrac{9F - 6 \cdot EA\alpha \cdot \Delta t_3}{5 + 4\sin^3 \beta}$ ∆)

For $\beta = 90^o$, the vertical displacement at the bar position C is: $v_C = \dfrac{FL}{EA} - \dfrac{6 \cdot \alpha \cdot \Delta t_3 \cdot L}{9}\,[\text{mm}]$

Note:

How to apply *Castigliano's Theorem* for assessing the displacement v_C ?:

As the system is prestressed by heating, *Castigliano's Theorem* can be applied only for assessing a **displacement caused with an external load (here F)** from **the balance position after the heating process** ($\Delta t_3 > 0$).

Task: Assess v_C, when the truss is loaded only with $\underline{F}$ ($\Delta t_3 = 0$).

Solution:

$$U = \frac{1}{2EA}\sum_i N_i^2 \cdot L_i = \frac{L}{2EA}\left[N_1^2 + N_2^2 \cdot \frac{1}{\sin\beta} + N_3^2\right] =$$

$$= \frac{L}{2EA}\left[\left(\frac{3F}{5+4\sin^3\beta}\right)^2 + \left(\frac{6F}{5+4\sin^3\beta}\cdot\sin^2\beta\right)^2\cdot\frac{1}{\sin\beta} + \left(-\frac{6F}{5+4\sin^3\beta}\right)^2\right]$$

$$v_{CF} = \frac{\partial U}{\partial F} = \frac{1}{EA}\sum_i N_i\cdot\frac{\partial N_i}{\partial F}\cdot L_i = \frac{L}{EA}\left[N_1\cdot\frac{\partial N_1}{\partial F} + N_2\cdot\frac{\partial N_2}{\partial F}\cdot\frac{1}{\sin\beta} + N_3\cdot\frac{\partial N_3}{\partial F}\right] =$$

$$= \frac{L}{EA}\left[\frac{3F}{5+4\sin^3\beta}\cdot\frac{3}{5+4\sin^3\beta} + \frac{6F}{5+4\sin^3\beta}\cdot\frac{6\cdot\sin^3\beta}{5+4\sin^3\beta} + \frac{6F}{5+4\sin^3\beta}\cdot\frac{6}{5+4\sin^3\beta}\right]$$

$$v_{CF} = \frac{L}{EA}\left[\frac{9F}{(5+4\sin^3\beta)^2} + \frac{36F\cdot\sin^3\beta}{(5+4\sin^3\beta)^2} + \frac{36F}{(5+4\sin^3\beta)^2}\right] = \frac{L}{EA}\cdot\frac{9F}{5+4\sin^3\beta} \quad ^{\blacktriangle\blacktriangle})$$

By comparing $^{\blacktriangle\blacktriangle})$ and $^{\blacktriangle})$, we proved (after taking $\Delta t_3 = 0$) that *Castigliano's Theorem* yielded a correct result.

For $\beta = 90^o$, the vertical displacement at the bar position C is: $v_C = \dfrac{FL}{EA}$
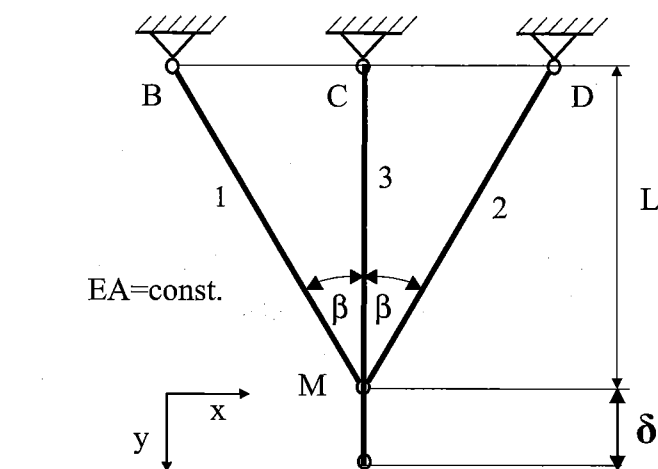
Conclusion:
The same result of displacement v_C we obtain even when substituting in the strain energy expression the **@)** relations of internal forces $N_{1,2,3}$, holding for the completely loaded truss as given in the task in headings, i.e. both F and $t_3 > 0$. **Proving is on you!**

Example 3.7.3.2 Series of trusses where the middle rod has imperfections of various kind
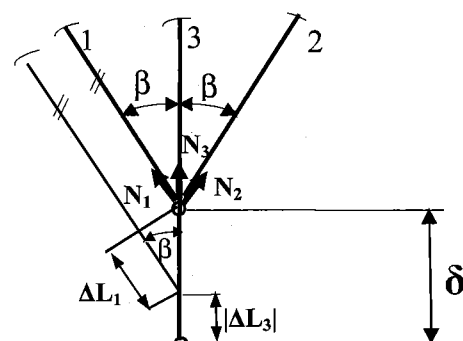
I/ Imperfection by inaccurate manufacturing (the middle rod was produced longer by $\delta \ll L$)

a) *Classical solution*

Item 1: SI 1° (after connecting)　　　　　　　**Item 2... Kinematically possible deformation**

Item 3: Equilibrium eqs. : Int. forces assumption: $N_1 > 0$; $N_2 > 0$; $N_3 > 0$

$$\left. \begin{array}{l} \textbf{x...} \ (N_1 - N_2)\sin\beta \Rightarrow N_1 = N_2 = N \\ \textbf{y...} \ N_1\cos\beta + N_2\cos\beta + N_3 = 2N\cos\beta + N_3 = 0 \end{array} \right\} \ N_1 = N_2 = N = -\frac{N_3}{2\cos\beta}$$

Item 4: Compatibility eq. (using Item 2) $\quad \delta = \dfrac{\Delta L_1}{\cos\beta} + \left|\Delta L_3\right| = \dfrac{\Delta L_1}{\cos\beta} - \Delta L_3$
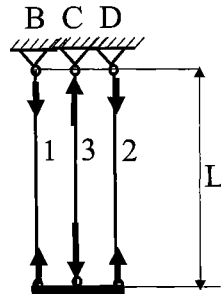
Item 5: Constitutive eqs. $\quad \Delta L_1 = \dfrac{N_1 \cdot L}{EA \cdot \cos\beta}$; $\quad \Delta L_3 = \dfrac{N_3 \cdot L}{EA}$

Combining Items 3+4+5, we have

$$\delta = \frac{\Delta L_1}{\cos\beta} - \Delta L_3 = \frac{N_1 \cdot L}{EA \cdot \cos^2\beta} - \frac{N_3 \cdot L}{EA} = -\frac{N_3 \cdot L}{2EA\cos^3\beta} - \frac{N_3 \cdot L}{EA} \Rightarrow$$

$$N_3\left[\frac{1}{2\cos^3\beta} + 1\right] = N_3\left[\frac{1 + 2\cos^3\beta}{2\cos^3\beta}\right] = -\frac{\delta EA}{L} \Rightarrow N_3 = -\frac{\delta EA}{L} \cdot \frac{2\cos^3\beta}{1 + 2\cos^3\beta} \quad < 0$$

$$N_1 = N_1 = N = -\frac{N_3}{2\cos\beta} = \frac{\delta EA}{L} \cdot \frac{\cos^2\beta}{1 + 2\cos^3\beta}\left[\frac{mm \cdot MPa \cdot mm^2}{mm} = N\right] > 0$$
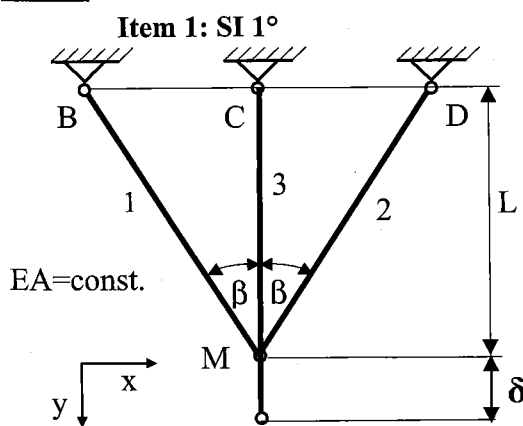
A simple checking of the results: 1/ the units (correct); 2/ a special simple shape and loading, e.g., $\beta = 0$:

$$N_1 = N_2 = \frac{1}{3}\frac{\delta EA}{L} \ ; \ N_3 = -\frac{2}{3}\frac{\delta EA}{L}$$

b) *Modified Second Castigliano's Theorem (MSCT) application*

It is necessary to choose the internal force N_3 (in the rod with imperfection) as **SI force** which will be used in MSCT:

Item 1: SI 1°

Item 2: It is not necessary to be applied!

Item 3: Equilibrium eqs.
(Inter. forces assumption: $N_1 > 0$; $N_2 > 0$; $N_3 > 0$)
x.... $N_1 - N_2\sin\beta = 0$
y.... $N_1\cos\beta + N_2\cos\beta + N_3 = 2N\cos\beta + N_3 = 0$

$$N_1 = N_2 = N$$

$$N_1 = N_2 = N = -\frac{N_3}{2\cos\beta}$$

Item 4: No compatibility eq. but the <u>MSCT application</u> :
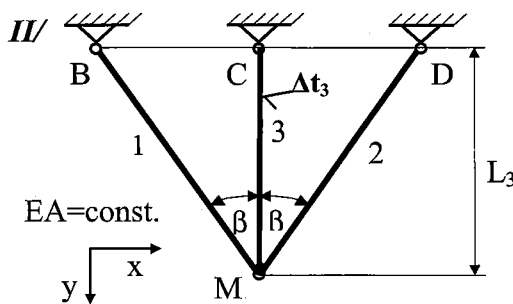
$$\frac{\partial U}{\partial N_3} = \frac{1}{EA}\sum_{i=1}^{3} N_i \cdot \frac{\partial N_i}{\partial N_3} \cdot L_i = \frac{1}{EA}\left[-2\frac{N_3}{2\cos\beta}\left(-\frac{1}{2\cos\beta}\right)\cdot\left(\frac{L}{\cos\beta}\right)+N_3\cdot L\right] = -\delta \Rightarrow$$

$$N_3 = \frac{-\delta EA}{L}\left[\frac{1}{2\cos^3\beta}+1\right] = N_3\left[\frac{1+2\cos^3\beta}{2\cos^3\beta}\right] = -\frac{\delta EA}{L} \Rightarrow N_3 = -\frac{\delta EA}{L}\cdot\frac{2\cos^3\beta}{1+2\cos^3\beta}$$

$$N_1 = N_2 = N = -\frac{N_3}{2\cos\beta} = \frac{\delta EA}{L}\cdot\frac{\cos^2\beta}{1+2\cos^3\beta}$$

i.e., the same results when using *the classical solution a)*

Analogously you can compute examples where imperfection δ is caused by change in temperature (<u>important note</u>: the trusses must be made always as symmetric structures):

II/

Only the **centre rod 3** is heated/cooled by Δt_3 .

The imperfection is **:**
either $\delta = \alpha \Delta t_3 L_3 > 0$, when the rod **3** is **heated**;

then

$$N_1 = N_2 = N = \frac{\alpha\cdot\Delta t_3\cdot L_3\cdot EA}{L}\cdot\frac{\cos^2\beta}{1+2\cos^3\beta}$$
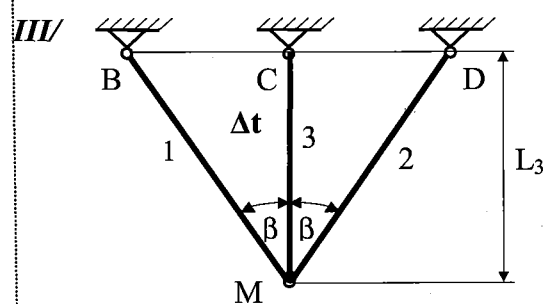
$$N_3 = -\frac{\alpha\cdot\Delta t_3\cdot L_3\cdot EA}{L}\cdot\frac{2\cos^3\beta}{1+2\cos^3\beta} ;$$

or $\delta = \alpha \Delta t_3 L_3 < 0$, when the rod **3** is **cooled**,

then

$$N_1 = N_2 = N = -\frac{\alpha\cdot\Delta t_3\cdot L_3\cdot EA}{L}\cdot\frac{\cos^2\beta}{1+2\cos^3\beta}$$

$$N_3 = \frac{\alpha\cdot\Delta t_3\cdot L_3\cdot EA}{L}\cdot\frac{2\cos^3\beta}{1+2\cos^3\beta} ;$$

III/
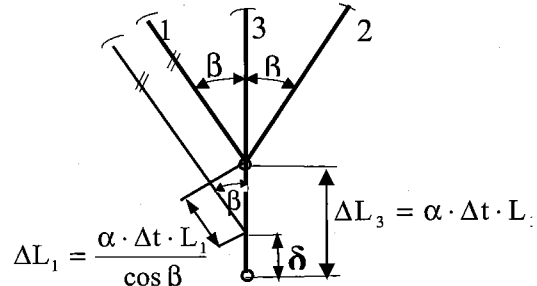
All the truss is heated/cooled by Δt .

The imperfection is:

$$\delta = \alpha\cdot\Delta t\cdot L_3 - \frac{\alpha\cdot\Delta t\cdot L_1}{\cos\beta} \quad \text{(see the figure beneath)}$$

$$\Delta L_1 = \frac{\alpha\cdot\Delta t\cdot L_1}{\cos\beta}$$

$$\Delta L_3 = \alpha\cdot\Delta t\cdot L$$

Depending on:
the materials of rods, the truss geometry
and the way of temperature influence,
the resulting imperfection can be:

$$\delta > 0 \Rightarrow N_{1,2} > 0, N_3 < 0;$$
$$\delta < 0 \Rightarrow N_{1,2} < 0, N_3 > 0;$$
$$\delta = 0 \Rightarrow N_{1,2,3} = 0$$

Example 3.7.3.3 Unsymmetric SI truss

Based on the SD truss solved in Chapter 2, Example 2.13.1, the SI 1° truss in Fig.e3.3.1 is created by adding the vertical rod 3, connecting the pin D with the pin support H. This problem can be solved by:

I/ Classical method (based on the truss kinematically possible deformation); *II/ Castigliano's Theorem*

$$L_1 = L/\sin\beta$$
$$L_2 = L/\text{tg}\beta$$
$$L_3 = L$$

$$N_1 > 0$$
$$N_2 > 0$$
$$N_3 > 0$$

Fig.3.7.3.3.1

Solution:

I/ Classical method:

Item 1: SI 1° *(three int. forces $N_{1,2,3}$ are unknown while two equilibrium equations are available]*

Item 2: Kinematically possible deformation

We can utilize **Example 2.13.1** from p.39.

Item 3: Equilibrium eqs :

$$\left.\begin{array}{l} \text{x...}\quad N_2 + N_1 \cdot \cos\beta = 0 \\ \text{y...}\quad F - N_3 - N_1 \cdot \sin\beta = 0 \end{array}\right\} \,*)$$

Item 4: Compatibility eq.

$$\Delta L_3 = \frac{\Delta L_1}{\sin\beta} + \frac{|\Delta L_2|}{\tan\beta}$$

Item 5: Constitutive relations

$$\Delta L_1 = \frac{N_1 \cdot L}{EA \cdot \sin\beta} \;;\; \Delta L_2 = \frac{N_2 \cdot L}{EA \cdot \tan\beta} \;;\; \Delta L_3 = \frac{N_3 \cdot L}{EA}$$

$$\Delta L_3 > 0$$

Fig. 3.7.3.3.2

Combining all the expressions, we have

$$\Delta L_3 = \frac{\Delta L_1}{\sin\beta} + \frac{|\Delta L_2|}{\tan\beta} \Rightarrow N_3 = \frac{N_1}{\sin^2\beta} - \frac{N_2}{\tan^2\beta} \Rightarrow$$

$$F - N_1 \cdot \sin\beta = \frac{N_1}{\sin^2\beta} + \frac{N_1 \cdot \cos^3\beta}{\sin^2\beta} \Rightarrow N_1 \cdot \left[\frac{1 + \cos^3\beta + \sin^3\beta}{\sin^2\beta}\right] = F \Rightarrow$$

$$N_1 = F \cdot \frac{\sin^2\beta}{1 + \cos^3\beta + \sin^3\beta};$$

$$N_2 = -N_1 \cdot \cos\beta = -F \cdot \frac{\sin^2\beta \cdot \cos\beta}{1 + \cos^3\beta + \sin^3\beta}$$

$$N_3 = F - N_1 \cdot \sin\beta = F \cdot \left[1 - \frac{\sin^2\beta}{1 + \cos^3\beta + \sin^3\beta}\right] = F \cdot \left[\frac{1 + \cos^3\beta + \sin^3\beta - \sin^2\beta}{1 + \cos^3\beta + \sin^3\beta}\right]$$
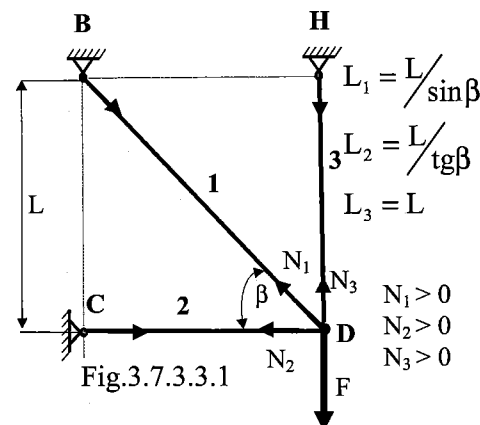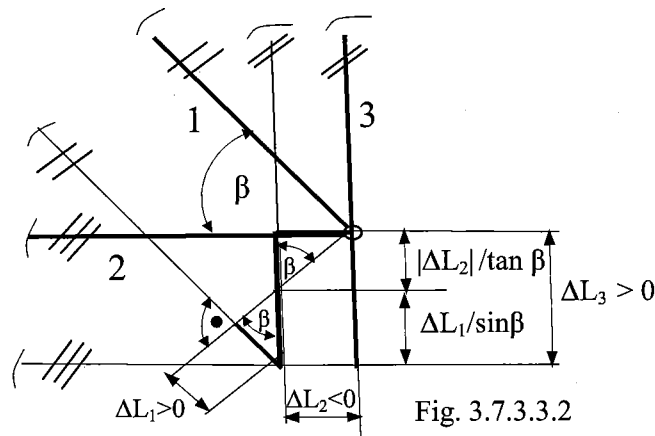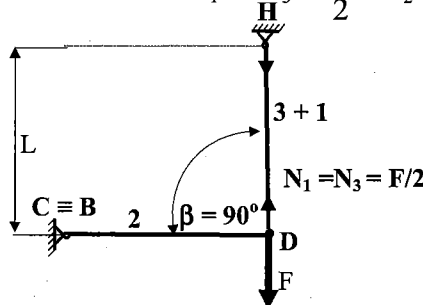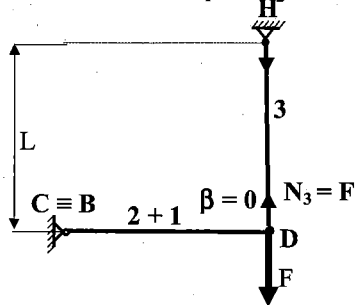
A simple checking of the results correctness:

a/ A truss with $\beta = 0$: $N_1 = N_2 = 0$; $N_3 = F$; b/ A truss with $\beta = 90^\circ$: $N_1 = N_3 = \dfrac{F}{2}$; $N_2 = 0$


II/ Castigliano's Theorem:

$$\frac{\partial U}{\partial N_3} = \frac{1}{EA}\sum_{i=1}^{3} N_i \cdot \frac{\partial N_i}{\partial N_3} \cdot L_i = 0 \Rightarrow$$

$$\frac{L}{EA}\left[N_1 \cdot \frac{\partial N_1}{\partial N_3} \cdot \frac{1}{\sin\beta} + N_2 \cdot \frac{\partial N_2}{\partial N_3} \cdot \frac{1}{\tan\beta} + N_3 \cdot \frac{\partial N_3}{\partial N_3} \cdot 1 = 0 \right]$$

When modifying eqs. *), we have: $N_1 = \dfrac{F - N_3}{\sin\beta}$; $\quad N_2 = -N_1 \cdot \cos\beta = -(F - N_3)\dfrac{\cos\beta}{\sin\beta}$,

and substituting to the expression above we assess subsequently **the internal forces**:

$$\frac{L}{EA}\left[\left(\frac{F - N_3}{\sin\beta}\right) \cdot \left(-\frac{1}{\sin\beta}\right) \cdot \frac{1}{\sin\beta} + (N_3 - F) \cdot \frac{\cos\beta}{\sin\beta} \cdot \frac{\cos\beta}{\sin\beta} \cdot \frac{\cos\beta}{\sin\beta} + N_3 \right] = 0 \Rightarrow$$

$$N_3 = F \cdot \frac{1 + \cos^3\beta}{1 + \cos^3\beta + \sin^3\beta};$$

$$N_1 = F \cdot \frac{\sin^2\beta}{1 + \cos^3\beta + \sin^3\beta}$$

$$N_2 = -N_1 \cdot \cos\beta = -F \cdot \frac{\sin^2\beta \cdot \cos\beta}{1 + \cos^3\beta + \sin^3\beta}$$

These results coincide with eqs. **) .
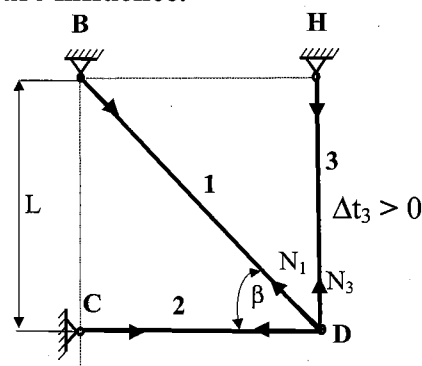
Again we found out that *Castigliano's Theorem* did not need to design kinematically possible deformations, which might be a quite difficult task when solving complex structures.

Example 3.7.3.4 Unsymmetric SI truss with temperature influence.

These 3-rod truss is, after assembly, subjected with heating the rod 3 about $\Delta t_3 > 0$. To assess the internal forces $N_{1,2,3}$ (which are assumed positive) , we will apply:

I/ Classical method;

II/ Modified Second Castigliano Theorem (MSCT)

Solution:

I/ Classical method:

Item 1: SI 1°

Item 2: Kinematically possible deformation (Example 2.13.1 or Ex 3.3 – Fig.e3.3.2 are utilized)

Item 3: Equilibrium eqs :

$$\left. \begin{aligned} \text{x...} \quad N_2 + N_1 \cdot \cos\beta = 0 \\ \text{y...} \quad N_3 + N_1 \cdot \sin\beta = 0 \end{aligned} \right\} \; *)$$

Item 4: Compatibility eq. (*see Example 3.7.3.3 – Fig.3.7.3.3.2*)

$$\Delta L_3 = \frac{\Delta L_1}{\sin\beta} + \frac{|\Delta L_2|}{\tan\beta}$$

Item 5: Constitutive relations

$$\Delta L_1 = \frac{N_1 \cdot L}{EA \cdot \sin\beta} \; ; \quad \Delta L_2 = \frac{N_2 \cdot L}{EA \cdot \tan\beta} \; ; \quad \Delta L_3 = \frac{N_3 \cdot L}{EA} + \alpha \cdot \Delta t_3 \cdot L$$

Combining all the expressions, we have

$$\Delta L_3 = \frac{\Delta L_1}{\sin\beta} + \frac{|\Delta L_2|}{\tan\beta} \Rightarrow N_3 + \alpha \cdot \Delta t_3 \cdot EA = \frac{N_1}{\sin^2\beta} - \frac{N_2}{\tan^2\beta} \Rightarrow$$

$$- N_1 \cdot \sin\beta + \alpha \cdot \Delta t_3 \cdot EA = \frac{N_1}{\sin^2\beta} + \frac{N_1 \cdot \cos^3\beta}{\sin^2\beta} \Rightarrow$$

$$\left. \begin{aligned} &N_1 \cdot \left[\frac{1 + \cos^3\beta + \sin^3\beta}{\sin^2\beta} \right] = \alpha \cdot \Delta t_3 \cdot EA \Rightarrow N_1 = \alpha \cdot \Delta t_3 \cdot EA \cdot \frac{\sin^2\beta}{1 + \cos^3\beta + \sin^3\beta} \\[2mm] &N_2 = -N_1 \cdot \cos\beta = -\alpha \cdot \Delta t_3 \cdot EA \cdot \frac{\sin^2\beta \cdot \cos\beta}{1 + \cos^3\beta + \sin^3\beta} \; ; \\[2mm] &N_3 = -N_1 \cdot \sin\beta = -\alpha \cdot \Delta t_3 \cdot EA \cdot \frac{\sin^3\beta}{1 + \cos^3\beta + \sin^3\beta} \end{aligned} \right\} \; **)$$

II/ Castigliano's Theorem:

Since the rod 3 is heated, we use *Castigliano's Theorem* as follows:

$$\frac{\partial U}{\partial N_3} = \frac{1}{EA} \sum_{i=1}^{3} N_i \cdot \frac{\partial N_i}{\partial N_3} \cdot L_i = -\alpha \cdot \Delta t_3 \cdot L_3 \Rightarrow$$

$$\frac{L}{EA} \left[N_1 \cdot \frac{\partial N_1}{\partial N_3} \cdot \frac{1}{\sin\beta} + N_2 \cdot \frac{\partial N_2}{\partial N_3} \cdot \frac{1}{\tan\beta} + N_3 \cdot \frac{\partial N_3}{\partial N_3} \cdot 1 = -\alpha \cdot \Delta t_3 \cdot L \right]$$

When modifying eqs. *), we have: $N_1 = -\dfrac{N_3}{\sin\beta} ; \quad N_2 = -N_1 \cdot \cos\beta = \dfrac{N_3}{\tan\beta} ,$

and substituting to the expression above we assess subsequently **the internal forces:**

$$\frac{1}{EA}\left[\left(-\frac{N_3}{\sin\beta}\right)\cdot\left(-\frac{1}{\sin\beta}\right)\cdot\frac{1}{\sin\beta}+\frac{N_3\cdot\cos\beta}{\sin\beta}\cdot\frac{\cos\beta}{\sin\beta}\cdot\frac{\cos\beta}{\sin\beta}+N_3\right]=-\alpha\cdot\Delta t_3 \Rightarrow$$

$$N_3=-\alpha\cdot\Delta t_3\cdot EA\cdot\frac{\sin^3\beta}{1+\cos^3\beta+\sin^3\beta};$$

$$N_1=-\frac{N_3}{\sin\beta}=\alpha\cdot\Delta t_3\cdot EA\cdot\frac{\sin^2\beta}{1+\cos^3\beta+\sin^3\beta};$$

$$N_2=\frac{N_3}{\tan\beta}=-\alpha\cdot\Delta t_3\cdot EA\cdot\frac{\sin^2\beta\cdot\cos\beta}{1+\cos^3\beta+\sin^3\beta}$$

These results coincide with eqs. **∗∗)** .

Once again we found out that *Castigliano's Theorem* did not need to design kinematically possible deformations, which might be a quite difficult task when solving complex structures.

4. Frameworks, trusses; application of Castigliano's theorem

In this chapter we shall discuss the ideal framework. It is a structure consisting of straight bars connected by ideal frictionless joints (pin connected bars). The framework is known as a *truss,* or plane framework, when all its bars lie in a plane; when this condition is not met, the structure is a space framework. All external forces acting on a ideal framework are applied at the joints, and the weight of each bar (when taken into account) is assumed concentrated at the two end points of the bar, that is, at the joints. It follows then from the conditions of equilibrium of any bar that the two forces transmitted to it from the joints at its ends must be equal in magnitude and opposite in orientation. The bars are consequently either in pure tension or in pure compression which, in structure diagrams, will be denoted by two arrows pointing (in respective bars) to /from each other, respectively.

4.1 Statically determinate frameworks

With frameworks, it is necessary to prove *static determinateness,* both *external* and *internal.* The former is ensured when a framework is supported in a statically determinate manner. For instance, in Fig.4.1.2, the frictionless pivot at B can transmit any horizontal and vertical reactions, and the frictionless slide at C can transmit any vertical reaction, which can be confirmed on the basis of the formula

$$s_e = \sum p - 3 , \qquad\qquad (4.1.1a)$$

where: s_e...the degree of external static indeterminateness

$\sum p$... the number of static parameters (reactions) in the supports

The latter can be proved by computing from the formula

$$s_i = n - 2m + 3 \qquad\qquad (4.1.1b)$$

where: s_i...the degree of internal static indeterminateness

n...the number of framework members

m...the number of ideal frictionless joints

When a statically determinate (SD) framework is subjected to known loads, the forces in its members can be calculated by means generally known from statics: *the methods of sections*; *Cremon's diagram.* Under these forces the members change their length and the elongations can be determined without difficulty if the stress-strain law of the material is known. The shape of an SD framework is completely determined by the length of its members and their arrangement. The displacement of a chosen joint of the framework can then be determined theoretically by step-by-step assessed elongations of its bars. The trouble is that the stretched lengths of the bars differ so little from the

initial lengths that they cannot be distinguished from each other in an engineering drawing. Nevertheless a framework bridge can easily deflect several tens of millimetres. The straightforward geometric approach is therefore not accurate enough for solving the purely geometric problem of obtaining the displacements of the joints of a framework from the known changes in the lengths of its members.

For this reason it is advisable to abandon this geometric approach (commonly used with simple frameworks solved in Secs.3.5; 3.7) and to calculate the displacements from *Castigliano's theorem*. Such a procedure can be learned readily when solving, for instance, displacements (at chosen joints and in chosen directions) of the simple truss shown in Fig.4.1.1.
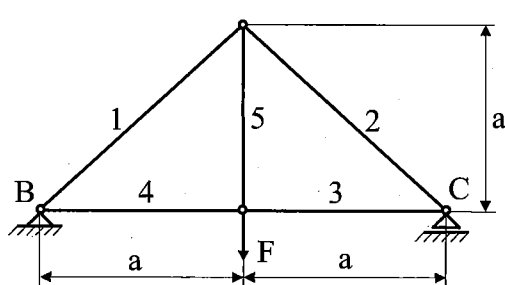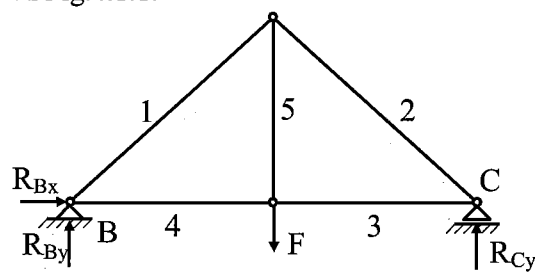
Fig.4.1.1   Fig.4.1.2

We can prove that the truss is SD by applying Eqs.(4.1.1a,b):

$$s_e = 3 - 3 = 0 \qquad \text{and} \qquad s_i = 5 - 2 \cdot 4 + 3 = 0$$

The strain energy accumulated in a truss is assessed when summing the strain energy of all its members ($U = \dfrac{1}{2}\sum_i \dfrac{N^2_i \cdot L_i}{E_i \cdot A_i}$, cf. Eq.2.12.3a) and, applying it on the truss in Fig.4.1.1 (where all bars are of the same cross-sectional area), we have $U = \dfrac{1}{2EA}\sum_{i=1}^{5} N^2_i \cdot L_i$.

Now, by applying *Castigliano's theorem* (cf. Eq.2.13.6), or the *"dummy"(unit) load method* (cf. Eq.2.13.7), respectively, we can determine:

a) Vertical displacement of the joint where load F is attached by the expressions

$$v_F = \frac{\partial U}{\partial F} = \frac{1}{EA}\sum_{i=1}^{5} N_i \cdot \frac{\partial N_i}{\partial F} \cdot L_i , \qquad \text{or} \qquad v_F = \frac{1}{EA}\sum_{i=1}^{5} N_i \cdot n_{i,F} \cdot L_i , \qquad (4.1.1a,b)$$

where: $n_{i,F}$ ... the internal force in the *i-th* bar (Fig.4.1.4) being in equilibrium with the external forces which consist of the dummy (unit) load, applied at the joint where load F is exerted, and its reactions.

Internal forces N_i can easily be obtained by means of *Cremon's diagram* (Fig.4.1.3). Analogously, internal forces $n_{i,F}$ are determined. All internal forces assessed in this way together with the bar lengths and the products of quantities showed in Formula (4.1.1b), are tabulated in Table 4.1.1, being arranged according the numbers n of the bars.
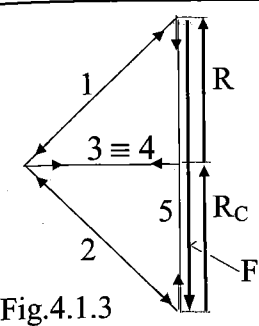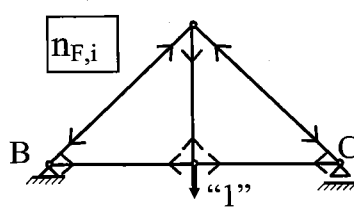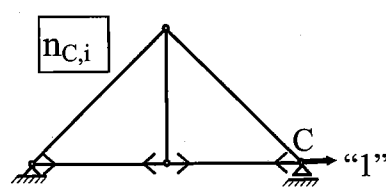
Fig.4.1.3   Fig.4.1.4   Fig.4.1.5

b) Horizontal displacement of the slide C by expressions (cf. Sec.2.13)

$$u_C = \left(\frac{\partial U}{\partial F}\right)_{\mathsf{F} \to 0} = \frac{1}{EA}\sum_{i=1}^{5}(N_i)_{\mathsf{F} \to 0} \cdot \frac{\partial N_i}{\partial F} \cdot L_i, \quad \text{or} \quad u_C = \frac{1}{EA}\sum_{i=1}^{5}N_i \cdot n_{i,C} \cdot L_i \quad (4.1.2a,b)$$

(Application of Eq. (4.1.2a) would require that we first attach an additional external (imaginary) force F to joint C, where no active concentrated force is exerted in the horizontal direction, and consequently express internal forces $N_i = Ni(F, \mathsf{F})$ and strain energy $U = U(F, \mathsf{F})$ as functions of the two external forces F and F. The procedure would be closed up by putting $\mathsf{F} \to 0$ in the result obtained; cf. Note in Sec.2.13.)

In Table 4.1.1, an extra column containing internal forces $n_{i,C}$, produced by the dummy (unit) load attached horizontally to the slide C (Fig.4.1.5), is added.

Table 4.1.1

n	N_i	$n_{i,F}$	$n_{i,C}$	L_i	$N_i \cdot n_{i,F} \cdot L_i$	$N_i \cdot n_{i,C} \cdot L_i$
1	$-F \cdot \frac{\sqrt{2}}{2}$	$-\frac{\sqrt{2}}{2}$	0	$a \cdot \sqrt{2}$	$F \cdot a \cdot \frac{\sqrt{2}}{2}$	0
2	$-F \cdot \frac{\sqrt{2}}{2}$	$-\frac{\sqrt{2}}{2}$	0	$a \cdot \sqrt{2}$	$F \cdot a \cdot \frac{\sqrt{2}}{2}$	0
3	$\frac{F}{2}$	$\frac{1}{2}$	1	a	$F \cdot a \cdot \frac{1}{4}$	$F \cdot a \cdot \frac{1}{2}$
4	$\frac{F}{2}$	$\frac{1}{2}$	1	a	$F \cdot a \cdot \frac{1}{4}$	$F \cdot a \cdot \frac{1}{2}$
5	F	1	0	a	$F \cdot a$	0
				Σ	$F \cdot a \cdot \left(\frac{3}{2} + \sqrt{2}\right)$	$F \cdot a$

Both looked-for displacements are obtained when utilizing the sums of the products of the respective quantities listed in the last two columns of Table 4.1.1. Thus, we have

$$v_F = \frac{F \cdot a}{EA} \cdot \left(\frac{3}{2} + \sqrt{2}\right) \qquad u_C = \frac{F \cdot a}{EA}$$

As the displacements are positive, they pass off in the orientations of the applied dummy loads.

4.2 Statically indeterminate frameworks

Statically indeterminate frameworks (trusses) are also called *redundant* frameworks.
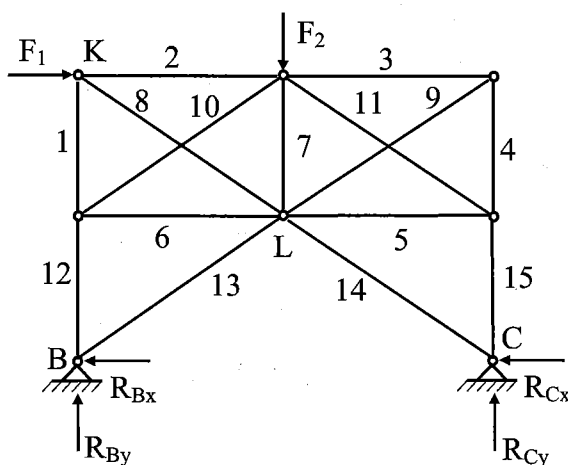
Fig.4.2.1

The procedure for solving SI frameworks will lose none of its universality when we demonstrate it on the truss in Fig.4.2.1.

The <u>degree of static indeterminateness</u> will be assessed by means of Eqs.(4.1.1a,b):
external SI

$$s_e = \sum p - 3 = 4 - 3 = 1;$$

internal SI

$$s_i = n - 2m + 3 = 15 - 2 \cdot 8 + 3 = 2;$$

which show that the <u>framework is SI to the third degree</u>.
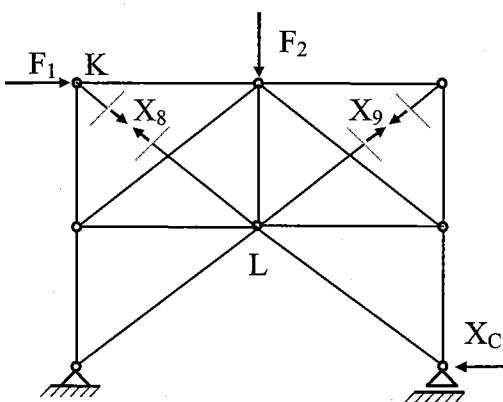
In the first step we shall <u>eliminate the superfluous support parameters and redundant rods and thus create the *basic (statically determinate) system*</u> of the framework. In this example we use fictitious sections to release the pivot C in the horizontal direction, while replacing this released support parameter with an unknown SI force X_C , and cause two redundant rods (any from *1* to *11* but none from *12* to *15* because the structure must not change into a mechanism), for instance, *8* and *9,* to be out of action (for the exerting

Fig.4.2.2

external loads F_1 , F_2) <u>by fictitious sections,</u> **(this is not clearly expressed)** while letting <u>them</u> transmit unknown SI forces X_8 and X_9 , respectively, Fig.4.2.2.

By applying Eq.2.12.3a, the strain energy can be expressed in the form

$$U = \frac{1}{2EA} \sum_{i=1}^{15} N_i^2 \cdot L_i \tag{4.2.1}$$

where the internal forces exerting in the rods are expressed by applying the <u>superposition principle</u> (Fig.4.2.2), as follows

$$N_i = Z_i + X_8 \cdot n_{i,8} + X_9 \cdot n_{i,9} + X_C \cdot n_{i,C} \tag{4.2.2}$$

where: Z_i ...internal forces exerting in the rods of the basic system, produced by the assigned external

loads F_1 and F_2;

$n_{i,8}$; $n_{i,9}$; $n_{i,C}$ ... .internal forces exerting in the rods of the basic system, produced by the dummy (unit) loads $X_8 = "1"$; $X_9 = "1"$; $X_C = "1"$, which are to be applied instead of the unknown SI forces X_8, X_9, X_C, respectively;

As the structure is SI to the third degree we have to write three compatibility relations, for which we will use Castigliano's theorem (analogously to Eqs.(4.1.1b) or (4.1.2b) we will express the partial derivatives):

$$\frac{\partial U}{\partial X_8} = \sum_{i=1}^{15} N_i \cdot n_{i,8} \cdot L_i = 0 \; ; \quad \frac{\partial U}{\partial X_9} = \sum_{i=1}^{15} N_i \cdot n_{i,9} \cdot L_i = 0 \; ; \quad \frac{\partial U}{\partial X_C} = \sum_{i=1}^{15} N_i \cdot n_{i,C} \cdot L_i = 0 \, .$$

$$(4.2.3a,b,c)$$

The last relation (4.2.3c) is easy to understand because the truss is in fact rigidly fixed at pivot C. However, the first two affirmations (4.2.3a,b), which state that the deformations of rods 8 and 9, respectively, do not differ from the deformations which the whole structure undergoes in the joints where these redundant rods are attached, deserve an explanation:

Consider the truss to be divided into two systems I and II, Fig.4.2.3. When applying Castigliano's theorem to each system we have

$$\frac{\partial U}{\partial X_9} = \frac{\partial U_I}{\partial X_9} + \frac{\partial U_{II}}{\partial X_9} = -\Delta L_9 + \Delta L_9 = 0$$
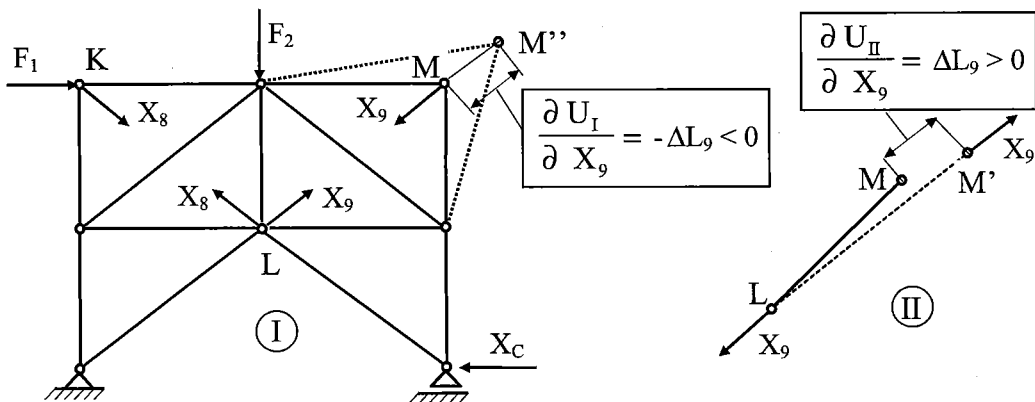
Fig.4.2.3

(The displacement MM'' of the connecting line LM in system I is negative, since it is executed in the opposite direction than force X_9 is acting. The strain energy of the further possible system III, comprising rod 8, does not include rod 9, and therefore there holds $\frac{\partial U_{III}}{\partial X_9} = 0$)

Eqs.(4.2.1a,b,c) are occasionally called *Castigliano's second theorem*, which in words states: *A statically indeterminate force quantity makes the strain energy of a structure become minimum.*

Substituting Eq.(4.2.2) into Eqs.(4.2.3a,b,c) we will obtain

$$\sum_{i=1}^{15} N_i \cdot n_{i,8} \cdot L_i = \sum_{i=1}^{15} Z_i \cdot n_{i,8} \cdot L_i + X_8 \cdot \sum_{i=1}^{15} n^2{}_{i,8} \cdot L_i + X_9 \cdot \sum_{i=1}^{15} n_{i,8} \cdot n_{i,9} \cdot L_i + X_C \cdot \sum_{i=1}^{15} n_{i,8} \cdot n_{i,C} \cdot L_i = 0$$

$$(4.2.4a)$$

71

$$\sum_{i=1}^{15} N_i \cdot n_{i,9} \cdot L_i = \sum_{i=1}^{15} Z_i \cdot n_{i,9} \cdot L_i + X_8 \cdot \sum_{i=1}^{15} n_{i,8} \cdot n_{i,9} \cdot L_i + X_9 \cdot \sum_{i=1}^{15} n^2_{i,9} \cdot L_i + X_C \cdot \sum_{i=1}^{15} n_{i,9} \cdot n_{i,C} \cdot L_i = 0$$

$$(4.2.4b)$$

$$\sum_{i=1}^{15} N_i \cdot n_{i,C} \cdot L_i = \sum_{i=1}^{15} Z_i \cdot n_{i,C} \cdot L_i + X_8 \cdot \sum_{i=1}^{15} n_{i,8} \cdot n_{i,C} \cdot L_i + X_9 \cdot \sum_{i=1}^{15} n_{i,9} \cdot n_{i,C} \cdot L_i + X_C \cdot \sum_{i=1}^{15} n^2_{i,C} \cdot L_i = 0$$

$$(4.2.4c)$$

Referring to Sec.4.1, we realize that the members of Eq.(4.2.4a) can be interpreted:

$$\frac{1}{EA} \cdot \sum_{i=1}^{15} Z_i \cdot n_{i,8} \cdot L_i = \Delta_{8,F} \quad \text{... displacement of connecting line } KL \text{ produced by external loads}$$

$$\frac{1}{EA} \cdot \sum_{i=1}^{15} n^2_{i,8} \cdot L_i = \delta_{8,8} \quad \text{...displacement of connecting line } KL \text{ produced by the unit load } X_8 = \text{"1"}$$

$$\frac{1}{EA} \cdot \sum_{i=1}^{15} n_{i,8} \cdot n_{i,9} \cdot L_i = \delta_{8,9} \quad \text{...displacement of connecting line } KL \text{ produced by the unit load}$$

$$X_9 = \text{"1"}$$

$$\frac{1}{EA} \cdot \sum_{i=1}^{15} n_{i,8} \cdot n_{i,C} \cdot L_i = \delta_{8,C} \quad \text{...displacement of connecting line } KL \text{ produced by the unit load}$$

$$X_C = \text{"1"}.$$

When proceeding analogously with the members of Eqs.(4.2.4b,c) we can rewrite Eqs.(4.2.4a,b,c) as

$$\Delta_{8,F} + \delta_{8,8} + \delta_{8,9} + \delta_{8,C} = 0$$
$$\Delta_{9,F} + \delta_{9,8} + \delta_{9,9} + \delta_{9,C} = 0 \qquad\qquad (4.2.5a,b,c)$$
$$\Delta_{C,F} + \delta_{C,8} + \delta_{C,9} + \delta_{C,C} = 0$$

Eqs.(4.2.5a,b,c) are called *canonical equations of the force method,* and can be conveniently expressed in the matrix form as follows

$$\{\Delta\} + [\delta]\{X\} = 0$$

4.3 Pre-stressed trusses; truss with a cooled-down member

We will determine the stress state in the truss shown in Fig.4.3.1, one member of which was cooled down by $\Delta t_4 < 0$. The truss comprises rods of uniform cross-sectional area A, made of the same material having the modulus of elasticity E and the coefficient of thermal expansion α.
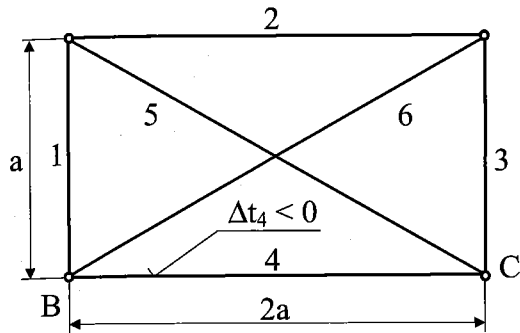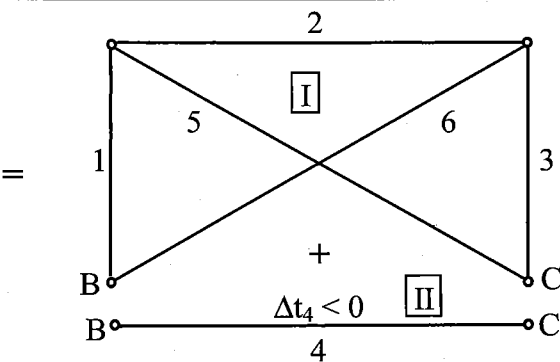
Fig.4.3.1   Fig.4.3.2

Referring to Sec.3.6, it appears to be more convenient - when solving a **SI structure influenced by a change in temperature** (in one or more structure members) - to release such a structure for it to become a SD system. In this way, we can determine the difference arising in the lengths of the members (when compared with their original state), due to the cooling of the relevant structure parts. Subsequently, when the structure is joined into a single unit again, tensions are produced in its members.
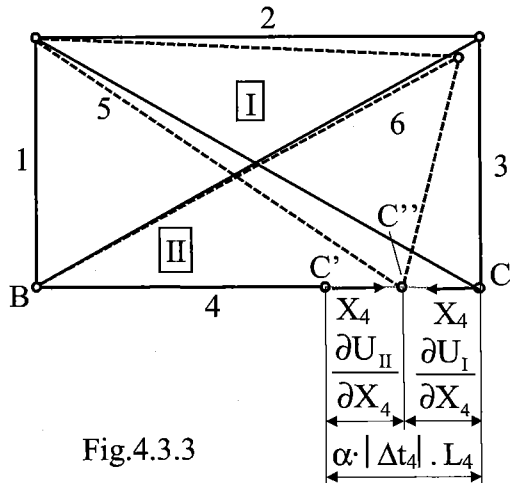
The strain energy accumulated in the truss

$$U = \frac{1}{2EA} \sum_{i=1}^{6} N^2{}_i \cdot L_i$$

should be divided, in this case, into two basic (SD) systems (see Fig.4.3.2 and Fig.4.3.3), as follows

$$U = U_I + U_{II} = \frac{1}{2EA} \cdot \left\{ \sum_{i=1, i \neq 4}^{6} N_i^2 \cdot L_i + X^2{}_4 \cdot L_4 \right\}$$

where *(4)* in front of the sum symbol means that the *4th* rod is not added to it.

Fig.4.3.3

The deformation condition (compatibility relation)

$$\frac{\partial U}{\partial X_4} = \frac{\partial U_I}{\partial X_4} + \frac{\partial U_{II}}{\partial X_4} = \alpha \cdot |\Delta t_4| \cdot L_4$$

is obtained by applying Castigliano's <u>first</u> theorem, because the structure is pre-stressed by tensions caused by cooling and therefore the minimum strain energy condition does not hold here.

The internal force in the *i-th* member and its partial derivative are

$$N_i = X_4 \cdot n_{i,4}; \qquad \frac{\partial N_i}{\partial X_4} = n_{i,4}$$

where: $n_{i,4}$ ... the internal force in the *i-th* bar being in equilibrium with the <u>dummy (unit) loads,</u> applied at the joints *BC* of the basic system *I*, respectively.

Applying the deformation condition and considering the above relations, we obtain successively

$$\frac{\partial U}{\partial X_4} = \frac{1}{EA} \cdot \left\{ \sum_{i=1,i\neq 4}^{6} N_i \cdot \frac{\partial N_i}{\partial X_4} \cdot L_i + X_4 \cdot L_4 \right\} = \frac{1}{EA} \cdot \left\{ \sum_{i=1,i\neq 4}^{6} X_4 \cdot n_{i,4}^2 \cdot L_i + X_4 \cdot L_4 \right\} = \alpha \cdot |\Delta t_4| \cdot L_4$$

$$\Rightarrow \frac{1}{EA} \cdot X_4 \cdot \left\{ \sum_{i=1,i\neq 4}^{6} n_{i,4}^2 L_i + L_4 \right\} = \alpha \cdot |\Delta t_4| \cdot L_4$$

And from this should follow the expression for the SI force X_4. However, as this depends on the bar cross-sectional area A, we have obtained the stress σ_4, which is independent of A, instead of the force X_4: hence,

$$\sigma_4 = \frac{X_4}{A} = \frac{\alpha \cdot |\Delta t_4| \cdot L_4 \cdot E}{\sum_{i=1,i\neq 4}^{6} n_{i,4}^2 \cdot L_i + L_4}$$

In conclusion we can determine the stress in all the members of the truss by applying the expression

$$\sigma_i = \frac{N_i}{A} = \frac{X_4}{A} \cdot n_{i,4} = \sigma_4 \cdot n_{i,4} \quad *)$$

Note 1: All the quantities entering the problem can readily be listed in a table:

Table 4.3.1

n	$n_{i,4}$	L_i	$n_{i,4}^2 \cdot L_i$	σ_i
1	$\frac{1}{2}$	a	$\frac{a}{4}$	$\frac{\alpha \cdot |\Delta t_4| \cdot E}{5\sqrt{5} + 9}$
2	1	$2 \cdot a$	$2 \cdot a$	$\frac{2 \cdot \alpha \cdot |\Delta t_4| \cdot E}{5\sqrt{5} + 9}$
3	$\frac{1}{2}$	a	$\frac{a}{4}$	$\frac{\alpha \cdot |\Delta t_4| \cdot E}{5\sqrt{5} + 9}$
4	1	$2 \cdot a$	$2 \cdot a$	$\frac{2 \cdot \alpha \cdot |\Delta t_4| \cdot E}{5\sqrt{5} + 9}$
5	$-\frac{\sqrt{5}}{2}$	$a \cdot \sqrt{5}$	$\frac{5}{4} \cdot a \cdot \sqrt{5}$	$-\frac{\sqrt{5} \cdot \alpha \cdot |\Delta t_4| \cdot E}{5\sqrt{5} + 9}$
6	$-\frac{\sqrt{5}}{2}$	$a \cdot \sqrt{5}$	$\frac{5}{4} \cdot a \cdot \sqrt{5}$	$-\frac{\sqrt{5} \cdot \alpha \cdot |\Delta t_4| \cdot E}{5\sqrt{5} + 9}$
	$\sum_{i=1,i\neq 4}^{6}$		$\frac{a}{2} \cdot (5\sqrt{5} + 5)$	

Note 2: How can we dimension cross-section A? First we must find out if the obtained stresses satisfy the strength criterion: $|\sigma_i| \leq \sigma_{all}$ **). Since, after substituting *) into **), the cross-sectional area A is missing it is evident that this cannot yield the dimension. It seems as if we could make it almost infinitely small in order to save material. Is this true? Naturally not! We shall find the necessary magnitude of A if we satisfy the *stability* criterion as far as the members under compression are concerned. This problem, known as *buckling*, will be dealt with next term.

Note 3: If the truss is heated instead of cooled, it is evident that the SI force X_4 will be negative (compression). Since it is better to assume SI always being in tension, this will lead to an inconsistency, which can be solved by adding a negative sign on the right hand side in the deformation relation (i.e., $\partial U / \partial X_4 = -\alpha \, \Delta t \, L_4$).

5. Stress and strain

5.1 Types of stress state

Referring to Sec.1.2.2, Fig.1.2.2.1, we determined the stress state in a general body in a section parallel to the yz plane (passing through point Q), which consisted of three components σ_x, τ_{xy}, τ_{xz}. Passing a section through Q parallel to the zx plane, we similarly define the stress components σ_y, τ_{yz}, τ_{yx}. Finally, a section through Q, parallel to the xy plane yields the components σ_z, τ_{zx}, τ_{zy}. In this way we obtained a *3D (spatial) stress state* generally comprising ***nine stress components.***
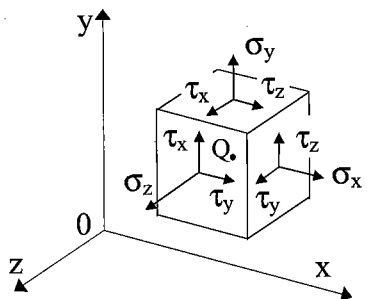
Fig.5.1.1

In the next section we will establish that, for instance, the stresses $\tau_{yx} = \tau_{xy} = \tau_z$ are *complementary shearing stresses* (they can be denoted by one subscript z, which expresses the axis to which both components are perpendicular) and in this way, we can simplify the notification of the shearing stress components, i.e.,

$$\tau_{xy} = \tau_{yx} = \tau_z; \quad \tau_{yz} = \tau_{zy} = \tau_x; \quad \tau_{zx} = \tau_{xz} = \tau_y; \text{see Fig.5.1.1.}$$

It follows from this that the stress state in an arbitrary point of a body is fully determined by ***six stress components***:

> ***three*** normal stress components... σ_x, σ_y, σ_z and
>
> ***three*** shearing stress components... τ_x, τ_y, τ_z

Fig.5.1.2

As we remarked at the time (cf. Sec.2.4), the same state of stress will be represented by a different set of components if the coordinate axes (and consequently the respective sections passing through an arbitrary point Q), are rotated, Fig.5.1.2.
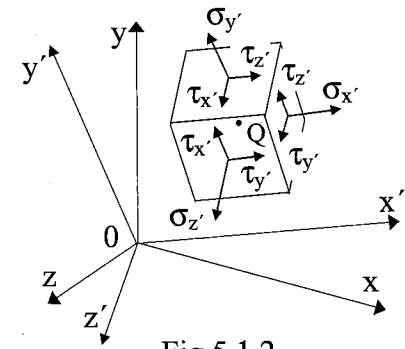
Our discussion of the transformation of stress will deal mainly with *2D (plane) stress*, i.e. with a situation in which two of the faces of the cubic element are free of stresses.

If the z axis is chosen perpendicular to these faces, we have $\sigma_z = \tau_x = \tau_y = 0$, and the only remaining stress components are : σ_x, σ_y, τ_z (cf. Sec.5.3). However, in the section 5.2, we will first conclude the discussion of the *uniaxial stress state* that we started in Section 2.4.

5.2 Uniaxial stress state; *complementary* shearing stresses

Consider now a one-force member, which is subjected to an axial force F (Fig.5.2.1). Proceeding in the same way as in Sec.2.4, we pass two sections ρ and ρ' forming an angle α with the normal plane (which is perpendicular to the rod axis) and draw the portion limited by these sections.
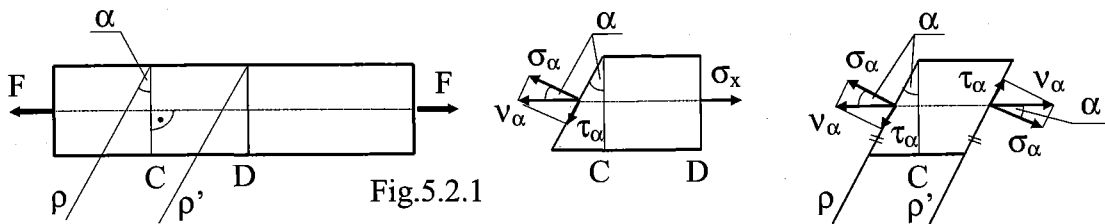
Fig.5.2.1

After decomposing F into normal N and shearing T forces, the average values of the corresponding resulting, normal and shearing stresses are the same as expressed in Eqs.(2.4.1a,b,c), from which we choose the expression for the shearing force:

$$\tau_\alpha = \frac{V}{A_\alpha} = \frac{F \cdot \sin \alpha}{\dfrac{A}{\cos \alpha}} = \sigma_x \cdot \sin \alpha \cdot \cos \alpha \qquad (5.2.1)$$

Now, we pass two other sections ψ and $\underline{\psi}$ (Fig.5.2.2), which are perpendicular to the first sections ρ and ρ' (with an angle, regarding the normal plane, of $\{\pi/2) - \alpha\}$) and having the area

$$\underline{A}_\alpha = \frac{A}{\cos\left[\left(\dfrac{\pi}{2}\right) - \alpha\right]} = \frac{A}{\sin \alpha}$$
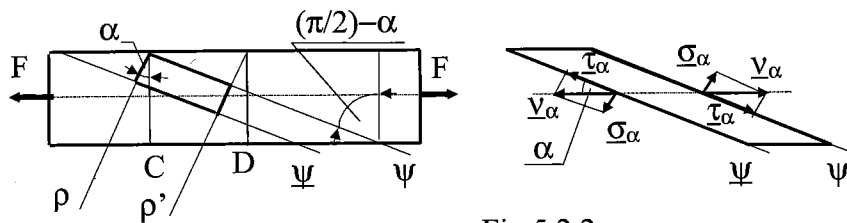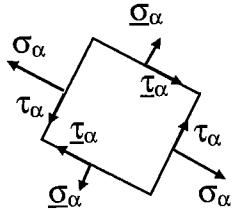
Fig.5.2.2

Acting on the section are:

normal force $\quad \underline{N} = F \cdot \cos\left[\left(\dfrac{\pi}{2}\right) - \alpha\right] = F \cdot \sin \alpha \Rightarrow \underline{\sigma}_\alpha = \dfrac{N}{\underline{A}_\alpha} = \dfrac{F \cdot \sin \alpha}{A/\sin \alpha} = \sigma_x \cdot \sin^2 \alpha$ **)

and shearing force $\quad \underline{V} = F \cdot \sin\left[\left(\dfrac{\pi}{2}\right) - \alpha\right] = F \cdot \cos \alpha \Rightarrow$

$$\underline{\tau}_\alpha = \frac{\underline{V}}{\underline{A}_\alpha} = \frac{F \cdot \cos \alpha}{A/\sin \alpha} = \sigma_x \cdot \sin \alpha \cdot \cos \alpha \qquad (5.2.2)$$

The resulting stress is $\qquad \underline{\nu}_\alpha = \dfrac{F}{\underline{A}_\alpha} = \sigma_x \cdot \sin \alpha$_

Comparing Eqs. (5.2.1) and (5.2.2), we find that

$$\tau_\alpha = \underline{\tau}_\alpha \qquad (5.2.3)$$

The relation (5.2.3) states that *the shearing stress components exerted on faces that are mutually perpendicular have equal values and their arrows point to/from the line of intersection of these faces.* This couple of shearing stresses is called **complementary** *shearing stresses*.

(Summing Eqs. (2.4.1a) and **), we find $\sigma_\alpha + \underline{\sigma}_\alpha = \sigma_x \cos^2 \alpha + \sigma_x \sin^2 \alpha = \sigma_x$)

Consequences following from *complementary shearing stresses*:

1) The *plane stress state* (Fig.5.2.3) is determined with only three stress components: σ_x, σ_y, τ_z.
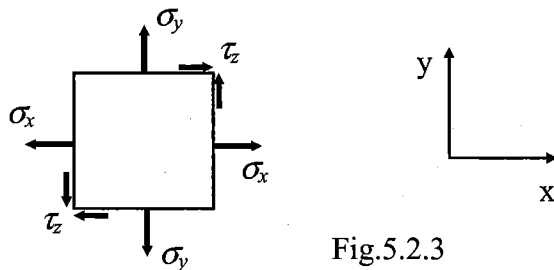
Fig.5.2.3

2) When a shearing stress is acting on a cross-section in the vicinity of the profile contour (Fig.5.2.4), then the direction of the shearing stress acts tangentially to the contour.

(If **no friction force** F_f acts on the bar surface, the stress $\tau_n = 0$: $\tau = \tau_t$)

The stress τ_n could exist only if a friction force F_f acted on the bar

resulting shear.stress
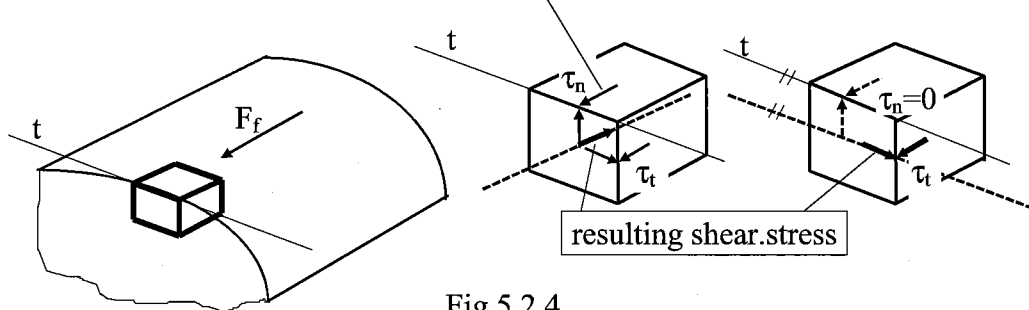
Fig.5.2.4

3) The same conclusion as for item 2) can be expressed for a corner on the profile contour (Fig.5.2.5), i.e., no shearing stress acts there, either.

4)
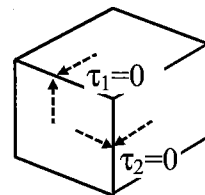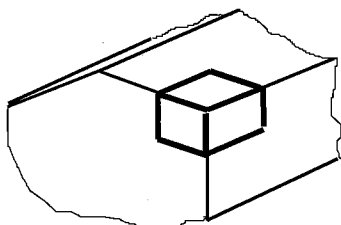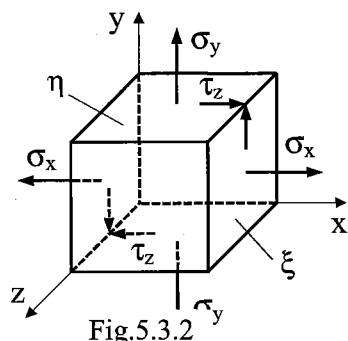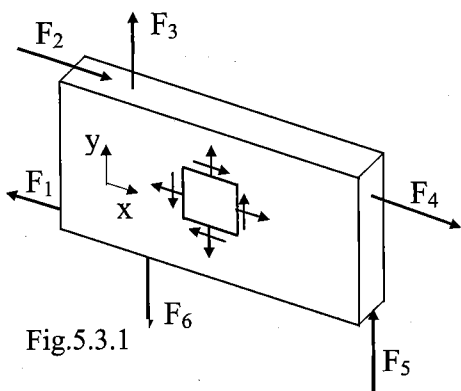
Fig.5.2.5

5.3 Plane stress state; Mohr's circle

A plane (2D) stress state occurs for instance in a thin plate subjected to forces acting in the midplane of the plate (Fig.5.3.1). In general, if an element is removed from a body it will be subjected to the normal stresses σ_x (acting on plane ξ) and σ_y (acting on plane η) together with the shearing stress τ_z (Fig.5.3.2).

Fig.5.3.1

Fig.5.3.2

5.3.1 Stresses in an inclined plane

To determine stress components associated with the element in Fig.5.3.2, after it has been rotated through an angle α about the z axis, we need to determine the stress components in an inclined plane ρ forming an angle α with the ξ plane, see Fig.5.3.3.

a)   b)   c)
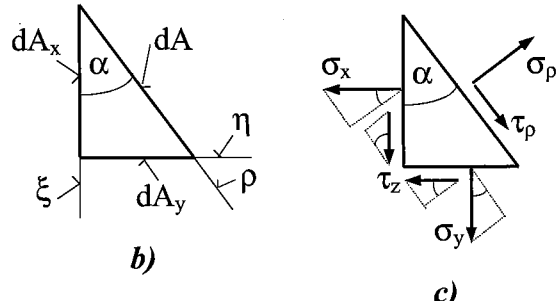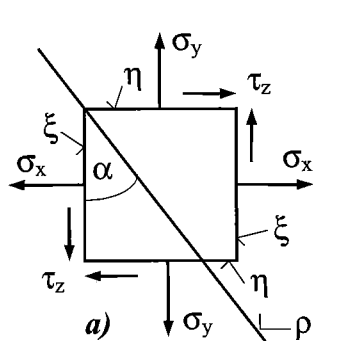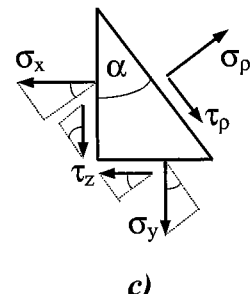
Fig.5.3.3

If we cut the element containing a given stress state σ_x, σ_y, τ_z by the ρ plane into two parts we must supply components σ_ρ and τ_ρ acting on the plane ρ in order to hold the separated portions in static equilibrium (Fig.5.3.3c). If we denote as dA the area cut in the element by plane ρ (Fig.5.3.3b), then for the areas belonging to the planes ξ and η, respectively, it holds

$$dA_x = dA \cdot \cos\alpha \qquad\qquad dA_y = dA \cdot \sin\alpha, \qquad\qquad (5.3.1a,b)$$

The subsequent equations of static equilibrium for forces acting in the σ_ρ and τ_ρ directions, respectively, are written, utilizing Figs.5.3.3b,c, in the forms

$$\sigma_\rho \cdot dA - \sigma_x \cdot \cos\alpha \cdot dA_x - \tau_z \cdot \sin\alpha \cdot dA_x - \sigma_y \cdot \sin\alpha \cdot dA_y - \tau_z \cdot \cos\alpha \cdot dA_y = 0$$

$$\tag{5.3.2a,b}$$

$$\tau_\rho \cdot dA - \sigma_x \cdot \sin\alpha \cdot dA_x + \tau_z \cdot \cos\alpha \cdot dA_x + \sigma_y \cdot \cos\alpha \cdot dA_y - \tau_z \cdot \sin\alpha \cdot dA_y = 0$$

Applying Eqs. (5.3.1a,b) in Eqs.(5.3.2a,b) we have after arrangements

$$\sigma_\rho = \sigma_x \cdot \cos^2\alpha + \sigma_y \cdot \sin^2\alpha + 2 \cdot \tau_z \cdot \sin\alpha \cdot \cos\alpha \tag{5.3.3a}$$

$$\tau_\rho = \left(\sigma_x - \sigma_y\right) \cdot \sin\alpha \cdot \cos\alpha - \tau_z \cdot \left(\cos^2\alpha - \sin^2\alpha\right) \tag{5.3.3b}$$

Introducing the following functions of double angles

$$\sin^2\alpha = \frac{1-\cos 2\alpha}{2} \quad , \quad \cos^2\alpha = \frac{1+\cos 2\alpha}{2} \quad a \quad \sin\alpha\cdot\cos\alpha = \frac{1}{2}\cdot\sin 2\alpha$$

we obtain Eqs. (5.3.3a,b) in the form

$$\sigma_\rho = \frac{\sigma_x+\sigma_y}{2}+\frac{\sigma_x-\sigma_y}{2}\cdot\cos 2\alpha+\tau_z\cdot\sin 2\alpha \tag{5.3.4a}$$

$$\tau_\rho = \frac{\sigma_x-\sigma_y}{2}\cdot\sin 2\alpha-\tau_z\cdot\cos 2\alpha \tag{5.3.4b}$$

By means of Eqs. (5.3.4a,b) we can determine the stress state σ_ρ, τ_ρ in an arbitrary inclined plane ρ based on a known plane stress state σ_x, σ_y, τ_z.

5.4 Mohr's circle for stress

All of the information contained in the above equations may be presented in a convenient graphical form known as *Mohr's circle*. In this representation normal stresses are plotted along the horizontal axis and shearing stresses along the vertical axis. The stresses σ_x, σ_y, and τ_z are plotted to scale and one member following one from Eqs.(5.3.4a,b) is successively interpreted in a geometric manner, see Fig.5.4.1, e.g.,

- the first member in Eq.(5.3.4a) represents the distance of the <u>circle centre C</u> (situated on the horizontal axis) which does not change its position when angle α varies;
- by combination of Eqs.(5.3.4a,b), with the exception of the first member in Eq.(5.3.4a), the triangle CRT is obtained, the shape and size of which does not change when angle α varies. The triangle CRT, when rotating about the centre C, creates a circle whose radius is defined by the hypotenuse of the triangle

$$r = \overline{CT} = \sqrt{\overline{CR}^2+\overline{RT}^2} = \sqrt{\left(\frac{\sigma_x-\sigma_y}{2}\right)^2+\tau_z^2}$$
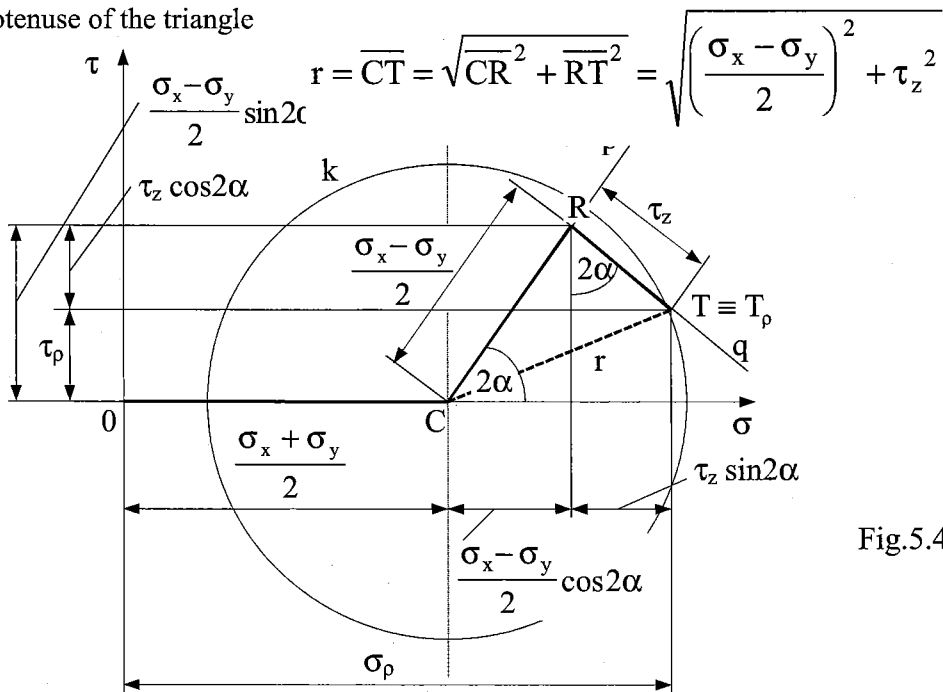
Fig.5.4.1

Thus, the point $T \equiv T_\rho$, lying on the circle and having coordinates σ_ρ, τ_ρ, represents the transformation of the original stress state (σ_x, τ_z), existing in the plane ξ, into the inclined plane ρ

when the plane ξ has been rotated (counterclockwise) by angle α, see Fig.5.3.3a, which is for better illustration introduced again as Fig.5.4.2a in this section. Therefore, we can return to the original stress state in the plane ξ when rotating back (clockwise) by angle α, which means that we put $\alpha = 0$ in Eqs.(5.3.5a,b). This substitution yields $\sigma_\xi = \sigma_x$ and $\tau_\xi = -\tau_z$, and the plane ρ will identify with ξ (Fig.5.4.2b). The triangle CRT will rotate by the <u>double</u> angle 2α and will occupy the hatched triangle $CR'T'$, where $T' \equiv T_\xi$ denotes the plane ξ position. The section η includes the angle $\pi/2$ with the section ξ. The stress state in the plane η will be <u>computed</u> when we substitute the double angle $2\alpha = \pi$ into Eqs. (5.3.5a,b), obtaining $\sigma_\eta = \sigma_y$ and $\tau_\eta = \tau_z$, and <u>plotted</u> as T_η in Fig.5.4.2b when we rotate the triangle $CR'T'$ by $2\alpha = \pi$. When summing the knowledge obtained above, and comparing Figs. 5.4.2a and 5.4.2b, we recognize that:

i) stress components σ_ρ, τ_ρ exerting in any section ρ carried out at a given point of a stressed body correspond to a certain point T_ρ on the Mohr's circle that was determined for the corresponding stress state;

ii) the position of such a section ρ in a stressed body is given by angle α, while the position of the corresponding point T_ρ on Mohr's circle is obtained by angle 2α, which is carried out in the same orientation (clockwise or counterclockwise) as angle α was determined in the element;
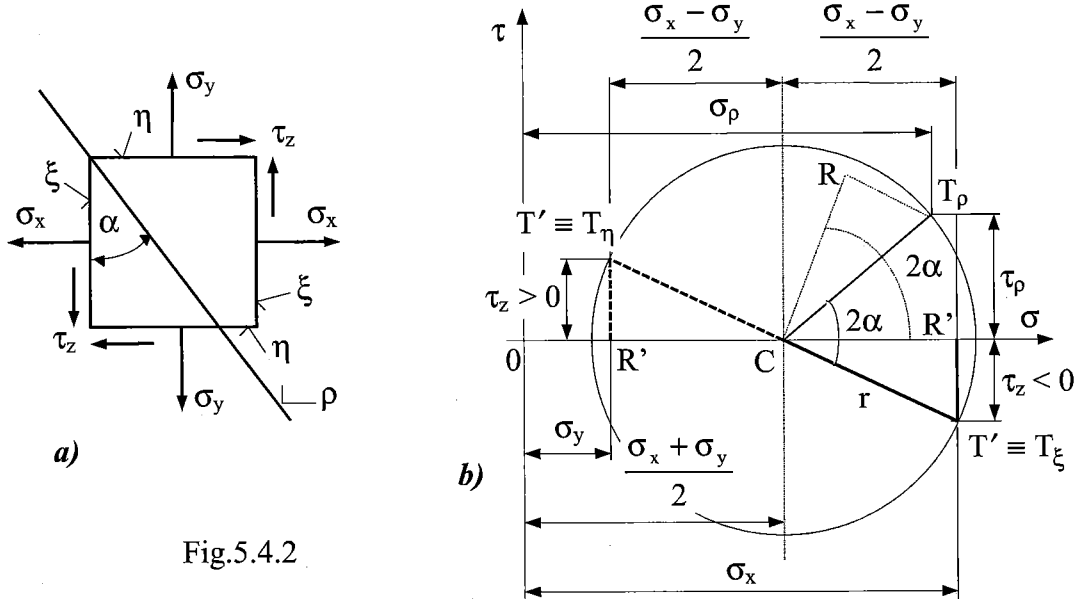
Fig.5.4.2

iii) with reference to the original rectangular element in Fig.5.4.2a, we shall introduce <u>the sign convention that *shearing stresses*</u> (applied to the Mohr's circle plotting (see Fig.5.4.2b)) <u>are positive if they tend to rotate the element clockwise, negative if they tend to rotate it counterclockwise;</u>

iv) based on the facts and rules presented above, <u>the procedure for constructing Mohr's circle can be described:</u>

knowing the stresses (σ_x, σ_y, and τ_z) exerting in two mutually perpendicular sections (ξ and η), the respective points T_ξ and T_η can be plotted in the Cartesian coordinates σ and τ, the connecting line of these points, representing the diameter of Mohr's circle, intersects the coordiante σ in the centre of the circle which can subsequently be drawn.

5.5 Principal stresses and principal planes

A plane stress state σ_x, σ_y, τ_z (Fig.5.5.1a) is plotted by means of Mohr's circle in Fig.5.5.1b.
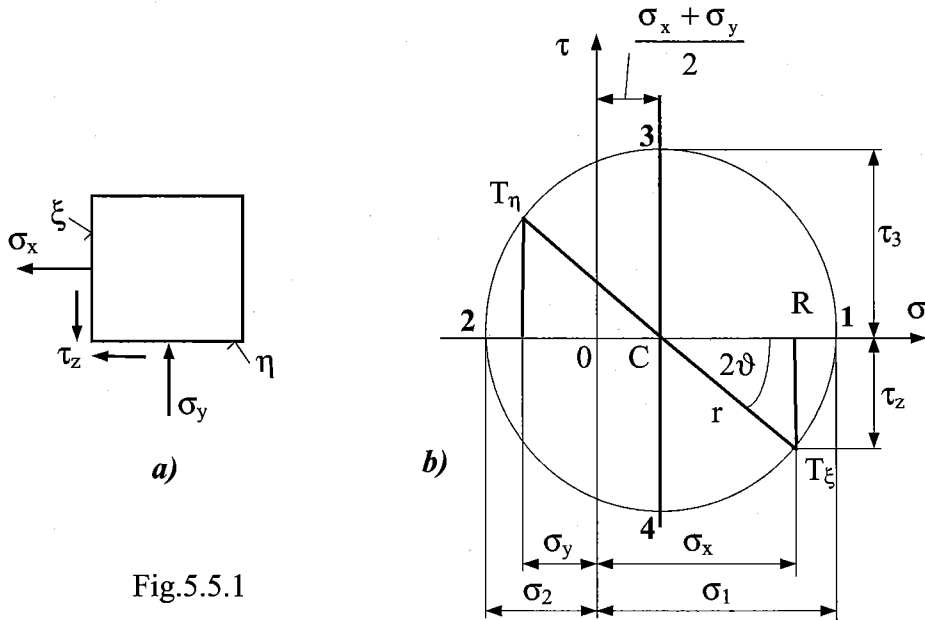
Fig.5.5.1

The two points *1* and *2* where the circle of Fig.5.5.1b intersects the horizontal axis are of special interest. Point *1* corresponds to the maximum value of the normal stress σ, while point *2* corresponds to its minimum value. In addition, these two points correspond to a zero value of the shearing stress τ. Thus the values ϑ of the parameter α, which corresponds to points *1* and *2*, may be obtained by setting $\tau_p = 0$ in Eq.5.3.4b. We write
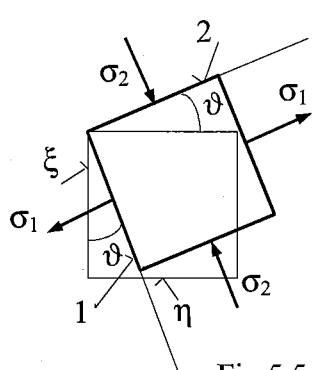
Fig.5.5.1c

$$tg2\vartheta = \left|\frac{2 \cdot \tau_z}{\sigma_x - \sigma_y}\right| \qquad (5.5.1)$$

This equation, defining the two values 2ϑ which are $180°$ apart, and thus the two values ϑ which are $90°$ apart, can be obtained geometrically when observing the triangle CRT_ξ in Fig.5.5.1b. Either of these values may be used to determine the orientation of the corresponding element (Fig.5.5.1c). The planes *1* and *2* containing the faces of the element obtained in this way are called the *principal plane of stress* at a given point (Q - see Fig.5.1.1) of a body, and the corresponding values $\sigma_{max} = \sigma_1$ and $\sigma_{min} = \sigma_2$ of the

normal stress exerted on these planes are called the *principal stresses* at Q. Since the two values ϑ defined by Eq.5.5.1 were obtained by setting $\tau_p = 0$ in Eq.5.3.4b, it is clear that no shearing stress is exerted on the principal planes.

We observe from Fig.5.5.1b that

$$\sigma_{1,2} = \overline{OC} \pm r = \sigma_{ave} \pm r$$

or

$$\sigma_{1,2} = \frac{\sigma_x + \sigma_y}{2} \pm \sqrt{\left(\frac{\sigma_x - \sigma_y}{2}\right)^2 + \tau_z^{\,2}} \qquad (5.5.2)$$

We can tell by inspection which of the two principal planes is subjected to σ_{max} and which to σ_{min}.

Referring again to the circle of Fig.5.5.1b, we note that the points *3* and *4* located on the vertical diameter of the circle correspond to the largest numerical value of the shearing stress $\tau_3 = \tau_4$. Observing from Fig.5.5.1b that the maximum value of the shearing stress is equal to the radius r of the circle, and recalling the second member in Eq.(5.5.2), we write

$$\tau_{3,4} = \frac{\sigma_1 - \sigma_2}{2} = \sqrt{\left(\frac{\sigma_x - \sigma_y}{2}\right)^2 + \tau_z^{\,2}} \qquad (5.5.3)$$
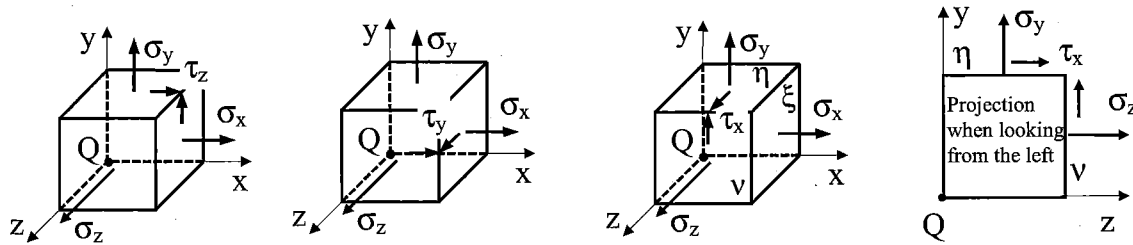
Likewise, it can be observed from Fig.5.5.1 that the normal stress corresponding to the conditions of maximum shearing stress is

$$\sigma_{3,4} = \sigma_{ave} = \frac{\sigma_1 + \sigma_2}{2} = \frac{\sigma_x + \sigma_y}{2} \qquad (5.5.4)$$

5.6 Application of Mohr's circle to various types of stress analysis

5.6.1 3D analysis of stress

If the elements shown in Fig.5.6.1.1a,b are rotated about one of the principal axes (i.e., an axis along which one of the principal stresses is exerted) at Q, say the $x \equiv 1$ axis, see Fig.5.6.1.1b, the corresponding transformation of stress may be analyzed by means of Mohr's circle as if it were a transformation of plane stress.

a)   Fig.5.6.1.1   *b)*

Indeed, the shearing stresses exerted on the faces perpendicular to the z axis remain equal to zero, and the normal stress $\sigma_x \equiv \sigma_1$ is perpendicular to the plane yz in which the transformation takes place and, thus, does not affect this transformation. From this it follows that, when first rotating the element

about the $x \equiv 1$ axis, the other principal axes (and Principal planes) *2* and *3* (and self-evidently the principal stresses σ_2 and σ_3) can be determined. We may therefore draw two additional Mohr's circles of diameter *12* and *13*. Thus, we use the circle of diameter *23* to determine the normal and shearing stresses exerted on the faces of the element as it is rotated about the $x \equiv 1$ axis: see Figs.5.6.1.1*b* and 5.6.1.2, where, for better understanding, concrete numerical values of the stresses (σ_x = 60 MPa, σ_y = 18 MPa, σ_z = -30 MPa, τ_x =30 MPa) were applied. Similarly, circles of diameter *12* and *13* may be used to determine the stresses on the element as it is rotated about the *2* and *3* axes, respectively. While our analysis will be limited to rotations about the principal axes, it could be shown that any other transformation of axes would lead to stresses represented in Fig.5.6.1.2 by a point located within the shaded area. Thus, the radius of the largest of the three circles yields the maximum value of the shearing stress at point Q. Noting that the diameter of that circle is equal to the difference between σ_{max} and σ_{min}

we write

$$\tau_{max} = \frac{1}{2} \cdot |\sigma_{max} - \sigma_{min}| \qquad (5.6.1.1)$$

Graphical solution:

Scale of stress

0 10 20 30 40 50
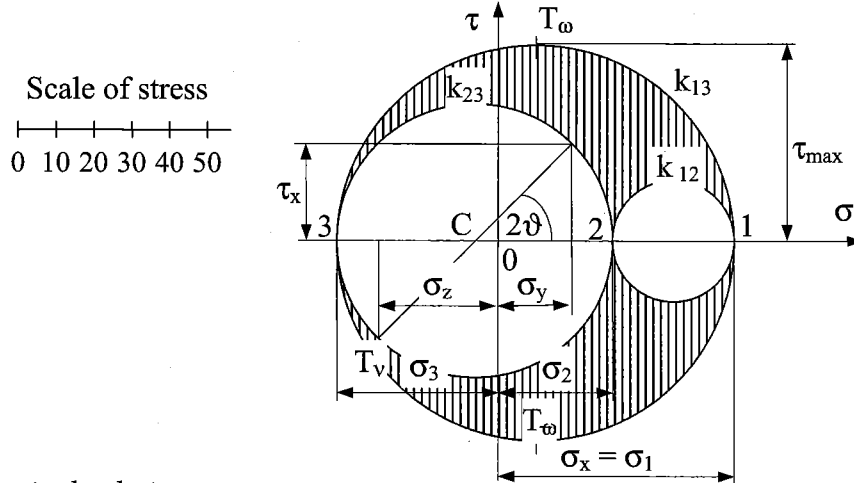
Fig.5.6.1.2

Numerical solution:

Principal stresses σ_2 and σ_3 are obtained by Eq.(5.5.2) adapted for other respective subscripts as follows

$$\sigma_{2,3} = \frac{\sigma_y + \sigma_z}{2} \pm \sqrt{\left(\frac{\sigma_y - \sigma_z}{2}\right)^2 + \tau_x^2} = \frac{18 + (-30)}{2} \pm \sqrt{\left[\frac{18 - (-30)}{2}\right]^2 + 30^2} =$$

$$= -6 \pm 38.4 = \left\langle \begin{array}{l} 32.4 \ [\text{MPa}] \\ -44.4 \ [\text{MPa}] \end{array} \right.$$

while the third principal stress has been determined as

$$\sigma_1 = \sigma_x = 60 \ \text{MPa}$$

The maximum shearing stress is computed from Eq.(5.6.1.1) in the form

$$\tau_{max} = \frac{\sigma_1 - \sigma_3}{2} = \frac{60 - (-44.4)}{2} = 52.2 \quad [\text{MPa}]$$

To determine positions of the principal planes 2 and 3 we apply Eq. (5.5.1)

$$\text{tg } 2\vartheta = \left| \frac{2 \cdot \tau_x}{\sigma_y - \sigma_z} \right| = \left| \frac{2 \cdot 30}{18 - (-30)} \right| = 1.25$$

$2\vartheta = 51^\circ 20'$ and thus $\vartheta = 25^\circ 40'$, which coincide with the graphical solution.
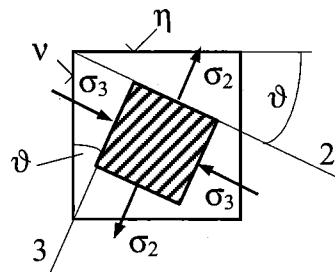
Fig.5.6.1.3

5.6.2 Particular cases of 2D analysis of stress

Let us now return to the particular case of *plane stress*, which was discussed in Secs.5.3 through 5.6.1. We recall that, if x and y are selected in the plane of stress, we have $\sigma_z = \tau_x = \tau_y = 0$. This means that the z axis, i.e., the axis perpendicular to the xy plane of stress, is one of the three principal axes of stress and the xy plane is one of the three principal planes (which is then denoted, for instance, as plane $xy \equiv 3$, see Fig.5.6.2.1). In a Mohr's-circle diagram, this axis corresponds to the origin 0, where $\sigma = \tau = 0$. We also recall that the other two principal axes and planes correspond to points 1 and 2, where Mohr's circle for the $xy \equiv 3$ plane intersects the σ axis. If 1 and 2 are located on opposite sides of the origin O (Fig.5.6.2.1), the corresponding principal stresses represent the maximum and minimum normal stresses at point Q, and the maximum shearing stress is equal to the maximum "in-plane" shearing stress. As noted in Sec.5.5, the planes of maximum shearing stress correspond to points 3 and 4 of Mohr's circle (Fig.5.5.1b), and are at 45° to the principal planes corresponding to points 1 and 2. They are, therefore, the shaded diagonal planes shown in Figs.5.6.2.2a,b.
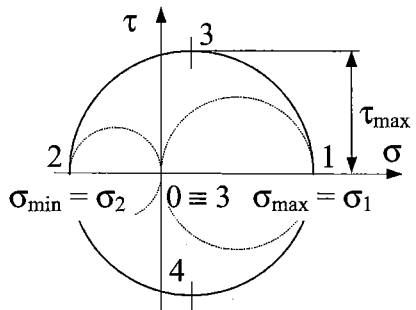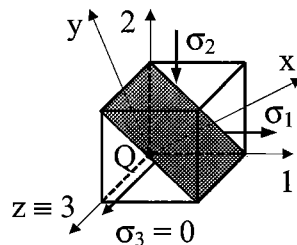
Fig.5.6.2.1

a) Fig.5.6.2.2 *b)*
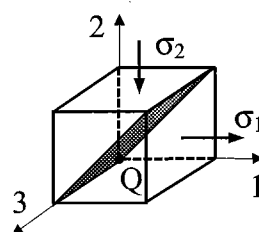
If, on the other hand, *1* and *2* are on the same side of *0*, that is, if σ_1 and σ_2 have the same sign, then the circle defining σ_{max}, σ_{min} and τ_{max} is *not* the circle corresponding to a transformation of stress within the *xy* plane. If $\sigma_1 > \sigma_2 > 0$, as assumed in Fig.5.6.2.3, we have $\sigma_{max} = \sigma_1$, $\sigma_{min} = \sigma_2$, and τ_{max} is equal to the radius of the circle defined by points $O \equiv 3$ and *1*, that is $\tau_{max} = (1/2).\sigma_{max}$. We also note that the planes of maximum shearing stress are obtained by rotating through 45° within the *13* planes. Thus, the planes of maximum shearing stress are the shaded diagonal planes shown in Figs.5.6.2.4*a,b*.

Fig.5.6.2.3

a) b)
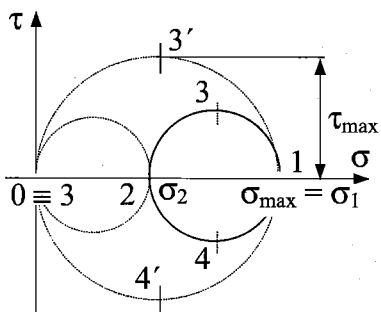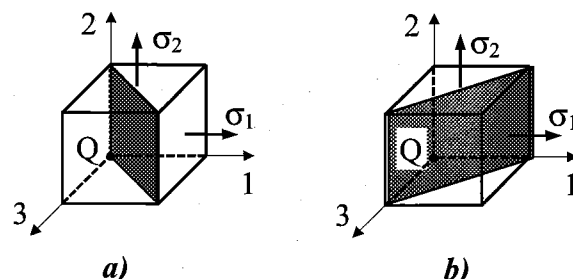
Fig.5.6.2.4

All variations occurring in cases of *plane stress* are for illustration arranged below in Figs.5.6.2.5*a,b*; Figs.5.6.2.6*a,b* and Figs.5.6.2.7*a,b*.

i)

$$\sigma_1 > \sigma_2 > 0 ; \sigma_3 = 0$$
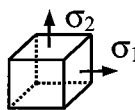
Fig.5.6.2.5*a*
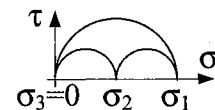
Fig.5.6.2.5*b*

ii)

$$\sigma_1 = 0 ; \sigma_3 < \sigma_2 < 0$$
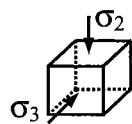
Fig.5.6.2.6*a*

Fig.5.6.2.6*b*

iii)
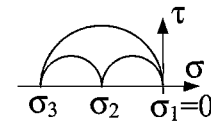
Fig.5.6.2.7*a*

$$\sigma_1 > 0 ; \sigma_2 = 0 ; \sigma_3 < 0$$
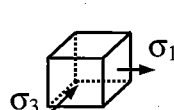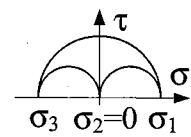
Fig.5.6.2.7*b*

5.6.3 Uniaxial stress state from the standpoint of 3D analysis of stress

Simple tension (or compression) executed in the *1* direction is a uniaxial stress state which can be interpreted as $\sigma_1 = F / A$ and $\sigma_2 = \sigma_3 = 0$ (Fig.5.6.3.1). The corresponding Mohr's diagram is constructed in Fig.5.6.3.2.
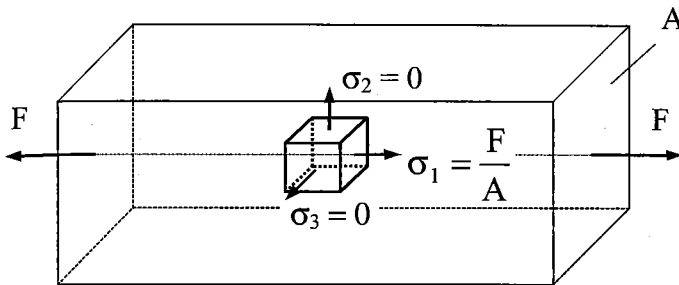
Fig.5.6.3.1
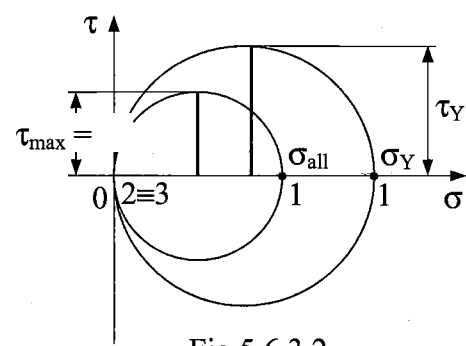
Fig.5.6.3.2

Points *2* and *3* (representing principal planes perpendicular to principal plane *1*) coincide and are placed in the origin *0*, in such a way that the circles between the principal planes *1* and *2* and the principal planes *1* and *3* coincide while the circle between the principal planes *2* and *3* degenerates in a point. Maximum shearing stress, being determined by the difference of the extreme principal

stresses, is defined by

$$\tau_{max} = \frac{\sigma_1}{2}$$

(5.6.3.1)

and is exerted in all the sections (in an infinite number) which include angle $\pi/2$ regarding the *1* direction. Eq.(5.6.3.1) can serve for <u>determining the limit values for shearing stress</u> in a tensile-test specimen based on corresponding limit values of normal stress, e.g.

yielding stress in shear... $\tau_Y = \dfrac{\sigma_Y}{2}$; allowable stress in shear... $\tau_{all} = \dfrac{\sigma_{all}}{2}$; etc. (5.6.3.2)

5.7 Stresses and strains in pure shear

When a circular bar (cf. Sec.8.1), either solid or hollow, is subjected to torsion, <u>shear</u> stresses act over the cross sections and on the longitudinal planes (Fig.5.7.1*a*). Such a type of <u>plane stress,</u> which is called *pure shear,* is represented by one couple of complementary shearing stress τ_z, while normal stresses are equal to zero, i.e., $\sigma_x = \sigma_y = 0$ (Fig.5.7.1*b*). Since twisted shafts are very important machine elements it is evident that <u>pure shear deserves special attention</u>. (This stress type occurs, self-evidently, not only with torsion but with many other stressed elements.)

Fig.5.7.1

a)

b)
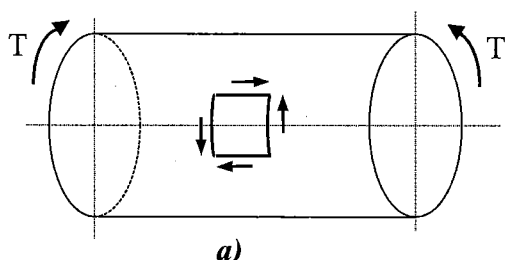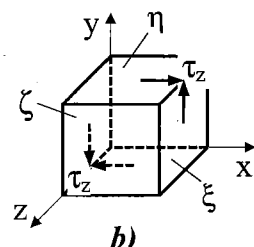
Mohr's diagram for pure shear (from the standpoint of 3D stress state) is shown in Fig.5.7.2a.
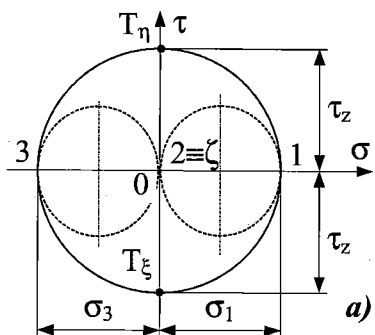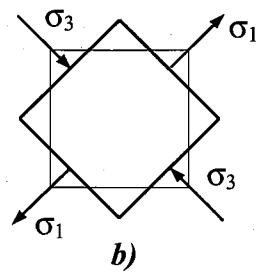
Fig.5.7.2

From Mohr's circle we can easily establish the principal stresses

$$\sigma_1 = \tau_z \ ; \qquad\qquad \sigma_2 = 0 \qquad\qquad \sigma_3 = -\tau_z$$

and the principal planes from which the planes *1* and *3* are oriented at an angle of 45° with regard to the respective original planes ξ and η, while the principal plane *2* (coinciding with the plane of the paper) is unchanged, see Fig.5.7.2b.

Strains corresponding to pure shear are shown in Fig.5.7.3, where the deformations are greatly exaggerated. The *shear strain* γ is the change in angle between two lines that were originally perpendicular to each other. Thus, the decrease in the angle at the lower left-hand corner of the element is the shear strain γ (measured in radians). This same change in angle occurs at the upper right-hand corner, where the angle decreases, and at the two other corners, where the angles increase. However, the lengths of the sides of the element, including the thickness perpendicular to the plane of the paper (xy), do not change when these shear deformations occur. Therefore, the element changes its shape from a rectangular parallelepiped (Fig.5.7.1b) to an oblique parallelepiped (Fig.5.7.3a). This change in shape is called *shear distortion*. If the material is linearly elastic, the shear stress for the element in Fig.5.7.1b is related to the shear strain by *Hooke's law in shear*:

$$\tau = \gamma \cdot G \qquad\qquad (5.7.1)$$

where the symbol G represents the **shear modulus of elasticity**.
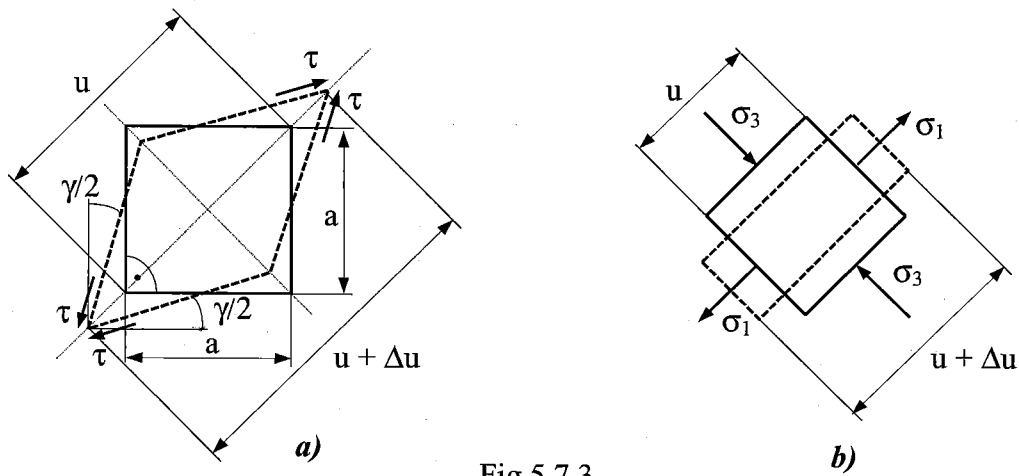
Fig.5.7.3

We can obtain a <u>relationship among the three material constants E, G and μ.</u> For this purpose, we utilize a comparison between Fig.5.7.3a and Fig.5.7.3b. Based on Fig.5.7.3a, we have

$$\frac{u + \Delta u}{2} = a \cdot \cos\left(\frac{\pi}{4} - \frac{\gamma}{2}\right) \Rightarrow u + \Delta u = a \cdot \sqrt{2}\left(\cos\frac{\gamma}{2} + \sin\frac{\gamma}{2}\right)$$

and since shearing strain γ is a very small quantity it holds

$$\cos\frac{\gamma}{2} \approx 1 \quad \text{and} \quad \sin\frac{\gamma}{2} \approx \frac{\gamma}{2}$$

Thus, we have

$$u + \Delta u = a \cdot \sqrt{2}\left(1 + \frac{\gamma}{2}\right) = u \cdot \left(1 + \frac{\gamma}{2}\right) \Rightarrow \Delta u = u \cdot \frac{\gamma}{2}$$

Substituting Hooke's law for shear, Eq.(5.7.1), into the last expression we have

$$\Delta u = \frac{u}{2} \cdot \frac{\tau_z}{G} \qquad (5.7.2a)$$

It is clear from Fig.5.7.3b that the expression for the diagonal elongation Δu can also be based on the principal stresses and we can write

$$\varepsilon_u = \frac{\Delta u}{u} = \frac{1}{E} \cdot \left[\sigma_1 - \mu \cdot \sigma_3\right] = \frac{\tau_z}{E} \cdot \left(1 + \mu\right) \Rightarrow \Delta u = u \cdot \frac{\tau_z}{E} \cdot \left(1 + \mu\right) \quad (5.7.2b)$$

where we have substituted *the generalized Hooke's law* (see Sec.5.8) since it is concerned with the plane stress state.

Comparing Eqs.(5.7.2a,b), we have

$$\frac{E}{G} = 2\left(1 + \mu\right) \qquad (5.7.3)$$

which is the relationship sought among the three elastic constants <u>holding for *homogeneous and isotropic* materials</u>.

5.8 Strain in the case of a 3D stress state; generalized Hooke's law

5.8.1 <u>Multiaxial loading</u>

We shall now consider a structural element subjected to loads acting in the directions of the principal axes and thus producing normal (principal) stresses σ_1, σ_2 and σ_3 which are all different from zero. This condition is referred to as *multiaxial loading*. In order to express the strain components ε_1, ε_2 and ε_3 in terms of the exerted stress components, we shall consider separately the effect of each element and combine the results obtained. The approach we propose will be used separately and is based on the *principle of superposition*. (We have already learned (cf. Sec.2.10) that this principle states that the effect of a given combined loading on a structure may be obtained by *determining separately the effects of the various loads and combining the results obtained*, providing that the following

conditions are satisfied: i) each effect is linearly related to the load which produces it; ii) the deformation resulting from any given load is small and does not affect the conditions of application of other loads. In the case of multiaxial loading, the first condition will be satisfied if the stresses do not exceed the proportional limit of the material, and the second condition will also be satisfied if the stress on any given face does not cause deformations of the other faces that are large enough to affect the computation of the stresses on those faces.)

Considering first the effect of the stress component σ_1, we recall from Sec.2.8 that σ_1 causes a strain equal to σ_1/E in the **1** axis direction, and strains equal to $-\mu\,\sigma_1/E$ in each of the **2** and **3** directions. Similarly, the stress component σ_2, if applied separately, will cause a strain σ_2/E in the **2** direction and strains $-\mu\,\sigma_2/E$ in the other two directions. Finally, the stress component σ_3 acts analogously. Combining the results obtained, we conclude that the components of strain corresponding to the given multiaxial loading are

$$\varepsilon_1 = \frac{1}{E} \cdot \left[\sigma_1 - \mu \cdot (\sigma_2 + \sigma_3)\right] \tag{5.8.1.1a}$$

$$\varepsilon_2 = \frac{1}{E} \cdot \left[\sigma_2 - \mu \cdot (\sigma_3 + \sigma_1)\right] \tag{5.8.1.1b}$$

$$\varepsilon_3 = \frac{1}{E} \cdot \left[\sigma_3 - \mu \cdot (\sigma_1 + \sigma_2)\right] \tag{5.8.1.1c}$$

5.8.2 Complex loading (a general stress condition)

For the general stress condition represented by stress components σ_x, σ_y, σ_z, τ_x, τ_y, and τ_z (Fig.5.1.1), and as long as none of the stresses involved exceeds the corresponding proportional limit, we may apply the principle of superposition and combine the results obtained in preceding sections.

We first use Eqs.(5.8.1.1a,b,c), while considering the directions x, y and z instead of the principal directions **1, 2** and **3** :

$$\varepsilon_x = \frac{1}{E} \cdot \left[\sigma_x - \mu \cdot (\sigma_y + \sigma_z)\right]$$

$$\varepsilon_y = \frac{1}{E} \cdot \left[\sigma_y - \mu \cdot (\sigma_z + \sigma_x)\right] \tag{5.8.2.1a,b,c}$$

$$\varepsilon_z = \frac{1}{E} \cdot \left[\sigma_z - \mu \cdot (\sigma_x + \sigma_y)\right]$$

which can easily be proved.

Then we add corresponding expressions for shearing stresses based on Eq.(5.7.1) as follows:

$$\gamma_x = \frac{\tau_x}{G} \; ; \; \gamma_y = \frac{\tau_y}{G} \; ; \; \gamma_z = \frac{\tau_z}{G} \tag{5.8.2.2a,b,c}$$

Eqs. (5.8.1.1a,b,c) or the set of Eqs. (5.8.2.1a,b,c) and (5.8.2.2a,b,c) are called *generalized Hooke's law*.

5.8.3 Mohr's circle for plane strain

It can be proved that, analogously to plane stress, we can obtain the relations

$$\varepsilon_\alpha = \frac{\varepsilon_x + \varepsilon_y}{2} + \frac{\varepsilon_x - \varepsilon_y}{2} \cdot \cos 2\alpha + \frac{\gamma_z}{2} \cdot \sin 2\alpha \qquad (5.8.3.1a)$$

$$\frac{\gamma_\alpha}{2} = \frac{\varepsilon_x - \varepsilon_y}{2} \cdot \sin 2\alpha - \frac{\gamma_z}{2} \cdot \cos 2\alpha \qquad (5.8.3.1b)$$

describing both normal strain ε_α and shearing strain γ_α in a general direction given by angle α.

(To derive these relations we start from the deformation of a rectangle in Fig.5.8.3.1, where its deformed shape is plotted with dashed lines. Neglecting small quantities of higher orders, we obtain

$$\Delta u = \left(a \cdot \varepsilon_x + b \cdot \gamma_z\right) \cdot \cos \alpha + b \cdot \varepsilon_y \cdot \sin \alpha \Rightarrow$$

$$\varepsilon_\alpha = \frac{\Delta u}{u} = \left(\frac{a}{u} \cdot \varepsilon_x + \frac{b}{u} \cdot \gamma_z\right) \cdot \cos \alpha + \frac{b}{u} \cdot \varepsilon_y \cdot \sin \alpha$$

After substituting $a/u = \cos\alpha$ and $b/u = \sin\alpha$ and applying known trigonometric relations, we will arrive at Eq.(5.8.3.1a). Based on a comparison of Eq.(5.3.4a) with

Fig.5.8.3.1

Eq.(5.8.3.1a), it follows that the normal stresses σ_x, σ_y correspond to the normal strains ε_x, ε_y, and, consequently, the shearing stress τ_z must correspond to one half of the shearing strain, i.e., $\gamma_z/2$. Analogously, based on Eq.(5.3.4b), we can write Eq.(5.8.3.1b)).

Since the equations for the transformation of plane strain are of the same form as the equations for the transformation of plane stress, the use of Mohr's circle may be extended to the analysis of plane strain. Constructing a plane coordinate system, we plot the normal strain components ε_x, ε_y on the abscissa and one half of the shearing strain component $\gamma_z/2$ on the ordinate. (An example, related with strains assessed by experiments, is presented in the next -5.9.2- section)

5.9 Examples on stress/strain states

5.9.1 3D stress state solvable by the Mohr's circle method.

Given: *Stress state:* $\sigma_x = -40 \ N/mm^2$, $\sigma_y = 10 \ N/mm^2$, $\sigma_z = 30 \ N/mm^2$, $\tau_y = -20 \ N/mm^2$

Plane ρ: inclined from plane yz about angle $\alpha = 30^o$

Task: Determine *principal stresses $\sigma_{1,2,3}$, principal planes 1,2,3, maximum shearing stress τ_{max}* and *the stresses in the given inclined plane ρ (σ_p, τ_p)*
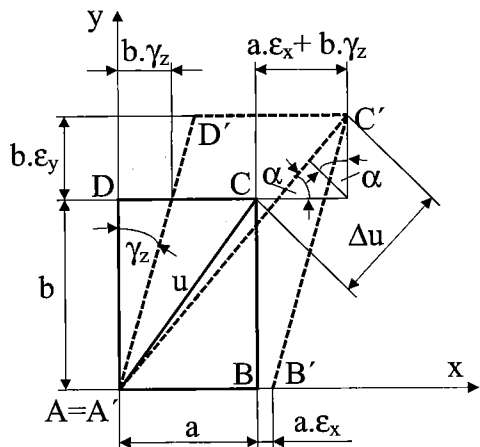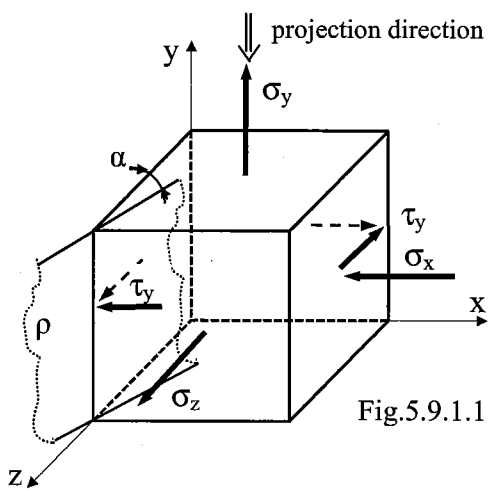
Solution: First draw a cube where the stress-state given is illustrated (all stresses are drawn according their signs, _Fig.5.9.1.1_):

i/ no problem is with normal stresses $\sigma_{x,y,z}$;

ii/ but mind that the shearing stress, $\tau_y = -20 \ N/mm^2$, having negative sign, has to be pointed in negative semi-axes x and z, and, after having done it, the origin negative sign is not further considered and <u>the shearing stress sign will be subject to a **different rule** when drawing the respective Mohr's circle.</u>
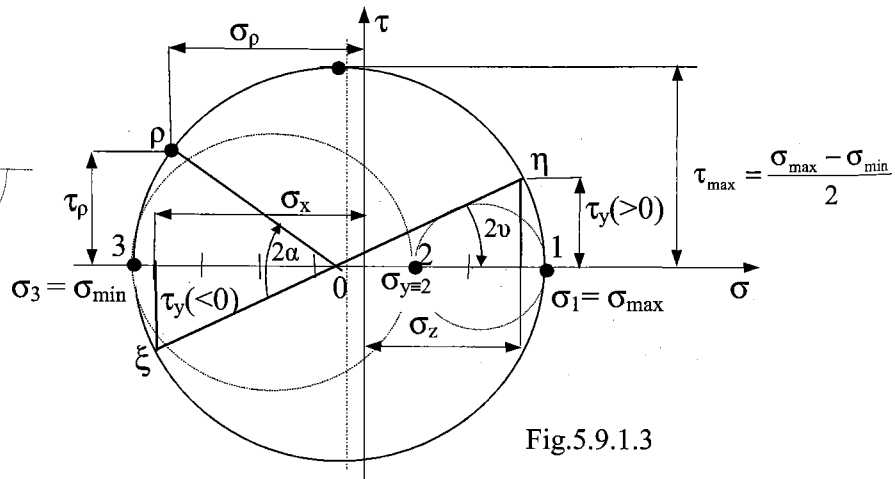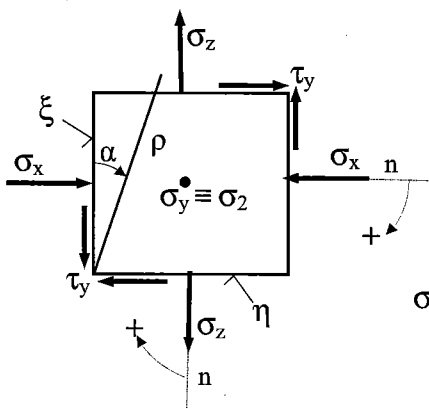
This rule says: When the normal of a plane is turned clockwise and falls to a shearing stress positive direction (Fig.5.9.1.2), then such a shearing stress shall be positive (and vice versa) in the respective Mohr's circle (Fig.5.9.1.3).

Fig.5.9.1.1

<u>Mohr's Circle method for a 3D stress state can be applied only when at least one of the planes is a principle plane.</u> When checking the stress state given, we see that in the plane having its normal parallel with y-axis is not a shearing stress, i.e., this plane is a principle one (say 2) and thus

$$\sigma_y \equiv \sigma_2 = 10 \ N/mm^2.$$

Then, when projecting the 3D stress state in the direction of y-axis, we obtain a partial 2D stress state where the principal stress σ_2 plays no role in equilibrium equations and Mohr's Circle method can be applied.

Fig.5.9.1.2

$$\tau_{max} = \frac{\sigma_{max} - \sigma_{min}}{2}$$

Fig.5.9.1.3

Numerical solution:

Principal stresses σ_1 and σ_3 are obtained by Eq.(5.5.2) adapted for other respective subscripts

$$\sigma_{1,3} = \frac{\sigma_x + \sigma_z}{2} \pm \sqrt{\left(\frac{\sigma_x - \sigma_z}{2}\right)^2 + \tau_y^2} = \frac{(-40) + 30}{2} \pm \sqrt{\left[\frac{(-40) - 30}{2}\right]^2 + 20^2} =$$

$$= -5 \pm 10 \cdot \sqrt{3.5^2 + 2^2} \; ;$$

$$\sigma_1 = -5 + 40.31 = 35.31 \quad \left[N / mm^2\right];$$

$$\sigma_3 = -5 - 40.31 = -45.31 \quad \left[N / mm^2\right] \quad \text{and}$$

$$\sigma_2 = \sigma_y = 10 \quad \left[N / mm^2\right]$$

Principal planes *1 and 3* are obtained by Eq.(5.5.1) adapted for other respective subscripts as follows

$$tg2\vartheta = \left|\frac{2 \cdot \tau_y}{\sigma_x - \sigma_z}\right| = \left|\frac{2 \cdot 20}{(-40) - 30}\right| = \frac{40}{70} = 0.5714 \Rightarrow \vartheta = 14°52'21''$$

Now the position of principal stresses and planes can be drawn in Fig.5.9.1.4.

Fig.5.9.1.4

Maximum shearing stress is given by

$$\tau_{max} = \frac{\sigma_{max} - \sigma_{min}}{2} = \frac{\sigma_1 - \sigma_3}{2} = 40.31 \quad \left[N / mm^2\right]$$
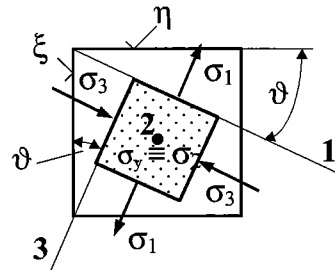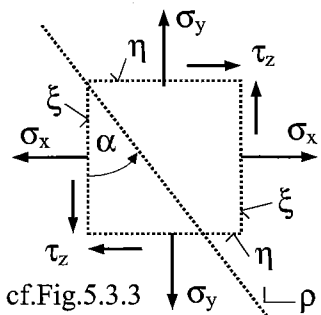
For answering the last task, it is recommendable to compare the origin stress state in Fig.5.3.3 (cf. Sec. 5.3.1), by which the Mohr's circle was derived, with the given stress state in Fig. 5.9.1.2.:

cf.Fig.5.3.3

Fig.5.9.1.2

Based on Eq. (5.3.4a,b): $\sigma_\rho = \dfrac{\sigma_x + \sigma_y}{2} + \dfrac{\sigma_x - \sigma_y}{2} \cdot \cos 2\alpha + \tau_z \cdot \sin 2\alpha$
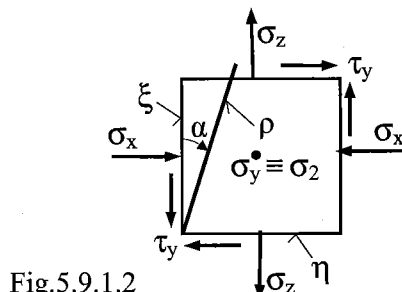
$$\tau_\rho = \frac{\sigma_x - \sigma_y}{2} \cdot \sin 2\alpha - \tau_z \cdot \cos 2\alpha \; ,$$

which can be adapted for other respective subscripts, it is possible to write similar equations for the given task:

$$\sigma_\rho = \frac{\sigma_x + \sigma_z}{2} + \frac{\sigma_x - \sigma_z}{2} \cdot \cos 2\alpha + \tau_y \cdot \sin 2\alpha \; ; \; \tau_\rho = \frac{\sigma_x - \sigma_z}{2} \cdot \sin 2\alpha - \tau_y \cdot \cos 2\alpha \quad *)$$

Comparing the stress senses and the angle senses of the inclined plane ρ in Fig.5.9.1.2 with those of the origin stress state and the plane ρ position in Fig.5.3.3 **will help us** to substitute proper stress and angle signs into Eqs.*):

$$\sigma_\rho = \frac{(-40)+30}{2} + \frac{(-40)-30}{2} \cdot \cos(2 \cdot 30°) + (-20) \cdot \sin(2 \cdot 30°) =$$

$$= -5 - 35 \cdot \frac{1}{2} + (-20) \cdot \frac{\sqrt{3}}{2} = -39.82 \quad [N/mm^2];$$
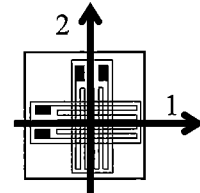
$$\tau_\rho = \frac{(-40)-30}{2} \cdot \sin(2 \cdot 30°) - \tau_z \cdot \cos(2 \cdot 30°) = -35 \cdot \frac{\sqrt{3}}{2} - (-20)\frac{1}{2} = -20.31 \quad [N/mm^2]$$

Note: The offset α of plane ρ (from plane ξ) is substituted as positive ($\alpha = 30° > 0$) into those expressions above since the **plane ρ** is **inclined** in the **same sense** (*here clockwise*) in the both figures (Fig.5.3.3 and Fig.5.9.1.2), while the **shearing stress** τ_y in Fig.5.9.1.2 is pointing to the different square edge than the **shearing stress** τ_y in Fig.5.3.3 and thus it is substituted as negative (*-20 N/mm²*).
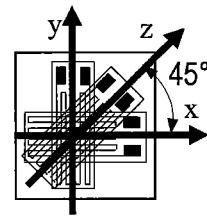
5.9.2 Experimental stress analysis.

One of experimental methods for assessing the 2D stress states of structures is application of so called strain-gauges. Generally, two basic strain-gauge sets are used:

1/ The strain-gauge cross, i,e., two mutually perpendicular strain-gages are used when knowing the principal stress/strain (σ_1/ε_1, σ_2/ε_2) directions.

2/ The strain-gauge rosette, i,e., three strain-gages are used when not knowing the principal stress/strain (σ_1/ε_1, σ_2/ε_2) directions.

Given: The structure material: $E = 2.1 \cdot 10^5 N/mm^2$, $\mu = 0.3$

The strains were measured by means of:

ad 1) the strain-gauge cross: $\varepsilon_1 = 407.5 \cdot 10^{-6}$, $\varepsilon_2 = 132.1 \cdot 10^{-6}$

ad 2) the strain-gauge rosette: $\varepsilon_x = 343.9 \cdot 10^{-6}$, $\varepsilon_y = 160.0 \cdot 10^{-6}$, $\varepsilon_z = 170.3 \cdot 10^{-6}$

Task: Determine the *principal strains and principal stresses,* cf. GHL (5.8.1.1a. b, c)

Solution:

Ad 1) In this case, the *principal strains* (ε_1 and ε_2) were measured (knowing their directions), so only the *principal stresses* (σ_1 and σ_2) are computed by applying GHL (5.8.1.1a,b,c) , which are modified:

$$\sigma_1 = \frac{E}{1-\mu^2} \cdot [\varepsilon_1 + \mu \cdot \varepsilon_2] = \frac{2.1 \cdot 10^5}{1-0.3^2} \cdot [(407.5 + 0.3 \cdot 132.1) \cdot 10^{-6}] = 103.2 [N/mm^2]$$

$$\sigma_2 = \frac{E}{1-\mu^2} \cdot [\varepsilon_2 + \mu \cdot \varepsilon_1] = \frac{2.1 \cdot 10^5}{1-0.3^2} \cdot [(132.1 + 0.3 \cdot 407.5) \cdot 10^{-6}] = 58.7 [N/mm^2] \qquad *)$$

Ad 2) Based on the measured strains (ε_x, ε_z, ε_y), the principal strains (ε_1, ε_2) are computed with

$$\varepsilon_{1,2} = \frac{\varepsilon_x + \varepsilon_y}{2} \pm \sqrt{\left(\frac{\varepsilon_x - \varepsilon_y}{2}\right)^2 + \left(\frac{\gamma}{2}\right)^2}$$, where the shearing strain $\gamma_z/2$ is assessed

by comparing the two equal triangles in Fig.5.9.2.

$$\frac{\gamma_z}{2} = \frac{\varepsilon_x + \varepsilon_y}{2} - \varepsilon_z =$$

$$= \left(\frac{343.9 + 160}{2} - 170.3\right) \cdot 10^{-6} =$$

$$= 81.65 \cdot 10^{-6}$$

$$\varepsilon_{1,2} = \frac{\varepsilon_x + \varepsilon_y}{2} \pm \sqrt{\left(\frac{\varepsilon_x - \varepsilon_y}{2}\right)^2 + \left(\frac{\varepsilon_x + \varepsilon_y}{2} - \varepsilon_z\right)^2}$$
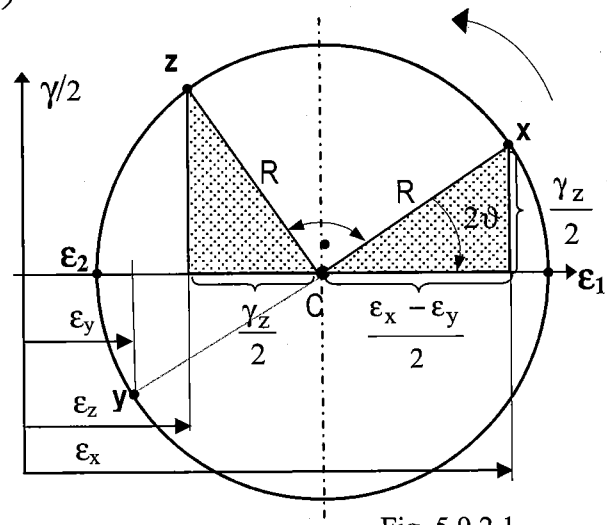
Fig. 5.9.2.1

$$\varepsilon_{1,2} = \left[\frac{343.9 + 160}{2} \pm \sqrt{\left(\frac{343.9 - 160}{2}\right)^2 + \left(\frac{343.9 + 160}{2} - 170.3\right)^2}\right] \cdot 10^{-6} \Rightarrow$$

$$\varepsilon_1 = 374.92 \cdot 10^{-6} ; \quad \varepsilon_2 = 128.98 \cdot 10^{-6}$$

The principal directions for this stress state can be assessed by means of the Mohr's circle (Fig. 5.9.2.1)

$$\tan 2\vartheta = \left|\frac{\frac{\gamma_z}{2}}{\frac{\varepsilon_x - \varepsilon_y}{2}}\right| = \frac{81.65 \cdot 10^{-6}}{\frac{343.9 - 160}{2} \cdot 10^{-6}} =$$

$$= 0.888 \Rightarrow \vartheta = 20°48'08''$$

Fig. 5.9.2.2

The strain-gauges (x, z, y) directions in the rosette with those of the principal strains (1, 2) are shown in Fig. 5.9.2.2. (Mind the same sequence of strain-gauges ($x \rightarrow y \rightarrow z$) in Fig. 5.9.2.1 and Fig. 5.9.2.1!!!)

Analogously to the expressions *), we obtain the principal stresses (by means of the rosette data):

$$\sigma_1 = 95.45 [N/mm^2] \quad \text{and} \quad \sigma_2 = 55.72 [N/mm^2]$$
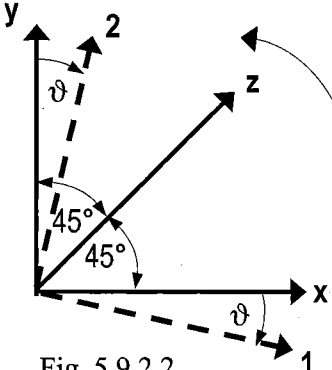
6. Strain energy

6.1 Introduction

In Sec.2.12 we discussed the elastic strain energy associated with <u>normal stresses</u> in members under axial loading, see Eqs.(2.12.3*a,b*) and (2.12.7*a,b*). The *strain-energy density,* being equal to the area under the stress-strain diagram of the material (Fig.2.12.1*c*), has been defined as the <u>strain energy per unit volume</u>

$$\lambda_\sigma = \frac{dU}{dV} = \frac{1}{2} \cdot \sigma(x) \cdot \varepsilon(x) = \frac{\sigma^2(x)}{2E}, \quad \text{see Eqs.(2.12.4) and (2.12.5).}$$

In Sec.6.2 we shall consider strain-energy density for a *general stress state*, which includes the strain energy associated with *shearing* stresses.

6.2 Strain energy for a general stress state

6.2.1 Strain energy for shearing stresses

When a material is subjected to *pure shear*, the originally perpendicular planes of an element, in which the shearing stresses τ are exerted, will undergo a shearing strain γ(Fig.6.2.1.1). The τ-γ curve is assumed linear. The shearing force $\tau_z \cdot dx \cdot dz$ brings about the total displacement $\gamma_z \cdot dy$. The strain energy accumulated in the element is determined from the product of the gradually increasing shearing force and the caused displacement in the form

$$dU = \frac{1}{2} \cdot \tau_z \cdot dx \cdot dz \cdot \gamma_z \cdot dy = \frac{1}{2} \cdot \tau_z \cdot \gamma_z \cdot dx \cdot dy \cdot dz = \frac{1}{2} \cdot \tau_z \cdot \gamma_z \cdot dV \qquad (6.2.1.1)$$

a)   *b)*
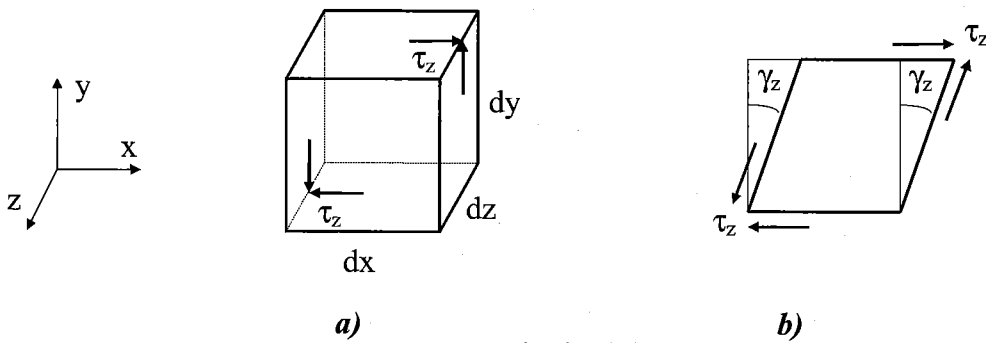
Fig.6.2.1.1

The *strain-energy density* in the case of *plane shearing stress* or *pure shear* is then

$$\lambda_\tau = \frac{dU}{dV} = \frac{1}{2} \cdot \tau_z \cdot \gamma_z = \frac{\tau_z^2}{2G} \qquad (6.2.1.2)$$

(when substituting Hooke's law for shear).

6.2.2 Strain energy for a general state of stress

In the preceding sections, we determined the strain energy of a body in a state of uniaxial stress (cf. Secs.2.12 and 6.1) and in a state of plane shearing stress (Sec.6.2.1). In the case of a body in a general state of stress characterized by the six stress components $\sigma_x, \sigma_y, \sigma_z, \tau_x, \tau_y$ and τ_z, the strain-energy density may be obtained by adding the expressions given in Eqs.(2.12.5) and (6.2.1.2), as well as the four other expressions obtained through a permutation of the subscripts .

In the case of the elastic deformation of an isotropic body, each of the six stress-strain relations involved is linear, and the strain-energy density may be expressed as

$$\lambda = \frac{dU}{dV} = \frac{1}{2}\left(\sigma_x \cdot \varepsilon_x + \sigma_y \cdot \varepsilon_y + \sigma_z \cdot \varepsilon_z + \tau_x \cdot \gamma_x + \tau_y \cdot \gamma_y + \tau_z \cdot \gamma_z\right) \qquad (6.2.2.1)$$

being sum of two independent parts

$$\lambda_\sigma = \frac{1}{2}\left(\sigma_x \cdot \varepsilon_x + \sigma_y \cdot \varepsilon_y + \sigma_z \cdot \varepsilon_z\right) \quad \text{and} \quad \lambda_\tau = \frac{1}{2}\left(\tau_x \cdot \gamma_x + \tau_y \cdot \gamma_y + \tau_z \cdot \gamma_z\right) \qquad (6.2.2.2a,b)$$

Recalling the relations (5.8.2.1a,b,c) and (5.8.2.2a,b,c) obtained in Sec.5.8.2, and substituting for the strain components into Eq.(6.2.2.1), we have, for the most general state of stress at a given point of an elastic body,

$$\lambda = \frac{1}{2 \cdot E}\left[\sigma_x^2 + \sigma_y^2 + \sigma_z^2 - 2 \cdot \mu \cdot \left(\sigma_x \cdot \sigma_y + \sigma_y \cdot \sigma_z + \sigma_z \cdot \sigma_x\right) + 2 \cdot (1+\mu) \cdot \left(\tau_x^2 + \tau_y^2 + \tau_z^2\right)\right]$$

$$(6.2.2.3)$$

If the principal axes at the given point are used as coordinate axes, the shearing stresses become zero and Eq.(6.2.2.3) reduces to

$$\lambda = \frac{1}{2}\left(\sigma_1 \cdot \varepsilon_1 + \sigma_2 \cdot \varepsilon_2 + \sigma_3 \cdot \varepsilon_3\right) = \frac{1}{2 \cdot E}\left[\sigma_1^2 + \sigma_2^2 + \sigma_3^2 - 2 \cdot \mu \cdot \left(\sigma_1 \cdot \sigma_2 + \sigma_2 \cdot \sigma_3 + \sigma_3 \cdot \sigma_1\right)\right]$$

$$(6.2.2.4)$$

where σ_1, σ_2, and σ_3 are the principal stresses at the given point.

In Chap.7, we shall deal with the limit state of a body subjected to a general state of stress. One of the criteria used to predict whether a given state of stress will cause a ductile material to yield is based on the determination of the energy per unit volume associated with the distortion, or change in shape, of that material, and will be called, among other names, the *maximum-distortion-energy criterion*. We shall, therefore, attempt to separate the strain-energy density λ at a given point into two parts, a part λ_v associated with a *change in volume* (also called the *volumetric strain energy per unit volume*) of the material at that point, and a part λ_d associated with a *distortion,* or *change in shape* (also called the *shear strain energy per unit volume*), of the material at the same point. We write, taking into account Eqs. (6.2.2.2a,b),

$$\lambda = \lambda_\sigma + \lambda_\tau = \lambda_v + \lambda_d \qquad (6.2.2.5a)$$

These relations can be further subdivided as

$$\lambda = \lambda_v + \lambda_d = \lambda_{v\sigma} + \lambda_{v\tau} + \lambda_{d\sigma} + \lambda_{d\tau} \qquad (6.2.2.5b)$$

where $\qquad \lambda_\sigma = \lambda_{v\sigma} + \lambda_{d\sigma} \qquad$ and $\qquad \lambda_\tau = \lambda_{v\tau} + \lambda_{d\tau} \qquad (6.2.2.5c,d)$

so that we may know how the normal and shearing stresses participate in the change in volume and in the change in shape, respectively.

In order to determine $\lambda_{v\sigma}$ and $\lambda_{d\sigma}$, we shall introduce the *average value* σ_{ave} of the normal stresses at the point under consideration,

$$\sigma_{ave} = \frac{\sigma_x + \sigma_y + \sigma_z}{3} \qquad (6.2.2.6)$$

and set

$$\sigma_x = \sigma_{ave} + (\sigma_x - \sigma_{ave}); \quad \sigma_y = \sigma_{ave} + (\sigma_y - \sigma_{ave}); \quad \sigma_z = \sigma_{ave} + (\sigma_z - \sigma_{ave}) \qquad (6.2.2.7)$$

a)   b)   Fig.6.2.2.1   c)
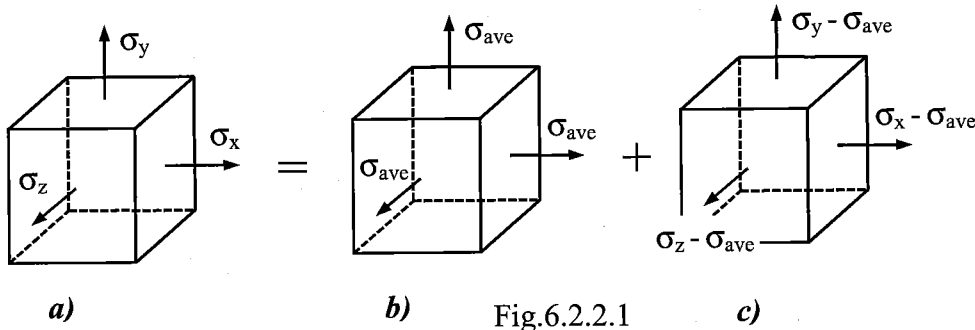
Thus, the given state of stress (Fig.6.2.2.1a) may be obtained by superposing the states of stress shown in Fig.6.2.2.1b and c. We note that the state of stress described in Fig.6.2.2.1b tends to change the volume of the element of material, but not its shape, since all the faces of the element are subjected to the same stress σ_{ave}. On the other hand, it follows from Eqs. (6.2.2.6) and (6.2.2.7) that

$$(\sigma_x - \sigma_{ave}) + (\sigma_y - \sigma_{ave}) + (\sigma_z - \sigma_{ave}) = 0 \qquad (6.2.2.8)$$

which indicates that some of the stresses shown in Fig.6.2.2.1c are tensile and others compressive. Thus, this state of stress tends to change the shape of the element. However, it does not tend to change its volume. Indeed, recalling Eq. (2.9.1) of Sec.2.9, and substituting for strains from generalized Hooke's law - Eqs.(5.8.2.1a,b,c) - we note that the dilatation Θ (i.e., the change in volume per unit volume) caused by this state of stress is

$$\Theta = \frac{1-2\mu}{E}\left[(\sigma_x - \sigma_{ave}) + (\sigma_y - \sigma_{ave}) + (\sigma_z - \sigma_{ave})\right] \qquad (6.2.2.9)$$

or $\Theta = 0$, in view of Eq. (6.2.2.8). We conclude from these observations that the portion $\lambda_{v\sigma}$ of the strain-energy density must be associated with the state of stress shown in Fig.6.2.2.1b, while the portion $\lambda_{d\sigma}$ must be associated with the state of stress shown in Fig.6.2.2.1c.

It follows that the portion $\lambda_{v\sigma}$ of the strain-energy density corresponding to a change in volume of the element may be obtained by substituting σ_{ave} for each of the normal stresses in Eq. (6.2.2.2a). We have

$$\lambda_{v\sigma} = \frac{1}{2 \cdot E} \cdot 3 \cdot \sigma_s^2 \cdot (1 - 2 \cdot \mu) = \frac{1 - 2 \cdot \mu}{6 \cdot E} \cdot \left(\sigma_x + \sigma_y + \sigma_z\right)^2 \tag{6.2.2.10}$$

while recalling Eq. (6.2.2.6) to express the last shape of Eq. (6.2.2.10).

To obtain the portion $\lambda_{d\sigma}$ of the strain-energy density corresponding to the distortion of the element, we shall solve Eq.(6.2.2.5c) for $\lambda_{d\sigma}$ and substitute for λ_σ and for $\lambda_{v\sigma}$ from Eqs.(6.2.2.2a) and (6.2.2.10), respectively. We write

$$\lambda_{d\sigma} = \lambda_\sigma - \lambda_{v\sigma} =$$

$$= \frac{1}{6E}\left[3 \cdot \left(\sigma_x^2 + \sigma_y^2 + \sigma_z^2\right) - 6\mu \cdot \left(\sigma_x\sigma_y + \sigma_y\sigma_z + \sigma_z\sigma_x\right) - \left(1 - 2\mu\right)\left(\sigma_x + \sigma_y + \sigma_z\right)^2\right]$$

Expanding the square and rearranging terms, we have

$$\lambda_{d\sigma} = \frac{1 + \mu}{6E}\left[\left(\sigma_x^2 - 2\sigma_x\sigma_y + \sigma_y^2\right) + \left(\sigma_y^2 - 2\sigma_y\sigma_z + \sigma_z^2\right) + \left(\sigma_z^2 - 2\sigma_z\sigma_x + \sigma_x^2\right)\right]$$

Noting that each of the parentheses inside the bracket is a perfect square, we obtain the following expression for the portion $\lambda_{d\sigma}$ of the strain-energy density, i.e., for the distortion energy per unit volume which is contributed by the normal stresses of the given general stress state,

$$\lambda_{d\sigma} = \frac{1 + \mu}{6E}\left[\left(\sigma_x - \sigma_y\right)^2 + \left(\sigma_y - \sigma_z\right)^2 + \left(\sigma_z - \sigma_x\right)^2\right] \tag{6.2.2.11}$$

In order to determine $\lambda_{v\tau}$ and $\lambda_{d\tau}$, we shall first substitute the stress state of pure shear $\sigma_1 = -\sigma_2 = \tau$ and $\sigma_3 = 0$ (cf. Sec.5.7) into Eq.(2.9.1) and obtain

$$\Theta = \varepsilon_1 + \varepsilon_2 + \varepsilon_3 = \frac{1 - 2\mu}{E}\left(\sigma_1 + \sigma_2 + \sigma_3\right) = 0$$

It follows from the result $\Theta = 0$ that shearing stresses do not contribute to the change in volume, i.e.,

$$\lambda_{v\tau} = 0$$

and the strain-energy density by shearing stresses is exerted only to the change in shape. According Eq.(6.2.2.2.b) we have

$$\lambda_{d\tau} = \frac{1 + \mu}{E} \cdot \left(\tau_x^2 + \tau_y^2 + \tau_z^2\right) \tag{6.2.2.12}$$

Based on the foregoing analysis we have:

- the resulting *volumetric strain energy per unit volume*

$$\lambda_v = \lambda_{v\sigma} = \frac{1 - 2 \cdot \mu}{6 \cdot E} \cdot \left(\sigma_x + \sigma_y + \sigma_z\right)^2 \tag{6.2.2.13}$$

- the resulting *shear strain energy per unit volume*

$$\lambda_d = \lambda_{d\sigma} + \lambda_{d\tau} =$$

$$= \frac{1+\mu}{6E}\left[\left(\sigma_x - \sigma_y\right)^2 + \left(\sigma_y - \sigma_z\right)^2 + \left(\sigma_z - \sigma_x\right)^2 + 6\cdot\left(\tau_x^2 + \tau_y^2 + \tau_z^2\right)\right] \qquad (6.2.2.14)$$

These relations can be expressed in terms of the principal stresses:

- the resulting *volumetric strain energy per unit volume*

$$\lambda_v = \frac{1-2\cdot\mu}{6\cdot E}\cdot\left(\sigma_1 + \sigma_2 + \sigma_3\right)^2 \qquad (6.2.2.15)$$

- the resulting *shear strain energy per unit volume*

$$\lambda_d = \frac{1+\mu}{6E}\left[\left(\sigma_1 - \sigma_2\right)^2 + \left(\sigma_2 - \sigma_3\right)^2 + \left(\sigma_3 - \sigma_1\right)^2\right] \qquad (6.2.2.16)$$

7. Limit analysis; theories of elastic failure

7.1 Introduction

*We can consider as a **limit state** (LS) any stress or strain state that is inadmissible for the proper function of a structure.*

The limit states listed below are those of very common practical applications:

1) *LS of elasticity:* when it is reached, the plastic flow of material starts to propagate in material macrovolumes.

2) *LS of ultimate strength (breakage) or fracture:* when it is reached, the cohesion of the material is broken.

3) *LS of fatigue:* this sets in when a structure failure occurs due to cyclic loading.

4) *LS of stability:* at certain values of compressive forces, a phenomenon known as *buckling of columns* can appear, which means the *stability failure* (by lateral deflection) of a long slender bar.

We shall concentrate on:

- the **LS of elasticity,** which (in most cases) must not be reached, or even exceeded, in structures made of **ductile materials,** and to which we relate a certain degree of safety loading (being expressed by the safety factor k_Y related to the yield strength σ_Y of the material);

- the **LS of fracture (breakage)** which must not be reached with a sufficient margin of safety when loading structures made of all kinds of material; it especially serves as a measure of safety for **brittle materials,** where the safety factor k_U related to the respective ultimate strength $\sigma_{U,t}$ (in tension) or $\sigma_{U,c}$ (in compression) of the material, is to be applied.

Note that in *both limit states listed here* the corresponding safety factors k_Y and k_U, respectively, must ensure that the *designed structures or components are stressed only elastically.*

Haigh's limit surface :

Using principal stresses σ_1, σ_2, and σ_3 as coordinates, we will create so-called *Haigh's space,* where we can plot *limit stress states* as points lying on a surface in this space, which is consequently called *Haigh's limit surface (Haigh's diagram).* Regarding homogeneity and isotropy of the materials, the axis of the first octant of Haigh's space coincides with the axis of Haigh's limit surface. There is also *Haigh's allowable surface,* which is derived from the limit surface by dividing all limit stress coordinates by the respective minimum safety factor k_{min}. Haigh's diagrams will be presented below in connection with individual *theories of elastic failure.*

7.2 Theories of elastic failure

7.2.1 Uniaxial loading.

In this case, issuing from tensile tests, we can simply compare the working stress (of a designed structure) with the respective limit strength (cf. Sec.2.6.3) :

- Ductile materials:

1) The *LS of elasticity* is more often called the *yield criterion:*

$$| \text{ Working stress } | \quad = \text{ Yield strength}, \qquad \text{i.e., } \quad |\sigma| = \sigma_Y \qquad \text{see Eq.(2.6.3.6)}$$

2) *Strength Criterion* (used by designers for computations of <u>allowable load-carrying capacity</u> of structures):

$$| \text{ Working stress } | \quad \leq \text{ Allowable stress}, \qquad \text{i.e., } \quad |\sigma| \leq \sigma_{\text{all}} \qquad \text{see Eq.(2.6.3.4)}$$

These criteria hold for both tension and compression.

- Brittle materials:

1) *Fracture (breakage) criteria:*

a) tension

Working stress = Ultimate strength in tension, i.e., $\sigma = \sigma_{\text{Ut}}$ see Eq.(2.6.3.7a)

b) compression

$| \text{ Working stress } | = $ *Ultimate strength in compression,* i.e., $|\sigma| = \sigma_{\text{Uc}}$ see Eq.(2.6.3.7b)

2) *Strength Criteria:*

a) tension

Working stress $\leq$ Allowable stress in tension , i.e., $\sigma \leq \sigma_{\text{all;t}}$ see Eq.(2.6.3.5a)

b) compression

$| \text{ Working stress } | \leq $ *Allowable stress in compression,* i.e., $\sigma \leq \sigma_{\text{all;c}}$ see Eq.(2.6.3.5b)

Haigh's diagram for uniaxial stress is shown in Fig.7.2.1.1:
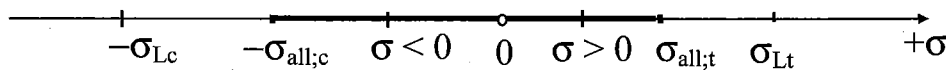
Fig.7.2.1.1

where points σ_{Lt} and σ_{Lc} correspond to the respective limit values of the material (i.e., to the yield strength for ductile materials and to the ultimate strength for brittle materials). Safety factors of working stress σ with respect to the limit values are determined by

$$k_L = \frac{\sigma_{Lt}}{\sigma} \quad (\text{for } \sigma > 0); \qquad k_L = \frac{\sigma_{Lc}}{|\sigma|} \quad (\text{for } \sigma < 0);$$

7.2.2 General stress state

When dealing with the design of structures or components, the physical properties of the constituent materials are usually found from the results of laboratory experiments which have only subjected the materials to the simplest stress conditions. The most usual test is the simple tensile test, in which the value of the stress at yield or at fracture (whichever occurs first) is easily determined. The strengths of materials under complex stress systems are not generally known, except in a few particular cases. In practice it is these complicated systems of stress that are more often encountered, and therefore it is necessary to have some basis for determining allowable working stresses so that failure will not occur. Thus, relevant *theories of elastic failure* must be postulated, the function of which is to predict from the behaviour of the materials in a simple test when elastic failure will occur under *any* condition of applied stress.

A number of theoretical criteria have been proposed, each seeking to obtain an adequate correlation between estimated component life and that actually achieved under service load conditions for both ductile and brittle material applications. The four main theories are:

For ductile materials:

a) Maximum shearing stress theory (Guest - Tresca)

b) Shear strain energy per unit volume (Huber - von Mises - Hencky)

For brittle materials:

c) Maximum principal stress theory (Rankine)

d) Mohr's modified shearing stress theory

In each case the value of the selected critical property implied in the title of the theory is determined for both the simple tension test and a three-dimensional complex stress system. These values are then equated to produce a so-called *criterion for failure* based on the respective theory.

7.3 Theories of elastic failure for ductile materials

7.3.1 Maximum-shearing-stress criterion (often denoted: "τ_{max}"; or Tresca's criterion; or Guest's criterion)

This theory states that *failure (i.e., critical state which prevent operational loading) can be assumed to occur when the maximum shearing stress in the complex stress system becomes equal to that at the yield point in the simple tensile test.*

This criterion is based on the observation that yield in ductile materials is caused by slippage of the material along oblique surfaces and is due primarily to shearing stresses. Recalling from Sec.5.6.3 that the maximum value of the shearing stress under a centric, axial load is equal to half the value of the corresponding normal, axial stress (Eq.5.6.3.2), we conclude that the maximum shearing stress in a tensile-test specimen is $\tau_{max} = \tau_Y = \dfrac{\sigma_Y}{2}$ as the specimen starts to yield. On the other hand, we saw in Sec.5.6.1, Eq.(5.6.1.1), that, for multiaxial stress, the maximum value τ_{max} of the shearing stress is equal to $\tau_{max} = \dfrac{1}{2} \cdot (\sigma_{max} - \sigma_{min})$. Thus, when equalling these expressions we have *Tresca's yield criterion* in the form

$$\sigma_{eq} = \sigma_{max} - \sigma_{min} = \sigma_Y \qquad (7.3.1.1)$$

where the symbol σ_{eq}, called *equivalent stress* (now representing the originally given complex stress system), means that we have transformed the original multiaxial stress as if into uniaxial stress.

The *strength criterion* for multiaxial stress (i.e., two- or three-dimensional stress) is then expressed analogically to Eq.(2.6.3.4) (cf. Sec.7.2) in the form

$$\sigma_{eq} = \sigma_{max} - \sigma_{min} \le \sigma_{all} \qquad (7.3.1.2)$$

Tresca's theory produces a fairly accurate correlation with experimental results and is often used for ductile materials in machine design. This is also one of the widely used laws of plasticity (which will be dealt with in the next course).

7.3.2 Maximum-shear-strain-energy (or distortion-energy) criterion (often denoted: "HMH" criterion[*]; or "von Mises" criterion)

This theory, based on determination of the distortion energy in a given material, i.e., of the energy associated with changes in shape (as opposed to the energy associated with changes in volume, see Sec.6.2.2) states that *failure occurs when the maximum shear strain energy component in the complex stress system is equal to that at the yield point in the tensile test,* i.e.

$$\lambda_d = \lambda_{dY} \qquad (7.3.2.1)$$

where λ_d in the case of a general stress state, is (Eq. 6.2.2.14)

$$\lambda_d = \frac{1+\mu}{6 \cdot E} \cdot \left[\left(\sigma_x - \sigma_y\right)^2 + \left(\sigma_y - \sigma_z\right)^2 + \left(\sigma_z - \sigma_x\right)^2 + 6 \cdot \left(\tau_x^2 + \tau_y^2 + \tau_z^2\right) \right]$$

or by means of the principal stresses (Eq. 6.2.2.16)

---

[*] The notation HMH is by Huber, von Mises, Hencky, who are three independent authors of the criterion.

$$\lambda_d = \frac{1+\mu}{6 \cdot E} \cdot \left[(\sigma_1 - \sigma_2)^2 + (\sigma_2 - \sigma_3)^2 + (\sigma_3 - \sigma_1)^2 \right]$$

When substituting in these expressions the stress at the *yield point in the tensile test*, i.e. $\sigma_1 = \sigma_Y$, $\sigma_2 = \sigma_3 = 0$, we have the limit distortion energy per unit volume in the form

$$\lambda_{dY} = \frac{1+\mu}{3 \cdot E} \cdot \sigma_Y^2$$

After substituting the above presented relations (Eqs.(6.2.2.14) and (6.2.2.16)) into the limit condition (Eq. 7.3.2.1) we obtain the *HMH yield condition* in the following shapes

for general stress

$$\frac{\sqrt{2}}{2} \cdot \sqrt{(\sigma_x - \sigma_y)^2 + (\sigma_y - \sigma_z)^2 + (\sigma_z - \sigma_x)^2 + 6 \cdot (\tau_x^2 + \tau_y^2 + \tau_z^2)} = \sigma_Y \qquad (7.3.2.2a)$$

for the stress state expressed by the principal stresses

$$\frac{\sqrt{2}}{2} \cdot \sqrt{(\sigma_1 - \sigma_2)^2 + (\sigma_2 - \sigma_3)^2 + (\sigma_3 - \sigma_1)^2} = \sigma_Y \qquad (7.3.2.2b)$$

If we denote the left hand sides of these relations as the equivalent stress σ_{eq} we can write the *HMH strength criterion* in the form

$$\sigma_{eq} \leq \sigma_{all} \qquad (7.3.2.3)$$

where the respective forms of the left hand sides are hidden in σ_{eq}.

This theory has received considerable verification in practice and is widely regarded as the most reliable basis for design.

7.3.3 Comparison of Tresca's and HMH yield criteria

It was stated at the end of the last two sections that each yield criterion presented there produces a fairly accurate correlation with experiments and is widely used in practice. Although yield criteria show a difference in results ranging from *0* to *15.5%*, designers are recommended to *consider both as exact*, and to apply them arbitrarily *for ductile materials*. Nevertheless, some advantages (or disadvantages) of their respective applications can be listed as below.

Advantages of Tresca's yield criterion:

1. Simple mathematical expression (but it is necessary to know the principal stresses)

Advantages of the HMH yield criterion:

1. It is not necessary to know the principal stresses (cf. Eq.7.3.2.2a)

2. It is not necessary to know the rank of the principal stress magnitudes.

3. All three principal stresses participate to express the equivalent stress and have the same significance.

(The advantages of one criterion mean disadvantages for the other. Though only one advantage is observed in Tresca's criterion, this is still used more frequently, mainly when dealing with problems of plasticity).

7.4 Graphical representation of the theories of elastic failure for ductile materials

Recalling Sec.7.1, the above presented theories of elastic failure enable not only mathematical assessment of the limit analysis or allowable working conditions of structures but also their geometric interpretation in the form of Haigh's limit or allowable surfaces, respectively.

7.4.1 Graphical representation of Tresca's criterion

Referring to the above obtained equivalent strength for Tresca's yield criterion (Eq.7.3.1.1) in the form

$$\sigma_{eq} = \sigma_{max} - \sigma_{min} = \sigma_Y$$

the corresponding Haigh's limit surface is defined when we consider each of the principal stresses, taking successively maximum or minimum value, respectively.

This procedure can be applied both for the 3D stress state or for the 2D (plane) stress state:

3D stress state:	2D (plane) stress state, e.g., $\sigma_3 = 0$:
$\sigma_1 - \sigma_2 = \sigma_Y$; $\sigma_2 - \sigma_1 = \sigma_Y$	$\sigma_1 - \sigma_2 = \sigma_Y$; $\sigma_2 - \sigma_1 = \sigma_Y$
$\sigma_2 - \sigma_3 = \sigma_Y$; $\sigma_3 - \sigma_2 = \sigma_Y$	$\sigma_2 = \sigma_Y$; $-\sigma_2 = \sigma_Y$
$\sigma_3 - \sigma_1 = \sigma_Y$; $\sigma_1 - \sigma_3 = \sigma_Y$	$-\sigma_1 = \sigma_Y$; $\sigma_1 = \sigma_Y$
i.e., **hexahedral prism** (HhP)	i.e., **hexagon** (Hn)

7.4.2 Graphical representation of HMH criterion

Recalling Sec.7.3.2, we will observe that, when raising the Eq.(7.3.2.2b) expression to the second power, we obtain

$$\sigma_{eq}^2 = \frac{1}{2} \cdot \left[(\sigma_1 - \sigma_2)^2 + (\sigma_2 - \sigma_3)^2 + (\sigma_3 - \sigma_1)^2 \right] = \sigma_Y^2$$

which represents a **circular cylinder** serving as the limit surface in Haigh's space. We can observe that Tresca's HhP is circumscribed by the HMH cylinder.
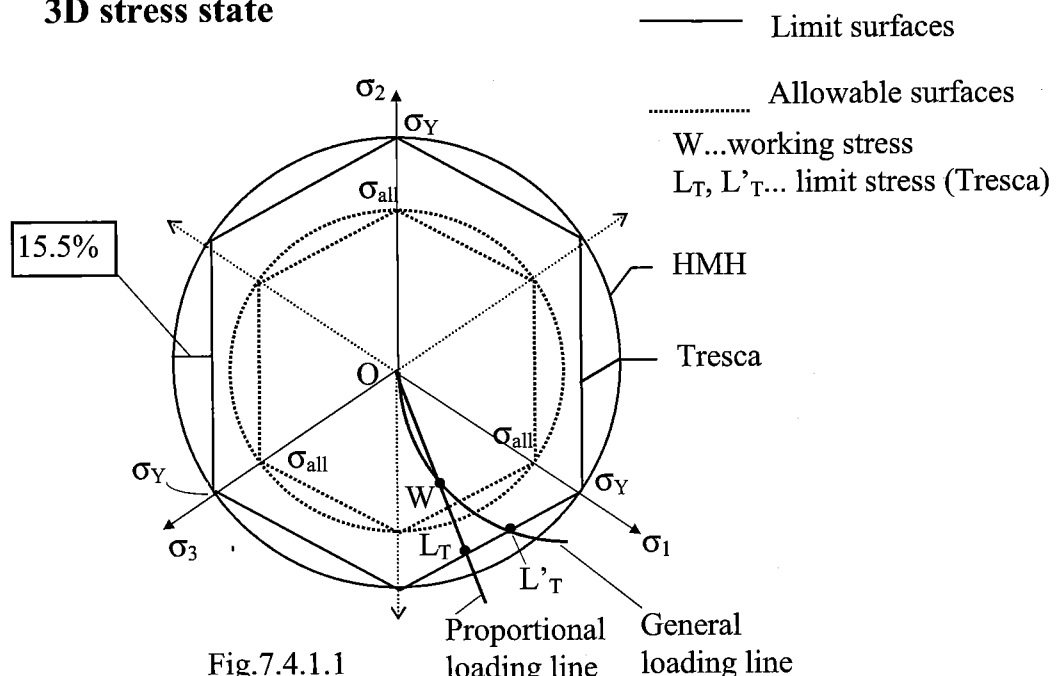
The corresponding Haigh's limit curve for the 2D (plane) stress state is obtained by putting one principal plane equal to zero, e.g. $\sigma_3 = 0$:

$$\sigma_{eq}^2 = \frac{1}{2} \cdot \left[(\sigma_1 - \sigma_2)^2 + \sigma_2^2 + \sigma_1^2 \right] = \sigma_Y^2$$
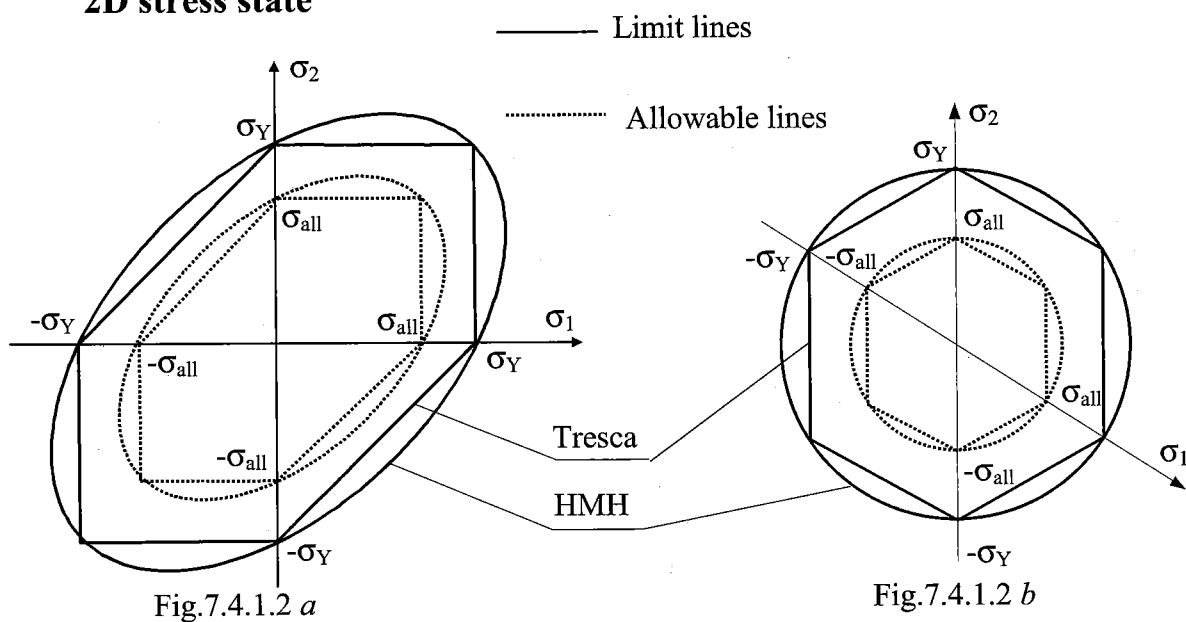
which represents an **ellipse** circumscribing Mohr's hexagon.

The above derived configurations, both for Tresca's and for HMH criteria, are shown in Fig.7.4.1.1 (Haigh's limit surfaces) and in Fig.7.4.1.2a,b (Haigh's limit lines). In order to make the geometric solution of plane stress problems for HMH criterion easier, the transformation of the limit ellipse into the corresponding limit circle, by using oblique coordinates, is shown in Fig.7.4.1.2b.

3D stress state

Fig.7.4.1.1

2D stress state

Fig.7.4.1.2 a

Fig.7.4.1.2 b

In Fig.7.4.1.1, two loading lines are plotted representing a <u>general</u> and a <u>proportional</u> type of loading, respectively. The loading lines intersect the respective limit lines at points representing the respective limit stress states (in Fig.7.4.1, only points L_T, L'_T, are denoted representing <u>limit stresses</u> with respect to <u>Tresca's limit</u> surface). Point W, which has coordinates $\sigma_1, \sigma_2, \sigma_3$, represents working stress.

The loading (straight) line of proportional type of loading, which occurs very often in practice, can be utilized for graphic expression of the respective factor of safety for given working stress $\sigma_1, \sigma_2, \sigma_3$ with respect to Tresca's criterion:

$$k_L = \frac{OL_T}{OW}$$

We can proceed analogously with respect to the HMH criterion and, when applying Fig.7.4.1.2a,b, the same procedure can be carried out for the 2D stress state.

7.5 Theories of elastic failure for brittle materials

As we saw in Chap. 2, brittle materials are characterized by the fact that, when subjected to a tensile test, they fail suddenly through rupture - or fracture - without any prior yielding. When a structural element or machine component made of a brittle material is under uniaxial tensile stress, the value of the normal stress which causes it to fail is equal to the ultimate strength σ_U of the material as determined from a tensile test, since both the tensile-test specimen and the element or component under investigation are in the same state of stress. However, when a structural element or machine component is in a state of complex stress, it is necessary to apply a suitable theory of failure.

7.5.1 <u>Maximum-normal-stress criterion</u> (often denoted as the "σ_{max}" criterion)

According to this criterion, *a given structural element fails when the* **<u>maximum normal stress</u>** σ_{max} *(in tension) in that component* <u>*reaches the ultimate strength*</u> σ_{Ut} *obtained from the tensile test of a specimen of the same material.* (It should be noted, however, that *failure could also occur in* <u>*compression*</u> *if the* **<u>minimum principal stress</u>** σ_{min} *were compressive and its* <u>*value reached the value of the ultimate strength in*</u> <u>*compression*</u> , *i.e.* $\sigma_{min} = -\sigma_{Uc}$, *for the material concerned before the value* σ_{Ut} *was reached in tension.)*

The *criterion of brittle fracture* is thus

- in tension $\qquad\qquad \sigma_{eq} = \sigma_{max} = \sigma_{Ut}$ $\qquad\qquad\qquad$ (7.5.1.1a)

- in compression $\qquad\quad \sigma_{eq} = -\sigma_{min} = \sigma_{Uc}$ $\qquad\qquad\qquad$ (7.5.1.1b)

The *strength criterion,* obtained in similar way, is

- in tension $\qquad\qquad \sigma_{eq} = \sigma_{max} = \sigma_{all;t}$ $\qquad\qquad\qquad$ (7.5.1.2a)

- in compression $\qquad\quad \sigma_{eq} = -\sigma_{min} = \sigma_{all;c}$ $\qquad\qquad\qquad$ (7.5.1.2b)

where the *allowable stresses* ($\sigma_{all;t}$, $\sigma_{all;c}$) are defined by Eqs.(2.6.3.3a,b), respectively.

7.5.2 Mohr's fracture criterion

According to German engineer Otto Mohr, this criterion states: *With a brittle material* (having σ_{Ut} < σ_{Uc}) *breakage (fracture) will onset in such cross-sections in which not only normal stress reaches a great magnitude but also a certain influence of shearing stress* (exerted simultaneously on those cross-sections) *will manifest* (Fig.7.5.2.1). (From Mohr's circles it is apparent that the limit points L, denoting the stress states in which the material fracture will take place, belong to the largest circle determined by the difference *(σ_{max} - σ_{min})*. This means that here, similarly as with Tresca's Criterion, medium stress plays no role.)
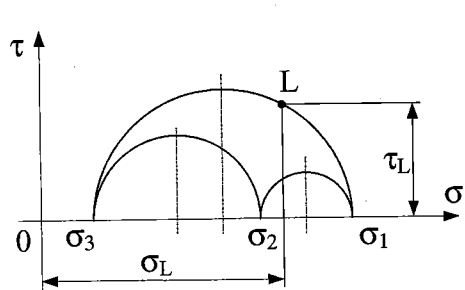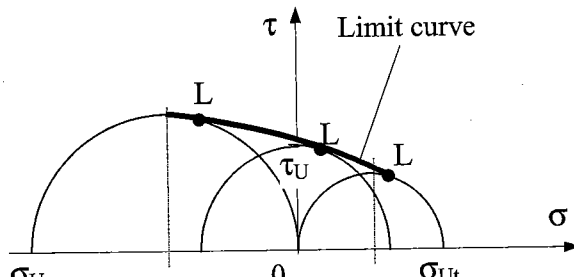
Fig.7.5.2.1 $\qquad\qquad\qquad\qquad\qquad$ Fig.7.5.2.2

Mohr's criterion can be defined when the results of various types of tests are available for that material. Let us first assume that a tensile test and a compressive test have been conducted and thus the two corresponding side Mohr's circles (having the limit values σ_{Ut}, σ_{Uc}) in Fig.7.5.2.2 have been obtained. Such analysis corresponds to the "σ_{max}" *Criterion,* because either tension or compression principal stresses exerted in a member are to be checked. In order to analyze the cases when the principal stresses in a member have opposite signs, we shall now assume that a torsion test has been conducted on the material and that its ultimate strength in shear τ_U has been determined. Drawing the circle centered at *0* representing the state of stress (i.e., pure shear, cf. Chap.8) corresponding to the failure of the torsion-test specimen (Fig.7.5.2.2), we observe that any state of stress represented by a circle entirely contained in that circle is also safe. Mohr's criterion is a logical extension of this observation: *A state of stress is safe if it is represented by a circle located entirely within the area bounded by the envelope of the circles corresponding to the available data (i.e., σ_{Ut}, σ_{Uc}, τ_U).*

It follows from experiments that this envelope, being curved only a little, can be approximated by the *tangent t* to the circles representing the limit uniaxial tension and compression, respectively (Fig.7.5.3).

Placing a circle representing a general stress state, given by $\sigma_{max} \equiv \sigma_1$, $\sigma_{min} \equiv \sigma_3$, which just touches that tangent t, and utilizing the hatched similar triangles in Fig.7.5.2.3, we shall obtain

the looked-for relation in the following form:

$$\frac{\dfrac{\sigma_1+\sigma_3}{2}-\dfrac{\sigma_{Ut}}{2}}{\dfrac{1}{2}\cdot\left[\sigma_{Ut}-\left(\sigma_1-\sigma_3\right)\right]}=\frac{\dfrac{\sigma_{Uc}}{2}+\dfrac{\sigma_{Ut}}{2}}{\dfrac{1}{2}\cdot\left(\sigma_{Uc}-\sigma_{Ut}\right)}$$

from which, after modification, we shall obtain:

$$\frac{\sigma_1}{\sigma_{Ut}}-\frac{\sigma_3}{\sigma_{Uc}}=1 \qquad\qquad (7.5.2.1)$$
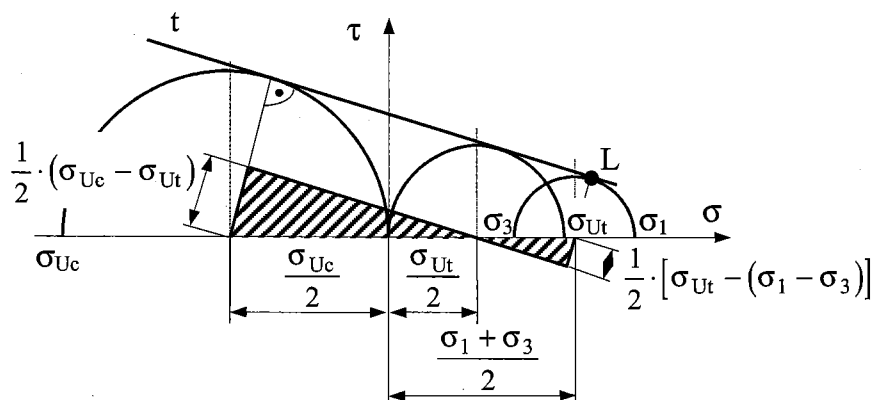
Fig.7.5.2.3

This expression, after being multiplied by the ultimate strength in tension σ_{Ut}, will yield

Mohr's fracture criterion:

$$\sigma_1-\frac{\sigma_{Ut}}{\sigma_{Uc}}\cdot\sigma_3=\sigma_{Ut}\;; \qquad \text{or} \qquad \sigma_1-\rho\cdot\sigma_3=\sigma_{Ut}$$

$$(7.5.2.2a,b)$$

where we denoted the ratio of the ultimate strength in tension and compression, respectively, as

$$\frac{\sigma_{Ut}}{\sigma_{Uc}}=\rho<1 \;;\text{(for the respective allowable stresses, it also holds } \frac{\sigma_{all;t}}{\sigma_{all;c}}=\rho<1\text{)}$$

$$(7.5.2.3a,b)$$

(Allowable working stresses $\sigma_{all;t}$ and $\sigma_{all;c}$ obey Eqs. (2.6.3.3a,b).)

Analogously, we can obtain *Mohr's strength criterion* :

$$\sigma_{eq}=\sigma_{max}-\rho\cdot\sigma_{min}\le\sigma_{all;t} \qquad\qquad (7.5.2.4)$$

7.5.3 Applicability of the criteria for brittle materials

Unlike the *Yield criteria*, i.e. *Tresca's* and *HMH criteria*, valid for ductile materials, the *Fracture criteria*, i.e. "σ_{max}" and *Mohr's*, to be applied to brittle materials, cannot substitute each other. Appropriate applicability of each of the Fracture criteria can be traced from the philosophy of the Mohr's criterion derivation, see Fig.7.5.2.2, where the exact limit curve *t* (connecting the limit points *L* of the respective Mohr's circles representing general stress states) passes from uniaxial compression to uniaxial tension through pure shear. It follows from this that *Mohr's criterion* holds for such a stress state where a combination of positive and negative stresses occurs.

Since the expression for *Mohr's criterion* was finally based on an approximate straight line *t* in Fig.7.5.2.3, this criterion would yield inadmissible factors of safety both for multiaxial tension and for compression (while being quite inappropriate for the latter because the limit straight line *t* does not cut the negative horizontal semi-axis of the diagram in Fig.7.5.2.3; cf. Sec.7.6.2, where the limit surface of Mohr's theory is derived) while the "σ_{max}" *criterion* holds very well for such a stress state where all stresses are positive or negative

In general: *that fracture criterion shall be applied which will yield the smaller factor of safety.*

7.6 Graphical representation of the theories of elastic failure for brittle materials

The theories of elastic failure for brittle materials, discussed in Sec.7.3, have their geometric interpretation in the form of Haigh's limit and allowable surfaces and lines, respectively, as follows.

7.6.1 Graphical representation of maximum-normal-stress-criterion ("σ_{max}")

Referring to the above obtained equivalent strengths for the "σ_{max}"-criterion for both tension and compression, see Eq. (7.5.1.1a,b), and taking into account that each of the principal stresses can assume either max. or min. values, we have:

3D stress state:

$$\sigma_1 = \sigma_{Ut}; \quad -\sigma_1 = \sigma_{Uc}$$

$$\sigma_2 = \sigma_{Ut}; \quad -\sigma_2 = \sigma_{Uc}$$

$$\sigma_3 = \sigma_{Ut}; \quad -\sigma_3 = \sigma_{Uc}$$

i.e., Haigh's limit surface is **cube**

2D (plane) stress state, e.g., $\sigma_3 = 0$:

$$\sigma_1 = \sigma_{Ut}; \; -\sigma_1 = \sigma_{Uc}$$

$$\sigma_2 = \sigma_{Ut}; \; -\sigma_2 = \sigma_{Uc}$$

i.e., Haigh's limit line is **square**

7.6.2 Graphical representation of Mohr's fracture criterion

Each of the principal stresses in this criterion, see Eqs. (7.5.2.2a,b), can assume either max. or min. values:

3D stress state:

$$\frac{\sigma_1}{\sigma_{Ut}} - \frac{\sigma_2}{\sigma_{Uc}} = 1; \qquad \frac{\sigma_2}{\sigma_{Ut}} - \frac{\sigma_1}{\sigma_{Uc}} = 1$$

$$\frac{\sigma_2}{\sigma_{Ut}} - \frac{\sigma_3}{\sigma_{Uc}} = 1; \qquad \frac{\sigma_3}{\sigma_{Ut}} - \frac{\sigma_2}{\sigma_{Uc}} = 1$$

$$\frac{\sigma_3}{\sigma_{Ut}} - \frac{\sigma_1}{\sigma_{Uc}} = 1; \qquad \frac{\sigma_1}{\sigma_{Ut}} - \frac{\sigma_3}{\sigma_{Uc}} = 1$$

i.e., Haigh's limit surface is a **hexahedral pyramid**

2D (plane) stress state, e.g., $\sigma_3 = 0$:

$$\frac{\sigma_1}{\sigma_{Ut}} - \frac{\sigma_2}{\sigma_{Uc}} = 1; \qquad \frac{\sigma_2}{\sigma_{Ut}} - \frac{\sigma_1}{\sigma_{Uc}} = 1$$

$$\frac{\sigma_2}{\sigma_{Ut}} = 1; \qquad -\frac{\sigma_2}{\sigma_{Uc}} = 1$$

$$-\frac{\sigma_1}{\sigma_{Uc}} = 1; \qquad \frac{\sigma_1}{\sigma_{Ut}} = 1$$

i.e., Haigh's limit line is a (deformed) **hexagon**

7.6.3 Plotting of Haigh's limit and allowable figures

Haigh's limit surfaces for ductile materials, i.e., graphical interpretation of *Tresca's* and *HMH* criteria in the case of a 3D stress state, which were a bottomless hexahedral prism and a circular cylinder, respectively, can be applied for graphical solution of problems owing to their simple projection. However, this is not the case for the above obtained Haigh's limit surfaces for brittle material according to the "σ_{max}" and *Mohr's criteria,* since both the cube and the hexahedral pyramid are closed and semi-closed, respectively. Therefore, only plane stress problems can have a graphical solution by applying a square and a deformed hexagon representing the limit lines of the "σ_{max}" and *Mohr's criteria,* respectively. In Fig.7.6.3.1, the respective limit lines are plotted with thick lines, and the respective allowable lines with thin lines.
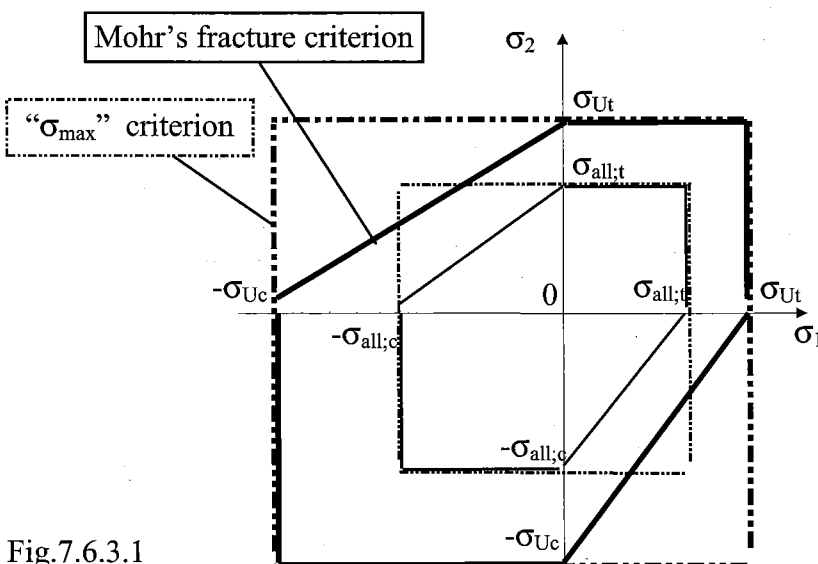
Fig.7.6.3.1

7.7 Examples
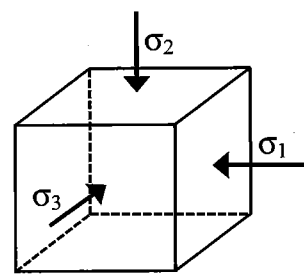
7.7.1 Ductile material dimensioning

Given: The stress-state in a rail, loaded with one wheel of a carriage, was assessed by experimental methods:

$\sigma_1 = -800\ N/mm^2$, $\sigma_2 = -1100\ N/mm^2$, $\sigma_3 = -900\ N/mm^2$.

The rail material: $\sigma_Y = 400\ N/mm^2$

Task: Assess the factor of safety: k_Y

Solution:

First we have to recognize the type of the material given and to know which theories of elastic failure are suitable for it. According to the fact that the *yielding strength* σ_Y is given, it is clear that this material is a **ductile** one, from which follows that the proper criteria are those of *Tresca* and *HMH*.

Numerical solution:

a/ Application of *Tresca* yielding criterion

$$\sigma_{eq} = \sigma_{max} - \sigma_{min} = \sigma_1 - \sigma_2 = (-800) - (-1100) = 300 [N/mm^2]\ ;\ k_{Y,T} = \frac{\sigma_Y}{\sigma_{eq}} = \frac{400}{300} = 1.\overline{3}$$

b/ Application of *HMH* yielding criterion

$$\sigma_{eq} = \frac{\sqrt{2}}{2} \cdot \sqrt{(\sigma_1 - \sigma_2)^2 + (\sigma_2 - \sigma_3)^2 + (\sigma_3 - \sigma_1)^2} =$$

$$= \frac{\sqrt{2}}{2} \cdot \sqrt{[(-800) - (-1100)]^2 + [(-1100) - (-900)]^2 + [(-900) - (-800)]^2} = 264.6 [N/mm^2]$$

$$k_{Y,HMH} = \frac{\sigma_Y}{\sigma_{eq}} = \frac{400}{264.6} = 1.51$$

Graphical solution:

$$k_{Y,T} = \frac{L_T O}{WO} = 1.3$$

$$k_{Y,HMH} = \frac{L_{HMH} O}{WO} = 1.5$$
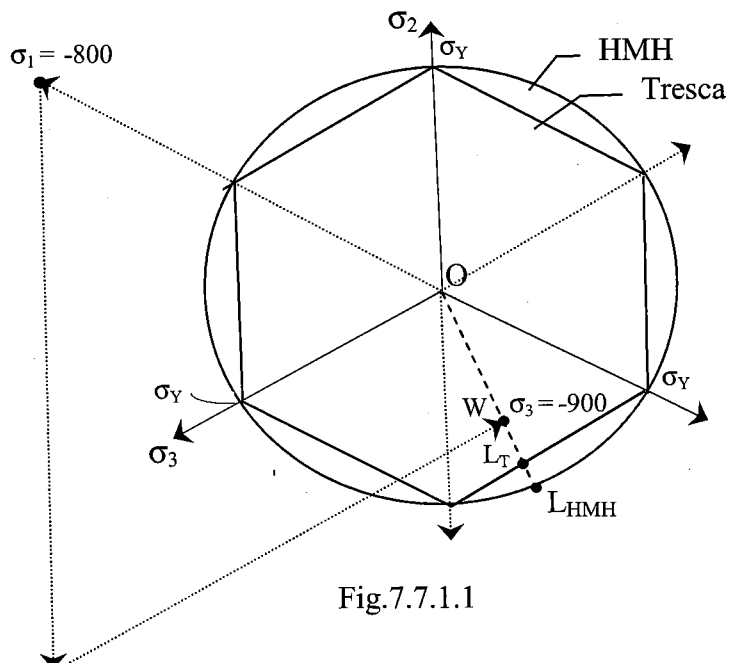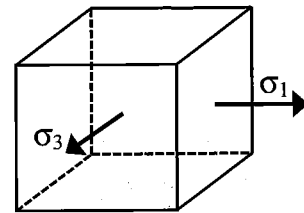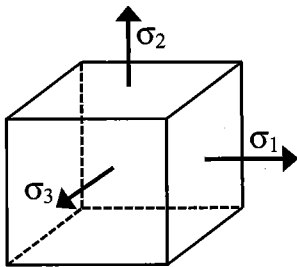
Fig.7.7.1.1

7.7.2 Brittle material dimensioning

Given: <u>Stress-states:</u>

$$2/ \ \sigma_1 = 80 \ N/mm^2, \ \sigma_2 = 0 \ N/mm^2,$$

$$\sigma_3 = 120 \ N/mm^2$$

<u>The brittle material ultimate strengths:</u> $\sigma_{Ut} = 160 \ N/mm^2$; $\sigma_{Uc} = 400 \ N/mm^2$

Task: <u>Determine factors of safety:</u> k_{Ut}

Solution:

We know that for brittle materials <u>two criteria of brittle fracture</u> could be basically applied:

a/ *"σ_{max}"criterion*; b/ *Mohr's criterion.*

But these two criteria depend also on the signs of the stresses applied.

Ad 1/ This is a <u>**3D tension** stress state</u> *($\sigma_1 = 80 \ N/mm^2$, $\sigma_2 = 20 \ N/mm^2$, $\sigma_3 = 120 \ N/mm^2$)*. When comparing the ***Haigh's limit surface*** of *"σ_{max}"criterion* (a cube) with that of ***Mohr's criterion*** (a hexahedral pyramid) in the first octant of $\sigma_{1,2,3}$ coordinates, we see that safer results can be obtained by the *"σ_{max}" criterion* application. At the same time, we see that such a 3D stress state can be solved only analytically.

Analytical (numerical) solution:

ad a/ *"σ_{max}" criterion*: $\sigma_{eq} = \sigma_{max} = \sigma_3 = 120 \left[N/mm^2 \right]$; $k_{Ut,\sigma} = \dfrac{\sigma_{Ut}}{\sigma_{eq}} = \dfrac{160}{120} = 1.3\overline{3}$

ad b/ *Mohr's criterion*:

$$\sigma_{eq} = \sigma_{max} - \frac{\sigma_{Ut}}{\sigma_{Uc}} \cdot \sigma_{min} = \sigma_3 - \frac{\sigma_{Ut}}{\sigma_{Uc}} \cdot \sigma_2 = 120 - \frac{160}{400} \cdot 20 = 112 \left[N/mm^2 \right]$$

$$k_{U,M} = \frac{\sigma_{Ut}}{\sigma_{eq}} = \frac{160}{112} = 1.43$$

The proper **factor of safety** is the minimum one, i.e., $k_U = 1.3\overline{3}$ by *"σ_{max}" criterion.*

Geometrical solution: <u>for brittle materials is not used with 3D stress states.</u>

Ad 2/ This is a <u>2D stress state with mixed stress signs:</u>

($\sigma_1 = 80 \ N/mm^2, \sigma_2 = 0 \ N/mm^2$, $\sigma_3 = -120 \ N/mm^2$),

i.e., *Mohr's criterion* is to be used. But for better imagination, we will try also the *"σ_{max}" criterion* .

Analytical (numerical) solution:

ad a/ *"σ_{max}" criterion:*

tension: $\sigma_{eq} = \sigma_{max} = \sigma_1 = 80\left[N/mm^2\right]$; $k_{Ut,\sigma} = \dfrac{\sigma_{Ut}}{\sigma_{eq}} = \dfrac{160}{80} = 2.0$

compression: $\sigma_{eq} = |\sigma|_{max} = |\sigma_3| = 120\left[N/mm^2\right]$; $k_{Uc,\sigma} = \dfrac{\sigma_{Uc}}{\sigma_{eq}} = \dfrac{400}{120} = 3.\overline{3}$

ad b/ *Mohr's criterion:*

$$\sigma_{eq} = \sigma_{max} - \frac{\sigma_{Ut}}{\sigma_{Uc}} \cdot \sigma_{min} = \sigma_1 - \frac{\sigma_{Ut}}{\sigma_{Uc}} \cdot \sigma_3 = 80 - \frac{160}{400} \cdot (-120) = 128\left[N/mm^2\right]$$

$$k_{U,M} = \frac{\sigma_{Ut}}{\sigma_{eq}} = \frac{160}{128} = 1.25$$

Graphical solution:

"σ_{max}" criterion:

tension:

$$k_{U_t,\sigma_{max}} = \frac{L_{\sigma_{max},t}O}{WO} = 2.0$$

compression:

$$k_{U_c,\sigma_{max}} = \frac{L_{\sigma_{max},c}O}{WO} = 3.\overline{3}$$

Mohr's criterion:

$$k_{U,M} = \frac{L_M O}{WO} = 1.25$$
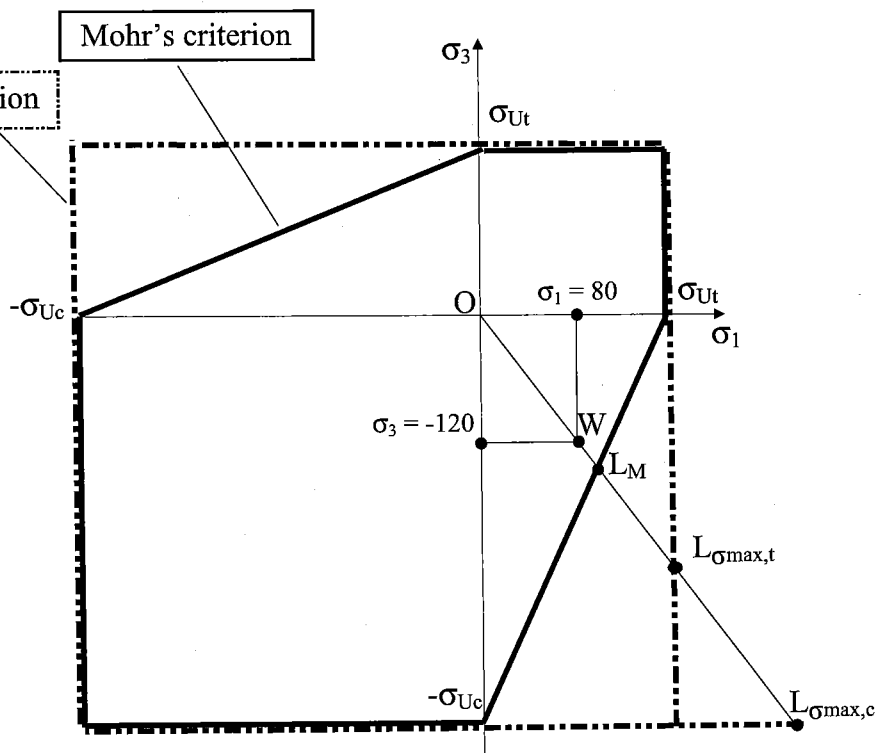
Fig.7.2.1

The resulting factor of safety is $k_{Ut,M} = 1.25$

8. Torsion of circular shafts

We shall analyze the stresses and strains in members of circular cross sections subjected to twisting couples, *torques*, **T** and **T'** (Fig.8.1.1.1). Both couples have a common magnitude **T** , and opposite senses (the couple **T'** can also be considered as the reaction from clamping, or support, or another machine member).

Members in torsion are encountered in many engineering applications. The most common application is provided by *transmission shafts,* which are used to transmit power from one point to another, e.g., from a steam turbine to an electric generator, or from a motor to a machine tool, or from the engine to the rear (or front) axle of an automobile. These shafts may be either solid or hollow.

8.1 Derivation of needed relations

Based on experiments, the following property of shafts is assumed: When a circular shaft is subjected to torsion, *every cross section remains plane and undistorted.* This property will enable us to determine the *distribution of shearing strains* in a circular shaft; the relations between displacement (angle of twist φ) and strain (shear strain γ), i.e., *geometrical relations*; and to conclude that the *shearing strain varies linearly with the distance from the axis of the shaft* (Sec.8.1.1).

Considering deformations in the *elastic range* and using Hooke's law for shearing stress and strain, we shall determine the relation between shear strain γ and stress τ, and, in addition, the *distribution of shearing stresses* in a circular shaft (Sec.8.1.2).

By applying the *equilibrium equation,* we can finally derive all the necessary *elastic torsion formulas*: the *strength* and *stiffness criteria* (Sec.8.1.3).

8.1.1 Geometrical relations

Detaching a cylinder of radius ρ from the shaft in Fig.8.1.1.1, we consider the small square element *AFCD* formed by two circles of radius ρ at a distance of *dx* and two adjacent straight lines *CA* and *DF* traced on the surface of the cylinder before any load is applied, Fig.8.1.1.2. As the shaft is subjected to a torsional load, the element will deform into a rhombus *A'F'CD*, while the originally right angle *ACD* will decrease by the shearing strain γ and the polar radius *OA* (changing into *OA'*) will undergo an angular displacement - *angle of twist $d\varphi$* - with respect to the polar radius *O'C*, see Fig.8.1.1.2. Arc *AA'* can be expressed in two relations

$$\overparen{AA'} = \rho \cdot d\varphi \quad \text{and} \quad \overparen{AA'} = \gamma \cdot dx \implies \gamma = \rho \cdot \frac{d\varphi}{dx}.$$
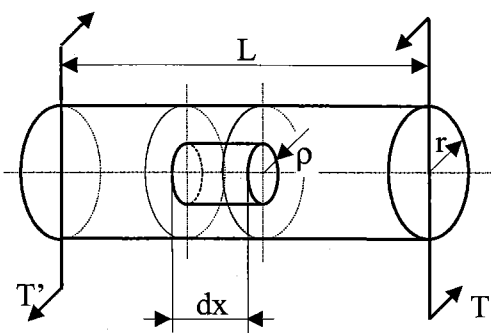
Fig.8.1.1.1
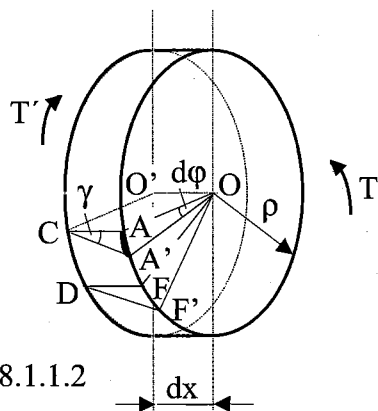
Fig.8.1.1.2

The latter relation can be rewritten as

$$\gamma = \rho \cdot \vartheta \qquad (8.1.1.1)$$

where we denote $d\varphi/dx$ by the symbol ϑ and refer to it as the *angle of twist per unit length*, or the *rate of twist*.

8.1.2 Torsional stresses in the elastic range

Since the shaft deformation is entirely expressed by one shearing strain γ it is dealt with as *pure shear*, and only one member of generalized Hooke's law is of use (it is of no use to write subscripts)

$$\gamma = \frac{\tau}{G}$$

When substituting here for γ from Eq.(8.1.1.1) we have

$$\tau = G \cdot \vartheta \cdot \rho \qquad (8.1.2.1)$$

Since the rate of twist ϑ does not change along a shaft of uniform cross-section subjected to a constant torque (Fig.8.1.1.1), the product

$$G \cdot \vartheta = c \qquad (8.1.2.2)$$

is constant and thus it holds

$$\tau = c \cdot \rho \qquad (8.1.2.3)$$

which expresses that shearing stress increases proportionally with its distance from the shaft axis: it has zero value at the shaft axis and reaches its maximum at the circumference of the circular profile, where $\rho = r$ (Fig.8.1.2.1).

A stress characteristic concerning *complementary* shearing stresses (cf. Sec.5.2) has the following consequences:

  1) In addition to τ exerted in the shaft cross-sections a complementary shearing stress acts in the
     shaft axial sections (Fig.8.1.2.1);

2) Shearing stress has to be tangent to the cross-sectional contour (which is fulfilled with the circular profile).
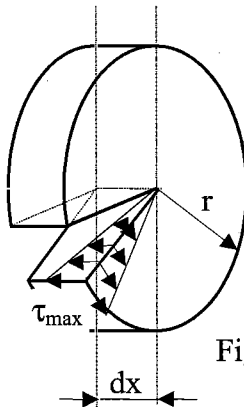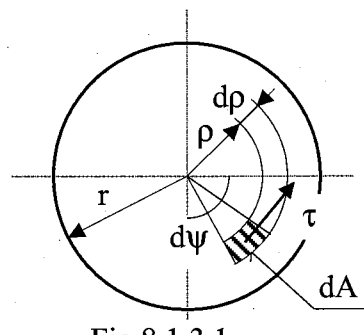
Fig.8.1.2.1   Fig.8.1.3.1

8.1.3 Torsion formulas

When solving tasks of statics, it is necessary that the problems obey *equilibrium equations*. With torsion of shafts, equilibrium between the external loading torque and the corresponding internal resistant torque (i.e., resulting from the produced shearing stresses) will provide the required relation between T and τ.

From the cross-section of a shaft, at an arbitrary radius ρ, we shall cut (using two cylindrical and two radial sections) an elementary area dA, where shearing stress $\tau(\rho)$, obeying Eqs.(8.1.2.1) and (8.1.2.3), is exerted (Fig.8.1.3.1). Based on this, we can express an elementary torque

$$dT = \rho \cdot \tau \cdot dA \quad \Rightarrow \quad dT = c \cdot \rho^2 \cdot dA$$

It holds, for the whole cross-sectional area A,

$$T = c \cdot \int_{(A)} \rho^2 \cdot dA \tag{8.1.3.1}$$

where the relation

$$\int_{(A)} \rho^2 \cdot dA = J \tag{8.1.3.2}$$

defines the *polar moment of inertia* or *polar second moment of area* so that we can write

$$T = c \cdot J \tag{8.1.3.3}$$

When expressing constant c from Eqs.(8.1.2.3.) and (8.1.3.3), we obtain successively the *relation between shearing strain and torque*:

$$c = \frac{\tau}{\rho}; \quad c = \frac{T}{J}, \quad \text{respectively,} \quad \Rightarrow \quad \tau(\rho) = \frac{T}{J} \cdot \rho \tag{8.1.3.4}$$

Since the maximum shearing stress in a cross-section of a shaft occurs at its outer fibres with radius $r = d/2$, we have

$$\tau_{max} = \frac{T}{J} \cdot r \quad \text{or} \quad \tau_{max} = \frac{T}{J} \cdot \frac{d}{2} \qquad (8.1.3.5a)$$

which can be written $\qquad\qquad \tau_{max} = \frac{T}{Z} \qquad\qquad\qquad (8.1.3.5b)$

By comparing Eqs.(8.1.3.5a,b), we have defined the quantity

$$Z = \frac{J}{r} \quad \text{or} \quad Z = \frac{2 \cdot J}{d} \qquad (8.1.3.6)$$

called the *polar section modulus* which is convenient for expressing the maximum shearing stress in a given cross-section of a twisted shaft.

By applying symbol Z we determine the shearing stress at the outer fibres, which here has its maximum value for a given cross-section of a twisted shaft. Considering that both the shaft diameter $d(x)$ and the exerted torque $T(x)$ can vary along the shaft length, it is always necessary to seek for such a site x of the shaft cross-section where the ratio T/Z reaches its maximum. The **torsional strength criterion** is then

$$\tau_{max} = \left(\frac{T}{Z}\right)_{max} \le \tau_{all} \qquad (8.1.3.7a)$$

This strength criterion for torsion recalls in form the strength criterion for tension-compression, see Eq.(2.6.3.4) in Sec.2.6.3, but there is an essential difference: **torsion** produces **a *plane state of stress,*** whereas **tension-compression** produces only a ***uniaxial state of stress.*** We learned from Chap.7 that, in the case of a multiaxial stress state, it is necessary to apply a suitable theory of elastic failure. In the case of torsion σ_{eq} is not determined, but the chosen theory is utilized for assessing the allowable shearing stress τ_{all} based on the allowable stress for tension σ_{all}. As was presented in Chap.7, members stressed predominantly in shear have to be produced from a ductile material, which means that either Tresca's theory or the HMH theory is to be applied. Thus, we have:

- for Tresca's theory it holds $\tau_{all} = \dfrac{\sigma_{all}}{2}$ (cf. Sec5.6.3 and 7.3.1); $\qquad (8.1.3.7b)$

- for the HMH theory, when we substitute into Eq.(7.3.2.2a) the stress state of pure shear (e.g.,$\sigma_x = \sigma_y =$

$= \sigma_z = \tau_x = \tau_y = 0; \ \tau_z = \tau_{all}$), we obtain $\tau_{all} = \dfrac{\sigma_{all}}{\sqrt{3}}$. $\qquad (8.1.3.7c)$

When substituting for c from Eq.(8.1.2.2) into Eq.(8.1.3.3) we have

$$T = \vartheta \cdot G \cdot J \quad \Rightarrow \quad \vartheta = \frac{T}{G \cdot J} \qquad (8.1.3.8)$$

which expresses the dependence between the *rate of twist* and the *torque*.

After limiting the rate of twist with a *maximum allowable value* ϑ_{all}, we obtain the **torsional stiffness criterion**

$$\vartheta = \frac{T}{G \cdot J} \leq \vartheta_{all} \,, \qquad (8.1.3.9)$$

while the quantity GJ is termed the *torsional rigidity* of the shaft and is thus given by

$$G \cdot J = \frac{T}{\vartheta} \qquad (8.1.3.10)$$

Taking into account definition $\vartheta = d\varphi / dx$, we obtain, from Eq. (8.1.3.8), the expression for the *elementary angle of twist* in the form

$$d\varphi = \frac{T}{G \cdot J} \cdot dx$$

For a constant torque T along a length L of the shaft we have

$$\varphi = \frac{T \cdot L}{G \cdot J} \qquad (8.1.3.11)$$

Formula (8.1.3.11) for the *angle of twist* may be used only if the shaft is homogenous (constant G), has a uniform cross-section, and is loaded at its ends. In the case of varying torque $T(x)$ and/or cross-section $J(x)$, the angle of twist can be calculated from

$$\varphi = \frac{1}{G} \cdot \int_{(L)} \frac{T(x)}{J(x)} \cdot dx \qquad (8.1.3.12)$$

8.2 Polar second moment of area (polar moment of inertia)

As stated above the *polar second moment of area* J is defined as

$$J = \int_{(A)} \rho^2 \cdot dA$$

where, according to Fig.8.1.3.1, it holds

$$dA = \rho \cdot d\psi \cdot d\rho$$

For a *solid shaft*

$$J_{(d)} = \int_0^r \rho^3 \cdot d\rho \cdot \int_0^{2\cdot\pi} d\psi = \frac{\pi \cdot r^4}{2} = \frac{\pi \cdot d^4}{32} \quad [\text{m}^4; \text{mm}^4] \qquad (8.2.1)$$

For a *hollow shaft* of outside diameter D (radius R) and inside diameter d (radius r), see Fig.8.2.1, we can obtain (since J is a result of integration) the resulting $J_{(D/d)}$ by subtracting $J_{(d)}$ (of the hole) from $J_{(D)}$,

i.e., $\quad J_{(D/d)} = J_{(D)} - J_{(d)} = \dfrac{\pi \cdot D^4}{32} - \dfrac{\pi \cdot d^4}{32} = \dfrac{\pi \cdot D^4}{32} \cdot \left[1 - \left(\dfrac{d}{D} \right)^4 \right] \qquad (8.2.2)$
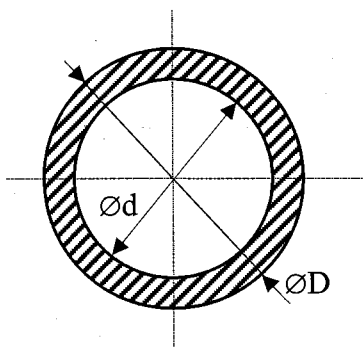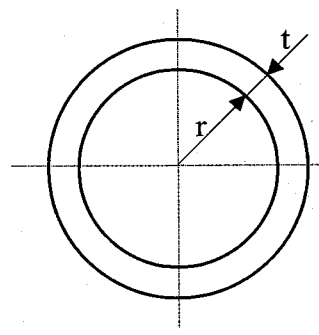
Fig.8.2.1   Fig.8.2.2

For the respective *polar section modulus,* see Sec.8.1.3, Eq.(8.1.3.6), it holds:

$$\text{for a } solid\ shaft \quad ... \quad Z_{(d)} = \frac{J_{(d)}}{d/2} = \frac{\pi \cdot d^3}{16} \qquad (8.2.3)$$

$$\text{for a } hollow\ shaft\ ... \quad Z_{(D/d)} = \frac{J_{(D/d)}}{D/2} = \frac{\pi \cdot D^3}{16} \cdot \left[1 - \left(\frac{d}{D}\right)^4\right] \qquad (8.2.4)$$

In the case of torsion of a thin-walled pipe (Fig.8.2.2), where $r >> t$, we have approximately

$$J = r^2 \cdot 2 \cdot \pi \cdot r \cdot t = 2 \cdot \pi \cdot r^3 \cdot t \quad ; \quad Z = \frac{J}{r} = 2 \cdot \pi \cdot r^2 \cdot t \qquad (8.4.5a,b)$$

Note: Since Z is not based on integration, this cannot be obtained by addition or subtraction and the looked-for *polar section modulus* of a shaft is defined by means of the corresponding *polar second moment of area* of the shaft divided by its outside radius.

8.3 Strain energy in torsion and application of *Castigliano's theorem*

Consider a shaft BC of length L subjected to one or several twisting couples. Denoting by J the *polar second moment of area* located at a distance x from B and by T the (internal) torque in that section, we recall that the shearing stresses in the section are $\tau = T\rho/J$.

Substituting for τ into the expression

$$dU_T = \lambda_\tau \cdot dV = \frac{\tau^2}{2G} \cdot dA \cdot dx,$$

we successively obtain

$$U_T = \int_{(V)} \frac{(T \cdot \rho)^2}{2GJ^2} dx \cdot dA = \int_{(L)} \frac{T^2}{2GJ^2} \cdot \left(\int_{(A)} \rho^2 \cdot dA\right) dx = \int_{(L)} \frac{T^2(x)}{2G(x) \cdot J(x)} dx \qquad (8.3.1)$$

For such a case, when the quantities T, G, J are constant along the shaft length L, the *strain energy for torsion* is given by (cf. Eq.2.12.3)

$$U = \frac{T^2 \cdot L}{2 \cdot G \cdot J}.$$

(8.3.2)

Knowledge of the *strain energy for torsion* will enable us to apply *Castigliano's theorem:*

If an external torque T_j is exerted in a cross-section j, then the angle of twist $\varphi_{(i-j)}$ of this cross-section j with respect to a chosen section i, being situated in a distance L,

yields from

$$\varphi_{(i-j)} = \frac{\partial U_{(i-j)}}{\partial T_j}$$

(8.3.3)

After substituting here from the expression for the strain energy, we shall obtain the following expression

$$\varphi_{(i-j)} = \int\limits_{(L)} \frac{T(x)}{G \cdot J(x)} \cdot \frac{\partial T(x)}{\partial T_j} dx$$

(8.3.4)

which is analogous to expression (2.13.6) used in Chap.2 (dealing with uniaxial loading - tension or compression), i.e., we can substitute $\dfrac{\partial T(x)}{\partial T_j} = t(x)$ and thus we have (cf. Eq.2.13.7)

$$\varphi_{(i-j)} = \int\limits_{(L)} \frac{T(x)}{G \cdot J(x)} \cdot t(x) \cdot dx$$

(8.3.5)

where: $T(x)$...internal torque in an arbitrary site x acting between sections i - j having mutual distance L (i.e., the sum of all external torques acting along one side of the shaft from one end up to point x)
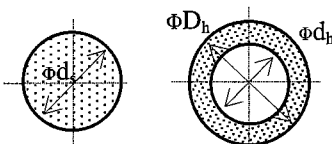
$t(x)$...internal torque in x produced by a dummy load (unit external torque) which is exerted in section j where we are to determine the angle of twist with respect to section i.

Example 8.3.1:
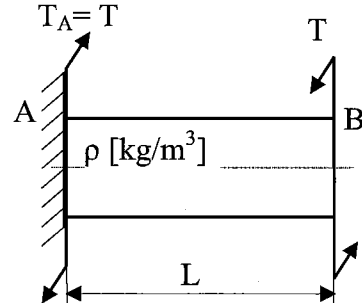
Given: Two types of shaft having:

1) **solid** profile (d_s);

2) **hollow** profile (D_h, d_h)

where: $D_h/d_h = 1.2$; $L = 1\,m$; $T = 1.2 \cdot 10^2$ kNm ;

$G = 8.1 \cdot 10^4$ N/mm^2 ; $\tau_{all} = 50$ N/mm^2
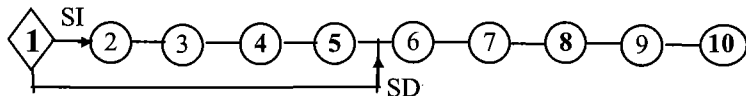
Task: Assess:

a/ Dimensions: solid shaft d_s ; hollow shaft (D_h, d_h);

b/ Mass ratio of the shafts: m_s / m_h ;

c/ The shafts angles of twist φ_{ABs}, φ_{ABh} at the torque locations B with respect to the shafts fixation A

Solution: (apply the flow diagram)

$$\langle 1 \rangle \xrightarrow{SI} (2)-(3)-(4)-(5)-(6)-(7)-(8)-(9)-(10)$$
$$\downarrow SD$$

Since the problem is *SD*, we start with **Items 6 + 7**: $T(x) = T$; $\tau(x) = \dfrac{T(x)}{Z_T} = \dfrac{T}{Z_T} = \tau_{max}$.

Item 8: Dimensioning. *Tresca's strength criterion* $\tau_{max} = \dfrac{T}{Z_T} \le \tau_{all}$

ad 1) <u>Solid profile:</u> $Z_{Ts} = \dfrac{\pi \cdot d_s^3}{16}$ => $d_s \ge \sqrt[3]{\dfrac{16 \cdot T}{\pi \cdot \tau_{all}}} = \sqrt[3]{\dfrac{16 \cdot 1.2 \cdot 10^8}{\pi \cdot 50}} = 230.4[\text{mm}]$

Chosen value: $d_s = 230[\text{mm}]$. Though this is a bit smaller diameter than that based on *Tresca*,

<u>mind</u> that $\tau_{all,HMH} = \tau_{all,T} \cdot \dfrac{2}{\sqrt{3}} = 57.73 \text{ N/mm}^2$ and the shaft safety is preserved

ad 2) <u>Hollow profile:</u> $Z_{Th} = \dfrac{\pi \cdot D_h^3}{16}\left[1 - \left(\dfrac{d_h}{D_h}\right)^4\right]$ =>

$$D_h \ge \sqrt[3]{\dfrac{16 \cdot T}{\pi \cdot \left[1 - \left(\dfrac{d_h}{D_h}\right)^4\right] \cdot \tau_{all}}} = \sqrt[3]{\dfrac{16 \cdot 1.2 \cdot 10^8}{\pi \cdot \left[1 - \left(\dfrac{1}{1.2}\right)^4\right] \cdot 50}} = 286.9[\text{mm}] \quad ;$$
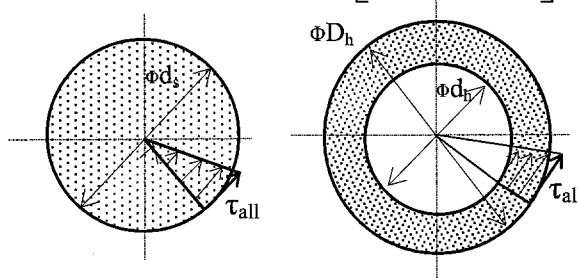
$$d_h = \dfrac{286.9}{1.2} = 239.1[\text{mm}]$$

Chosen values: $D_h = 290[\text{mm}]$; $d_h = 240[\text{mm}]$ ($D_h/d_h = 290/240 = 1.21$)

Mass ratio: ad 1) <u>Solid profile:</u> $m_s = V \cdot \rho = \dfrac{\pi \cdot d_s^2}{4} \cdot L \cdot \rho$

ad 2) <u>Hollow profile:</u> $m_h = V \cdot \rho = \dfrac{\pi \cdot D_h^2}{4} \cdot \left[1 - \left(\dfrac{d_h}{D_h}\right)^2\right] \cdot L \cdot \rho$

$$\dfrac{m_s}{m_h} = \dfrac{d_s^2}{D_h^2 \cdot \left[1 - \left(\dfrac{d_h}{D_h}\right)^2\right]} = 2.1$$

Item 9: Checking of the resulting stress.

ad 1) <u>Solid profile:</u> $\tau_{max} = \dfrac{T}{Z_{Ts}} = \dfrac{1.2 \cdot 10^8}{\dfrac{\pi \cdot 230^3}{16}} = 50.23 \text{N} / \text{mm}^2 \approx \tau_{all,T} < \tau_{all,HMH}$

ad 2) <u>Hollow profile:</u> $\tau_{max} = \dfrac{T}{Z_{Ts}} = \dfrac{1.2 \cdot 10^8}{\dfrac{\pi \cdot 290^3}{16}\left[1-\left(\dfrac{240}{290}\right)^4\right]} = 47.2\,\text{N}\,/\,\text{mm}^2 < \tau_{all,T}$

Item 10: Deformation. Angles of twist (since $\tau = \dfrac{T}{Z_T} = \text{const}$, *Eq, (8.1.3.12)* is to be applied)

ad 1) <u>Solid profile:</u> $\varphi_s = \dfrac{T \cdot L}{G \cdot \dfrac{\pi \cdot d_s^4}{32}} = \dfrac{1.2 \cdot 10^8 \cdot 10^3}{8.1 \cdot 10^4 \cdot \dfrac{\pi \cdot 230^4}{32}} = 5.3924 \cdot 10^{-3}\,\text{rad} = 18'32''$

ad 2) <u>Hollow profile:</u>

$\varphi_h = \dfrac{T \cdot L}{G \cdot \dfrac{\pi \cdot D_h^4}{32} \cdot \left[1-\left(\dfrac{d}{D}\right)^4\right]} = \dfrac{1.2 \cdot 10^8 \cdot 10^3}{8.1 \cdot 10^4 \cdot \dfrac{\pi \cdot 290^4}{32}\left[1-\left(\dfrac{240}{290}\right)^4\right]} = 4.0187 \cdot 10^{-3}\,\text{rad} = 13'49''$

Conclusion: i) the hollow shaft is <u>two times lighter</u> then the solid shaft, and ii) at the same time the hollow shaft is <u>stiffer</u> then the solid shaft

8.4 Statically indeterminate problems in torsion.

Such problems frequently arise in the case of torsional loadings. In Chap.3, dealing with statically indeterminate problems in tension and compression, a generally applicable procedure (containing 5 items) leading to the solution of SI problems was presented, see Sec.3.2.

We shall apply this procedure on the following example 8.4.1:

Example 8.4.1: Determine the reactive torques at the fixed ends of the circular shaft shown in Fig.8.4.1*a*, loaded by the couples $T_1=3.10^7 N.mm$ and $T_2=4.10^7 N.mm$ the location of which is given by: $a = c = 400\ mm;\ b = 300\ mm$. The cross-section of the bar is constant along the length. When $G = 8.10^{4\ 2}$ and $\tau_{all} = 60\ N/mm^2$ hold for the material of the shaft, dimension its diameter ϕd.

Solution:

The solution is analogous to a fixed rod to which we would apply axial forces F_1 and F_2 instead of torques T_1 and T_2 being exerted in the shaft and then we could proceed in such a way that we would release the rod, for instance at the clamping B and write one equilibrium equation and one compatibility relation ($\Delta L_B = 0$)., for the given shaft, we can write one *equilibrium equation* as follows

$$T_A + T_1 - T_2 - T_B = 0 \qquad\qquad (8.4.1)$$

containing two unknown reactive torques T_A and T_B at the fixed ends, which confirms the member is statically indeterminate to the first degree. We release the shaft at point B and substitute this removed support B with a <u>statically indeterminate torque</u> T_B (which is considered as active during the solution)

while a <u>reactive torque</u> T_A will be exerted at the remaining support A (Fig.8.4.1b). By the following *compatibility relation*

$$\varphi_B = 0 \qquad (8.4.2)$$

we express the reality that point B was originally fixed (Fig.8.4.1a), and, subsequently, no angle of twist could arise there. We can specify this condition by superposing all <u>active torques</u> which twist cross-section B with respect to cross-section A, thus obtaining

a)

b)

c)

Fig.8.4.1

$$\varphi_B = \varphi_{B;T_B} - \varphi_{B;T_1} + \varphi_{B;T_2} = 0 \qquad (8.4.3)$$

Individual respective *constitution relations* are

$$\varphi_{B;T_B} = \frac{T_B \cdot L}{G \cdot J} \; ; \qquad \varphi_{B;T_1} = \frac{T_1 \cdot (a+b)}{G \cdot J} \qquad ;$$

$$\varphi_{B;T_2} = \frac{T_2 \cdot a}{G \cdot J} \qquad (8.4.4)$$
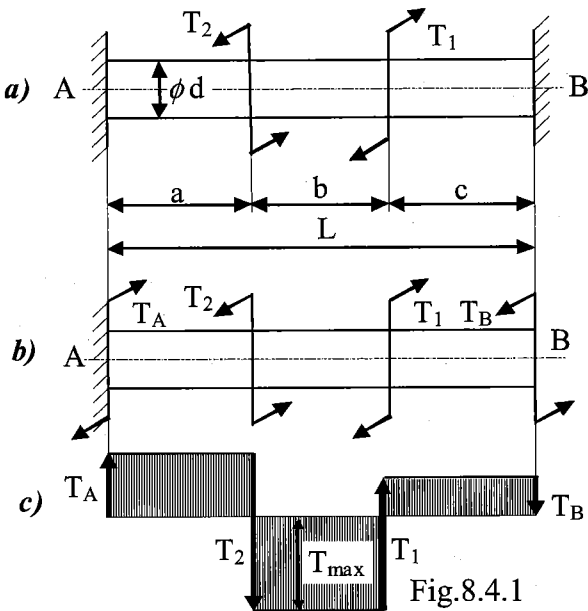
By combining Eqs.(8.4.3) and (8.4.4), we obtain the <u>statically indeterminate torque</u> T_B (while substituting the given numerical values) in the form

$$T_B = T_1 \cdot \frac{a+b}{L} - T_2 \cdot \frac{a}{L} \approx 0.45 \cdot 10^7 \left[N \cdot mm \right]$$

The torque in the section a is identical with the reactive torque T_A, which we will calculate from the equilibrium equation (after substituting for T_B) in the form

$$T_A = T_2 - T_1 + T_B = T_2 \cdot \frac{b+c}{L} - T_1 \cdot \frac{c}{L} \approx 1.45 \cdot 10^7 \left[N \cdot mm \right]$$

The moment distribution is plotted in Fig.8.4.1c while having its maximum value in section b

$$T_{max} = \left| T_A - T_2 \right| \approx 2.55 \cdot 10^7 \left[N \cdot mm \right]$$

The diameter of the shaft is determined by the application of relevant strength criterion, see Eqs.(8.1.3.7) and (8.2.3),

$$T_{max} \leq Z \cdot \tau_{all} \quad ; \quad \text{where} \quad Z = \frac{\pi \cdot d^3}{16}$$

From that we assess

$$d = \sqrt[3]{\frac{16 \cdot T_{max}}{\pi \cdot \tau_{all}}} \approx 130 \left[mm \right]$$

Example 8.4.2: Another example is a shaft composed of two materials, a tube of *steel* surrounding a tube of *copper,* with the entire assembly being subjected to a twisting moment (Fig.8.4.2).

Solution:

As usual, the applicable *statics equations* (in this case being one, i.e.,

$$T = T_{Cu} + T_{Fe}$$

expressing that each tube will carry a respective part of the applied torque according to its stiffness) must be
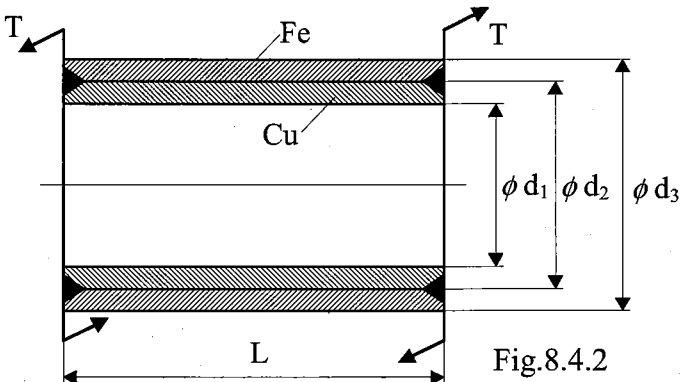
Fig.8.4.2

supplemented by additional *equations based upon the deformations* of the structure in order to furnish a number of equations equal to the number of unknowns. Because of the $1°$ SI of the member, there is only one such equation, i.e.,

$$\varphi_{Cu} = \varphi_{Fe} \Rightarrow \frac{T_{Cu} \cdot L}{G_{Cu} \cdot J_{Cu}} = \frac{T_{Fe} \cdot L}{G_{Fe} \cdot J_{Fe}}$$

stating that the angles of twist of the two materials are equal.

Based on these relations, the torques of the copper and steel tube will be

$$T_{Cu} = T \cdot \frac{G_{Cu} \cdot J_{Cu}}{G_{Cu} \cdot J_{Cu} + G_{Fe} \cdot J_{Fe}} \; ; \; T_{Fe} = T \cdot \frac{G_{Fe} \cdot J_{Fe}}{G_{Cu} \cdot J_{Cu} + G_{Fe} \cdot J_{Fe}}, \text{ respectively.}$$

Note: This example is analogous to the example of parallel members connected with a rigid plate solved in Sec.3.4. (Either "*St*" or "*Fe*" subscripts denoting a **steel** member are used in technical literature.)

8.5 Close-coiled helical springs subjected to axial load *W*

Springs are energy absorbing units whose function it is to store energy and release it slowly or rapidly depending on the particular application. In motor vehicle applications the springs act as buffers between the vehicle itself and the external forces applied through the wheels by uneven road conditions. In such cases the shock loads are converted into strain energy of the spring and the resulting effect on the vehicle is much reduced. In some cases springs are merely used as positioning devices whose function it is to return mechanisms to their original positions after some external force has been removed. From a design point of view "good" springs store and release energy but do not significantly absorb it. Should they do so then they will be prone to failure.

8.5.1 Types of stress in close-coiled helical springs

Let us consider a helical spring constructed from wire in the form of a helix and subjected to axial load W, as shown in Fig.8.5.1.1. By application of the *method of sections* on a cross-section of the spring, sufficiently distant from the spring ends, we can determine its state of stress, in a plane including the spring axis, which is produced by load W and couple $M = W.D / 2$.
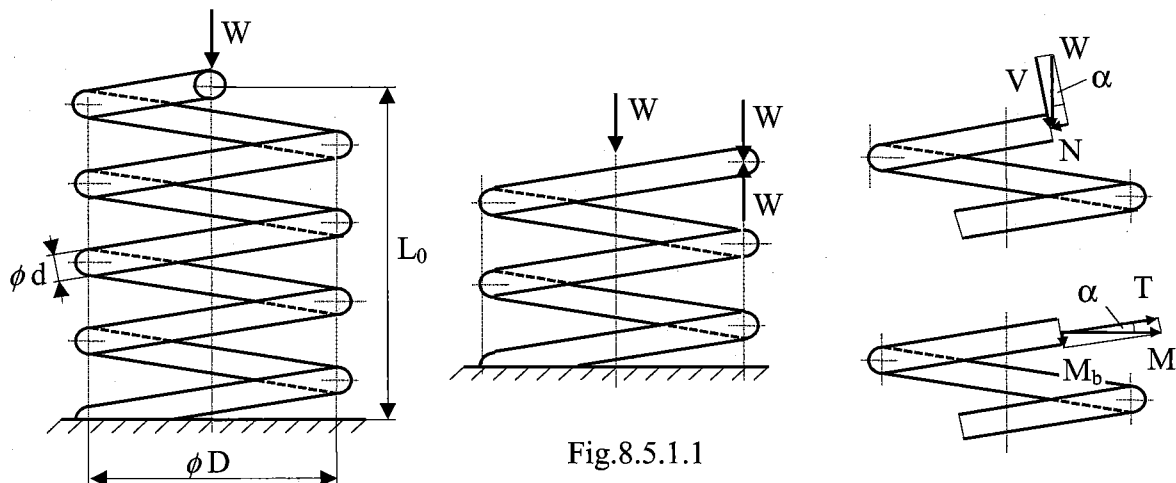
Fig.8.5.1.1

Consider a cross-section perpendicular to the tangent of the wire axis. In the considered cross-section (tangent to the wire axis), we decompose these two loading factors in the directions perpendicular and tangent to the wire axis, respectively, thus obtaining the basic types of stress state, as follows:

1. Compression component ... $N = W \cdot \sin \alpha$

2. Shear component ... $V = W \cdot \cos \alpha$

3. Bending component ... $M_b = \dfrac{W \cdot D}{2} \cdot \sin \alpha$

4. Twisting component ... $T = \dfrac{W \cdot D}{2} \cdot \cos \alpha$

We observe that such a helix spring has a relatively complicated state of stress. But if the spring is *close-coiled*, i.e., constructed in such a way that each turn of the helix is close to the adjacent turn, we can consider the *helix angle α* to be so small that it may be neglected, i.e., each turn may be considered to lie on a horizontal plane (if the central axis of the spring is vertical). Consequently, it holds $\sin \alpha \approx 0$ and $\cos \alpha \approx 1$ and thus, the bending M_b and compression N components can be neglected. The only remaining components loading *close-coiled helix* spring are *shearing force* $V \approx W$ and *torque*

$$T \approx \frac{W \cdot D}{2} \qquad\qquad (8.5.1.1)$$

If, in addition, the helix spring (with diameter D) is constructed of a wire (with diameter d) being relatively thin, and thus having so-called *spring index D/d* that is relatively high, i.e., $D/d >> 10$, then

even a small load W (multiplied by arm $D/2$) causes a considerable torque. Therefore, with **close-coiled helix springs made of a thin wire** it is possible to **neglect the shearing force** $V \approx W$ and **consider only torque** producing shearing stress as follows

$$\tau = \frac{T}{Z} = \frac{\dfrac{W \cdot D}{2}}{\dfrac{\pi \cdot d^3}{16}} = \frac{8 \cdot W \cdot D}{\pi \cdot d^3} \approx 2.5 \cdot W \cdot \frac{D}{d^3} \qquad (8.5.1.2)$$

This stress must obey the *strength criterion* $\qquad \tau_{max} \le \tau_{all} \qquad (8.5.1.3)$

Most springs in production do not differ greatly from the presented assumptions and thus, it is possible to carry out the dimensioning of springs in the manner discussed above. With springs having spring index $D/d < 10$, it is necessary to define the computation of spring dimensions, i.e. to consider the <u>combined stress of torque and shear.</u> This procedure (cf. Sec.13.3) leads to the finding that maximum stress occurs at the inner side of the wire section.

For instance, in the following relation

$$\tau_i = \kappa \cdot 2.5 \cdot W \cdot \frac{D}{d^3},$$

presented in technical literature, <u>coefficient</u> $\kappa \in \langle 1.514 \div 1.134 \rangle$, corresponding to <u>spring index</u> $D/d \in \langle 3 \div 10 \rangle$, respectively, holds for <u>helix angle</u> $\alpha = 0°$. With **open-coiled** *helical springs,* similar coefficients can be obtained <u>including the influence of bending and compression</u> (or tension):

for $\alpha = 15°$ ... $\kappa \in \langle 1.441 \div 1.091 \rangle$; for $\alpha = 30°$ ... $\kappa \in \langle 1.241 \div 0.966 \rangle$

Note: Springs are manufactured either by hot- or cold-working processes, depending on the size of the material, the spring index, and the properties desired. In general, winding the spring induces residual stresses through bending, but these are normal to the direction of the torsional working stresses in a coil spring. Quite frequently in spring manufacture, these are relieved, after winding, by a mild thermal treatment. A wide variety of spring materials are available to the designer, including plain carbon steels, alloy steels, and corrosion-resisting steels, as well as nonferrous materials such as phosphor bronze, spring brass, etc. An excellent material for highly stressed springs requiring long life and subjected to shock loading is **chrome silicon,** which has high values of allowable strength of about $\tau_{all} = 500 \ N/mm$.

8.5.2 Deflection of close-coiled helical springs

By means of Castigliano's theorem (cf. Sec.2.13) we can easily assess the deflection of close-coiled helical spring. Utilizing the above mentioned (Sec.8.5.1) simplifications, we substitute corresponding quantities into Eq.(8.3.2) and have the strain energy accumulated in the spring in the form

$$U = \frac{T^2 \cdot L}{2 \cdot G \cdot J} = \frac{\left(\frac{W \cdot D}{2}\right)^2 \cdot \pi \cdot D \cdot n}{2 \cdot G \cdot \frac{\pi \cdot d^4}{32}} = \frac{4 \cdot W^2 \cdot D^3 \cdot n}{G \cdot d^4}$$

where the length of the spring wire L was obtained as the circumferential length of one coil πD multiplied by the number of active coils n, i.e., $L = \pi D.n$; and that of the wire cross-section was substituted for J.

By applying Castigliano's theorem we obtain the following expression for the spring deflection

$$y_W = \frac{\partial U}{\partial W} = W \cdot \frac{8 \cdot D^3 \cdot n}{G \cdot d^4} \qquad (8.5.2.1)$$

This expression can (by analogy with Eq.(2.7.4b)) be rewritten as

$$y_W = W \cdot \frac{1}{k}$$

By comparing the last two relations we express the *spring rate* (i.e. *spring stiffness*)

$$k = \frac{G \cdot d^4}{8 \cdot D^3 \cdot n} \qquad \left[N \cdot mm^{-1}\right] \qquad (8.5.2.2)$$

Example 8.5.1: A close-coiled helical spring should have a stiffness of *90 N/mm* and should exert a force of *3 kN* ; the mean diameter of the coils should be *75 mm* and the maximum stress should not exceed *240 N/mm²*. Calculate the required number of coils and the diameter of the steel rod from which the spring should be made.

Solution: The solution is obtained from the strength criterion (Eqs. 8.5.1.2 and 8.5.1.3)

$$\tau = \frac{T}{Z} \approx 2.5 \cdot W \cdot \frac{D}{d^3} \le \tau_{all} \Rightarrow d \ge \sqrt[3]{\frac{2.5 \cdot W \cdot D}{\tau_{all}}} = \sqrt[3]{\frac{2.5 \cdot 3 \cdot 10^3 \cdot 75}{240}} \approx 13 \, mm$$

By applying the stiffness criterion that can be derived from Eq.(8.5.2.2) in the form

$$k = \frac{G \cdot d^4}{8 \cdot D^3 \cdot n} \ge k_{all}$$

we can calculate the required number of coils as

$$n \le \frac{G \cdot d^4}{8 \cdot D^3 \cdot k_{all}} = \frac{8 \cdot 10^4 \cdot 13^4}{8 \cdot 75^3 \cdot 90} = 7.52 \Rightarrow n = 7$$

Example 8.5.2: Now we can return back to the **impact loading** discussed in **Chapter 2**, namely to the mine lift (mass $m=10^3$ *kg* and velocity $v=1$ *m/s*), cf. Example 2.12.1. We shall design a suitable closely coiled helical spring ($D/d \approx 10$) made of a special material ($\tau_{all} = 5x10^8 \, N/m^2$, $G = 8.1x10^{10} \, N/m^2$).

Solution: First we shall dimension the wire diameter d (using the strength criterion and estimating the spring diameter $D = 0.2$ *m*.

$$\tau = \frac{T}{Z} \approx 2.5 \cdot W \cdot \frac{D}{d^3} \le \tau_{all} \Rightarrow d \ge \sqrt[3]{\frac{2.5 \cdot W \cdot D}{\tau_{all}}} = \sqrt[3]{\frac{2.5 \cdot 9.81 \cdot 10^3 \cdot 0.2}{5 \cdot 10^8}} = 0.021\,m = 21mm$$

(the design requirement $D/d \approx 10$ is obeyed)

Expressing strain energy accumulated in helical springs and comparing with the lift kinetic energy

$$U = \frac{4 \cdot W^2 \cdot D^3 \cdot n}{G \cdot d^4} = \Delta K = \frac{m \cdot v^2}{2} \text{ (where the lift weight } W=mg),$$

we see that only one free parameter to be assessed is the number of coils n:

$$n \ge \frac{m \cdot v^2 \cdot G \cdot d^4}{8 \cdot (m \cdot g)^{2\cdot} \cdot D^3} = \frac{1^2 \cdot 8.1 \cdot 10^{10} \cdot 0.021^4}{8 \cdot 10^3 \cdot 9.81^2 \cdot 0.2^3} = 2.55 \approx 3,$$

from which we obtain that the minimum number of coils shall be $n = 3$.

Summary: The resulting parameters of the spring are: $D \ge 200$ *mm*, $d = 21$ *mm*, $n \ge 3$ which can

accumulate the strain energy of $\quad \Delta K = \dfrac{m \cdot v^2}{2} = \dfrac{10^3 \cdot 1^2}{2} = 0.5 \cdot 10^3 \left[\dfrac{kg \cdot m}{s^2} \cdot m = J\right] = 5 \cdot 10^2 [kJ]$

8.5.3 Springs in series

If two springs of different stiffness are joined end-on and carry a common load W, they are said to be *connected in series* (Fig.8.5.3.1). This task being *statically determinate,* the combined stiffness and deflection are given by the following equations.

Deflection $\quad y = \dfrac{W}{k} = y_1 + y_2 = \dfrac{W}{k_1} + \dfrac{W}{k_2} \Rightarrow \qquad (8.5.3.1)$

Stiffness $\quad \dfrac{1}{k} = \dfrac{1}{k_1} + \dfrac{1}{k_2} \Rightarrow \quad k = \dfrac{k_1 \cdot k_2}{k_1 + k_2} \qquad (8.5.3.2)$

From this and from Eq.(8.5.4.3) (cf. Sec.8.5.4) we see that *spring stiffness* behaves like *capacity in electrotechnics.*
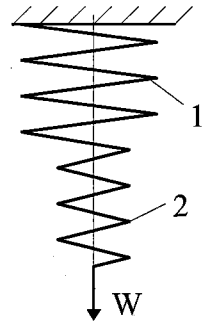
Fig.8.5.3.1

8.5.4 Springs in parallel

If two springs are joined in such a way that they have a common deflection y they are said to be *connected in parallel* (Fig.8.5.4.1). This task is *statically indeterminate* and its solution could be mathematically identical with the case of "Parallel members connected with a rigid plate" in Sec.3.4 and "Tube of copper surrounded with tube of steel", see example 8.4.2, if we there substituted (for the respective materials)

$$\frac{E_{St;Al} \cdot A_{St;Al}}{L} = k_{t\,St;Al} \qquad ; \qquad \frac{G_{Fe;Cu} \cdot J_{Fe;Cu}}{L} = k_{T\,Fe;Cu}$$

which are stiffness in tension (compression) and torsion, respectively, and would diversify only when the respective expressions for the respective stiffness is substituted back. In this case the load carried is shared between the two springs and total load

$$W = W_1 + W_2 \qquad (8.5.4.1)$$

Now
$$y = \frac{W}{k} = \frac{W_1}{k_1} = \frac{W_2}{k_2} \qquad (8.5.4.2)$$

so that
$$W_1 = W \cdot \frac{k_1}{k} \quad ; \quad W_2 = W \cdot \frac{k_2}{k}$$

Substituting in Eq.(8.5.4.1)

$$W = W \cdot \frac{k_1}{k} + W \cdot \frac{k_2}{k} = \frac{W}{k} \cdot \left(k_1 + k_2\right)$$

Fig.8.5.4.1

i.e., **combined stiffness**
$$k = k_1 + k_2 \qquad (8.5.4.3)$$

Where $k_1 = \dfrac{G_1 \cdot d_1^{\,4}}{8 \cdot D_1^{\,3} \cdot n_1}$ and $k_2 = \dfrac{G_2 \cdot d_2^{\,4}}{8 \cdot D_2^{\,3} \cdot n_2}$
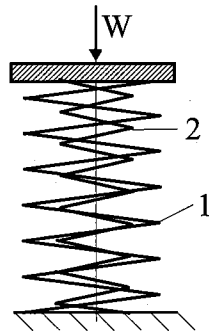
Note: Now we can summarize all the parallel problems, we have mentioned so far.

Chapter 2: Tension and compression – *3.4 Parallel members connected with a rigid plate:*

$$N_{Al} = F \cdot \frac{k_{Al}}{k_{Al} + k_{St}} = F \cdot \frac{E_{Al} \cdot A_{Al}}{E_{Al} \cdot A_{Al} + E_{St} \cdot A_{St}} \; ; \quad N_{St} = F \cdot \frac{k_{St}}{k_{Al} + k_{St}} = F \cdot \frac{E_{St} \cdot A_{St}}{E_{Al} \cdot A_{Al} + E_{St} \cdot A_{St}}$$

Where $k_{Al} = \dfrac{E_{Al} \cdot A_{Al}}{L}$; $k_{St} = \dfrac{E_{St} \cdot A_{St}}{L}$ and $L_{Al} = L_{St} = L$

Chapter 8: Torsion - *Example 8.4.2:*

$$T_{Cu} = T \cdot \frac{k_{Cu}}{k_{Cu} \cdot k_{Fe}} = T \cdot \frac{G_{Cu} \cdot J_{Cu}}{G_{Cu} \cdot J_{Cu} + G_{Fe} \cdot J_{Fe}} \; ; \quad T_{Fe} = T \cdot \frac{k_{Fe}}{k_{Cu} \cdot k_{Fe}} = T \cdot \frac{G_{Fe} \cdot J_{Fe}}{G_{Cu} \cdot J_{Cu} + G_{Fe} \cdot J_{Fe}}$$

where $k_{Cu} = \dfrac{G_{Cu} \cdot J_{Cu}}{L_{Cu}}$; $k_{Fe} = \dfrac{G_{Fe} \cdot J_{Fe}}{L_{Fe}}$ and $L_{Cu} = L_{Fe} = L$

9. <u>Geometric characteristics of a cross-section</u>

The topics covered in this chapter include *centroids* and how to locate them, *moments of inertia, polar moments of inertia, products of inertia, parallel-axis theorem, rotation of axes,* and *principal axes.* Only plane areas are considered.

The terminology used in this chapter may appear puzzling to some readers. For instance, the term "moment of inertia" is clearly a misnomer when referring to the properties of an area, since no mass is involved. Even the word "area" is used inappropriately in the preceding discussions. When we say "plane area", we really mean "plane surface". Strictly speaking, area is a measure of the *size* of a surface and is not the same thing as the surface itself. In spite of these deficiencies, this terminology is used in most present-day English and American technical literature and is so entrenched in the engineering literature that it rarely causes confusion. However, instead of "(polar) moment of inertia" some modern writers prefer to refer to *(polar) second moment of area.*

9.1 Centroids of plane areas

To obtain formulas for locating centroids, we will refer to Fig.9.1.1, which shows a plane area of irregular shape with its centroid at point C. The yz coordinate system is oriented arbitrarily with the origin in any point O (dA is a differential element of area having coordinates y and z).

We define the coordinates y_C and z_C of the centroid, respectively, as follows:

$$y_C = \frac{Q_z}{A} = \frac{\int\limits_{(A)} y \cdot dA}{\int\limits_{(A)} dA}$$

(9.1.1.*a,b*)

$$z_C = \frac{Q_y}{A} = \frac{\int\limits_{(A)} z \cdot dA}{\int\limits_{(A)} dA}$$
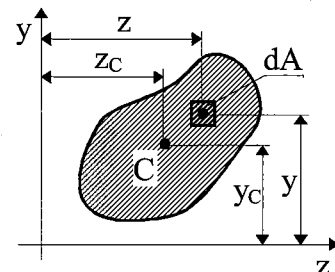
Fig.9.1.1

where Q_y and Q_z ... represent *first moments of area* with respect to the y and z axes, respectively;

A ... represents the area of the cross-section.

9.2 Second moments of area (moments of inertia of a plane area)

The *second moments of area* (Fig.9.2.1) with respect to the y and z axes, respectively, are defined by the integrals

$$I_y = \int\limits_{(A)} z^2 \cdot dA \quad ; \quad I_z = \int\limits_{(A)} y^2 \cdot dA \qquad \left[m^4 ; mm^4 \right]$$

(9.2.1*a,b*)

in which y and z are the coordinates of the differential element of area dA. Because the element dA is multiplied by the square of the distance from the reference axis, *moments of inertia* have become called *second moments of area*. Also, we see that second moments of area (unlike *first moments*) are always positive quantities. If a different set of axes is selected, the second moments of area will have different values.
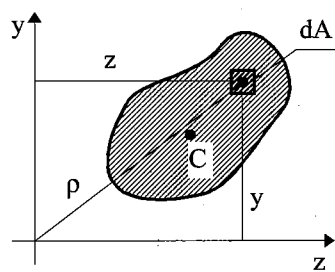
Fig.9.2.1

To illustrate how second moments of area are obtained by integration, we will consider a rectangle having width b and height h (Fig.9.2.2). The y and z axes have their origin at the centroid C. For convenience, we use a differential element of area dA in the form of a thin horizontal strip of width b and height dy (therefore, $dA = b\,dy$). Since all parts of an elemental strip are the same distance from the z axis, we can express the second moment of area I_z with respect to the axis z as follows:

$$I_z = \int_{(A)} y^2 \cdot dA = \int_{-h/2}^{h/2} y^2 \cdot b \cdot dy = \frac{b \cdot h^3}{12}$$

In a similar manner, we can use an element of area in the form of a vertical strip with area $dA = h\,dz$ and obtain the second moment of area with respect to the y axis: $I_y = (hb^3)\,/\,12$.
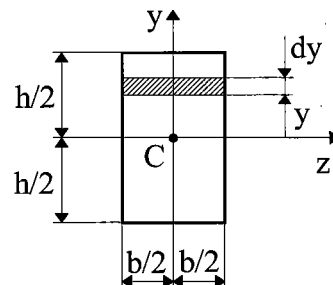
Fig.9.2.2

The second moment of area of a *composite area* with respect to any particular axis is the sum of the second moments of area of its parts with respect to that same axis.

A distance known as the *radius of area* (*radius of gyration* of a plane area) is occasionally encountered in mechanics. The radius of area of a cross-section is defined as the square root of the second moment of area divided by the area itself of that cross-section; thus,

$$r_y = \sqrt{\frac{I_y}{A}} \qquad ; \qquad r_z = \sqrt{\frac{I_z}{A}} \qquad [\mathrm{m;\,mm}] \qquad (9.2.2a,b)$$

in which r_y and r_z denote the radii of area with respect to the y and z axes, respectively. Since the second moment of area has units of length to the fourth power and area has units of length to the second power, the radius of area (radius of gyration of a plane area) has units of length. Although the radius of area does not have an obvious physical meaning, we may consider it to be the distance (from the reference axis) at which the entire area could be concentrated and still have the same second moment of area as the original area.

9.3 Products of inertia

The product of inertia of a plane area is defined with respect to a set of perpendicular axes lying in the plane of the area. Thus, referring to the area shown in Fig.9.2.1, we define the *product of inertia*

with respect to the y and z axes as follows:

$$I_{yz} = \int_{(A)} y \cdot z \cdot dA \qquad \left[m^4; mm^4 \right] \tag{9.3.1}$$

From this definition we see that each differential element of area dA is multiplied by the product of its coordinates. As a consequence, products of inertia may be positive, negative, or zero, depending upon the position of the yz axes with respect to the area. If the area lies entirely on the first quadrant of the axes (as in Fig.9.2.1), then the product of inertia is positive because every element dA has positive coordinates y and z, etc. When the area is located in more than one quadrant, the sign of the product of inertia depends upon the distribution of the area within the quadrants. A special case arises when one of the axes is an **axis of symmetry** of the area. We can easily learn that *the product of inertia of an area is zero with respect to any pair of axes in which at least one axis is an axis of symmetry of the area and corresponding axes are called the principal axes.*

9.4 Polar second moment of area (polar moment of inertia)

We have encountered the *polar second moment of area* in Chap.8 concerning the torsion of shafts. Referring to Fig.9.2.1 we observe

$$J = \int_{(A)} \rho^2 \cdot dA = \int_{(A)} \left(y^2 + z^2 \right) \cdot dA = \int_{(A)} y^2 \cdot dA + \int_{(A)} z^2 \cdot dA \qquad \Rightarrow \qquad J = I_z + I_y \tag{9.4.1}$$

This equation shows the definition of the *polar second moment of area* in its first integral. (Note also that the polar second moment of area with respect to an axis perpendicular to the plane of the figure at any point O is equal to the sum of the second moments of area with respect to <u>any</u> two perpendicular axes y and z passing through that same point and lying in the plane of the figure.)

For convenience, we usually refer to J simply as the polar second moment of area with respect to point O, without mentioning the axis perpendicular to the plane of the figure. Also, to distinguish them from *polar* second moments of area, we sometimes refer to I_y and I_z as *rectangular* second moments of area.

9.5 Properties of second moments of area

9.5.1 Parallel-axis theorem for second moments of area

The *parallel-axis theorem* gives the relationship between the second moment of area with respect to a *centroidal* axis and the second moment of area with respect to any parallel axis. To derive the theorem, we consider an area of arbitrary shape with centroid C (Fig.9.5.1.1). We also consider two sets of coordinate axes: (1) the y_C, z_C axes with their origin at the centroid, and (2) a set of parallel yz axes with their origin at any point O. The distances between the two sets of parallel axes are denoted d_1 and d_2. Also, we identify a differential element of area dA having coordinates y and z with respect to

the centroidal axes.

From the definition of the second moment of area, we can write the following equation for the second moment of area I_y with respect to the y axis

$$I_y = \int\limits_{(A)} (z+d_2)^2 \cdot dA = \int\limits_{(A)} z^2 \cdot dA + 2d_2 \cdot \int\limits_{(A)} z \cdot dA + d_2{}^2 \cdot \int\limits_{(A)} dA$$

The first integral on the right-hand side is the second moment I_{y_C} with respect to the y_C axis. The second integral is the first moment of area with respect to the y_C axis (this integral equals zero because the y_C axis passes through the centroid). The third integral is the area A itself. Therefore, the preceding equation and the equation that would be obtained analogously with respect to the z axis reduce, respectively, to

Fig.9.5.1.1

$$I_y = I_{y_C} + A \cdot d_2{}^2 \quad ; \quad I_z = I_{z_C} + A \cdot d_1{}^2 \qquad (9.5.1.1a,b)$$
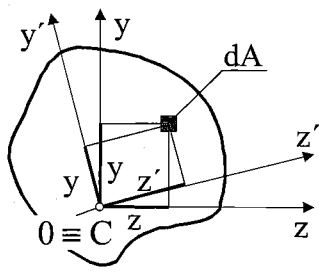
Equations $(9.5.1.1a,b)$ represent the **parallel-axis theorem** for **second moments of area**: *The second moment of area of a cross-section with respect to any axis in its plane is equal to the second moment of area with respect a parallel centroidal axis plus the product of the area and the square of the distance between the two axes.* When using the parallel-axis theorem, it is essential to remember that one of the two parallel axes must be a centroidal axis.

Products of inertia of an area with respect to parallel sets of axes are related by a **parallel-axis theorem** that is analogous to the corresponding theorems for second moments of area (moments of inertia) stating (see Fig.9.5.1.1)
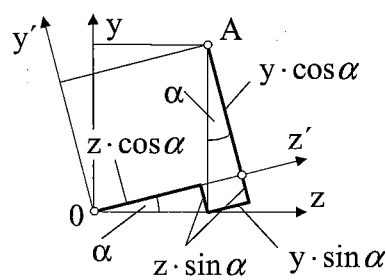
$$I_{yz} = I_{y_C z_C} + A \cdot d_1 \cdot d_2 \qquad (9.5.1.2)$$

9.5.2 Rotation of axes

The second moments of area (moments of inertia) of a plane figure depend upon the position of the origin and the orientation of the reference axes. For a given origin, the moments and product of inertia vary as the axes are rotated about that origin. The manner in which they vary, and the magnitudes of maximum and minimum values, are discussed in this and the following sections.

a)   Fig.9.5.2.1   *b)*

Let us consider the plane area shown in Fig.9.5.2.1*a*, and let us assume that the *yz* axes are a pair of centroidal reference axes, i.e., passing arbitrarily through origin *0* coinciding with centroid *C* of this area (*0* ≡ *C*). The *y'*, *z'* axes have the same origin but are rotated through a counterclockwise angle α with respect to the *yz* axes. To obtain the moments and product of inertia $I_{y'}$, $I_{z'}$, and $I_{y'z'}$ to the rotated axes, we first express the following geometric relations, based on Fig.9.5.2.1*b*,

$$y' = y \cdot \cos\alpha - z \cdot \sin\alpha \quad ; \quad z' = z \cdot \cos\alpha + y \cdot \sin\alpha$$

Applying Eqs.(9.2.1*a,b*) and (9.3.1), respectively, we obtain successively

$$I_{z'} = \int_{(A)} y'^2 \cdot dA = \int_{(A)} (y \cdot \cos\alpha - z \cdot \sin\alpha)^2 \cdot dA =$$

$$= \cos^2\alpha \cdot \int_{(A)} y^2 \cdot dA - 2\sin\alpha \cdot \cos\alpha \cdot \int_{(A)} y \cdot z \cdot dA + \sin^2\alpha \cdot \int_{(A)} z^2 \cdot dA \qquad (9.5.2.1a)$$

or, after substituting,

$$I_{z'} = I_z \cos^2\alpha - I_{yz} \cdot 2\sin\alpha \cdot \cos\alpha + I_y \sin^2\alpha,$$

and

$$I_{y'z'} = \int_{(A)} y' \cdot z' \cdot dA = \int_{(A)} (y \cdot \cos\alpha - z \cdot \sin\alpha) \cdot (z \cdot \cos\alpha + y \cdot \sin\alpha) dA = ... =$$

$$= I_{yz} \cdot \cos^2\alpha + I_z \cdot \sin\alpha \cdot \cos\alpha - I_y \cdot \sin\alpha \cdot \cos\alpha - I_{yz} \cdot \sin^2\alpha \qquad (9.5.2.1b)$$

Now we introduce the following trigonometric identities (the same as in Sec.5):

$$\cos^2\alpha = \frac{1}{2} \cdot (1 + \cos 2\alpha); \quad \sin^2\alpha = \frac{1}{2} \cdot (1 - \cos 2\alpha) \; ; \quad 2\sin\alpha \cdot \cos\alpha = \sin 2\alpha$$

Then Eqs. (9.5.2.1*a,b*) become

$$I_{z'} = \frac{1}{2} \cdot (I_z + I_y) + \frac{1}{2} \cdot (I_z - I_y) \cdot \cos 2\alpha - I_{yz} \cdot \sin 2\alpha \qquad (9.5.2.2a)$$

$$I_{y'z'} = \frac{1}{2} \cdot (I_z - I_y) \cdot \sin 2\alpha + I_{yz} \cdot \cos 2\alpha \qquad (9.5.2.2b)$$

These equations are called the *transformation equations for* **moments and products of inertia.**

Note that these transformation equations have the same form as the transformation equations for plane stress (Eq. 5.3.4*a,b* of Sec.5) except the signs at several members. Therefore, we can also analyze moments and products of inertia with the use of **Mohr's circle** (Fig.9.5.2.2).


Fig.9.5.2.2

136
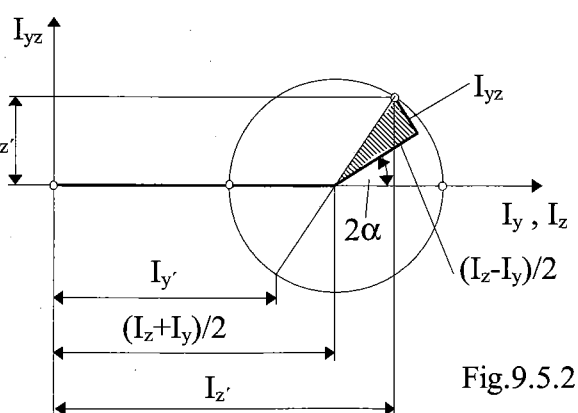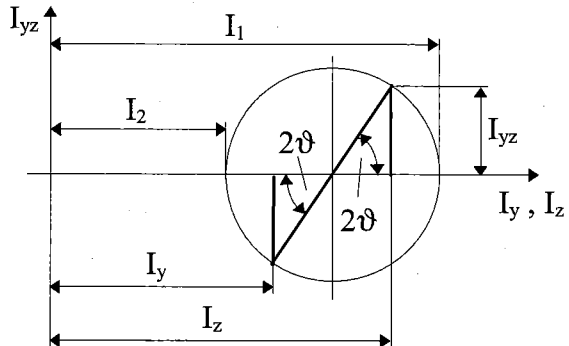
Of special interest are the maximum and minimum values of the second moment of area (moment of inertia) where the products of inertia are equal to zero. These values are known as the *principal second moments of area*, and the corresponding axes are known as *principal axes* (which, when passing through the centroid of the figure in question, are called the *principal **centroidal** axes* and, consequently, the corresponding second moments of area are known as the *principal **centroidal** second moments of area*).

Based upon Fig.9.5.2.3 (which we have drawn with the hatched triangle, see Fig.9.5.2.2, rotated into its basic position for $\alpha = 0$), we get angle

$$\tan 2\vartheta = \left| \frac{2 I_{yz}}{I_z - I_y} \right|, \qquad (9.5.2.3)$$

Fig.9.5.2.3   which denotes the <u>angle defining a principal axis</u> (cf. Eq. 5.5.1), and the principal second moments of area, see Eq.(5.5.2), in the form

$$I_{1,2} = \frac{I_z + I_y}{2} \pm \sqrt{\left(\frac{I_z - I_y}{2} \right)^2 + I_{yz}^2} \qquad (9.5.2.4)$$

A convention for plotting angle ϑ determined from Eq.(9.5.2.3) into a given cross-section, to obtain the position of the respective principal axes, has not been settled. Nevertheless, it can be observed that when a **negative** <u>product of inertia</u> ($I_{yz} < 0$) has been obtained, the <u>principal axis *1*</u> corresponding to the **maximum** <u>second moment of area</u> I_1 will pass through the **first and third** <u>quadrants</u> of the *yz* coordinates; conversely, for $I_{yz} > 0$ ... <u>the **second and fourth** quadrants</u> will be passed through; in both cases angle ϑ is measured from that coordinate axis (*y* or *z*) with respect to which the larger second moment of inertia (I_y or I_z) is obtained.

9.5.3 Example

Determine the orientations of the principal centroidal axes and the magnitudes of the principal centroidal second moments of area for the cross-sectional area of the *Z-section* shown in Fig.9.5.3.1. Use the following numerical data: height $h = 200 \ mm$, width $b = 90 \ mm$, and thickness $t = 15 \ mm$.

Solution: Let us use the *y*, *z* axes (Fig.9.5.3.1) as the reference axes through the centroid *C*. The moments and product of inertia with respect to these axes can be obtained by dividing the area into three rectangles and using the parallel-axis theorems.

<u>Second moments of area</u> about the coordinate system - axes y, z going through the total centroid C_T:
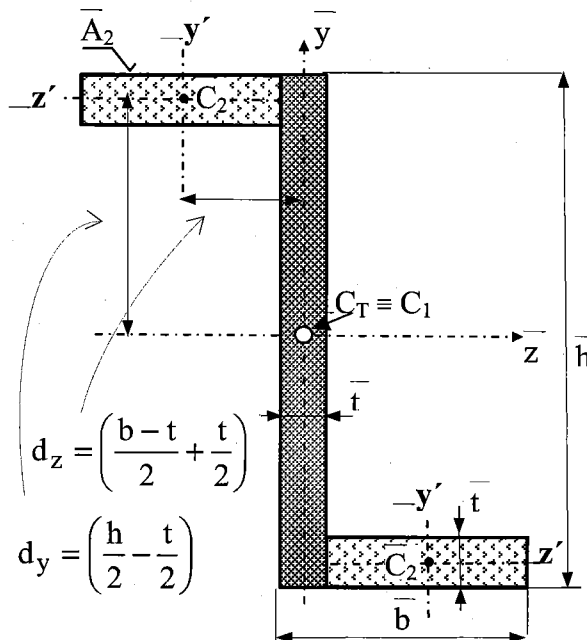
Fig.9.5.3.1

$$I_{zC_1} = \frac{1}{12} \cdot h^3 \cdot t = 10 \cdot 10^6 \text{ mm}^4$$

$$I_{zC_2} = \frac{1}{12} \left[t^3 \cdot (b-t) \right] ; \quad A_2 \cdot d_y^2 = ((b-t) \cdot t) \cdot \left(\frac{h}{2} - \frac{t}{2} \right)^2 ;$$

$$I_{zC_2} = \left(I_{z'C_2} + A_2 \cdot d_y^2 \right) \cdot 2 = 19.29 \cdot 10^6 \text{ mm}^4 ;$$

$$I_z = I_{zC_1} + I_{zC_2} = 29.29 \cdot 10^6 \text{ mm}^4$$

$$I_{yC_1} = \frac{1}{12} \cdot t^3 \cdot h = 56.25 \cdot 10^3 \text{ mm}^4$$

$$I_{y'C_2} = \frac{1}{12} \cdot \left[(b-t)^3 \cdot t \right] ;$$

$$A_2 \cdot d_z^2 = ((b-t) \cdot t) \cdot \left(\frac{b-t}{2} + \frac{t}{2} \right)^2 ;$$

$$I_{yC_2} = \left(I_{y'C_2} + A_2 \cdot d_z^2 \right) \cdot 2 = 5.61 \cdot 10^6 \text{ mm}^4 ;$$

$$I_y = I_{yC_1} + I_{yC_2} = 5.667 \cdot 10^6 \text{ mm}^4$$

<u>Product of inertia</u> about the same centroidal axes:

$$I_{yz} = I_{yzC_1} + 2 \cdot I_{y'z'C_2} + A_2 \cdot d_y \cdot (-d_z) + A_2 \cdot (-d_y) \cdot d_z =$$

$$= 0 + 2 \cdot 0 - 2 \cdot ((b-t) \cdot t) \cdot \left(\frac{h}{2} - \frac{t}{2} \right) \cdot \left(\frac{b-t}{2} + \frac{t}{2} \right) = -9.366 \cdot 10^6 \text{ mm}^4$$

Note: Products of inertia about the profile axes of symmetry equal zero (see Fig.9.5.1.1)

Substituting these results into Eqs.(9.5.2.3) and (9.5.2.4) for the angle ϑ and the principal second moments of area I_1 and I_2, respectively, we get

$$\tan 2\vartheta = \left| \frac{2 I_{yz}}{I_z - I_y} \right| = 0.7930 \qquad \Rightarrow \vartheta = \frac{38.4^\circ}{2} = 19.2^\circ$$

$$I_{1,2} = \frac{I_z + I_y}{2} \pm \sqrt{\left(\frac{I_z - I_y}{2} \right)^2 + I_{yz}^2} = (17.48 \pm 15.07) \cdot 10^6 \Rightarrow$$

$$I_1 = 32.6 \cdot 10^6 \text{ mm}^4 ; \quad I_2 = 2.40 \cdot 10^6 \text{ mm}^4$$

The principal axis *1*, for the maximum second moment of area I_1, were plotted in Fig.9.5.3.2 as passing through the first and third quadrants, while the principal axis *2* passes through the second and forth quadrants, since $I_{yz} < 0$.
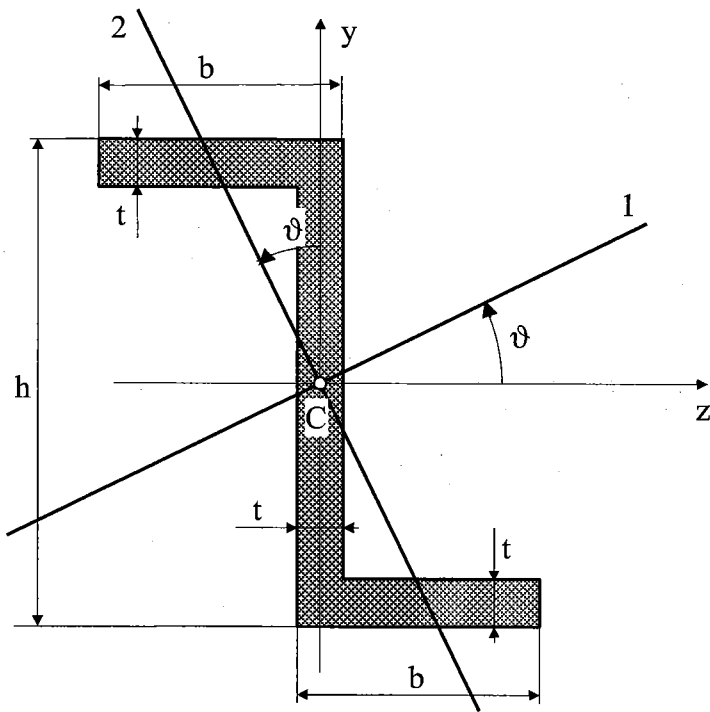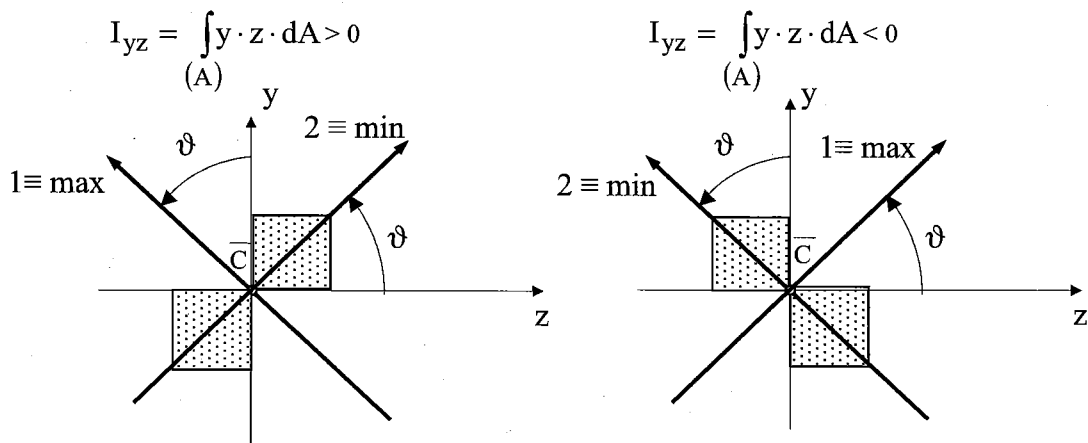
Fig.9.5.3.2

**Note:** How to determinate the positions of maximum and minimum principal centroidal exes, respectively?

We utilize simple, but illustrative, figures:

$$I_{yz} = \int\limits_{(A)} y \cdot z \cdot dA > 0 \qquad\qquad I_{yz} = \int\limits_{(A)} y \cdot z \cdot dA < 0$$

Just with a simple imagination about the maximum and minimum moments of inertia of these areas, we can determine their positions.

10. Beams in bending

10.1 Basic concepts

10.1.1 Introduction

Structural members are usually classified according to the types of loads they support. An *axially loaded bar* supports forces whose vectors are directed along the axis of the bar, and a *bar (shaft) in torsion* supports torques (or couples) whose moment vectors are directed along the axis. In this chapter we begin our study of **beams**, which are structural members subjected to lateral loads, that is, to forces or moments whose vectors are perpendicular to the axis of the bar. The beams to be discussed in this chapter are classified as *planar structures*, because they lie in a single plane which is assumed to be a plane of symmetry of the beam. If all loads act in that plane, and all deflections occur in that plane, then we refer to that plane as a *plane of bending* and so-called **planar bending** will be obtained (i.e., the beam deflection curve will lie in that plane). We will also encounter so-called **unsymmetric** (or **spatial**) **bending** of a beam, when its deflection is a spatial curve, see Chap.13.

10.1.2 Types of beams, loads, and reactions

When drawing sketches of beams, we identify the supports with *conventional symbols* indicating the manner in which the beam is restrained, and also the nature of the reactive forces and moments. *However those symbols do not represent the actual physical construction.* The task of representing a real structure by an *idealized model* is an important aspect of engineering work. The model should be simple enough to facilitate mathematical analysis and yet complex enough to represent the actual behaviour of the structure with reasonable accuracy. All types of beams shown in this section will be plotted in two modes: a) more realistic sketches; b) simple computational models; subsequently, we will generally use the latter approach.

If a beam is supported at only one end, and in such a manner that the axis of the beam cannot rotate at that point, it is called a **cantilever beam**, see Fig.10.1.2.1*a,b*: the left end *A* of the bar is free to deflect but

a)   b)
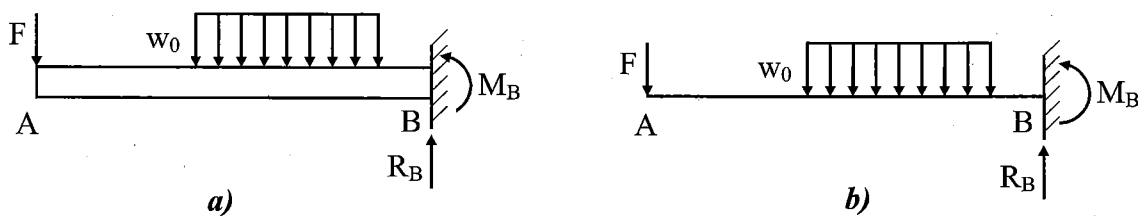
Fig.10.1.2.1

the right end *B* is rigidly *clamped* (or *fixed*). The right end *B* is said to be „restrained". The reaction of the supporting wall upon the beam consists of a vertical force R_B together with a couple M_B acting in the plane of the applied loads.

A beam that is freely supported at the both ends (a *pin support* at end A preventing translation, and a *roller support* at end B preventing translation in the vertical but not in the horizontal direction) is called a *simple beam*. The term „freely supported" implies that the end supports are capable of exerting only forces upon the bar (vertical reactions R_A and R_B at both the pin and roller supports may act *either* upwards *or* downwards) and are not capable of exerting any moments. Thus no restraint is offered to the angular rotation of the ends of the bar at the supports as the bar deflects under the loads. Note that at least one of the supports must be capable of undergoing horizontal movement so that no force will exist in the direction of the axis of the beam. If neither end were free to move horizontally, then some axial force would arise in the beam as it deforms under the load. Problems of this nature will not be considered in this textbook.
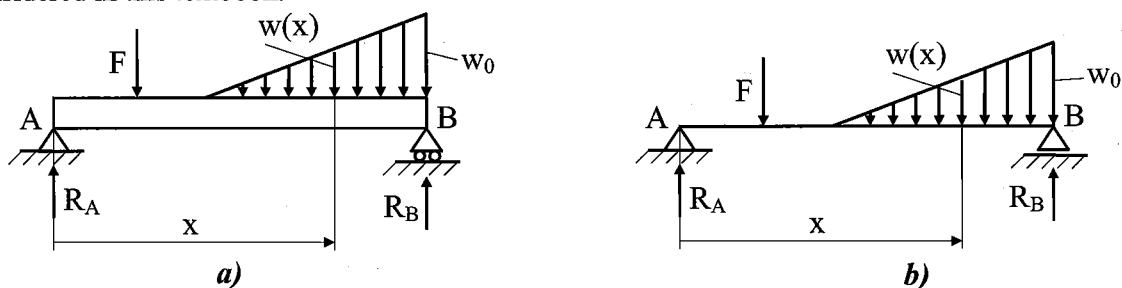

Fig.10.1.2.2

A beam freely supported at two points (that is a pin support at A and a roller support at B) and with one or both ends extending beyond these supports is termed an *overhanging beam.*
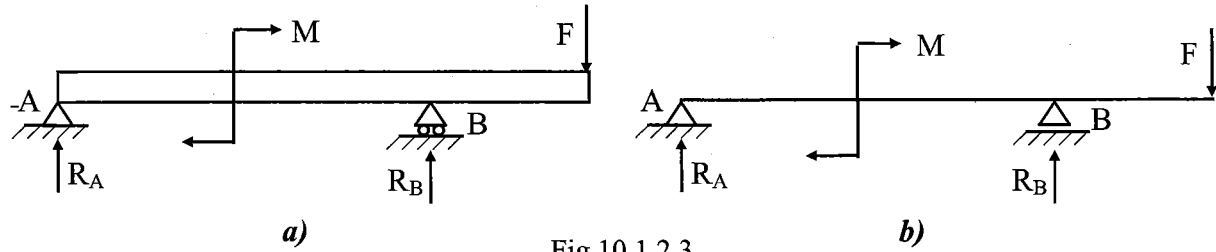
Fig.10.1.2.3

(It is clear that if a horizontal force loads the presented beams, the pin or fixed support, respectively, will be capable of exerting a corresponding horizontal reaction to carry that force)

Statically determinate beams

All the beams considered above, *cantilevers, simple beams,* and *overhanging beams,* are beams in which the reactions of the supports may be determined by equations of static equilibrium. The values of these reactions are independent of the deformations of the beam. Such beams are said to be *statically determinate.*

Statically indeterminate beams

If the number of reaction components exerted upon the beam exceeds the number of equations of static equilibrium, then the static equations must be supplemented by equations based upon the deformation of the beam. In such a case the beam is said to be *statically indeterminate,* see Chap.12.

Types of loading

Earlier pictures showed: *concentrated load* (applied at a point, see forces *F*); *uniformly distributed load* (such as the load w_o in Fig.10.1.2.1), in which case the magnitude is expressed as a certain number of newtons per millimeter of length of the beam, or *uniformly varying load* (such as the load *w(x)* in Fig.10.1.2.2); and a *couple* (the load *M* in Fig.10.1.2.3).

10.2 Shearing forces and bending moments

10.2.1 Method of sections

When a beam is loaded by forces and couples, internal stresses arise in the bar. In general, both normal and shearing stresses will occur. In order to determine the magnitude of these stresses at any section of the beam, it is necessary to know the resultant force and moment acting at that section. These may be found by means of the *method of sections,* i.e., by applying the equations of static equilibrium.

Suppose several concentrated forces act on a simple beam as in Fig.10.2.1.1.
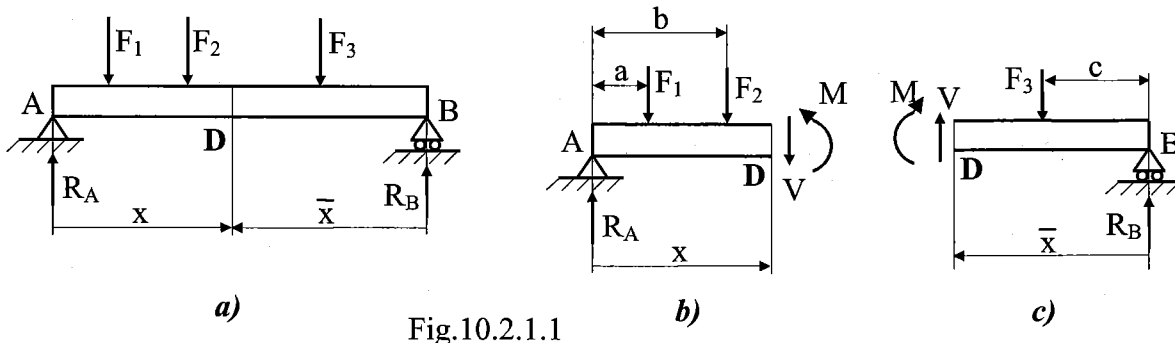
a)   Fig.10.2.1.1   b)   c)

We want to study the internal stresses across the section at *D*, located at a distance *x* from the left end of the beam. Let us therefore consider the beam to be cut at *D* and the portion of the beam to the right of *D* to have been removed. The portion removed must then be replaced by the effect it exerted upon the portion to the left of *D*, and this effect will consist of a vertical shearing force together with a couple, as represented by the vectors *V* and *M*, respectively, in the free-body diagram of the left portion of the beam shown in Fig.10.2.1.1*b*. (To be better demonstrated, *M* is not drawn in the form of vector from the mathematical stand-point). The force *V* and the couple *M* hold the left portion of the bar in equilibrium under the action of forces R_A , F_1 , F_2 , and the right portion under the action of forces R_B , F_3 (Fig.10.2.1.1*c*). The quantities *V* and *M* are taken to be positive if they have the senses indicated above, with respect to the sense of access to section *D*.

Resisting moment and bending moment

The couple *M* shown in Fig.10.2.1.1*b* above is called the *resisting moment* at section *D*, and its magnitude may be found by a static equation which states that the sum of the moments of all forces, and couples, respectively, about an axis through *D* and perpendicular to the plane of the page is zero.

$$\sum M_D = M - R_A \cdot x + F_1 \cdot (x - a) + F_2 \cdot (x - b) = 0 \Rightarrow M = R_A \cdot x - F_1 \cdot (x - a) - F_2 \cdot (x - b)$$

Thus the resisting moment M is the moment at point D created by the moments of the reaction at A and the applied forces F_1 and F_2. The resisting moment is the resultant couple due to the stresses that are distributed over the vertical section at D. These stresses act in the horizontal direction and are tensile in certain portions of the cross-section, and compressive in others. Their nature will be discussed in Sec.10.3. *The algebraic sum of the moments of the external forces, and couples, respectively, to one side of section **D*** (defined by an arbitrary longitudinal coordinate x) *about an axis through **D** is called the **bending moment** at x*:

$$M(x) = R_A \cdot x - F_1 \cdot (x - a) - F_2 \cdot (x - b)$$

Thus the bending moment is opposite in direction to the resisting moment, but is of the same magnitude. When taking into account the right part, see Fig.10.2.1.1c, we obtain

$$M(\bar{x}) = R_B \cdot \bar{x} - F_3 \cdot (\bar{x} - c)$$

It must hold $\qquad\qquad M(x) = M(\bar{x})$

The bending moment rather than the resisting moment is ordinarily used in calculations, because it can be represented directly in terms of external loads without drawing the free-body diagram.

Resisting shear and shearing force

The vertical force V shown in Fig.10.2.1.1b is called the ***resisting shear*** at section D (placed at x). For equilibrium of forces in the vertical direction,

$$\sum F_D = R_A - F_1 - F_2 - V(x) = 0 \qquad \Rightarrow \qquad V(x) = R_A - F_1 - F_2$$

When examining the equilibrium of forces in the right part (Fig.10.2.1.1c) we obtain the shearing force

$$V(\bar{x}) = -R_B + F_3$$

When expressing the reactions we can easily prove that it holds $V(x) = V(\bar{x})$. This force V is actually the resultant of shearing stresses distributed over the vertical section D at x. The nature of these stresses will be studied in Sec.10.5. *The algebraic sum of all vertical external forces to one side, either to the left or to the right, of section **D** (at x) is called the **shearing force** at that section.* The shearing force is opposite in direction to the resisting shear but of the same magnitude.

Sign conventions

A force that tends to bend the beam in such a way that it is concave upward is said to produce a positive bending moment (we can also say that upward external forces produce positive bending moments), see Fig.10.2.1.2a. A force that tends to shear the left portion of the beam upward with respect to the right portion is said to produce a positive shearing force, see Fig.10.2.1.2b. Both rules are summed in Fig.10.2.1.2c, illustrating positive and negative sets of these internal stress resultants V and M for an approach from the left and from the right.
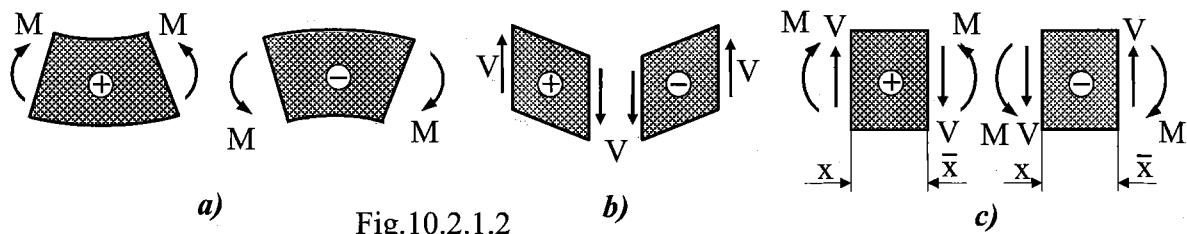
a)   Fig.10.2.1.2   *b)*   *c)*

10.2.2 Relationships between loads, shearing forces, and bending moments

We will now obtain some important relationships between loads, shearing forces, and bending moments in beams. These relations are quite useful when investigating the shear forces and bending moments throughout the entire length of a beam (which is very **suitable** when **distributed loads are exerted** on a beam), and they are **especially helpful** when **constructing shearing-force and bending-moment diagrams**.

As a means of obtaining the relationships, let us consider an element of a beam cut out between two cross-sections that are a distance *dx* apart (Fig.10.2.2.1). The load acting on the top surface of the element will be a distributed force that is considered to be **positive** when acting **downwards**. The shearing forces and bending moments acting on the sides of the element are shown in their positive orientations. In general, shearing forces and bending moments vary along the axis of the beam There, when proceeding from the left, their values on the right-hand face of the element may be different by infinitesimal increments *dV* and *dM,* respectively, from their values on the left-hand face, see Fig.10.2.2.1.
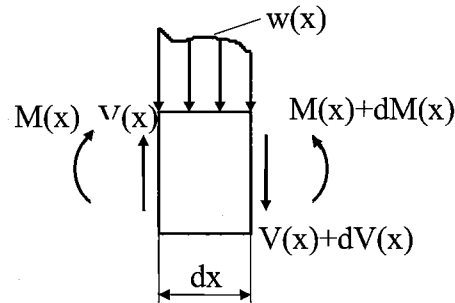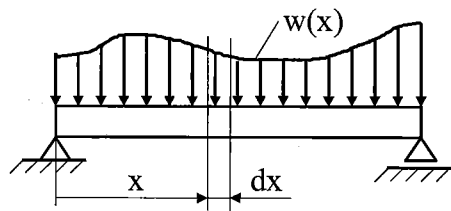
Fig.10.2.2.1.

Now, we can write two equations of equilibrium for the element - one equation for the equilibrium of forces in the vertical direction,

$$V(x) - w(x) \cdot dx - [V(x) + dV] = 0 \quad \Rightarrow \quad -w(x) = \frac{dV}{dx} \qquad (10.2.2.1a)$$

and one for the equilibrium of moments about, say, an axis at the right-hand side of the element,

$$M(x) + V(x) \cdot dx - w(x) \cdot dx \cdot \frac{dx}{2} - [M(x) + dM] = 0 \quad \Rightarrow V(x) = \frac{dM}{dx} \qquad (10.2.2.1b)$$

The latter result was obtained when discarding the product of the differentials (because they are negligible compared to the other terms).

When differentiating Eq.(10.2.2.1*b*) once more and substituting Eq.(10.2.2.1*a*), we have successively

$$\frac{dV}{dx} = \frac{d^2M}{dx^2} \quad \Rightarrow -w(x) = \frac{d^2M}{dx^2} \qquad (10.2.2.1c)$$

When <u>proceeding from the **right**</u> we obtain analogous relations with changed signs in the first two:

$$w(\overline{x}) = \frac{dV}{d\overline{x}} \quad ; \quad -V(\overline{x}) = \frac{dM}{d\overline{x}} \quad ; \quad -w(\overline{x}) = \frac{d^2M}{d\overline{x}^2} \qquad (10.2.2.2a,b,c)$$

10.2.3 <u>General comments</u>

When <u>calculating</u> the distribution of shearing forces $V(x)$ and bending moments $M(x)$ along beams, application of the *method of sections* is in most cases preferable to the above obtained *relations between V and M*. On the other hand, when <u>plotting diagrams</u> $V(x)$ and $M(x)$, we always take the *relations between V and M* (Eqs.10.2.2.1a,b,c or 10.2.2.2a,b,c) into account since it holds that the ordinates from the distributed load $w(x)$ are proportional to the slopes of the shearing force $V(x)$ (cf. Eq.10.2.2.1a or 10.2.2.2a), and the ordinates of the shearing force $V(x)$ are proportional to the slopes of the bending moments $M(x)$ (cf. Eq.10.2.2.1b or 10.2.2.2b).

Example 10.2.3.1: Construct the shear-force and bending-moment diagrams for simple beams with concentrated loads: a) Symmetric; b) Anti-symmetric

<u>Ad a) Symmetric concentrated loads.</u>
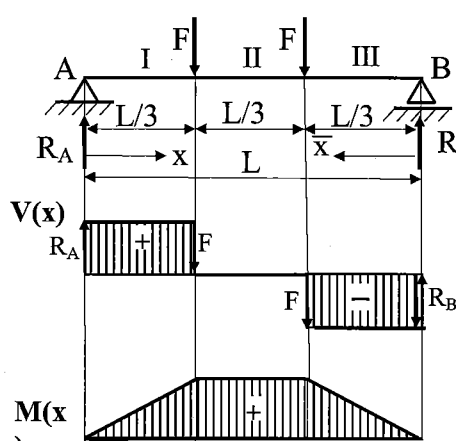
Fig.10.2.3.1

Note: The graphs are for:
    load... **symmetric**
    *shearing force...**anti-symmetric***
    *moment... **symmetric***

*1) Solution by applying the **method of sections**:*
<u>Reactions.</u>

$$M_B: \quad R_A \cdot L - F \cdot \frac{2}{3}L - F \cdot \frac{1}{3}L = 0 \quad \Rightarrow \quad R_A = F$$

$$M_A: \quad R_B \cdot L - F \cdot \frac{2}{3}L - F \cdot \frac{1}{3}L = 0 \quad \Rightarrow \quad R_B = F$$

Note: This result can be obtained simply from the symmetry.

<u>Shearing forces and bending moments.</u>
Proceeding from the left:

I. $(0 < x < L/3)$: $V_I(x) = R_A = F$; $\quad M_I(x) = R_A \cdot x = F \cdot x$

II. $(L/3 < x < 2L/3)$: $V_{II}(x) = R_A - F = 0$;
$$M_{II}(x) = R_A \cdot x - F \cdot (x - L/3) = F \cdot L/3$$

III. $(2L/3 < x < L)$:
$$V_{III}(x) = R_A - F - F = -F;$$
$$M_{III}(x) = R_A \cdot x - F \cdot (x - L/3) - F(x - 2L/3) = F \cdot (L - x)$$

Proceeding from the right (span III only: III. $(0 < \overline{x} < L/3)$: $V_{III}(\overline{x}) = R_B = -F$; $\quad M_{III}(\overline{x}) = R_A \cdot \overline{x} = F \cdot \overline{x}$

Note: Mind different signs of $V_{III}(x) = -F$ (from the left), than $V_{III}(\overline{x}) = F$ (from the right), see Fig.10.2.2.1.

Try to substitute $\overline{x} = (L - x)$ into $M_{III}(\overline{x})$ to obtain $M_{III}(x)$!

*2) Solution by applying the **relations between w, V and M** (cf. Eqs.(10.2.2.1a,b):*

As having three spans (Fig.10.2.3.2), we should apply six differential equations, while needed six static boundary conditions and thus we could obtain three shearing forces (V(x)) and three bending moments (M(x)) distributions, which we have obtained much more easily by the *method of sections* (see above).

But when using: i) the geometrical interpretation of the *relations between w, V and M* and ii) the *boundary conditions*, we can draw the shapes of *V(x)* and *M(x)* distribution quite correctly even without a computation.

Ad b) Anti-symmetric concentrated loads.

load... *anti-symmetric*
shearing force... *symmetric*
moment... *anti-symmetric*

Fig.10.2.3.2

The analytical solution by *the method of sections* is here again more convenient than that of *the relations between w, V and M*, while for the graphical illustration, it is conversely.

Reactions.

$$M_B: \quad R_A \cdot L - F \cdot \frac{2}{3}L + F \cdot \frac{1}{3}L = 0 \quad \Rightarrow \quad R_A = \frac{F}{3}$$

$$M_A: \quad R_B \cdot L + F \cdot \frac{2}{3}L - F \cdot \frac{1}{3}L = 0 \quad \Rightarrow \quad R_B = -\frac{F}{3}$$

Note: Since the reaction R_B is negative (which means - when concerning *external forces* - that our assumption of the reaction pointing was wrong), we must change that (cf. Fig.2.3.3)!

1) Solution by applying the method of sections:

Shearing forces and bending moments.

Proceeding from the left:

I. $(0 < x < L/3)$: $V_I(x) = R_A = \frac{F}{3}$; $M_I(x) = R_A \cdot x = \frac{F}{3} \cdot x$

II. $(L/3 < x < 2L/3)$: $V_{II}(x) = R_A - F = -\frac{2F}{3}$; $M_{II}(x) = R_A \cdot x - F \cdot \left(x - \frac{L}{3}\right) = \frac{F \cdot L}{3}\left(1 - 2 \cdot \frac{x}{L}\right)$

Proceeding from the right:

III. $(0 < \bar{x} < L/3)$: $V_{III}(\bar{x}) = R_B = \frac{F}{3}$; $M_{III}(\bar{x}) = R_B \cdot \bar{x} = -\frac{F}{3} \cdot \bar{x}$

2) Geometric interpretation by applying the relations between w, V and M:

Shearing force distribution:
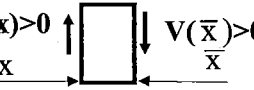
From the left:

$-w(x) = \frac{dV}{dx}$, here $w(x) = 0 \Rightarrow \alpha_V = 0$;

From the right:

$w(\bar{x}) = \frac{dV}{d\bar{x}}$, here $w(\bar{x}) = 0 \Rightarrow \bar{\alpha}_V = 0$,

i.e., the zero slope is in all the $V(x)$ or $V(\bar{x})$ spans.

<u>Boundary coditions for drawing $V(x)$</u>: i/ Apply *forces R_A, F, F and R_B* <u>in scale.</u>
ii/ <u>Mind the $V(x)$ / $V(\bar{x})$ signs when proceeding from the left/right</u>, respectively:

$V(x)>0$ $\uparrow$ □ $\downarrow$ $V(\bar{x})>0$
x ———→   ←——— $\bar{x}$

Bending moment distribution:

From the left :

$$V(x) = \frac{dM}{dx}, \Rightarrow \alpha_M \text{ depends}$$

on the $V(x)$ signs and values

From the rightt:

$$-V(\bar{x}) = \frac{dM}{d\bar{x}}, \Rightarrow \bar{\alpha}_M \text{ depends}$$

on the $V(\bar{x})$ signs and values

Boundary conditions for drawing:
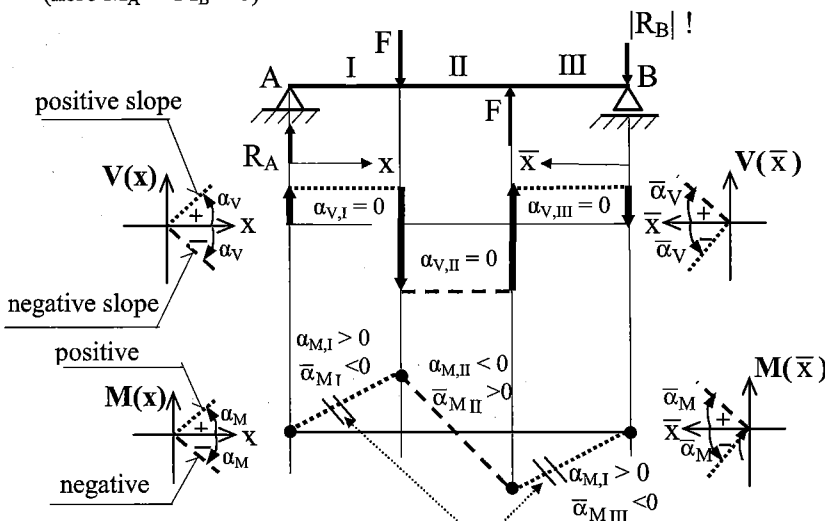
i) Basic BC are at the ends (from the *left* or *right*):

$x = 0$, $M(x = 0) = M_A$, or $\bar{x} = L$, $M(\bar{x} = L) = M_A$,

$x = L$, $M(x = L) = M_B$, or $\bar{x} = 0$, $M(\bar{x} = 0) = M_B$

(here $M_A = M_B = 0$)

$M(x)>0$ □ $M(\bar{x})>0$
x $\bar{x}$

Detail
(from the left)
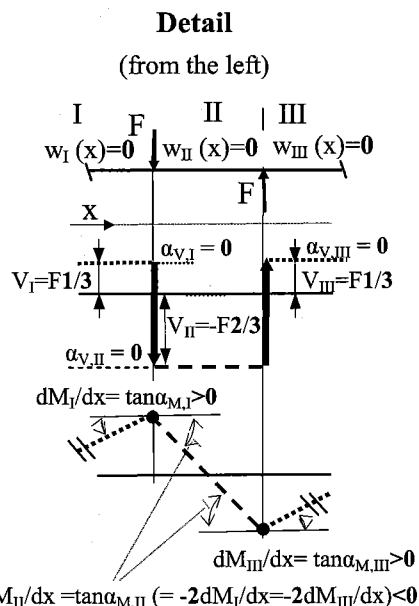
Since $V_I = V_{III}$, these lines are parallel

Fig.10.2.3.3

$dM_{III}/dx= \tan\alpha_{M,III}>0$
$dM_{II}/dx =\tan\alpha_{M,II} (= -2dM_I/dx=-2dM_{III}/dx)<0$

Example 10.2.3.2: Construct the shear-force and bending-moment diagrams for a simple beam with a uniform load of intensity w_o acting over part of the span (Fig.10.2.3.4).

*1) Solution by applying the **method of sections**:*

<u>Reactions.</u> We begin the analysis by determining the reactions of the beam from the free-body diagram of the entire beam (Fig.10.2.3.4). Taking the moments about ends B and A gives two equations of equilibrium, from which we find, respectively,

$$M_B: \quad R_A \cdot L - w_o \cdot b \cdot (b/2 + c) = 0 \quad \Rightarrow \quad R_A = \frac{w_o \cdot b \cdot (b + 2c)}{2 \cdot L}$$

$$M_A: \quad R_B \cdot L - w_o \cdot b \cdot (b/2 + a) = 0 \quad \Rightarrow \quad R_B = \frac{w_o \cdot b \cdot (b + 2a)}{2 \cdot L}$$

As a check on these results we can write an equation of equilibrium in the vertical direction, and can verify that it reduces to an identity.

Shearing forces and bending moments. To obtain $V(x)$ and $M(x)$ for the entire beam, we must consider the three segments of the beam individually.

Proceeding from the left: I. $(0 < x < a)$: $V_I(x) = R_A$; $M_I(x) = R_A \cdot x$

II. $(a < x < a + b)$: $V_{II}(x) = R_A - w_o \cdot (x - a)$; $M_{II}(x) = R_A \cdot x - \dfrac{w_o \cdot (x-a)^2}{2}$

Proceeding from the right: III. $(0 < \overline{x} < a)$: $V_{III}(\overline{x}) = -R_B$; $M_{III}(\overline{x}) = R_B \cdot \overline{x}$

Fig.10.2.3.4

2) *Solution by applying the relations between V and M* :

In this approach it is not necessary to start with the determination of the reactions.

Shearing forces and bending moments. To obtain $V(x)$ and $M(x)$ for the entire beam, we must consider the three segments of the beam individually.

Proceeding from the left while applying Eqs.(10.2.2.1a,b):

I. $(0 < x < a)$:

$$V_I(x) = -\int w_I(x) \cdot dx = C_1; \quad \text{for } w_I(x) = 0$$
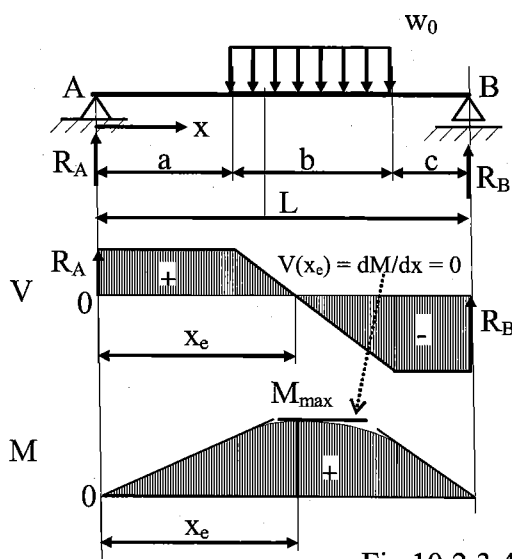
$$M_I(x) = \int V_I(x) \cdot dx = \int C_1 \cdot dx = C_1 \cdot x + C_2$$

II. $(a < x < a + b)$:

$$V_{II}(x) = -\int w_{II}(x) \cdot dx = -w_o \cdot x + C_3; \quad \text{for } w_{II}(x) = w_o$$

$$M_{II}(x) = \int V_{II}(x) \cdot dx = \int (-w_o \cdot x + C_3) \cdot dx = -w_o \cdot \frac{x^2}{2} + C_3 \cdot x + C_4$$

Proceeding from the right while applying Eqs.(10.2.2.2a,b):

$(0 < \overline{x} < a)$: $V_{III}(\overline{x}) = \int w_{III}(\overline{x}) \cdot d\overline{x} = C_5; \quad \text{for } w_{III}(\overline{x}) = 0$

$$M_{III}(\overline{x}) = -\int V_{III}(\overline{x}) \cdot d\overline{x} = -\int C_5 \cdot d\overline{x} = -C_5 \cdot \overline{x} + C_6$$

In order to obtain the integration coefficients $C_1 \div C_6$, we apply six static boundary conditions as follows:

1) for $x = 0$; $M_I (x=0) = 0$; 2) and 3) for $x = a$; $V_I (x=a) = V_{II} (x=a)$ and $M_I (x=a) = M_{II} (x=a)$;

4) and 5) for $x = a+b$ and $\overline{x} = c$; $V_{II} (x = a+b) = V_{III} (\overline{x} =c)$; $M_{II} (x = a+b) = M_{III} (\overline{x} = c)$;

6) for $\overline{x} = 0$; $M_{III} (\overline{x} =0) = 0$

from which (after substitution in the respective equations) we have:

$$C_1 = R_A; \quad C_2 = C_6 = 0; \quad C_3 = R_A + w_o \cdot a; \quad C_4 = -\frac{w_o \cdot a^2}{2}; \quad C_5 = -R_B$$

It can be readily found that after substituting these determined integral coefficients into the respective equations from above (according the relations between $V(x)$ and $M(x)$) we obtain identical solutions with those determined by applying the method of sections.

We now construct the shearing-force and bending-moment diagrams (Figs.10.2.3.4). The shearing-force diagram consists of horizontal straight lines in the unloaded regions of the beam and an inclined straight line with negative slope in the loaded region, as expected from Eqs.(10.2.2.1a) and (10.2.2.2a). The bending-moment diagram consists of two inclined straight lines in the unloaded portions of the beam and a parabolic curve in the loaded portion. The inclined lines have slopes equal to R_A and $-R_B$, respectively, as expected from Eqs.(10.2.2.1b) and (10.2.2.2b). Also, each of these inclined lines is tangent to the parabolic curve at the point where it meets the curve. This conclusion follows from the fact that there are no abrupt changes in the magnitude of $V(x)$ at these points. Hence, from Eqs.(10.2.2.1b) and (10.2.2.2b), we see that the slope of the bending-moment diagram does not change abruptly at these points.

Maximum bending moment. The maximum moment occurs where the shearing force equals zero. This point can be found by setting $V_{II}(x) = 0$ and the obtained value $x = x_e$, denoting the position of the extreme, is then substituted into $M_{II}(x_e) = M_{max}$,
which yields

$$x_e = a + \frac{b}{2 \cdot L} \cdot (b + 2 \cdot c) \quad \Rightarrow \quad M_{max} = \frac{w_o \cdot b}{8 \cdot L^2}(b + 2 \cdot c)\left(4 \cdot a \cdot L + 2 \cdot d \cdot c + b^2\right)$$

Conclusions. The maximum positive and negative bending moments in a beam may occur at the following cross-sections: i) where a concentrated load is applied and the shearing force changes signs; ii) where the shearing force equals zero; iii) at a point on an inner-span support where a vertical reaction is present; iv) where a couple is applied. When several loads act on a beam, it may be preferable to obtain bending-moment diagrams by superposition (or summation) of the diagrams obtained for each of the loads acting separately.

10.3 Stresses in beams

The effect of forces or couples (that lie in a plane containing the longitudinal axis of the beam and act perpendicular to the longitudinal axis, and the plane containing the forces is assumed to be a plane of symmetry of the beam) is to impart deflection perpendicular to the longitudinal axis of the bar and to set up both normal and shearing stresses on any across-section of the beam perpendicular to its axis.

Types of bending

If couples are applied to the ends of the beam and no forces act on it, the bending is termed *pure bending* and such a beam has only normal stresses with no shearing stresses set up in it. *Pure bending*

will be dealt with in Sec.10.3.1. Bending produced by forces that do not form couples is called *ordinary bending*, and a beam subjected to it has <u>both normal and shearing stresses</u> acting within it. Problems connected with <u>shearing stresses</u> in a beam will be discussed in Sec.10.3.2.

10.3.1 <u>Bending formulas</u>

<u>Nature of beam action for *pure bending*</u>

It is convenient to imagine a beam to be composed of an infinite number of thin longitudinal rods or fibers. Each longitudinal fibre is assumed to act independently of each other fibre, i.e., there are no lateral pressures or shearing stresses between adjacent fibres. The beam of Fig.10.3.1.1, for example, will deflect downward and the fibres in the lower part of the beam will undergo extension, while those in the upper part are shortened. These changes in the lengths of the fibres set up stresses in them. Those that are extended have tensile stresses acting on the fibres in the direction of the longitudinal axis of the beam, while those that are shortened are subject to compressive stresses. There is always one surface in the beam that contains fibres that do not undergo any extension or compression, and thus are not subjected to any tensile or compressive stress. This surface is called the *neutral surface* of the beam. The intersection of the neutral surface with any cross-section of the beam perpendicular to its longitudinal axis is called the *neutral axis*. All fibres on one side of the neutral axis are in a state of tension, while those on the opposite side are in compression.
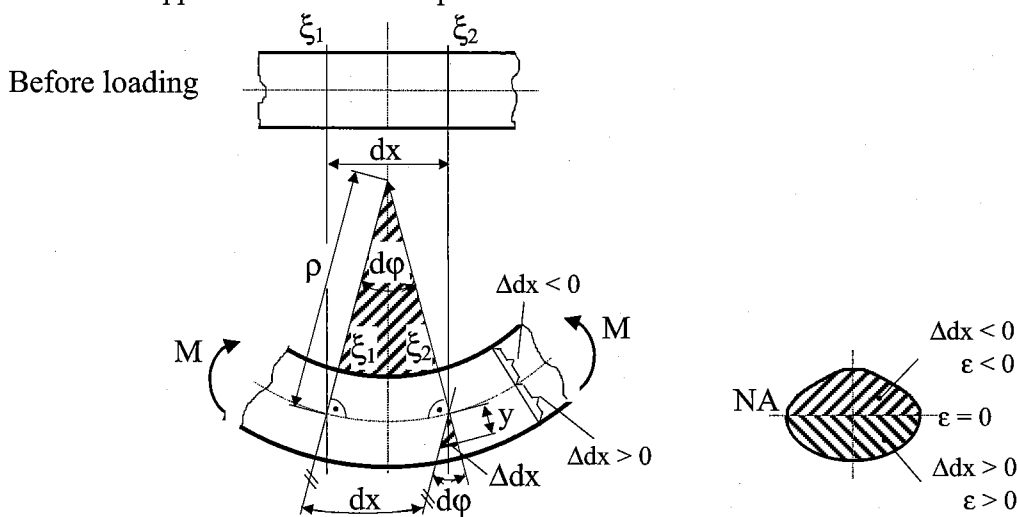

Fig.10.3.1.1

A hypothesis known as **Bernoulli's hypothesis** has been proved for pure bending. It states:
Plane sections, which were perpendicular to the longitudinal beam axis before the beam was deformed, remain plane and perpendicular to the deformed longitudinal beam axis.

In order to derive the necessary relations we can proceed analogously to the torsion of shafts:

1) <u>The relation between the *displacement* and *strain.*</u>

Comparing the hatched similar triangles (having the same angle $d\varphi$) in this picture we can write:

$$\frac{dx}{\rho} = \frac{\Delta dx}{y} \quad ,$$

where ρ represents the curvature radius of the deformed longitudinal axis of the beam and we can express the *curvature* $\kappa = 1/\rho$ of the deformed axis (which plays here the role of a *displacement*). We will solve the equation in such a way that the *strain* ε is obtained and expressed as a function of the *curvature* κ, i.e.,

$$\frac{\Delta dx}{dx} = \frac{1}{\rho} \cdot y \quad \Rightarrow \quad \varepsilon = \kappa \cdot y \qquad \text{(cf. Eq.8.1.1.1)} \qquad (10.3.1)$$

2) The relation between *stress* and *strain*

Application of Hooke's law combined with Eq. (10.3.1) yields

$$\sigma = E \cdot \varepsilon = E \cdot \kappa \cdot y = c \cdot y \quad \Rightarrow \quad c = \frac{\sigma}{y} \quad \text{or} \quad c = E \cdot \kappa \quad \text{(cf. Eq.8.1.2.3)} \quad (10.3.2a,b)$$

from which follows that the stress magnitude is proportional to its distance from the neutral axis (*NA*) having its extreme values σ_1 and σ_2 at the most distant fibres with ordinates $y = e_1$; e_2 , respectively (Fig.10.3.1.2a,b). To plot the stress diagram with respect to the beam cross-section, it is necessary to turn it into the cross-sectional plane, see Fig.10.3.1.2b.
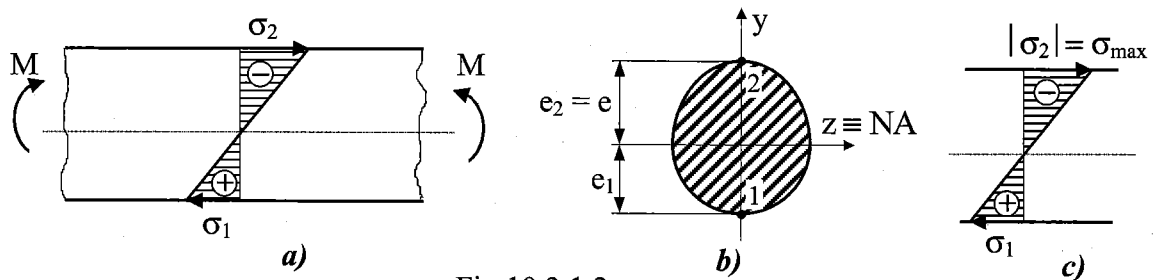

Fig.10.3.1.2

3/ Equations of *static equilibrium.*

When deriving bending formulas we need to apply **three** *equations of static equilibrium*, since we must find out (Fig.10.3.1.3):
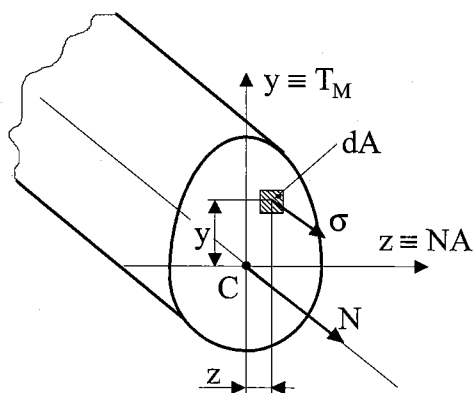

Fig.10.3.1.3

α) the *position of the neutral axis* given by the following answers:

    a) what cross-sectional point does it pass through?

    b) how is the neutral axis inclined to the given coordinate system?

β) the relation between the *bending moment* and *stress*

ad α)   a) We will find out this answer when applying the equilibrium equation for the forces acting upon the beam in the *longitudinal* direction. Since no external force is

exerted on the beam in this direction the sum of the internal normal forces (Eq.10.3.2 was applied)

must equal zero
$$N = \int_{(A)} \sigma \cdot dA = \int_{(A)} c \cdot y \cdot dA = c \cdot \int_{(A)} y \cdot dA = 0$$

The last integral in this expression means the *first moment of the cross-sectional area* and this is equal to zero only if the **neutral axis passes through the centroid.**

ad α) b) We will find out this answer when applying the equilibrium equation saying: <u>if the forces acting upon the beam, and producing bending moments, lie in the plane containing the x and y axes</u> and thus intersecting the cross-sectional plane in the track (denoted T_M) which coincides with the axis y, then the <u>moments of the internal forces with respect to the cross-sectional axis $y \equiv T_M$, must equal zero.</u> Let us now consider that the *neutral axis* coincides with the axis z ($z \equiv NA$), then we can write

$$M_y = \int_{(A)} z \cdot \sigma \cdot dA = c \cdot \int_{(A)} z \cdot y \cdot dA = c \cdot I_{yz} = 0$$

We see that this condition can be fulfilled only when the <u>product of inertia of the cross-sectional area I_{yz} with respect to the axes $y \equiv T_M$ and $z \equiv NA$ equals zero.</u>

(It follows from this, for instance, that if T_M coincides with one of the principal axes, e.g., $y \equiv 2$, NA will coincide with the second principal axis $z \equiv 1$, being perpendicular to y. Otherwise, the axes $y \equiv T_M$ and $z \equiv NA$ must form a <u>skew coordinate system</u> for which it holds that $I_{y,z} = 0$.)

ad β) When expressing the moment of the internal forces with respect to the axis $z \equiv NA$:

$$M = \int_{(A)} y \cdot \sigma \cdot dA = c \cdot \int_{(A)} y^2 \cdot dA = c \cdot I_z \quad \Rightarrow \quad c = \frac{M}{I_z} \qquad (10.3.3)$$

and afterwards substituting here for c from Eq.(10.3.2a), we will find the relation $\{M, \sigma\}$ the so-called *flexure formula* in the form
$$\sigma = \frac{M}{I_z} \cdot y \quad \text{(cf. Eq.8.1.3.4)} \qquad (10.3.4)$$

This bending stress acquires extreme values in the extreme fibres of the cross-section at distances e_1, e_2 from NA, respectively, see Fig.10.3.1.2b,

Maximum tensile stress	*Maximum compression stress*	
$\sigma_1 = \dfrac{M}{I_z} \cdot e_1 = \dfrac{M}{\dfrac{I_z}{e_1}}$	$\sigma_2 = -\dfrac{M}{I_z} \cdot e_2 = -\dfrac{M}{\dfrac{I_z}{e_2}}$	$(10.3.5a,b)$

The *Strength criterion* for a beam made of a *ductile material* (loaded in pure bending) is obtained for a fibre of the beam cross-section that is at the extreme distance e from NA:

$$\sigma_{max} = \frac{M}{\dfrac{I_z}{e}} = \frac{M}{Z_b} \le \sigma_{all} \quad \text{(cf. Eq.8.1.3.4)} \qquad (10.3.6)$$

To obtain the *Strength criterion* for *brittle material* (pure bending) it is necessary to check both tension and compression (cf. Secs.2.6.3 and 7.2.1): $\sigma_1 \leq \sigma_{all;t}$; $|\sigma_2| \leq \sigma_{all;c}$ (respectively). (10.3.7a,b)

The so-called *section modulus in bending*
$$Z_b = \frac{I_{NA}}{e}$$
(10.3.8)

(where I_{NA} ... the second moment of area with respect to *NA*) was introduced in Eq.(10.3.6), analogously as for the torsion of shafts (Eq.8.1.3.6).

10.4 Strain energy in bending

Since pure bending is a uniaxial stress state, we will start from Eq.(2.12.5) for strain energy. Consider now a loaded beam and let M be the bending moment at a distance x from one end. Neglecting for the time being the effect of shear, and taking into account only the normal stresses given by the *flexure formula* (Eq.10.3.3), we substitute this expression into Eq.(2.12.5) and write

$$U = \int_{(V)} \frac{\sigma^2}{2E} \cdot dV = \int_{(V)} \frac{M^2(x) \cdot y^2}{2E \cdot I_z^2} \cdot dV$$

Setting $dV = dA\, dx$, where dA represents an element of the cross-sectional area and dx an element of the length of the beam, and recalling that $M^2/2EI_z$ is a function of x alone, we have

$$U = \int_{(L)} \frac{M^2(x)}{2E \cdot I_z^2} \left(\int_{(A)} y^2 \cdot dA \right) \cdot dx = \int_{(L)} \frac{M^2(x)}{2E \cdot I_z} \cdot dx$$
(10.4.1)

where we recall that the integral in parentheses represents the second moment of area of the cross-section about its *NA*.

10.5 Shearing stress in beams (ordinary bending)

Ordinary bending is very common in practice, because in a beam loaded by transverse forces acting perpendicular to the axis of the beam, not only are the bending stresses parallel to the axis of the bar produced (due to the bending moment *M*), but the shearing stresses (due to the shear force V) also act over cross-sections of the beam perpendicular to the axis of the bar. We will study this problem now to find out **when we can neglect** the influence of **shearing stress, and when we cannot.**

10.5.1 Distribution of the shearing stress in a beam with a rectangular cross-section

The actual distribution of the shearing stress in a beam cross-section of a general shape is difficult to define. But when dealing with tall, narrow sections, we can define it quite easily. Let us consider a rectangular section (Fig.10.5.1.1) with a height to width ratio of **h/b ≥ 2.** For this we can assume: i) the shearing stresses are parallel with the vertical shear force *V*, i.e. with the axis *y*, and they depend on the position *y*, i.e. $\tau_z(y)$; ii) the shearing stresses are uniform along the whole section width, i.e. along the *z* axis. Cutting an element *dx* from the beam in the longitudinal direction we realize that, due to different

values of bending moments in section x, *i.e.* $M(x)$, and in the section $x + dx$, *i.e.* $M(x) + dM$, there are different magnitudes of normal stresses depending on the positions of the sections on the x axis, *i.e.* $\sigma(x)$ and $\sigma(x) + d\sigma$, respectively. From that element we shall use only the lower part cut at a distance y from the neutral axis $NA \equiv z$. Evidently, such an element (being loaded in the longitudinal direction with the resulting normal forces $N(x)$ and $N(x) + dN$, to the left and to the right, respectively) would not rest in static equilibrium if a certain shear force (resulting from the shearing stress τ_z) did not exert on its upper surface.
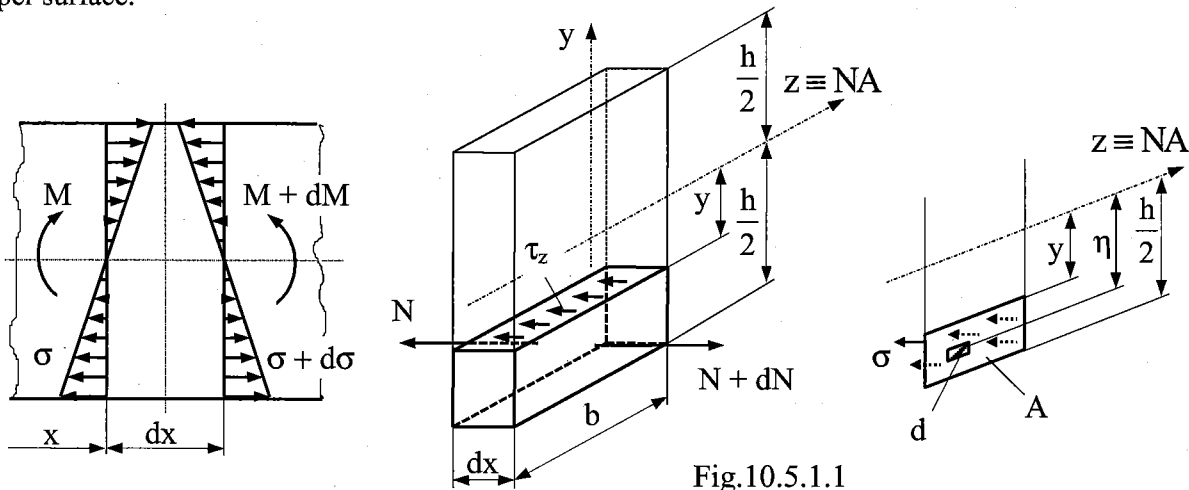

Fig.10.5.1.1

The equilibrium equation is

$$N + dN - N - \tau_z \cdot b \cdot dx = 0$$

The resulting normal force exerted on the left hand side of the element is given by

$$N = \int_{(A)} \sigma \cdot dA = \int_{(A)} \left(\frac{M}{I_z} \cdot \eta\right) \cdot dA = \frac{M}{I_z} \cdot \int_{(A)} \eta \cdot dA = \frac{M}{I_z} \cdot Q$$

The integral $\int_{(A)} \eta \cdot dA = Q$ expresses the first moment of the area A (a part **cut off** from the cross-section at an arbitrary ordinate y) with respect to the neutral axis NA. Analogously, we will obtain the resulting force acting on the right hand side of the element $N + dN = \dfrac{M + dM}{I_z} \cdot Q$. After substituting into the equilibrium equation and rearranging it (and applying the differential relation between the *bending moment M* and the *shear force V*, see Eq.(10.2.2.1b), we obtain the shearing stress in the form

$$\tau = \frac{V \cdot Q}{I_z \cdot b} \tag{10.5.1.1}$$
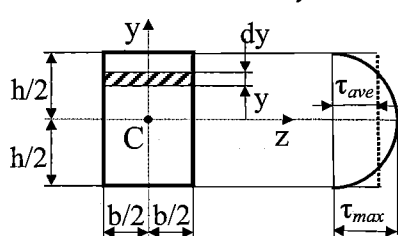
(This formula is known also as *Zhurawski's theorem*)

    (*V*... the shear force acting in the particular cross-section of the beam;

    Q... the first moment with respect to the *NA* of the part of the cross-sectional area that is separated by a horizontal line passing at a distance y from the *NA,* or briefly: *the first moment of the cut-off part of the cross-section;*

I_z...the second moment of the cross-sectional area with respect to *NA*;

b... the width of the section in the investigated locality)

As an example we recommend you to continue solving the given section while applying this expression. You will assess that the shearing stress distribution obeys the parabola law with its maximum value at *NA*, where $y = 0$, hence, $\tau_{max} = (3/2)\,\tau_{ave}$.
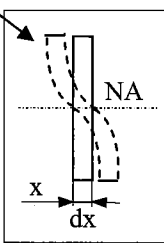
$$\tau_z = \frac{V \cdot Q}{I_z \cdot b} = \frac{V \cdot b \cdot \displaystyle\int_y^{h/2} y \cdot dy}{\dfrac{h^3 \cdot b}{12} \cdot b} = \frac{3}{2} \cdot \tau_{ave} \cdot \left[1 - \left(\frac{2y}{h}\right)^2 \right] \quad (10.5.1.2)$$
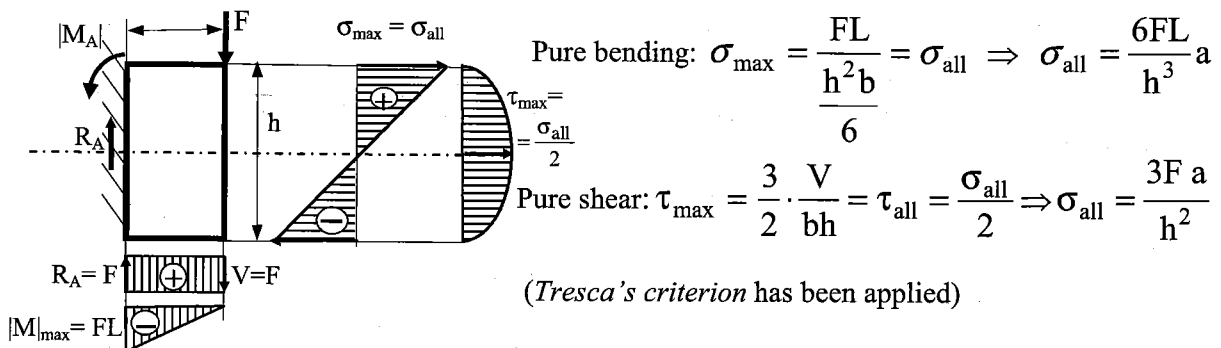
(The average shearing stress $\tau_{ave} = V/bh$ is based on its imaginary uniform distribution over the section.)

(Analogously to Eq.(10.5.1.2), the distribution of the shearing stress can be derived, based on Eq.(10.5.1.1), for *other sections having a relatively narrow wall thickness.* Note that the assessment of shearing stresses will be important mainly for *thin-walled sections*. It should be observed that we always cut a given cross-section in the direction of the smallest thickness at the investigated place in the section.)

The **influence of shearing stress** will produce **deplanation (warping) of the cross-section** of the beam ensuing from the fact that the individual section each other, undergo the shear strain in a different intensity according to the magnitude of the shearing stress which is the largest in the *NA*, while in the upper and lower extreme fibers, the shearing stress equals zero. Of course, this is in contradiction with *Bernoulli's hypothesis*, according to which "beam sections being plane before deformation remain plane after deformation". Owing to this fact, the normal stress distribution will also not remain linear. Clearly, since *the stress state* of beams under ordinary bending contains both normal and shearing stresses, this is a plane stress state and the normal bending stress will not be the *principal stress*. **Bernoulli's hypothesis** and the linear distribution of normal bending stress (being the principal stress) would *hold exactly only under* **pure bending**. Thus, some small deviations from *Bernoulli's hypothesis* arise when dealing with ordinary bending which produces shear as well. These deviations can be neglected if the effect of the bending moment outweighs the shear force effect, which is confirmed for instance by the following example:

Determine the limit ratio h/L for a cantilever of length *L* with the rectangular section of height/width = h/b = a, when the influence of the shearing stress will have the same effect on the beam strength as does the normal stress.

Pure bending: $\sigma_{max} = \dfrac{FL}{\dfrac{h^2 b}{6}} = \sigma_{all} \Rightarrow \sigma_{all} = \dfrac{6FL}{h^3} a$

Pure shear: $\tau_{max} = \dfrac{3}{2} \cdot \dfrac{V}{bh} = \tau_{all} = \dfrac{\sigma_{all}}{2} \Rightarrow \sigma_{all} = \dfrac{3F\,a}{h^2}$

(*Tresca's criterion* has been applied)

Comparing the two results, we obtain the limit ratio $h/L = 2$. Evidently, this represents a very short beam with a very high section. It follows from this that for a 'normally grown beam' (slim) we can neglect the influence of shear and consider only the normal bending stress (as principal stress) being produced in such beams.

10.5.2 Distribution of the shearing stress in thin-walled open sections (shear centres)

This section consists of two principal parts: first, evaluating the shearing stress acting on the cross-section when bending occurs about one of the principal axes, and second, determining the resultant of those stresses. The so-called *shear centre* (or *centre of flexure*) is located on the line of action of the resultant.

Let us investigate the shearing stress in the *channel section* of Fig.10.5.2.1. loaded by a shear force V acting perpendicularly to z, which is the axis of symmetry of this channel section and where, thus, the shear centre must self-evidently be located. We begin by considering the shearing stress at section s in the top flange. When applying Eq.(10.5.1.1) we have

$$\tau_y = \frac{V \cdot Q}{I_z \cdot b} = \frac{V \cdot \left(s \cdot t_f \cdot \dfrac{h}{2}\right)}{I_z \cdot t_f} = \frac{V \cdot h}{2 \cdot I_z} \cdot s \qquad (10.5.2.1)$$

As this equation shows, the shearing stress increases linearly with distance s. When substituting $s = b$, we obtain the maximum stress $\tau_{y;max}$ in the flange. In a section located at a distance y from NA, the shearing stress τ_z acting in the web is calculated as follows:

$$\tau_z = \frac{V \cdot Q}{I_z \cdot b} = \frac{V \cdot \left[b \cdot t_f \cdot \dfrac{h}{2} + t_w \left(\dfrac{h}{2} - y\right) \cdot \dfrac{1}{2}\left(\dfrac{h}{2} + y\right) \right]}{I_z \cdot t_w} = \frac{V \cdot \left[b \cdot t_f \cdot h + t_w \left(\dfrac{h^2}{4} - y^2\right) \right]}{2 I_z \cdot t_w}$$

$$(10.5.2.2)$$
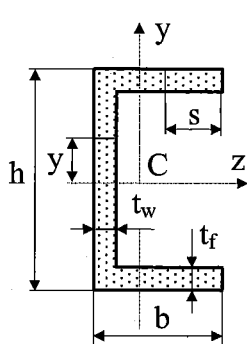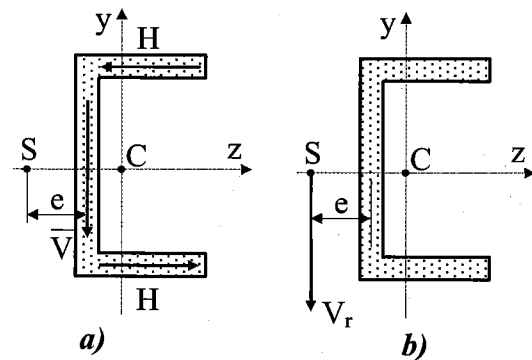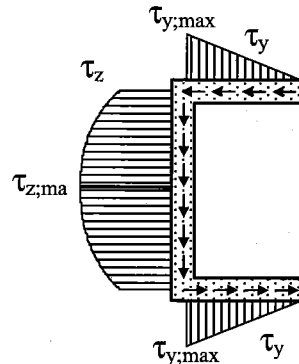
Fig.10.5.2.1   Fig.10.5.2.2

The stress τ_z in the web acts downward and increases in magnitude until *NA* is reached. When $y = h/2$, we obtain $\tau_z\ (h/2) = \tau_y\ (b)\ .\ (t_f\ /t_w)$, while for $y = 0$ this equation gives the maximum shearing stress,

$$\tau_{z;max} = \frac{V \cdot Q}{I_z \cdot b} = \frac{V \cdot h}{2 \cdot I_z} \cdot \left(b \cdot \frac{t_f}{t_w} + t_w \cdot \frac{h}{4} \right) \qquad (10.5.2.3)$$

The shearing stresses in the web vary parabolically, as shown in Fig.10.5.2.1, although the variation is not large. The ratio of τ_{max} to $\tau_z\ (h/2)$, if we take, for instance, typical values of $h = 2b$ and $t_f = 2t_w$, is $\tau_{max}\ /\tau_z\ (h/2) = 1.25$.

The horizontal shear force *H* in either flange and the vertical shear force *V* in the web can be found by

$$H = \int_0^b \tau_y \cdot t_f \cdot ds = \int_0^b \frac{V \cdot h \cdot s}{2 I_z} \cdot t_f \cdot ds = \frac{V \cdot h \cdot t_f \cdot b^2}{4 I_z}; \quad \overline{V} = \int_0^b \tau_z \cdot t_w \cdot dy = V \quad (10.5.2.4)$$

(Try for yourself. Compute $\overline{V}$ by substituting from Eq. (10.5.2.1) and thus confirming the shown identity.)

The three internal forces acting on the cross-section (Fig.10.5.2.1) have a resultant $V_r = V$ that intersects the *z* axis at the shear center *S* (Fig.10.5.2.2a). Hence, the moment of the three forces about any point (here *S*) in the cross-section must be equal to the moment of the force V_r about the same point:

$$H \cdot h - V \cdot e = 0 \quad \Rightarrow \quad e = \frac{H \cdot h}{V} = \frac{h^2 \cdot t_f \cdot b^2}{4 I_z} \qquad (10.5.2.5)$$

where e is the distance from the centerline of the web to the shear centre *S*, and the moment of the resultant force V_r is zero (Fig.10.5.2.2b). Note that a channel beam will undergo bending without twisting whenever it is loaded by forces acting through the shear centre. If the loads act parallel to the *y* axis but through some point other than the shear centre, they can be replaced by a statically equivalent force system consisting of loads through the shear centre and a twisting couple.

10.5.3 Strain energy in shear

Strain energy in shear produced by shearing force V and accumulated in a beam of length L and a rectangular cross-section of height h and width b (i.e., $A = bh$), where the vertical shearing stress distribution τ_z is given by Eq.(10.5.1.2), the beam volume element by $dV = b.dx.dy$ and $\tau_{ave} = V/A$, is successively expressed as follows:

$$U = \int_{(V)} \frac{\tau_z^{2}}{2G} \cdot dV = \int_0^L \left\{ \frac{b}{2G} \cdot \frac{9}{4} \cdot \tau^2_{ave} \cdot \int_{-h/2}^{h/2} \left[1 - \left(\frac{2y}{h} \right)^2 \right]^2 \cdot dy \right\} \cdot dx = \frac{6}{5} \cdot \int_0^L \frac{V^2}{2GA} \cdot dx$$

We observe that this expression differs from the expected shape (to be analogous to the other strain energies obtained so far - cf. Eqs. (2.12.7a), (8.3.2) and (10.4.1)) by a coefficient $\beta = 6/5 = 1.2$, holding for the **rectangular** cross-section. Coefficient β, depending on the considered type of the beam cross-section, must of course be derived case by case. Other special cases:

for a *circular profile*... $\beta = 32/27 \approx 1.18$;   for *W-beams (I-profile)*... $\beta = 2.4 \div 3.8$

10.5.4 Examples

10.5.4.1 Thin-walled pipe with a very narrow gap

1) Determine **the shear centre** of a thin-walled pipe with a very narrow gap caused when the pipe weld is broken.


Fig. 10.5.4.1

Use Eq. (10.5.1.1), $\tau = \dfrac{V \cdot Q^{cut}}{I_z \cdot b}$,

where substitute (using polar coordinates and expressions for thin pipes, because $\dfrac{r}{t} \geq 5$):

$$Q_z^{cut} = \int_0^{\varphi} r \cdot \sin\psi \cdot \underbrace{t \cdot r \cdot d\psi}_{dA_\psi} = r^2 t (1 - \cos\varphi),$$

$$I_z = \frac{J}{2} = \frac{1}{2} \int_0^{2\pi} r^2 \cdot \underbrace{t \cdot r \cdot d\varphi}_{dA_\varphi} = \pi r^3 t, \quad b = t$$

and obtain
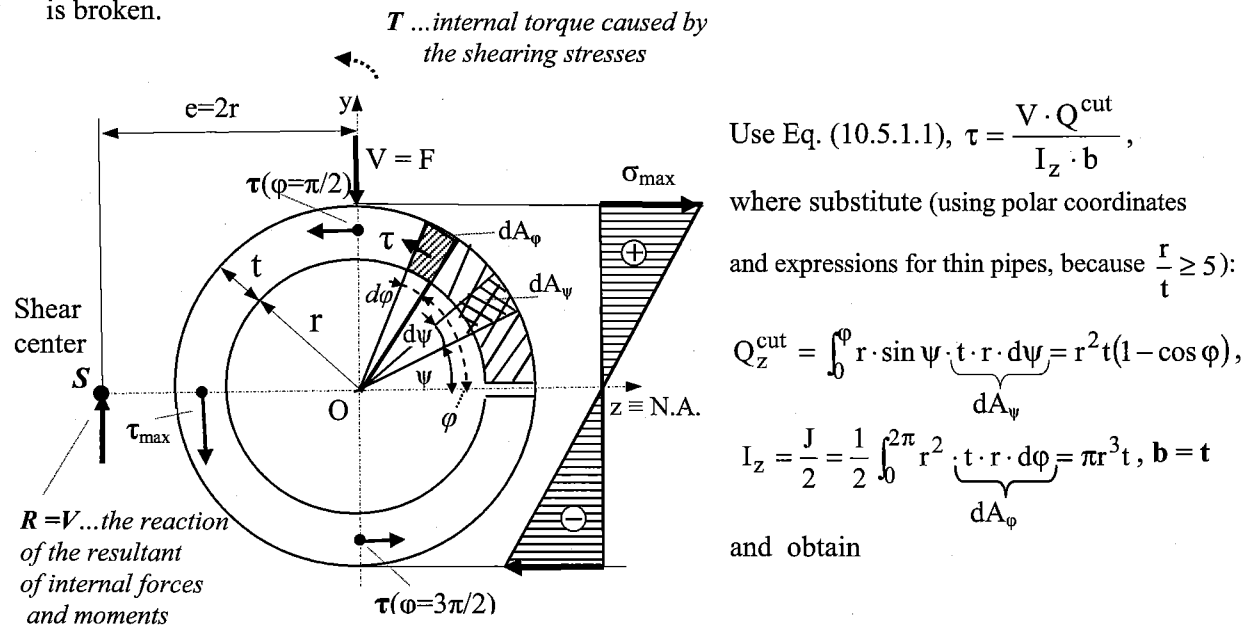
$$\tau(\varphi) = \frac{V \cdot Q_z^{cut}}{I_z \cdot b} = \frac{V \cdot r^2 t (1 - \cos\varphi)}{\pi r^3 t \cdot t} = \frac{V}{\pi r t} \cdot (1 - \cos\varphi)$$

Interesting shearing stress values: $\tau(\pi) = \dfrac{V}{\pi rt} \cdot [1 + (-1)] = 2 \cdot \dfrac{V}{\pi rt} = \tau_{max}$

$\tau(0) = \tau(2\pi) = \dfrac{V}{\pi rt} \cdot (1 - 1) = 0$; $\tau(\pi/2) = \tau(3\pi/2) = \dfrac{V}{\pi rt} \cdot (1 - 0) = \dfrac{V}{\pi rt}$;

The internal torque T, caused by the shearing stresses when summing their moments about the pole O, is:

$$T = \int_0^{2\pi} dT = r \cdot \int_0^{2\pi} \tau \cdot dA_\varphi = r \cdot \dfrac{V}{\pi rt} \cdot \int_0^{2\pi} (1 - \cos\varphi) \cdot t \cdot r \cdot d\varphi = r \cdot \dfrac{V}{\pi} \cdot [\varphi - \sin\varphi]_0^{2\pi} = r \cdot \dfrac{V}{\pi} \cdot [2\pi] = 2 \cdot V \cdot r$$

The external couple $V \cdot e$ has to be equal to the internal torque T, which yields the _shear center position S_:
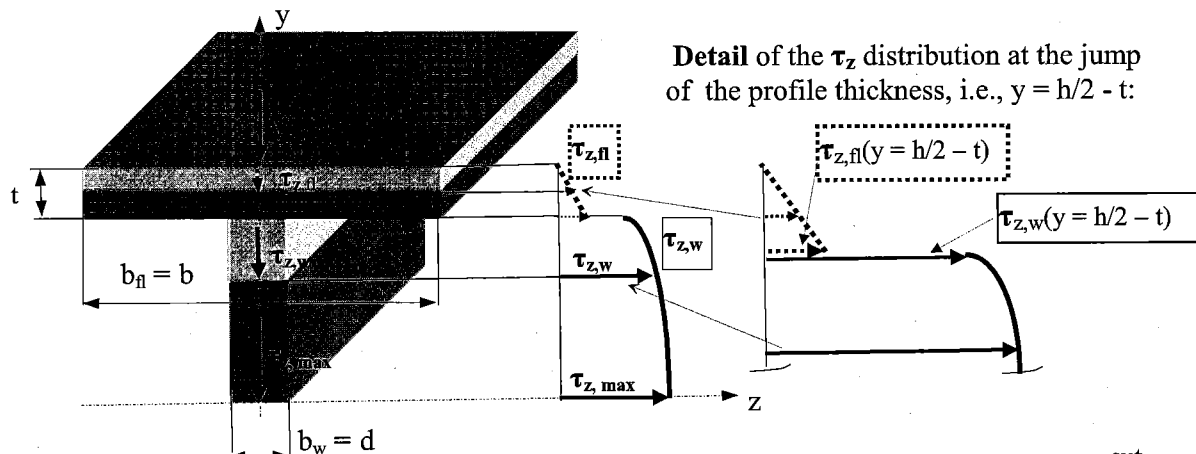
$$e = 2r \quad \text{(see Fig. 10.5.4.1)}$$

Note: A discussion about important consequences, following from non-coinciding the _cross-section_ _center O_ with the _shear center S_, will be carried out in the Chapter 13 – **Combined loading**, where the pipe is used as a cantilever bearing a vertical load F at its free end (Complement 13.7).

10.5.4.2 Example on Zhurawski's theorem application

This example should help you with the proper _Zhurawski's theorem_ application and with your imagination of the shearing stress distribution in thin-walled beams. We will show that on a W- profile.

1) The vertical shearing stress (τ_z) distribution in the web and flanges.

Detail of the τ_z distribution at the jump of the profile thickness, i.e., $y = h/2 - t$:

The vertical shearing stress distribution (along the W-profile heights h): $\tau_{z,fl,w}(y) = \dfrac{V \cdot Q^{cut}}{I_z \cdot b_{fl,w}}$

_a)_ **Flanges**: From the comparison of $\tau_{z,fl}$ ($y = h/2 - t$) with that exerted in the web, $\tau_{z,w}$ ($y = h/2 - t$), we can see the influence of the sudden jump in the profile thickness.

(For the _horizontal_ cutting: $Q^{cut} = b \cdot (h/2 - y) \cdot \dfrac{(h/2 + y)}{2} = b \cdot \left[\left(\dfrac{h}{2}\right)^2 - y^2\right] \cdot \dfrac{1}{2}$

$\tau_{z,fl}\left(y = h/2 - t\right) = \dfrac{V \cdot t \cdot (h/2 - t/2)}{I_z} \ll \tau_{z,w}\left(y = h/2 - t\right) = \dfrac{V \cdot [b \cdot t \cdot (h/2 - t/2)]}{I_z \cdot d}$)
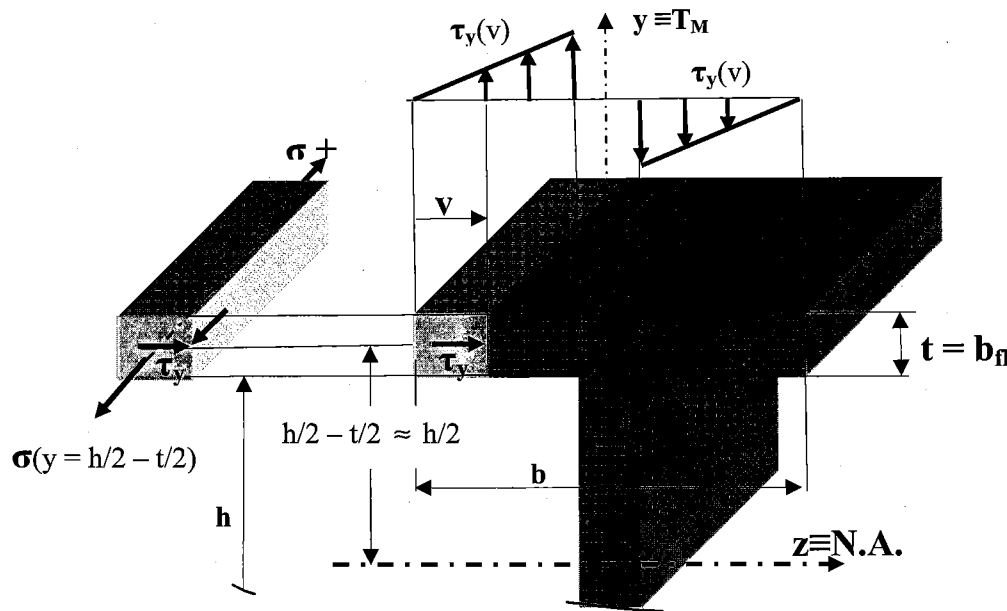
At the same time, we know that the flange being cut with *horizontal* sections contradicts to the requirement that the *Zhurawski's theorem* can be applied only for narrow profiles.

b) **Web:** It is evident that the web obeys this requirement and we have
(when neglecting t compared with h)

$$Q^{cut} = b \cdot t \cdot \left(\frac{h}{2} - \frac{t}{2}\right) + d \cdot \left(\frac{h}{2} - t - y\right) \cdot \left(\frac{\frac{h}{2} - t - y}{2} + y\right) \approx b \cdot t \cdot \frac{h}{2} + d \cdot \left(\frac{h^2}{8} - \frac{y^2}{2}\right)$$

$$\tau_{z,w}(y) \approx \frac{V \cdot \left[b \cdot t \cdot \frac{h}{2} + d \cdot \left(\frac{h^2}{8} - \frac{y^2}{2}\right)\right]}{I_z \cdot d} \ ; \ \tau_{z,max} \approx \frac{V \cdot \left[b \cdot t \cdot \frac{h}{2} + d \cdot \frac{h^2}{8}\right]}{I_z \cdot d}$$

2) The horizontal shearing stress (τ_y) distribution in the flanges

$$\tau_{y,fl}(v) = \frac{V \cdot Q^{cut}}{I_z \cdot b_{(fl)}} = \frac{V \cdot (v \cdot t) \cdot \left(\frac{h}{2} - \frac{t}{2}\right)}{I_z \cdot t} \approx \frac{V \cdot t \cdot \frac{h}{2}}{I_z \cdot t} \cdot v \ ,$$

Note: As the symbol $b_{(fl)}$, in the denominator of the *Zhurawski Theorem*, there has to be applied such a profile thickness **which is perpendicular to the shearing stress to be assessed**
(i.e., here $b_{(fl)} = t$ for $\tau_{y,fl}$)

11. Deflections of beams

11.1 Introduction

When a beam with a straight longitudinal axis is loaded by lateral forces or couples, the axis is deformed into a curve *v(x)* (see Fig.10.3.1.1), called the deflection curve of the beam. In Sec.10.3 we used the curvature of the deflection curve to determine the normal strains and stresses in a beam. However, we did not develop a method for finding the deflections themselves. In this chapter, we will determine the equation of the deflection curve (Sec.11.2) and also find deflections at specific points along the axis of the beam by applying *Castigliano's theorem* and its derivations (Sec.11.3). The calculation of deflections is an important part of structural analysis and design. It is, for instance, an essential ingredient in the analysis of statically indeterminate beams (Chap.12).

11.2 Differential equation of the deflection curve

In Sec.10.3 we derived Eqs.(10.3.2*b*) and (10.3.3), from which we obtain successively the relation between the curvature of beam and the bending moment in the form (the *x* in the parentheses stresses that these quantities are in general functions of the longitudinal coordinate *x*)

$$E \cdot \kappa(x) = \frac{M(x)}{I_z(x)} \quad \Rightarrow \quad \kappa(x) = \frac{M(x)}{E \cdot I_z(x)} \tag{11.2.1}$$

Based on *differential geometry* we have

$$\kappa = \frac{1}{\rho} = \pm \frac{v''}{\left[1 + (v')^2\right]^{3/2}} \tag{11.2.2}$$

where ... $v' = dv/dx$ and $v'' = d^2 v /(dx)^2$ represent the respective derivatives of the deflection curve with respect to *x*.

Since the deflections of the beams are very shallow, it holds $(v')^2 << 1$ for the quadrate of the slopes of the deflections, and Eq.(11.2.2) can be simplified as $\kappa \approx v''$ (we can also take $v' = tg\varphi \approx \varphi$). Based on this simplification, and taking into account that positive bending moments produce concave deflection curves for which it holds $v'' < 0$, the combination of Eqs.(11.2.1) and (11.2.2) yields the basic *differential equation of the deflection curve* of a beam (*Bernoulli's equation*):

$$v'' = -\frac{M(x)}{E \cdot I_z(x)} \tag{11.2.3}$$

161

This (slightly rearranged) equation can undergo two further differentiations with respect to x, and then the *relations between w, V and M* (Eqs.10.2.2.1*a,b*) can be substituted, which yields successively

$$E \cdot I_z \cdot v'' = -M \; ; \quad E \cdot I_z \cdot v''' = -M' = -V; \quad E \cdot I_z \cdot v^{IV} = -M'' = w \qquad (11.2.4a,b,c)$$

We will refer to these equations as the *bending-moment equation,* the *shearing-force equation,* and the *load equation,* respectively. The general procedure consists of integrating the equations and then evaluating the constants of integration from the *boundary conditions (BC)* pertaining to the beam. There are two types of the *boundary conditions* pertaining to the beam:

  1) **static** *B.C* ... knowledge of V and/or M at specific sections of the beam;

  2) **geometric** *B.C* ... knowledge of φ and/or v at specific sections of the beam

11.3 Application of Castigliano's theorem

Referring to Sec.2.13, *Castigliano's theorem* provides a means for finding the deflections of a structure from the strain energy of the structure. To illustrate how to proceed with beams, consider a cantilever beam of uniform cross-section with a concentrated load F acting at the free end (Fig.11.3.1). The strain energy of this beam is obtained from Eq.(10.4.1), where it is substituted $M = -F.x$:

$$U = \frac{1}{2EI_z} \cdot \int_0^L (-F \cdot x)^2 \cdot dx = \frac{F^2 \cdot L^3}{6EI_z}$$

Now take the derivative of this expression with respect to the load F:

$$v(0) = \frac{\partial U}{\partial F} = \frac{\partial}{\partial F} \left(\frac{F^2 \cdot L^3}{6EI_z} \right) = \frac{F \cdot L^3}{3EI_z} \qquad (11.3.1)$$
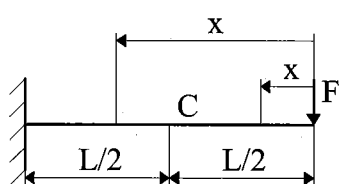

Fig.11.3.1

(The only displacements that can be found from Castigliano's theorem are those that correspond to loads acting on the structure. If we wish to calculate a displacement at a point on a structure where there is no load, then an imaginary load $\mathcal{F}$ *corresponding to the desired displacement* must be applied to the structure. We can then determine the displacement by evaluating the strain energy and taking the partial derivative with respect to the imaginary load $\mathcal{F}$. The result is the displacement produced by the actual loads and the imaginary load acting simultaneously. By setting the imaginary *(fictitious, or dummy)* load equal to zero ($\mathcal{F} \to 0$), we obtain the displacement produced only by the actual load, cf. Note in Sec. 2.13.)

11.3.1 Differentiation under the integral sign

As we can observe from Eq.(10.4.1), finding the strain energy requires the integration of the *square* of the bending moment. This may lead in general to lengthy integrations, especially when more than two loads act on the beam. For instance, if the bending moment expression has three terms, its square may have as many as six terms, each of which must be integrated. After the integrations have been completed and the strain energy has been determined, we differentiate the strain energy to obtain the deflections. However, we can bypass the step of finding the strain energy by differentiating *before* integrating:

$$v_i = \frac{\partial U}{\partial F_i} = \frac{\partial}{\partial F_i} \int_{(L)} \frac{M^2(x)}{2EI_z} \cdot dx = \int_{(L)} \frac{M(x)}{EI_z} \cdot \frac{\partial M}{\partial F_i} \cdot dx \qquad (11.3.1.1a)$$

(The indication *M(x)* in the integrals is to stress that we must express the bending moment at an arbitrary beam point determined by coordinate *x*). This procedure, which does not eliminate the integrations but makes them much simpler, is called *Mohr's integral*. Considering that the bending moment *M(x)* is always a linear function of the concentrated load F_i (either a real or a *dummy* load), Eq.(11.3.1.1a) can be rewritten in the form:

$$v_i = \int_{(L)} \frac{M(x)}{EI_z} \cdot m_i(x) \cdot dx \qquad (11.3.1.1b)$$

where $m_i = \partial M / \partial F_i$ represents the rate of change of the bending moment *M(x)* with respect to the load F_i, that is, it is equal to the bending moment produced by a (*dummy*) load of **unit** value applied at point (*i*) and in the desired direction of the looked-for displacement (cf. Sec.2.13: Eq.(2.13.7); Sec.4.1: Eqs.(4.1.1b) and (4.1.2b); and Sec.8.3: Eq.(8.3.5)). To confirm that you understand this method, recall the beam in Fig.11.3.1 and determine the deflection at its centre (point *C*) by applying a *(dummy) unit force* at point *C*. After using Eq.(11.3.1.1b).

(Note that the integral will separate into two integrals: for $0 \le x \le L/2$, and $L/2 \le x \le L$) you will obtain

$$v_C = \frac{1}{EI} \left\{ \int_0^{L/2} (-F \cdot x) \cdot 0 \cdot dx + \int_{L/2}^{L} (-F \cdot x) \cdot \left[-\left(x - \frac{L}{2}\right) \right] \cdot dx \right\} = \frac{5}{48} \cdot \frac{F \cdot L^3}{EI} \qquad (11.3.1.2)$$

Eqs.(11.3.1.1a,b) can be slightly modified in order to determine the slope of the deflection curve of a beam at a desired point *i*, where either the *real* or the *imaginary* couple M_i is exerted, as follows

$$\varphi_i = \frac{\partial U}{\partial M_i} = \int_{(L)} \frac{M(x)}{EI_z} \cdot \frac{\partial M}{\partial M_i} \cdot dx = \int_{(L)} \frac{M(x)}{EI_z} \cdot m_i(x) \cdot dx \qquad (11.3.1.3)$$
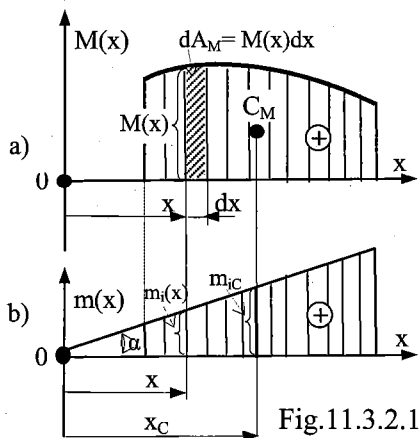
where $m_i = \partial M / \partial M_i$ represents the rate of change of the bending moment $M(x)$ with respect to the couple M_i, that is, it is equal to the bending moment produced by a (*dummy*) couple of **unit** value applied at the point *i*.

11.3.2 Geometric interpretation of Mohr's integral (Verescagin's rule)

Considering that $m_i(x) = x\ tg\alpha$ is always a linear function (Fig.11.3.2.1), Mohr's integral can be rearranged successively in the form

$$\int_{(L)} M(x) \cdot x \cdot tg\alpha \cdot dx = tg\alpha \cdot \int_{(L)} x \cdot dA_M = tg\alpha \cdot Q_{A_M} = A_M \cdot x_C \cdot tg\alpha = A_M \cdot m_{iC}$$

Fig.11.3.2.1

where the quantities have been substituted as follows:

$dA_M = M(x) \cdot dx$ ... the elementary moment area;

A_M ... the moment area;

$$Q_{A_M} = \int_{(L)} x \cdot dA_M = A_M \cdot x_C$$

...the first moment of the moment area about the origin;

m_{iC} ...the ordinate of the (dummy) unit force moment under the centroid of A_M

Since both A_M and m_{iC} can generally consist of a number *n* of types of areas we define the expression

$$v_i; \varphi_i = \frac{1}{EI} \cdot \sum_{j=1}^{n} A_{M;j} \cdot m_{iC;j} \qquad (11.3.2.1)$$

known as *Verescagin's rule*. This is the counterpart to Eq.(11.3.1.1*b*) and thus serves for determining the deflection of a beam at point *i* when m_{iC} is produced by a *dummy* unit load, or the counterpart to Eq.(11.3.1.2). It thus also serves for determining the slope of the deflection curve of a beam at point *i* when m_{iC} is produced by a *dummy* unit couple.

Note: When applying the *bending-moment equation*, the *shear-force equation*, and *load equation* (Eqs.11.2.4*a,b,c*) on the cantilever in Fig.11.3.1, where $w(x) = 0$, we obtain successively (while proceeding from the right):

$$EI \cdot v^{IV}(x) = 0; \quad EI \cdot v''' = C_1 = V(x); \qquad EI \cdot v''(x) = C_1 \cdot x + C_2 = -M(x);$$

$$EI \cdot \varphi(x) \approx EI \cdot v'(x) = C_1 \cdot \frac{x^2}{2} + C_2 \cdot x + C_3; \qquad EI \cdot v(x) = C_1 \cdot \frac{x^3}{6} + C_2 \cdot \frac{x^2}{2} + C_3 \cdot x + C_4$$

Boundary conditions:

I) static *BC*: for $x = 0$ hold 1) $V(0) = F \Rightarrow$ $C_1 = F$

2) $M(0) = 0 \Rightarrow$ $C_2 = 0$

II) geometric *BC*: for $x = L$ hold   3) $\varphi(L) \approx v' = 0 \Rightarrow \qquad C_3 = -FL^2 / 2$

4) $v(L) = 0 \Rightarrow \qquad C_4 = -FL^3 / 3$

After substituting for the integration constants obtained, we have:

$$V(x) = F; \quad M(x) = -F \cdot x; \quad \varphi(x) \approx \frac{F \cdot L^2}{2EI} \cdot \left[\left(\frac{x}{L}\right)^2 - 1\right]; \quad v(x) = \frac{F \cdot L^3}{6EI} \cdot \left[\left(\frac{x}{L}\right)^3 - 3 \cdot \frac{x}{L} + 2\right]$$

When setting $x = 0$ and $x = L/2$ into the last two expressions, we obtain deformations at the free end and in the middle of the beam, respectively:

- **slope** of the deflection curve:

$$\varphi(0) \approx -\frac{F \cdot L^2}{2EI} \text{ (note the negative sign corresponding to the coordinate system in Fig.11.3.1)}$$

$$\varphi\left(\frac{L}{2}\right) \approx -\frac{3}{8} \cdot \frac{F \cdot L^2}{2EI} \text{ (in the middle of the cantilever at point } C)$$

- **deflection**:

$$v(0) = \frac{F \cdot L^3}{3 \cdot EI} \text{ (compare this result with Eq.11.3.1, obtained by Castigliano's theorem)}$$

$$v\left(\frac{L}{2}\right) = \frac{5}{48} \cdot \frac{F \cdot L^3}{EI} \text{ (compare this result with Eq.11.3.1.2, obtained by Mohr's integral)}$$

11.4 Influence coefficients; Maxwell's theorem of reciprocal displacements

11.4.1 Influence coefficients

Influence coefficient $\qquad\qquad \eta_{ij} = \frac{v_i}{F_j} \quad \left[mm \cdot N^{-1}\right] \qquad\qquad$ (11.4.1.1)

expresses the deflection at a given point *i* of a beam produced by a unit load $F_j = 1$ acting at another given point *j* of the beam. It follows from this definition that the above defined *influence factor* is in substance the *flexibility* of the beam with respect to points *i* and *j*.

Analogous *influence coefficients:* $\qquad\qquad\qquad\qquad\qquad\qquad\qquad$ (11.4.1.2a,b,c)

$\psi_{ij} = \frac{\varphi_i}{F_j} \quad \left[N^{-1}\right]$ ...the slope of the deflection curve at *i* produced by $F_j = 1$ at *j*

$\overline{\eta}_{ij} = \frac{v_i}{M_j} \quad \left[N^{-1}\right]$ ...the deflection of the beam at *i* produced by a unit couple $M_j = 1$ at *j*

$$\overline{\Psi}_{ij} = \frac{\varphi_i}{M_j} \quad \left[\left(mm \cdot N\right)^{-1}\right] \text{...the slope of the deflection curve at } i \text{ produced by } M_j = 1 \text{ at } j$$

All the *influence coefficients* can be calculated, for instance, by applying *Verescagin's rule*:

a load F, or a couple M, being equal to unit, i.e., $F_j = 1$ (or $M_j = 1$), is applied at point j where the beam is to be loaded and a *dummy* unit load (or couple) "1" is applied at i, where the required deflection (or slope of the deflection curve) is to be calculated, respectively.

11.4.2 Maxwell's theorem of reciprocal displacements

Consider a beam subjected to two loads F_i and F_j at points i and j, respectively, as shown in Fig.11.4.2.1. Let F_i be gradually applied first, producing a deflection $v_i = F_i \, \eta_{ii}$ at i.

$$\text{Work done} = \frac{1}{2} \cdot F_i \cdot F_i \cdot \eta_{ii}$$

When F_j is applied it will produce a deflection $v_j = F_j \, \eta_{jj}$ at j and an additional deflection $F_j \, \eta_{ij}$ at i (the latter occurring in the presence of a now constant load F_i).

$$\text{Extra work done} = \frac{1}{2} \cdot F_j \cdot F_j \cdot \eta_{jj} + F_i \cdot F_j \cdot \eta_{ij}$$

$$\text{total work done ... } W_A = \frac{1}{2} \cdot F_i \cdot F_i \cdot \eta_{ii} + \frac{1}{2} \cdot F_j \cdot F_j \cdot \eta_{jj} + F_i \cdot F_j \cdot \eta_{ij} \qquad (11.4.2.1)$$

Similarly, if the loads were applied in reverse order and the load F_i at i produced an additional deflection $F_i \eta_{ji}$ at j, then

$$\text{total work done ... } W_B = \frac{1}{2} \cdot F_j \cdot F_j \cdot \eta_{jj} + \frac{1}{2} \cdot F_i \cdot F_i \cdot \eta_{ii} + F_j \cdot F_i \cdot \eta_{ji} \qquad (11.4.2.2)$$
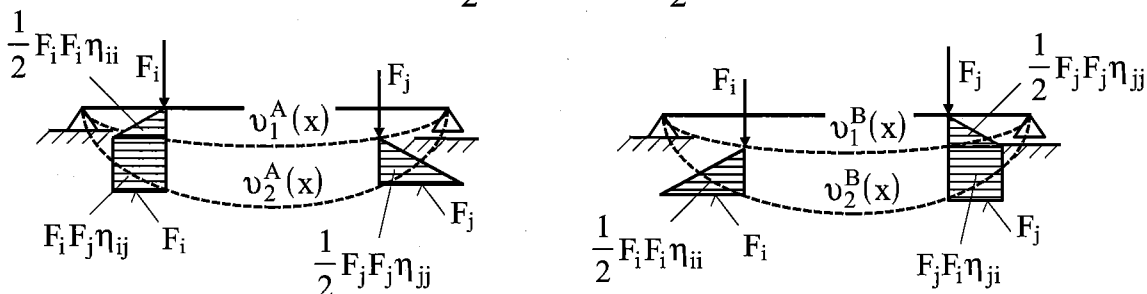

Fig.11.4.2.1

Equaling eqs.(11.4.2.1) and (11.4.2.2) we obtain *Maxwell's theorem of reciprocal displacements*

$$1) \quad \eta_{ij} = \eta_{ji} \left[mm \cdot N^{-1}\right]; \; 2) \, \overline{\Psi}_{ij} = \overline{\Psi}_{ji} \left[\left(mm \cdot N\right)^{-1}\right]$$

$$3) \quad \psi_{ij} = \psi_{ji} \left[N^{-1}\right]; \; 4) \, \overline{\eta}_{ij} = \overline{\eta}_{ji} \left[N^{-1}\right]; \; 5) \, \psi_{ij} = \overline{\eta}_{ji} \left[N^{-1}\right]$$

In the above expressions, the other four modes of influence coefficients are also presented - note the compatibility of the units at all the modes. Fig.11.4.2.2 shows the influence coefficients of mode 5), which are equal numerically to each other.
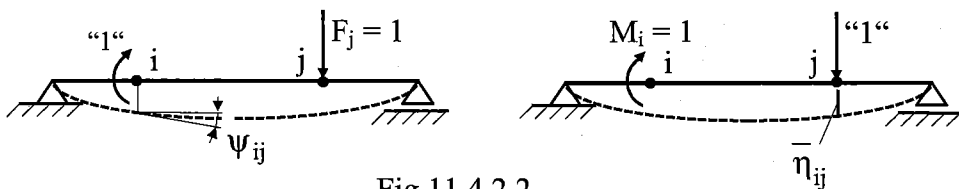

Fig.11.4.2.2

11.5 Examples

11.5.1 Model beam example with anti-symmetric distributed load.

Given: Load ... $w_0 = 5$ N/mm

Material ... $E = 2.1 \times 10^5$ MPa; $\sigma_{all} = 180$ N/mm^2

Dimension ... L= 1.5 m; h/b = 2 (rectangle)
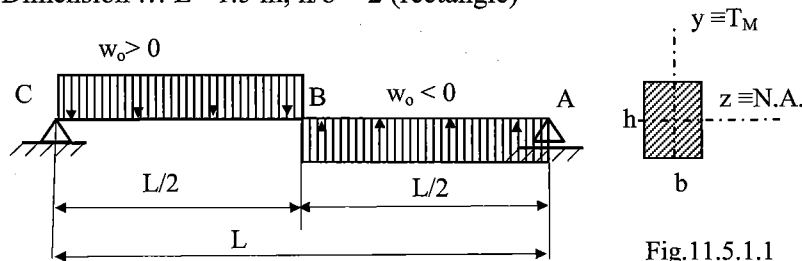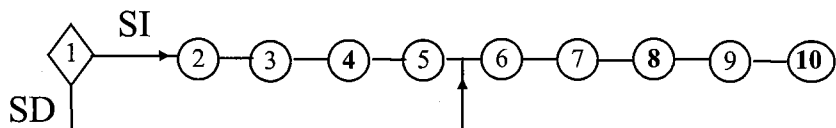
Fig.11.5.1.1

Task: Use the general flow diagram (Chap.3) for assessing all the important beam parameters

The first consideration:

Since having **two equilibrium eqs.** available for **two unknown reactions** (a plane system of parallel forces), the beam is **statically determinate (SD)** and we will start form the item 6.

Solution:
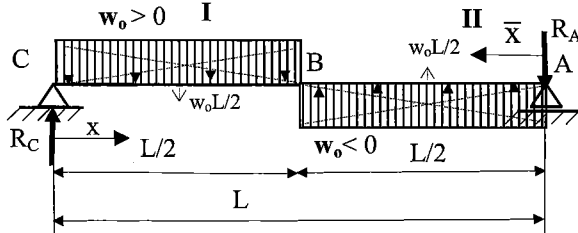
Fig.11.5.1.2

Reactions: (needed only when applying *the method of sections*)

Supposing the reaction senses (Fig.11.5.1.2) and then **applying** *two* *__moment equilibrium eqs.,__* we have:

$$M_C : R_A \cdot L - w_o \cdot \frac{L}{2} \cdot \frac{3L}{4} + w_o \cdot \frac{L}{2} \cdot \frac{L}{4} = 0 \Rightarrow R_A = w_o \cdot \frac{L}{4} = 5 \cdot \frac{1500}{4} = 1875 \quad [\text{N}] \quad > 0,$$

$R_A > 0$, i.e., <u>our supposition of the R_A sense was correct</u>

$$M_A : R_C \cdot L - w_o \cdot \frac{L}{2} \cdot \frac{3L}{4} + w_o \cdot \frac{L}{2} \cdot \frac{L}{4} = 0 \Rightarrow R_C = w_o \cdot \frac{L}{4} = 5 \cdot \frac{1500}{4} = 1875 \quad [\text{N}] \quad > 0,$$

$R_C > 0$, i.e., <u>our supposition of the R_C sense was correct</u>

Now we can apply __the force equilibrium eq. for checking:__ $R_C - R_A - w_o \cdot \dfrac{L}{2} + w_o \cdot \dfrac{L}{2} = 0$

i.e., the **reactions were computed correctly.**

Item 6: Shearing force $V(x)$, bending moment $M(x)$:

*1) Applying the **method of sections:***
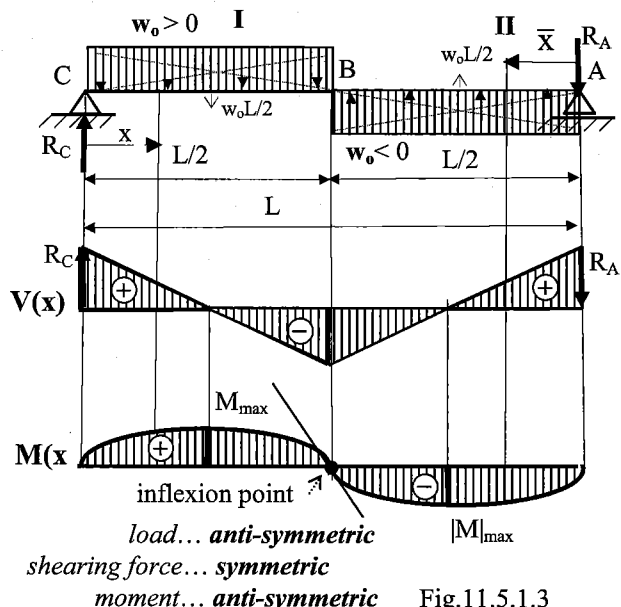
load... *anti-symmetric*
shearing force... *symmetric*
moment... *anti-symmetric*   Fig.11.5.1.3

Span I: $0 \le x \le L/2$ (from the left)

$V(x) = R_C - w_o x = w_o L/4 - w_o x$ [N]

$V(L/2) = w_o L/4 - w_o L/2 = - w_o L/4$ [N]

$M(x) = R_C x - w_o x \cdot x/2 = w_o L/4 \cdot x - w_o x^2/2$ [Nmm]

$M(L/2) = w_o L^2/8 - w_o L^2/8 = 0$ [Nmm]

$M_{max} = M(L/4) = w_o L/4 \cdot L/4 - w_o (L/4)^2/2 = $
$$= w_o L^2/32 \ [\text{Nmm}]$$

Span II: $0 \le \bar{x} \le L/2$ (from the right)

$V(\bar{x}) = R_A - w_o \bar{x} = w_o L/4 - w_o \bar{x}$ [N]

$V(L/2) = w_o L/4 - w_o L/2 = - w_o L/4$ [N]

$M(\bar{x}) = - R_A \bar{x} + w_o \bar{x} \cdot \bar{x}/2 = $
$$= - w_o L/4 \cdot \bar{x} + w_o \bar{x}^2/2 \ [\text{Nmm}] \ ;$$

$M(L/2) = w_o L^2/8 - w_o L^2/8 = 0$ [Nmm]

$|M|_{max} = M(L/4) = w_o L^2/32$ [Nmm]

*2) Applying the **relations between w, V and M:***

Span I: $0 \le x \le L/2$ (from the left): ;

$$-w(x) = \frac{dV}{dx} \Rightarrow V(x) = -\int w_o \cdot dx = -w_o \cdot x + C_1 ;$$

$$V(x) = \frac{dM}{dx} \Rightarrow M(x) = \int V(x) \cdot dx = \int (-w_o \cdot x + C_1) \cdot dx = -w_o \cdot \frac{x^2}{2} + C_1 \cdot x + C_2$$

Span II: $0 \le \bar{x} \le L/2$ (from the right)

$$w(\bar{x}) = \frac{dV}{d\bar{x}} \Rightarrow V(\bar{x}) = \int w_o \cdot d\bar{x} = w_o \cdot \bar{x} + C_3 ;$$

$$-V(\bar{x}) = \frac{dM}{d\bar{x}} \Rightarrow M(\bar{x}) = -\int V(\bar{x}) \cdot d\bar{x} = -\int (w_o \cdot \bar{x} + C_3) \cdot d\bar{x} = -w_o \cdot \frac{\bar{x}^2}{2} - C_3 \cdot \bar{x} + C_4$$

$(*)$

Static boundary conditions (SBC):

From the left: 1) $x = 0 : M(0) = 0 \Rightarrow 0 = -w_o \cdot \dfrac{0^2}{2} + C_1 \cdot 0 + C_2 \Rightarrow C_2 = 0$

From the right: 2) $\quad \overline{x} = 0 : M(0) = 0 \Rightarrow 0 = -w_o \cdot \dfrac{0^2}{2} - C_3 \cdot 0 + C_4 \Rightarrow C_4 = 0$

At the boundary position B: 3)
$$\begin{cases} x = \dfrac{L}{2} \text{ and } \quad \overline{x} = \dfrac{L}{2} \Rightarrow M\left(x = \dfrac{L}{2}\right) = M\left(\overline{x} = \dfrac{L}{2}\right) \Rightarrow \\ -w_o \cdot \dfrac{L^2}{2} + C_1 \cdot \dfrac{L}{2} = -w_o \cdot \dfrac{L^2}{2} - C_3 \cdot \dfrac{L}{2} \Rightarrow C_1 = -C_3 \end{cases}$$

4)
$$\begin{cases} x = \dfrac{L}{2} \text{ and } \quad \overline{x} = \dfrac{L}{2} \Rightarrow V\left(x = \dfrac{L}{2}\right) = V\left(\overline{x} = \dfrac{L}{2}\right) \Rightarrow \\ -w_o \cdot \dfrac{L}{2} + C_1 = w_o \cdot \dfrac{L}{2} + C_3 \Rightarrow C_1 - C_3 = 2 \cdot w_o \cdot \dfrac{L}{2} \Rightarrow \\ C_1 = -C_3 = w_o \cdot \dfrac{L}{2} \end{cases}$$

After substituting the integration constants assessed, we obtain the **concluding results** which coincide with those (*) computed by the *method of sections* (above).

Item 7: Bending (normal) stresses:

$$\sigma(x) = \frac{M(x)}{Z_b} = \frac{M(x)}{\dfrac{h^2 \cdot b}{6}} = \frac{3 \cdot M(x)}{b^3} \left[\frac{N \cdot mm}{mm^3} = N/mm^2\right]$$
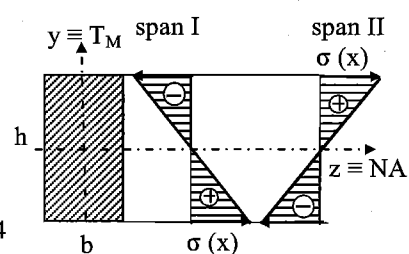
Fig.11.5.1.4

Item 8: Dimensioning

$$\sigma_{max} = \frac{M_{max}}{Z_b} = \frac{\dfrac{w_o \cdot L^2}{32}}{\dfrac{h^2 \cdot b}{6}} = \frac{3}{16} \cdot \frac{w_o \cdot L^2}{4b^3} \le \sigma_{all} \Rightarrow b \ge \sqrt[3]{\frac{3 \cdot w_o \cdot L^2}{64 \cdot \sigma_{all}}} = \sqrt[3]{\frac{3 \cdot 1.5 \cdot \left(1.5 \cdot 10^3\right)^2}{64 \cdot 180}} = 13.93[mm]$$
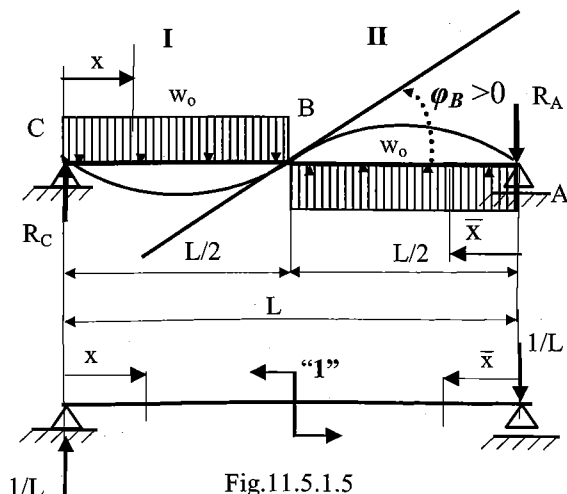
Based on this, chose next highest size: e.g., **b = 15 [mm], h = 2b = 30 [mm]**

Item 9: Checking

$$\sigma_{max} = \frac{3}{16} \cdot \frac{5 \cdot 1500^2}{4 \cdot 15^3} = 156[MPa] < \sigma_{all} = 180 \text{ [MPa], which is suitable.}$$

Item 10: Deformation by the Mohr's Integral (MI)

A specific task: Assess the tangent slope at the inflection point B (φ_B) using MI:


$$\varphi_B = \int\limits_{(L)} \frac{M(x)}{EI_z} \cdot m_B(x) \cdot dx$$

Span	I – from the left	II – from the right
$M(x)$	$w_o \cdot \dfrac{L}{4} \cdot x - w_o \cdot \dfrac{x^2}{2}$	$w_o \cdot \dfrac{\overline{x}^2}{2} - w_o \cdot \dfrac{L}{4} \cdot \overline{x}$
$m_B(x)$	$\dfrac{1}{L} \cdot x$	$-\dfrac{1}{L} \cdot \overline{x}$
boundar	$0 \le x \le L/2$	$0 \le \overline{x} \le L/2$

Fig.11.5.1.5

$$\varphi_B = \frac{1}{EI_z} \int_0^{L/2} M(x) \cdot m_B(x) \cdot dx + \frac{1}{EI_z} \int_0^{L/2} M(x) \cdot m_B(x) \cdot dx = \frac{2}{EI_z} \int_0^{L/2} \left(w_0 \cdot \frac{L}{4} \cdot x - \frac{w_0 \cdot x^2}{2} \right) \cdot \left(\frac{1}{L} \cdot x \right) \cdot dx =$$

$$= \frac{2}{EI_z} \int_0^{L/2} \left(w_0 \cdot \frac{x^2}{4} - \frac{w_0 \cdot x^3}{2L} \right) \cdot dx = \frac{w_0 \cdot L^3}{EI_z} \left[\frac{1}{2} \cdot \frac{1}{3} \cdot \left(\frac{x}{L} \right)^3 - \frac{1}{4} \cdot \left(\frac{x}{L} \right)^4 \right]_0^{L/2}$$

$$= \frac{1}{192} \cdot \frac{w_0 \cdot L^3}{EI_z} = \frac{1}{192} \cdot \frac{5 \cdot 1500^3}{2 \cdot 10^5 \cdot \dfrac{30^3 \cdot 15}{12}} = 0.0043[\text{rad}] = 0.249^\circ = 14'56''$$

Since $\varphi_B > 0$, it turns counterclockwise, as it was assumed by the unit "dummy couple".

11.5.2 Beam with a hinge

When a beam is designed with a hinge at a certain position, then the beam lacks here its ability to transfer *bending moments*, while the *shearing force* transfer is not interrupted (Fig.11.5.2.1).
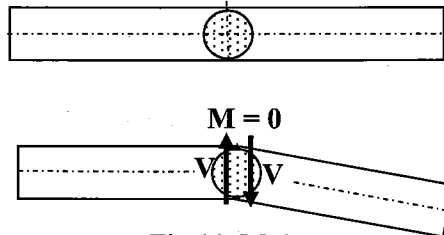
Fig.11.5.2.1

Assess the distribution of shearing forces $V(x)$ and bending moments $M(x)$ in the beam bellow.
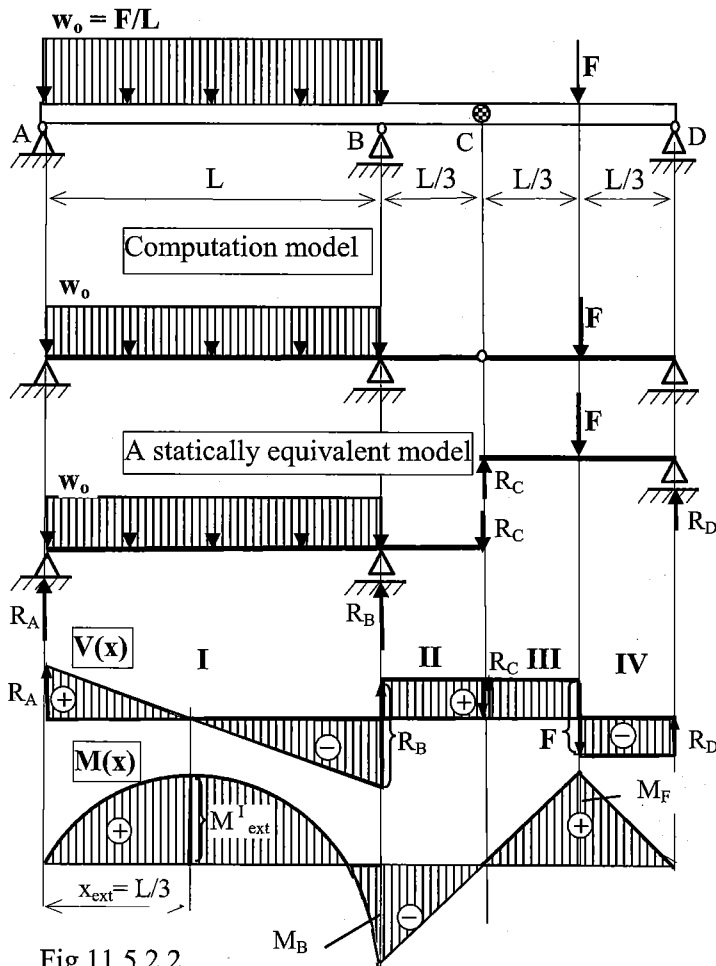
Fig.11.5.2.2

Solution:

It is necessary to start with the beam part (CD) which is situated between two hinges (here between the hinge C – the one in the beam – and the hinge D – the support hinge where the beam can be bent freely).

In this way, the reaction R_C of the part CD can be then applied as an action R_C to the part ABC.

Results:

$$R_A = \frac{1}{2} w_0 \cdot L - \frac{1}{6} F = \frac{1}{3} F;$$

$$R_B = \frac{1}{2} w_0 \cdot L + \frac{2}{3} F = \frac{7}{6} F;$$

$$R_C = R_D = \frac{1}{2} F$$

$$M^I_{\text{ext}} = \frac{1}{9} F \cdot L; \quad M_B = -\frac{1}{6} F \cdot L$$

$$M_F = \frac{1}{6} F \cdot L$$

Note:

This beam, having 3 supports, looks like to be SI 1°, but the hinge C decreases the degree of statical indeterminateness, i.e., this beam is SI 0° = SD.

Warning:

Generally, the position of hinges changes the beam SI degree.

Let us see the **originally SI 2° beam** where a certain number of hinges is added:
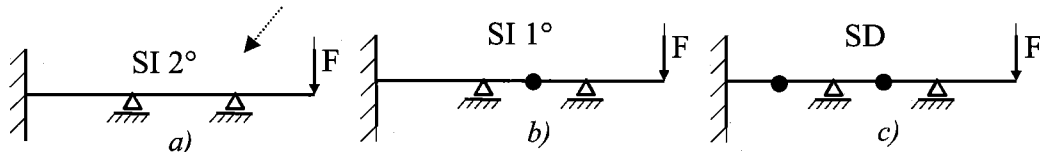
Fig.11.5.2.3

But not always the added hinges make the beam to become SD.

On the contrary, the hinges can even make the beam a mechanism (of several degrees of freedom).
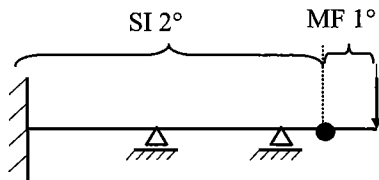
Fig.11.5.2.4

For instance, if one hinge is added into the overhanging part of the originally SI 2° beam (Fig.11.5.2.3a), this does not influence the SI degree of the whole beam. Its prevailing part remains SI 2°, while one part changes into a mechanism of one degree of freedom (MF 1°) (see Fig.11.5.2.4).

12. Statically indeterminate beams

If a beam loaded by transversal (vertically oriented) loads or by couples is supported with $n > 2$ static parameters (corresponding to n reactive forces), it is said to be *statically indeterminate to the (n-2) degree*.

12.1 General procedure for the solution of *SI* structures applied on beams

In Sec.3.2, we defined the procedure for solving *SI* structures. This was applied again in Sec.8.4, although in the first case we were dealing with the tension and compression of rods, and in the second case with the torsion of shafts. In a similar manner, we can apply the same items to the solution of *SI* beams. We will give an example and will proceed in various modes:

A beam of circular section (ϕd; $EI = const$), with an overhang, is clamped at A and supported by a roller support at B (Fig.12.1.1). Determine the deflection of the beam at the point of application of load F.
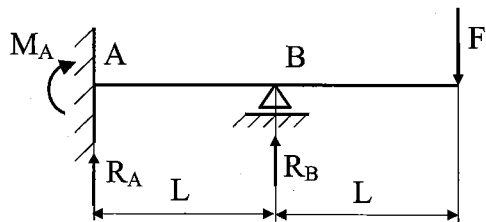

Fig.12.1.1

Solution: As we know from Sec.3.1, a displacement of an *SI* structure can be solved only after the corresponding *SI* forces (or couples) have been determined and the strength criterion has been applied (used for structure dimensioning).

The determination of *SI* forces (couples) will be performed in two modes:
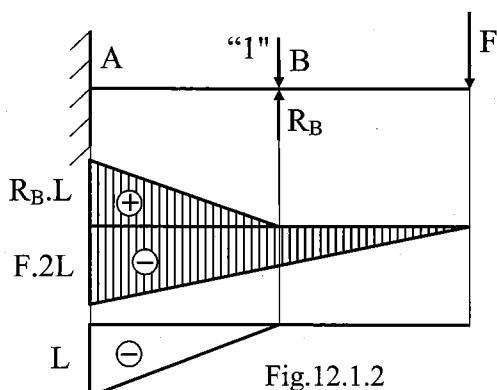
Fig.12.1.2

Mode I (Fig.12.1.2): The basic (*SD*) system will be obtained (in this case it will be a cantilever) when removing the roller support B and compensating it with *SI* force R_B. The *compatibility relation* (in combination with the corresponding *Verescagin constitutive relation*) is expressed for this basic system as follows (a *dummy unit force* is applied at B):

$$v_B = 0 = \frac{1}{EI} \cdot \sum A_{M;i} \cdot m_{C;i} \Rightarrow$$

$$0 = \left[R_B L \frac{L}{2}\left(-\frac{2}{3}L\right) + \left(-FL\frac{L}{2}\right)\cdot\left(-\frac{1}{3}L\right) + \left(-F2L\frac{L}{2}\right)\cdot\left(-\frac{2}{3}L\right) \right] \Rightarrow \quad R_B = \frac{5}{2}F$$

*Mode II* (Fig.12.1.3): The basic (*SD*) system will be obtained (in this case it will be a simple beam with an overhang) when removing the fixation *A* and compensating it with *SI* couple M_A. The *compatibility relation* (in combination with the corresponding *Verescagin constitutive relation*) is expressed for this basic system as follows (a *dummy unit couple* is applied at *A*):
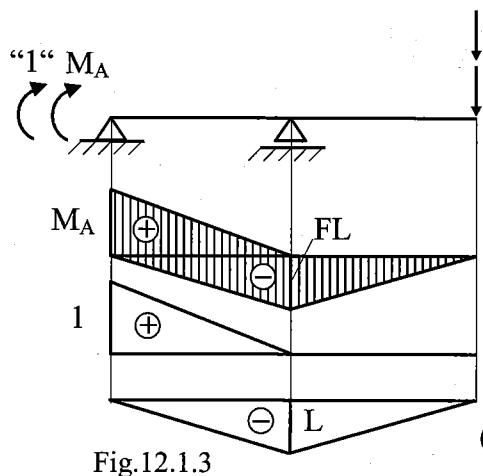
$$\varphi_A = 0 = \frac{1}{EI} \cdot \sum A_{M;i} \cdot m_{C;i} \quad \Rightarrow$$

$$0 = M_A \frac{L}{2} \cdot \frac{2}{3} + \left(-FL\frac{L}{2}\right) \cdot \frac{1}{3} \quad \Rightarrow \quad M_A = \frac{FL}{2}$$

Fig.12.1.3

We can easily prove that the two results correspond with each other by expressing the couple at the fixation *A* by substituting for R_B from the solution obtained in *Mode I*:

$$M_A = R_B \cdot L - F \cdot 2L = \frac{5}{2} F \cdot L - F \cdot 2L = \frac{FL}{2}$$

Now, to dimension the beam, we determine the *maximum bending moment*. It can be exerted at *A* or at *B*. The latter bending moment being $M_B = -F \cdot L$,

we write the <u>strength criterion</u> as follows:

$$\sigma_{max} = \frac{M_{max}}{Z} \leq \sigma_{all} \quad \Rightarrow \quad \sigma_{max} = \frac{|M_B|}{Z} = \frac{F \cdot L}{\frac{\pi \cdot d^3}{32}} \leq \sigma_{all}$$

From this we can determine either dimension ⌀*d* or allowable load *F*. Finally, utilizing Fig.12.1.3 and adding another *dummy unit load* at point *F* (where *F* is applied), we can determine the required deflection

$$v_F = \frac{1}{EI} \cdot \left[2 \cdot \left(-FL\frac{L}{2}\right) \cdot \left(-\frac{2}{3}L\right) + M_A \frac{L}{2} \cdot \left(-\frac{1}{3}L\right)\right] = \frac{7}{12} \cdot \frac{FL^3}{E \cdot \frac{\pi \cdot d^4}{64}}$$

Note: Beams that have more than one span and that are continuous through their lengths are known as **continuous beams.** It is usually advantageous to select the bending moments at the intermediate supports as redundant. This choice simplifies the calculations because it leads to a set of simultaneous equations in which no more than three unknowns appear in any one equation, regardless of the number of redundant intermediate supports. Because of this fact, this variation of the method of superposition is known as the *method of three moments.* (Another advantage of this method is that the deflection calculations are simpler because only simple beams are involved.) The *method of three moments* will be discussed at lectures and seminars.

12.2 Examples

12.2.1 Complete solution of a SI beam.

A beam with four supports, loaded with a concentrated force F and a distributed load w_o (Fig.12.2.1.1), is to be solved by the general flow diagram (see Chap.3).
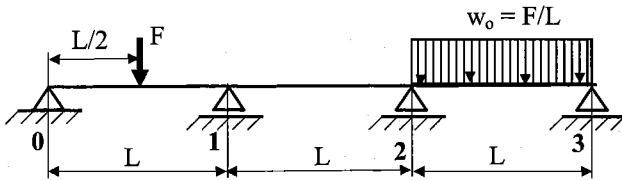
Item 1:

For four unknowns, there are two equilibrium eqs. available, i.e., the beam is SI $2°$ and thus two static parameters shall be removed to obtain **a basic SD system.**

Fig.12.2.1.1

Item 2:

Now there is a question how such a basic SD system can be obtained. Generally, three essential releasing modes exist.

*Mode 1 – by **removing two supports**, here the middle ones, and **substituting them** with the **SI forces** $R_{1,2}$ (this mode is usually a first idea of students), while the forces $R_{0,3}$ being reactions:*

(**Item 3:** The equilibrium eqs. - needed for assessing all the reactions - will be different for all the modes and can be applied after assessing the SI forces/moments)
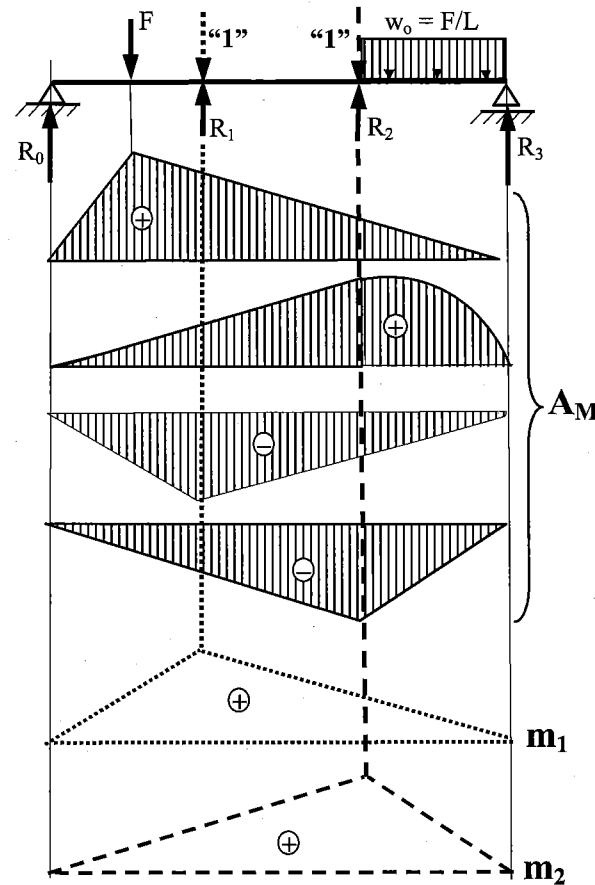
Item 4 (depending on the releasing mode applied) leads to the **compatibility eqs:**
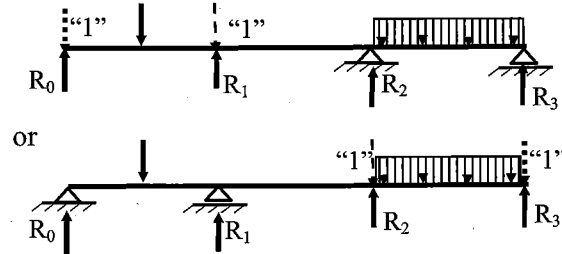
$$v_1 = 0 = \frac{1}{EI}\sum_{i=1}^{n} A_{Mi} \cdot m_{1Ci}$$

$$v_2 = 0 = \frac{1}{EI}\sum_{j=1}^{n} A_{Mj} \cdot m_{2Cj}$$

(Vertical lines, denoting the breaks of the respective *unit dummy loads*, are cutting the respective moment areas A_M into a number of partial areas A_{Mi}, which are very difficult to compute with. So you can see that such *a mode I* would be very much time-consuming).

Note:

A better approach is obtained when two **side supports** are removed, i.e., $R_{0,1}$ or $R_{2,3}$ become the SI forces. Such a task is recommendable for individual study.

Fig.12.2.1.2

Mode 2 – by <u>cutting</u> the beam through the supports on the <u>three SD simply supported beam parts</u> and <u>connecting</u> these parts with the so-called <u>support bending moments $M_{1,2}$</u>
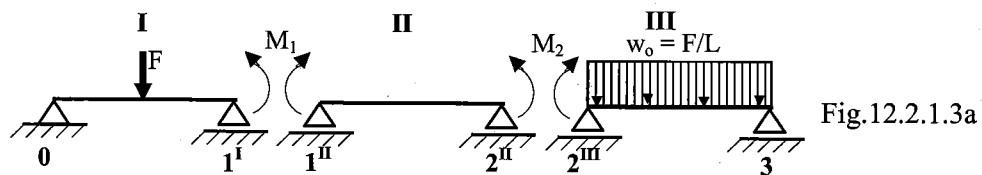

Fig.12.2.1.3a

Item 4: Compatibility equations easily follow from comparing the support tangent angles (Fig.12.2.1.3b):

$$\varphi_1^I = -\varphi_1^{II}; \quad \varphi_2^{II} = -\varphi_2^{III}$$

(Mind the negative signs at the right side of the equations, which is clear when comparing Fig.12.2.1.3b and Fig.12.2.1.3c)
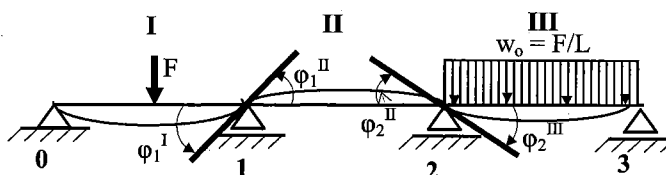

Fig.12.2.1.3b

**Item 5:** <u>Verescagin Rule</u> is recommended as **the constitutive relations** (Fig.12.2.1.3c)
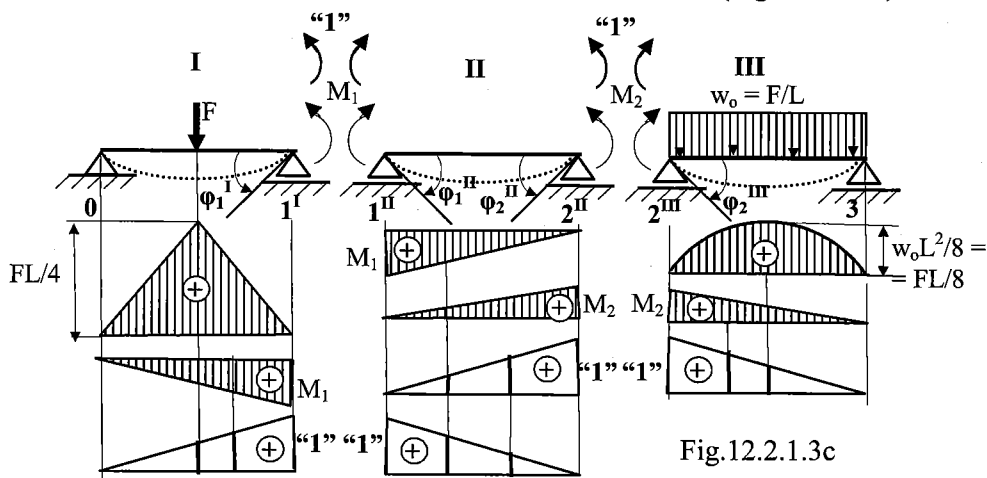
Fig.12.2.1.3c

$$\varphi_1^I = \frac{1}{EI}\left[\left(\frac{FL}{4}\cdot L\cdot\frac{1}{2}\right)\cdot\frac{1}{2}+\left(M_1\cdot L\cdot\frac{1}{2}\right)\cdot\frac{2}{3}\right]; \quad \varphi_1^{II} = \frac{1}{EI}\left[\left(M_1\cdot L\cdot\frac{1}{2}\right)\cdot\frac{2}{3}+\left(M_2\cdot L\cdot\frac{1}{2}\right)\cdot\frac{1}{3}\right];$$

$$\varphi_2^{II} = \frac{1}{EI}\left[\left(M_1\cdot L\cdot\frac{1}{2}\right)\cdot\frac{1}{3}+\left(M_2\cdot L\cdot\frac{1}{2}\right)\cdot\frac{2}{3}\right];$$

$$\varphi_2^{III} = \frac{1}{EI}\left[\left(M_2\cdot L\cdot\frac{1}{2}\right)\cdot\frac{2}{3}+\left(\frac{w_0 L^2}{8}\cdot L\cdot\frac{2}{3}\right)\cdot\frac{1}{2}\right]$$

After substituting into the **compatibility equations** and rearranging, these relations yield:

$$M_1 = -\frac{FL}{12}; \quad M_2 = -\frac{FL}{24}$$

**Item 6: M(x), i.e.,** the bending moment distribution.
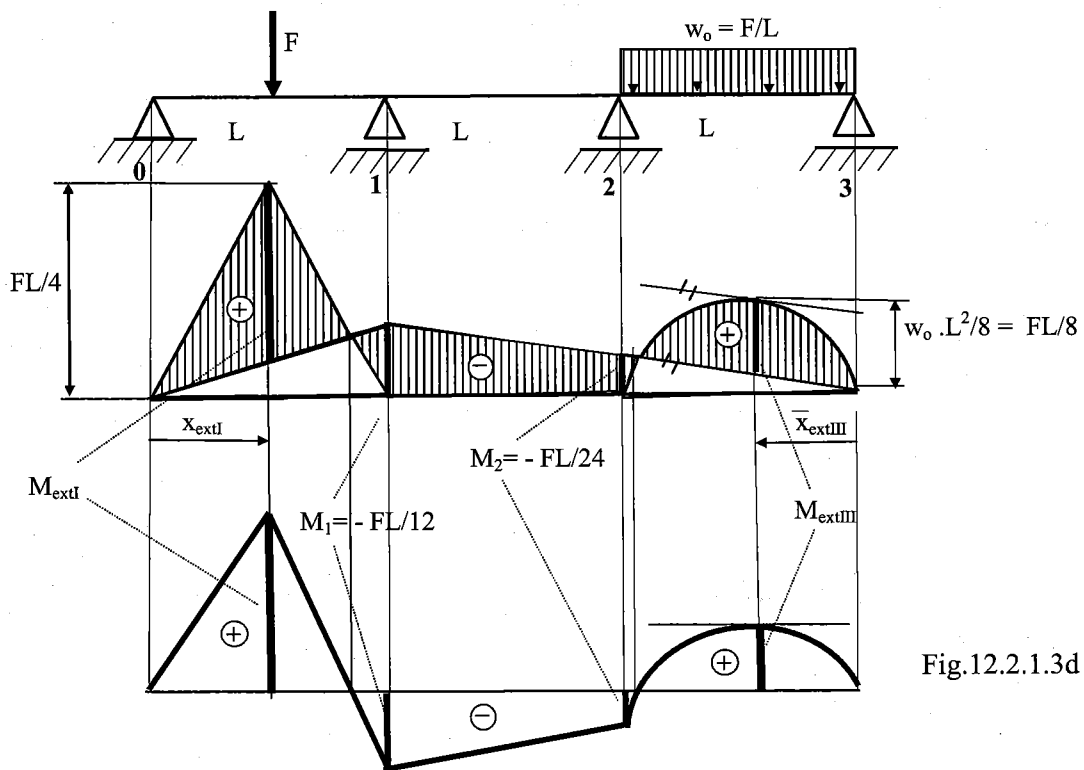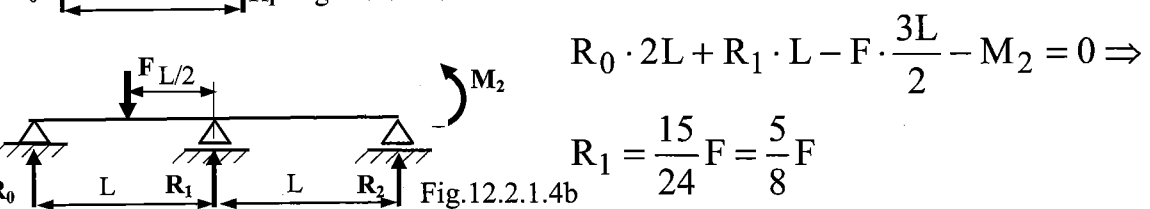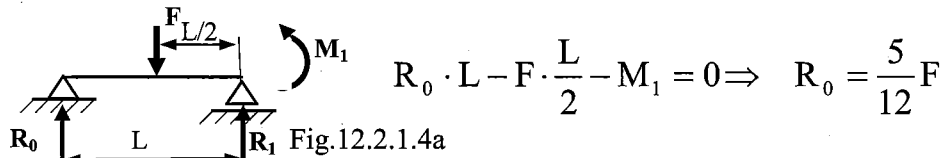
Fig.12.2.1.3d

Computing reactions:

α) If all the reactions are needed:

$$R_0 \cdot L - F \cdot \frac{L}{2} - M_1 = 0 \Rightarrow \quad R_0 = \frac{5}{12}F$$

Fig.12.2.1.4a

$$R_0 \cdot 2L + R_1 \cdot L - F \cdot \frac{3L}{2} - M_2 = 0 \Rightarrow$$

$$R_1 = \frac{15}{24}F = \frac{5}{8}F$$

Fig.12.2.1.4b

When applying Fig.12.2.1.2, we obtain

$$R_0 \cdot 3L + R_1 \cdot 2L + R_2 \cdot L - F \cdot \frac{5L}{2} - w_0 \cdot \frac{L^2}{2} = 0 \Rightarrow \quad R_2 = \frac{12}{24}F = \frac{F}{2}$$

The last reaction R_3 can be assessed span from the last span:

Fig.12.2.1.4c

$$R_3 \cdot L - \frac{w_0 L^2}{2} - M_2 = R_3 \cdot L - \frac{FL}{2} - M_2 = 0 \Rightarrow \quad R_3 = \frac{11}{24} \cdot w_0 L = \frac{11}{24}F$$
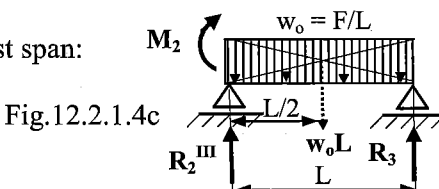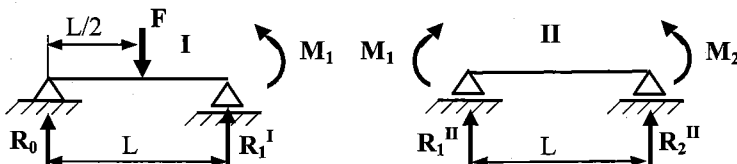
Checking: <u>Equilibrium equation of forces in the vertical direction is satisfied:</u>

$$F + w_0 \cdot L - R_0 - R_1 - R_2 - R_3 = 2F - \frac{5}{12}F - \frac{5}{8}F - \frac{1}{2}F - \frac{11}{24}F =$$

$$= F \cdot \frac{48 - 10 - 15 - 12 - 11}{24} = 0$$

β) If <u>only a middle reaction</u> is needed, e.g., R_1:

$$R_1^I \cdot L - F \cdot \frac{L}{2} + M_1 = 0 \Rightarrow \quad R_1^I = \frac{7}{12}F; \quad R_1^{II} \cdot L + M_1 - M_2 = 0 \Rightarrow \quad R_1^{II} = \frac{1}{24}F$$

$$R_1 = R_1^I + R_1^{II} = \frac{7}{12}F + \frac{1}{24}F = \frac{14}{24}F + \frac{1}{24}F = \frac{15}{24}F = \frac{5}{8}F \ \dots\text{resulting } R_1$$

Item 8: Dimensioning

Extreme bending moments can be assessed using Fig.12.2.1.3d, Fig.12.2.1.4a and Fig.12.2.1.4d:

In <u>the span I</u>, based on Fig.12.2.1.4a, we compute:
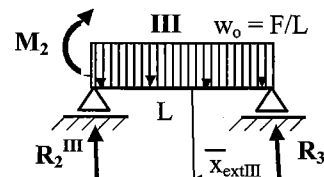
$$M_{extI} = R_0 \cdot \frac{L}{2} = \frac{5}{12}F \cdot \frac{L}{2} = \frac{5}{24}FL = 0.21FL$$

In <u>the span III</u>, we have to determine first the **extreme position** $\overline{x}_{extIII}$ according <u>the relation</u>

$V(\overline{x}) = dM/d\overline{x}$. Then M_{ext3} is at the position where $V(\overline{x}_{extIII}) = 0$.

Using Fig.12.2.1.4d we have:

$$V(\overline{x}_{extIII}) = R_3 - w_0 \cdot \overline{x}_{extIII} = 0 \Rightarrow$$

$$\overline{x}_{extIII} = \frac{R_3}{w_0} = \frac{11}{24} \cdot w_0 L / w_0 = \frac{11}{24}L$$

$$M_{extIII} = R_3 \cdot x_{extIII} - \frac{w_0 \overline{x}_{extIII}^2}{2} = \frac{11}{24}w_0 L \cdot \frac{11}{24}L - \frac{w_0\left(\frac{11}{24}L\right)^2}{2} = \quad \text{Fig.12.2.1.4d}$$

$$= \frac{121}{1152}w_0 L^2 = \frac{121}{1152}FL = 0.105 \cdot FL$$

Comparing M_{extI} with M_{extIII}, we conclude that: $\quad M_{max} = M_{extI} = 0.21 \cdot FL$

and then the **strength criterion** is: $\quad M_{max} = 0.21 \cdot FL \le Z_b \cdot \sigma_{all}$

from which i) either <u>*the necessary dimension*</u> (hidden in modulus in bending Z_b),

ii) or <u>*the allowable load F_{all}*</u> can be assessed.

Item 9: Checking is applied with numerically solved examples.

Item 10: Deformation

For instance, the beam deflection v_F (at the force F position) is to be assessed.
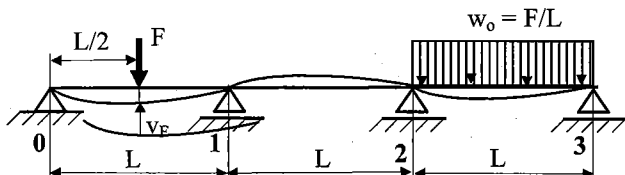

Fig.12.2.1.5a

This operation is not necessary to perform with the SI task, but with a basic SD system.

We showed **four** basic SD systems in the **Item 2**. When comparing them from the point of deflection assessment, it is even more clear how disadvantageous would be to apply the releasing modes with removing two supports, e.g., see Fig.12.2.1.2, and then compute deflections dealing with the whole beam of those three spans.

The deflection v_F assessment will be very easy, when applying the releasing mode 2, where only the span 1 is necessary for this task. For this purpose we utilize Fig.12.2.1.4a and apply the respective unit "dummy load": "1"
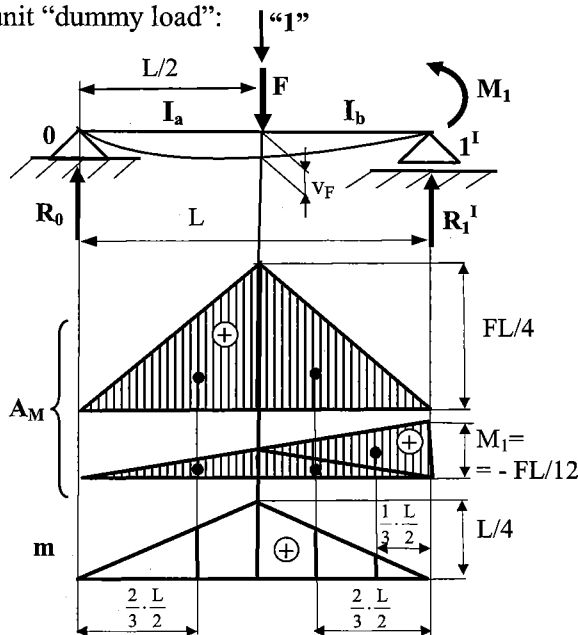

Fig.12.2.1.5b

Since the moment shapes are simple, we use

Verescagin rule (VR): $v_F = \dfrac{1}{EI} \cdot \sum_{j=1}^{n} A_{M;j} \cdot m_{F;C;j}$

(Important note:
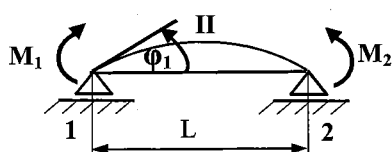
Before starting *VR*, we look for a possible **break** in the *m(x)* course. If **that** is found, all the *M(x)* courses is to be divided at this position.)

$$v_F = \frac{1}{EI} \cdot \left[\left(\frac{FL}{4} \cdot \frac{L}{2} \cdot \frac{1}{2} \right) \cdot \left(\frac{2}{3} \cdot \frac{L}{4} \right) \cdot 2 + \right.$$

$$\left. + \left(\frac{M_1}{2} \cdot \frac{L}{2} \cdot \frac{1}{2} \right) \cdot \left(\frac{2}{3} \cdot \frac{L}{4} \right) \cdot 2 + \left(M_1 \cdot \frac{L}{2} \cdot \frac{1}{2} \right) \cdot \left(\frac{1}{3} \cdot \frac{L}{4} \right) \right] \Rightarrow$$

$$v_F = \frac{1}{EI} \cdot \left[\frac{FL^3}{48} + M_1 \cdot \frac{L^2}{16} \right] = \frac{1}{EI} \cdot \left[\frac{FL^3}{48} + \left(-\frac{FL}{12} \right) \cdot \frac{L^2}{16} \right] = \frac{3}{192} \cdot \frac{FL^3}{EI} > 0$$

(i.e., downwards as the unit dummy load pointing)

Task: Assess the beam tangent slope at the support 1 (φ_1) as individual study. The simplest solution is when using the span II:

Result:

$$|\varphi_1| = \frac{5}{144} \cdot \frac{FL^2}{EI}$$

13. Combined loading

13.1 Introduction

The objective of analysing combined loadings is to determine the largest stresses anywhere in the structure. To do this, critical points should be selected at cross-sections where the stress resultants have their largest values. Furthermore, within these cross-sections, points should be selected where normal stresses and/or shearing stresses have their largest values. By using good judgment in selecting the points, we often can be reasonably certain of obtaining the absolute maximum stresses in the structure. However, it is sometimes difficult to recognize in advance where the maximum stresses in the member are to be found. Then it may be necessary to investigate the stresses at a large number of points, perhaps even using trial-and-error in the selection of points. Other strategies may also prove fruitful - such as deriving equations specific to the problem at hand or making simplifying assumptions to facilitate an otherwise difficult analysis.

13.2 Unsymmetric bending

Our analysis of both pure and ordinary bending has been limited so far to members possessing at least one plane of symmetry and subjected to couples acting in that plane. Because of the symmetry of such members, and of their loadings, we conclude that the members will remain symmetric with respect to the plane of couples, and will thus bend in that plane, i.e., *plane bending* will take place. In other words: *NA* (neutral axis) is perpendicular to T_M (track of the acting moment). Strictly speaking, we have assumed couples acting in a plane which intersects the cross-sectional plane in the track T_M coinciding with one of the centroidal principal axes of the cross-section. Consequently, *NA* of this bending coincides with the other centroidal principal axis.

We shall now consider situations where bending couples do **not** act in a plane of symmetry of the member, either because they act in a different plane, or because the member does not possess any plane of symmetry. In such situations, we cannot assume that the member will still bend in the plane of the couples, i.e., *unsymmetric bending,* or more generally, *spatial* or *oblique bending* takes place (its deflection curve is a spatial curve). Such tasks of combined stress are *1D - tasks.*

Unsymmetric bending can be solved as a combined load of two plane bendings. Let us assume that the *yz* axes of the cross-section in Fig.13.2.1 are the principal axes. The bending moment vector *M* (being perpendicular to the plane in which it is exerted) will be decomposed into

$$M_y = M \cdot \sin\alpha; \qquad M_z = M \cdot \cos\alpha$$
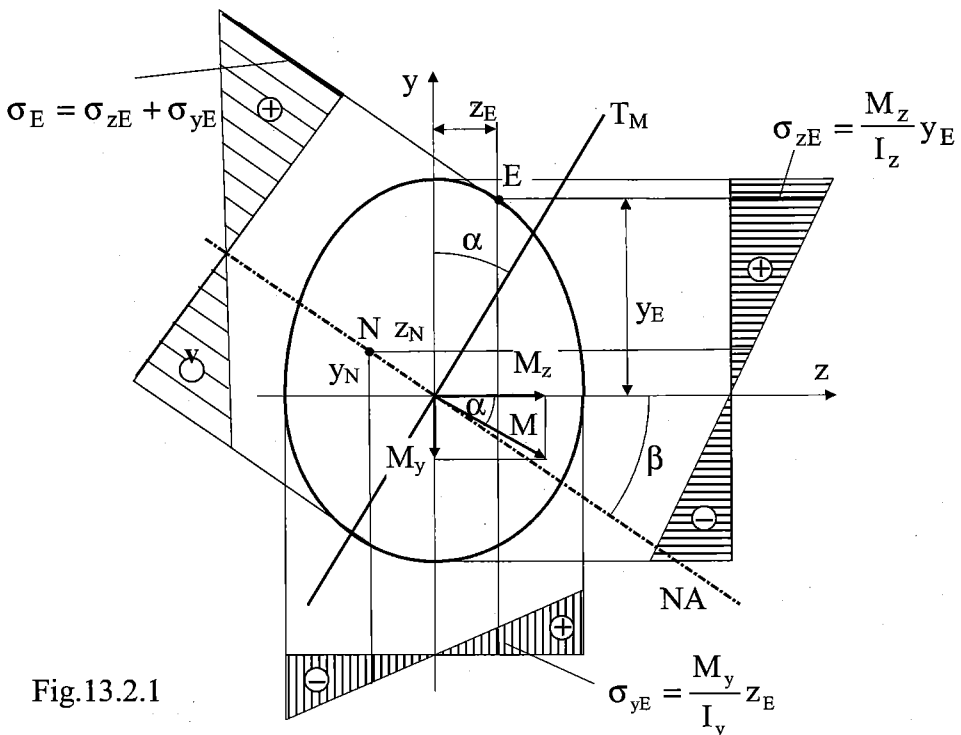
Fig.13.2.1

We shall first determine the position of NA. Assuming that point $N(y_N, z_N)$ lies on NA, the resulting stress at N must be equal to zero, i.e.,

$$\sigma_N = \frac{M_y}{I_y} \cdot z_N + \frac{M_z}{I_z} \cdot y_N = M \cdot \left[\frac{\sin\alpha}{I_y} \cdot z_N + \frac{\cos\alpha}{I_z} \cdot y_N\right] = 0$$

which yields

$$\frac{y_N}{z_N} = -\frac{I_z}{I_y}\,\text{tg}\alpha \qquad (13.2.1a)$$

This relation can be rewritten as

$$\frac{\text{tg}\beta}{\text{tg}\alpha} = \frac{I_z}{I_y} \qquad (13.2.1b)$$

and interpreted as follows:

When angle α is measured from principal axis y to T_M (the track of the exerted couple) then angle β is measured from principal axis z to NA (the neutral axis of the combination) in the same sense.

The maximum stress of the unsymmetric bending occurs at point E, which has the maximum distance from NA, and, observing that we are dealing with **uniaxial stress**, the *strength criterion* is expressed as

$$\sigma_{max} = M_{max} \cdot \left[\frac{\sin\alpha}{I_y} \cdot z_E + \frac{\cos\alpha}{I_z} \cdot y_E\right] \leq \sigma_{all}, \qquad (13.2.2)$$

where M_{max} indicates that, in addition to the maximally stressed cross-sectional point E, we must find that cross-section of the investigated beam at which the maximum bending moment is acting.

Conclusion: This stress combination deals with all types of beam profile

Example 13.2.1
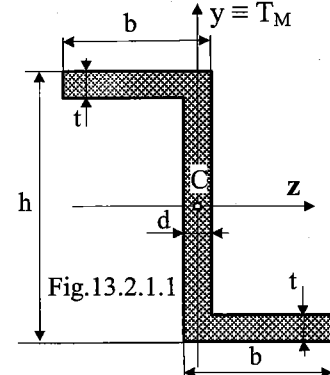
Given: Z 10 section, where the vertical axis y coincides with the track of moments T_M, i.e., $y \equiv T_M$.

Size:
$h = 100$ mm
$b = 55$ mm
$d = 6.5$ mm
$t = 8$ mm

Material:
$E = 2.1 \cdot 10^5 \text{ N/mm}^2$

$\sigma_{all} = 120 \text{N/mm}^2$

Fig.13.2.1.1

Task: Find out the allowable bending moment M_{all} the profile can bear.

Step by step solution:

1) a) Assessing the principal second moments of area I_1 and I_2 and the position (ϑ) of the principal axes *1(max)* and *2(min)*, cf. Example 9.5.1.

Results: $I_1 = 27.0 \times 10^5 \text{ mm}^4$, $I_2 = 2.4 \times 10^5 \text{ mm}^4$, $\text{tg}\vartheta = 0.492 \rightarrow \vartheta = 26.2° = \alpha$

b) Decomposing given couple M (exerted in the vertical plane and intersecting the cross-section in the moment track $y \equiv T_M$ – which is not a principal axis and thus an unsymmetric bending arises) into two plane bending components:

$M_1 = M \cos \alpha$ (exerted in the plane going through the principal axis *2* and having its neutral axis

$- NA_1$ - in the principal axis *1*)

$M_2 = M \sin \alpha$ (exerted in the plane going through the principal axis *1* and having tits neutral axis

$- NA_2$ - in the principal axis *2*)
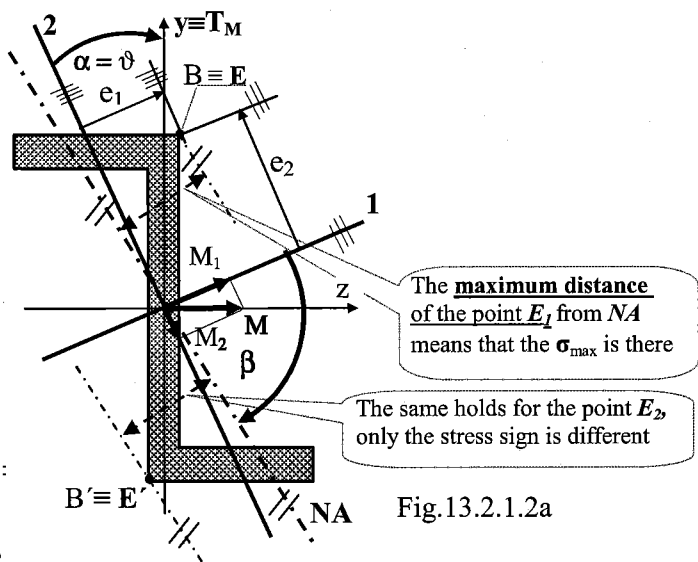
2) a) Assessing the **NA position** of **unsymmetric** bending by using **Eq.13.2.1.2b**.

$$\frac{\text{tg}\beta}{\text{tg}\alpha} = \frac{I_1}{I_2} \Rightarrow \text{tg}\beta = 5.55$$

b) Assessing the maximum stress position $E(E')$ as maximum distance from *NA* (Fig.13.2.1.2a)

c) Assessing the allowable bending moment to be borne by the profile

$$\sigma_{max} = \sigma_{1E} + \sigma_{2E} =$$

$$= \frac{M_1}{I_1} e_2 + \frac{M_2}{I_2} e_1 =$$

$$= M \left[\frac{\cos \alpha}{I_1} e_2 + \frac{\sin \alpha}{I_2} e_1 \right] \leq \sigma_{all} :$$

$$M_{all} \approx 1.9 \cdot 10^6 \text{Nmm} = 1.9 [\text{kNm}]$$

The **maximum distance of the point E_1** from *NA* means that the σ_{max} is there

The same holds for the point E_2, only the stress sign is different

Fig.13.2.1.2a

c) <u>Geometrical assessment of the unsymmetric</u>
<u>bending *NA*</u>

For this purpose we draw the stress distribution the two plane bendings in scale (<u>this supposes to draw the solved profile in scale</u> <u>from the start</u>):

$$\frac{\sigma_{1A}}{\sigma_{2B}} = \frac{M \cdot \dfrac{\cos \alpha}{I_1} a_2}{M \cdot \dfrac{\sin \alpha}{I_2} b_1} = 0.48$$

Ratios measured from Fig.13.2.1.2*b* are

$$\frac{a_2}{b_1} = 2.67 \text{ and } \frac{e_1}{e_2} = 0.59$$

Fig.13.2.1.2b

Then $\dfrac{e_2}{\dfrac{h}{2}} \approx \cos \alpha \Rightarrow e_2 \approx \dfrac{h}{2} \cdot \cos \alpha = \dfrac{100}{2} \cdot \cos 26.2° = 44.9 [\text{mm}]$

These relations yield: $e_1 \approx 44.9 \cdot 0.59 = 26.5 = [\text{mm}]$

When comparing Figs.13.2.1.2a,b, it is clear that points E, E′ coincide with B, B′, which can be used for the geometrical checking of the maximum stress: $\sigma_{max} = \sigma_{1E} + \sigma_{2E} = \sigma_{1B} + \sigma_{2B}$

**The more precise drawing, the more precise results.**

13.3 Bars with axial loads

Structural members are often subjected to the simultaneous action of bending loads and axial loads. This happens, for instance, when a beam is loaded with a force having a different angle than 90° with respect to the beam axis. In such a case, besides *shear force V* and *bending moment M, normal force N* is exerted in the cross-section of the beam.

Another load developing a simultaneous *bending moment M* and *normal force N* action in the cross-section of a bar (but without *shear force V*) is an **eccentric axial load**, which is an axial load (normal with respect to the cross-section) that does **not** act through the centroid of the cross-section. An example is shown in Fig.13.3.1, where the bar is subjected to a tensile load *N* acting on the *z* axis (which is the axis of symmetry) at distance *e* from the *x* axis (the *x* axis passes through the centroids of the cross-sections). The distance *e* is called the *eccentricity* of the load.

Fig.13.3.2

a)   Fig.13.3.1   b)   Fig.13.3.3
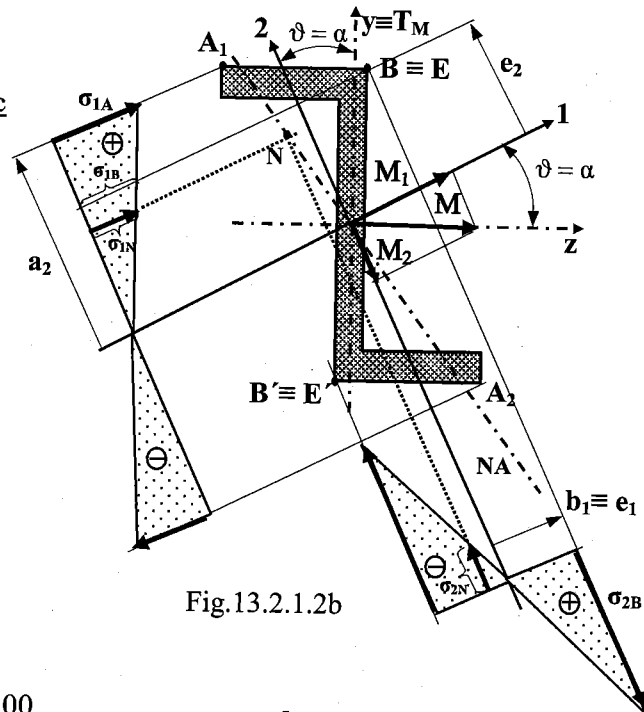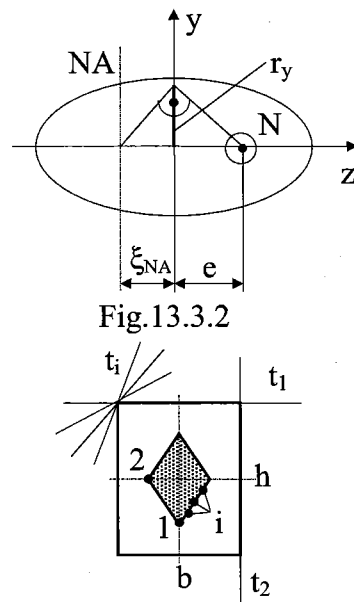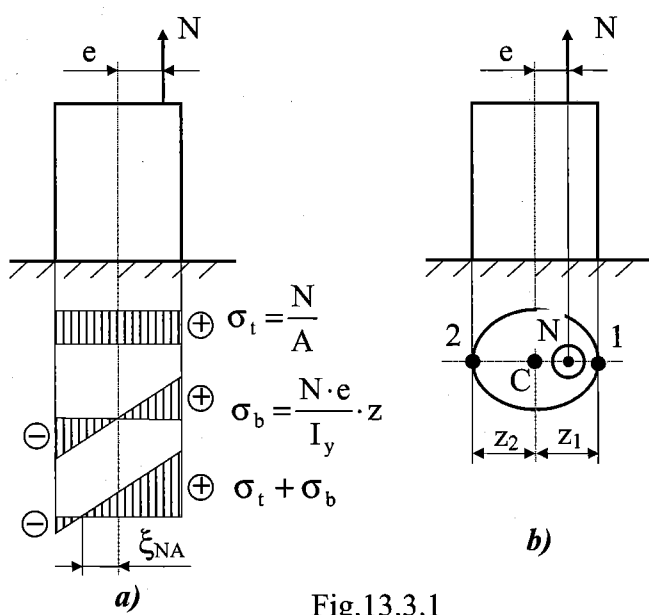
The eccentric load N is statically equivalent to a *normal force* N acting along the x axis and a *bending moment* $M = N.e.$, both being constant along the x axis. The normal stress at any point in the bar is (Fig.13.3.1a)

$$\sigma = \sigma_t + \sigma_b = \frac{N}{A} + \frac{N \cdot e}{I_y} \cdot z \qquad (13.3.1)$$

The extreme stresses are in the extreme fibers *1* and *2* (see Fig.13.3.1b, where distances z_1 and z_2 are considered absolute values)

$$\sigma_1 = \frac{N}{A} + \frac{N \cdot e}{I_y} \cdot z_1 \qquad \text{and} \qquad \sigma_2 = \frac{N}{A} - \frac{N \cdot e}{I_y} \cdot z_2 \qquad (13.3.2)$$

This problem, being a problem of **uniaxial stress state**, has the *strength criteria* holding for **ductile** and **brittle** materials, respectively,

$$\max\left(|\sigma_1|;|\sigma_2|\right) \leq \sigma_{all} \qquad \text{and} \qquad |\sigma_1| \wedge |\sigma_2| \leq \sigma_{all;t} \wedge \sigma_{all;c} \qquad (13.3.3)$$

The position of NA (the neutral axis of the combination) can be obtained from Eq.(13.3.1) by setting the stress σ equal to zero and solving for the coordinate z, which we now denote as ξ_{NA}. Expressing the second moment of area I_y by the radius of area r_y according to Eq.(9.2.2a), the result is

$$\sigma_{NA} = 0 = \frac{N}{A} + \frac{N \cdot e}{A \cdot r_y^2} \cdot \xi_{NA} = \frac{N}{A}\left(1 + \frac{\xi_{NA}}{\frac{r_y^2}{e}}\right) \qquad \Rightarrow \qquad \xi_{NA} = -\frac{r_y^2}{e} \qquad (13.3.4)$$

The negative sign means that NA lies at the side opposite (with respect to the coordinate origin) to that at which load N is applied. Eq. (13.3.4) can be geometrically interpreted by means of *Euclid's theorem*, as shown in Fig.(13.3.2).

If the load point $N(e_y, e_z)$ does not lie on one of the centroidal principal axes we obtain the **triple combined load**: *tension (compression)* and **unsymmetric bending** *(i.e., plane bending + plane bending)*, and we solve such problems by combining procedures from Secs.13.2 and 13.3. Analogously to Eq. (13.3.4) <u>the position of NA of this combination</u> is then given by two intercepts (η_{NA}, ξ_{NA}) of the two **principal** axes $y \equiv 2$, $z \equiv 1$, respectively:

$$\eta_{NA} = -\frac{r_z^2}{e_y} \qquad\qquad \xi_{NA} = -\frac{r_y^2}{e_z} \qquad (13.3.5a,b)$$

From Eqs.(13.3.4) and (13.3.5a,b), respectively, we see that the eccentricity e_y, e_z is reduced, the distances η_{NA}, ξ_{NA} increase and NA moves away from the centroid. In the limit, as e_y, e_z approach zero, the load acts at the centroid, NA is at an infinite distance, and the stress distribution is uniform. If the eccentricity is increased, the distances η_{NA}, ξ_{NA} decrease and NA moves toward the centroid. In the limit, as e_y, e_z become extremely large, the load acts at an infinite distance, NA passes through the centroid, and the stress distribution is the same as in pure bending.

The **core of a cross-section (CCS)**: If the axial load is applied with a small eccentricity, NA may lie outside the beam. When that happens, the normal stresses will have the same sign throughout the cross-section, and the bar will be entirely in tension or entirely in compression. This condition is important, for instance, when a compressive load acts on a material that is very weak in tension, such as concrete, stone, or ceramics. <u>With such materials we must be sure that the load produces only compression on the cross-sections; and this will be accomplished only when loads will act</u> **inside, or at the boundaries,** of the so-called **core of the cross-section**. How to define CCS: imagining that NA can at most be tangent to a given cross-section, we try all possibilities and from each attempt we obtain the respective coordinates η_{NA}, ξ_{NA}, and Eqs.(13.3.5a,b) will subsequently yield the looked-for coordinates e_y, e_z of CCS. (As an example, CCS is constructed for a rectangular cross-section in Fig.13.3.3, where points *1* and *2* of the core correspond to tangents t_1 and t_2 to the rectangle, respectively, and the points *i* on the right bottom abscissa of the core correspond to the bundle of vertex tangents t_i to the left upper corner of the rectangle).

Conclusion: This stress combination deals with <u>all types of beam profile</u>

13.4 Bending and torsion

Recalling Chap.8, we acknowledge that shafts are important machine members, which for instance transfer, by means of <u>torsion,</u> the power from the engine to the wheels of cars, etc. Unfortunately, torsion is almost always accompanied by <u>bending</u>. From that standpoint, we can consider <u>bending as a parasite</u> which deteriorates the resulting effect.

Fig.13.4.1*a* shows a cross-section of a shaft, subjected to simultaneous bending and torsion. The maximum bending stresses are at fibers *C* and *D* (cf. Sec.10.3: Eqs.(10.3.5a,b) and (10.3.6)) and the maximum shearing stresses (produced by torsion) are exerted in the cross-section circumference

(cf. Sec.8.1.3: Eqs.8.1.3.5*a,b*). It follows from this that the maximum stresses of the combined load are at fibers *C* and *D*.
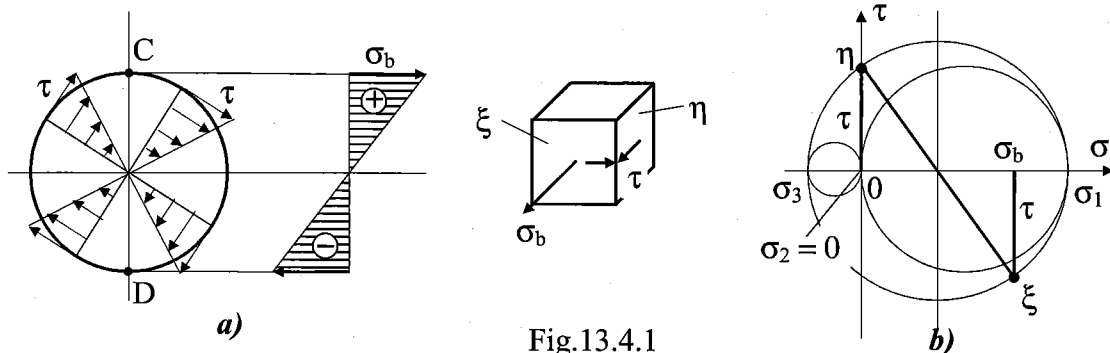

Fig.13.4.1

Taking an element from these maximally stressed fibers, we observe that we are dealing with a **plane** stress state for which we will find, by means of *Mohr's circle*, principal stresses as follows (Fig.13.4.1*b*):

$$\sigma_{1,3} = \frac{\sigma_b}{2} \pm \sqrt{\left(\frac{\sigma_b}{2}\right)^2 + \tau^2}; \qquad \sigma_2 = 0 \qquad (13.4.1)$$

Because shafts need <u>ductile</u> materials (due to the exerted shearing stress), *Tresca's* (Eq.7.3.1.2) and *HMH* (Eq.7.3.2.2*a*) *strength criteria* must be applied and we have, respectively,

$$\sigma_{eq} = \sigma_1 - \sigma_3 = \sqrt{\sigma_b^2 + 4 \cdot \tau^2} \le \sigma_{all} \quad \text{and} \quad \sigma_{eq} = \sqrt{\sigma_b^2 + 3 \cdot \tau^2} \le \sigma_{all} \qquad (13.4.2a,b)$$

($\sigma_x = \sigma$, $\sigma_y = \sigma_z = 0$ and $\tau_x = \tau_y = 0$, $\tau_z = \tau$ were substituted in Eq.(7.3.2.2*a*)).

Eqs.(13.4.2*a,b*) can be expressed by one relation:

$$\sigma_{eq} = \sqrt{\sigma_b^2 + (\alpha \cdot \tau)^2} \le \sigma_{all} \qquad (13.4.2c)$$

where $\alpha = 2$ for *Tresca's criterion* and $\alpha = \sqrt{3}$ for *HMH criterion*.

When substituting from Eq.(10.3.6) and Eq.(8.1.3.5*b*) into Eq.(13.4.2*c*), we obtain the *strength criterion* for the combined *bending + torsion* as follows:

$$\sigma_{eq} = \sqrt{\left(\frac{M}{Z_b}\right)^2 + \left(\alpha \cdot \frac{T}{Z_T}\right)^2} \le \sigma_{all} \qquad (13.4.3)$$

where we have added the respective subscripts to the respective *section moduli* of <u>circular</u> profiles:

$$\text{for bending} \quad \dots \quad Z_b = \frac{\pi \cdot d^3}{32} \quad \text{and for torsion} \quad \dots \quad Z_T = \frac{\pi \cdot d^3}{16} = 2 \cdot Z_b \qquad (13.4.4a,b)$$

Issuing from the relation in Eq.(13.4.4*b*), we can rewrite Eq.(13.4.3) in the form

$$\sigma_{eq} = \frac{1}{Z_b} \cdot \sqrt{M^2 + \left(\alpha \cdot \frac{T}{2}\right)^2} = \frac{M_{eq}}{Z_b} \le \sigma_{all}, \qquad (13.4.4)$$

from which we can, for instance, calculate the shaft diameter

$$d \geq \sqrt[3]{\frac{32 \cdot M_{eq}}{\pi \cdot \sigma_{all}}}$$

(13.4.5)

Conclusion: This 2D stress combination, concerning shafts, deals only with <u>circular profiles</u>

Example 13.4.1

Given: A simply supported overhanging shaft (Fig. 13.4.1), with two cog-wheels, transmitting power from the wheel *1 (F₁)* to the wheel *2(F₂)*:

Shaft length:	*Shaft material:*	*Maximum torque:* $T_{max} = 10\,kNm$
$3L = 1.5\,m$	$E = 2.1 \cdot 10^5\,N/mm^2$	
Wheels size:	$\sigma_{all} = 150 N/mm^2$	
$d_1 = 1m;\ d_2 = 0.8\,m$	$\mu\ \ = 0.3$	

Task: Assess the shaft diameter *d* satisfying the ***strength*** *criterion*.
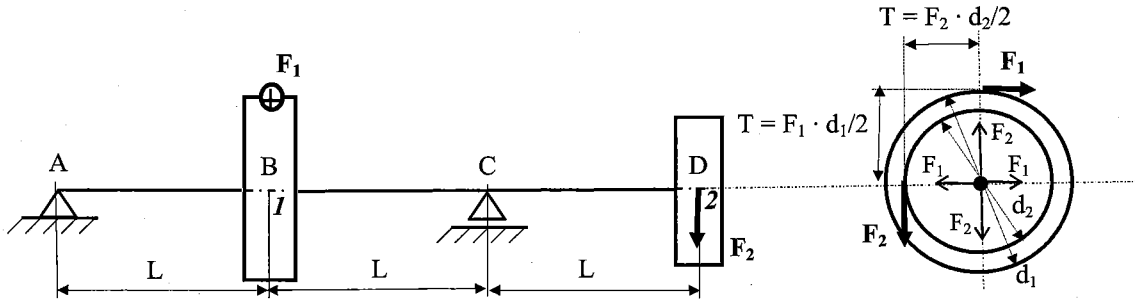

Fig.13.4.1.1

<u>Solution:</u>

This problem (Fig.13.4.1.1) is a combination of torsion and bending. <u>The torsion is the agent of transmitting the power,</u> while the bending is a "parasite" which causes an excessive shaft mass to be designed and has no direct contribution to the power transmission. At the same time, the bending is here exerted in two planes (the vertical and horizontal ones), i.e., we encounter with another combination of two plane bendings. <u>But, as shaft profiles are always **circular**, it results only in a **plane** bending.</u> The resulting bending moments is then obtained by a geometrical summing:

$$M = \sqrt{M_v^2 + M_h^2}$$

The explanation, which follows, should help us with solving similar structures subjected to combined stresses. The solution of a structure subjected to combined stress consists in looking for:

1) the maximally loaded structure section, and then

2) the section point where the combined stress reaches its maximum.

ad1)

vertical bending
$$M_{C;v} = F_2 \cdot L;$$

$$M_{B;v} = \frac{M_{C;v}}{2} = \frac{F_2 \cdot L}{2}$$

horizotal bending
$$M_{B;h} = \frac{F_1 \cdot L}{2}$$

torsion
$$T_B = F_1 \cdot \frac{d_2}{2} = T_D = F_2 \cdot \frac{d_2}{2}$$
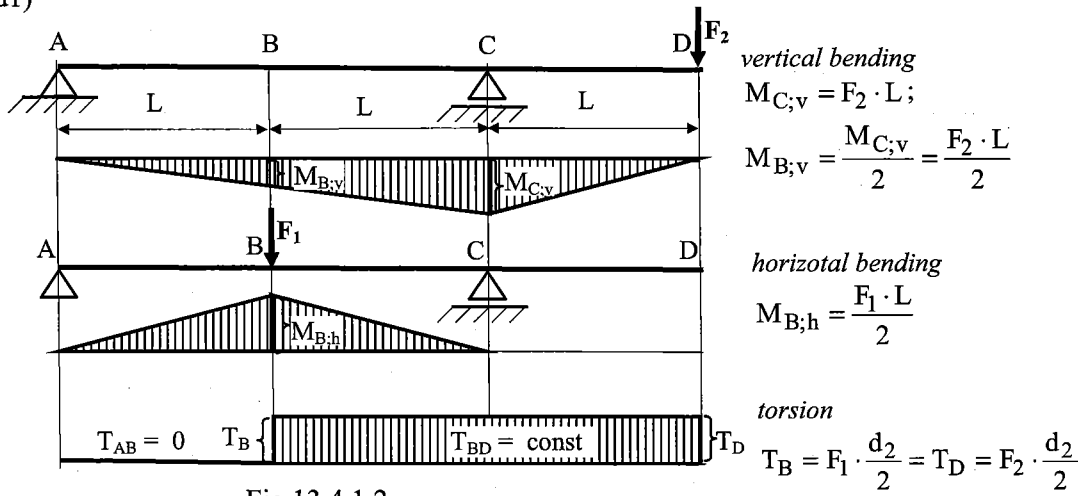
Fig.13.4.1.2

The maximum loaded structure section need not be obvious for the first look, i.e., there can be several possible sections where the combination of internal forces/moments could be maximum. In the given problem, such possible sections are: the section B (where the load F_1 is exerted) or the section C (a support). This conclusion comes from the extreme positions with the vertical/horizontal bending moment courses and with the torque course. The first span AB is excluded, since the $T_{AB} = 0$ and the bending moment combination cannot reach its maximum there as well.

The loads assessment:

According Fig.13.4.1.1, we have

$$T = F_1 \cdot \frac{d_1}{2} = F_2 \cdot \frac{d_2}{2} \Rightarrow F_1 = 2 \cdot \frac{T}{d_1} = 2 \cdot \frac{10}{1} = 20[kN] \quad \text{and } F_2 = 2 \cdot \frac{T}{d_2} = 2 \cdot \frac{10}{0.8} = 25[kN]$$

$$M_{C;v} = F_2 \cdot L = 25 \cdot 0.5 = 12.5[kNm]; M_{B;v} = \frac{F_2 \cdot L}{2} = 6.25[kNm];$$

$$M_{B;h} = \frac{F_1 \cdot L}{2} = \frac{20 \cdot 0.5}{2} = 5[kNm]; \qquad M_{C;h} = 0[kNm]$$

The resulting bending moments: $M_B = \sqrt{M_{B;v}^2 + M_{C;v}^2} = 8[kNm]$; $M_C = M_{C;v} = 12.5[kNm]$

As $T_B = T_C = 10[kNm]$, the decisive indicator is that of the bending moment $M_C = 12.5[kNm]$, i.e., the section C is the maximally loaded section.

ad 2) It was derived in the section (13.4) that, due to necessity of using ductile materials in the shaft production, *Tresca's* or *HMH* strength criteria are to be applied (Eq. 13.4.4) - here at the section C:

$$\sigma_{eq;C} = \frac{1}{Z_b} \cdot \sqrt{M_C^2 + \left(\alpha \cdot \frac{T_C}{2}\right)^2} = \frac{M_{eq;C}}{Z_b} \leq \sigma_{all} \Rightarrow d \geq \sqrt[3]{\frac{32 \cdot M_{eq;C}}{\pi \cdot \sigma_{all}}} = 0.1028[m] = 102.8[mm]$$

(*Tresca's* strength criterion was applied, i.e., $\alpha = 2$)

Now it is on the designer to choose the suitable diameter d (satisfying both the technological and economical conditions).

Note: The bending moment (though being the parasite) is chosen as the equivalent agent $M_{eq} = \sqrt{M^2 + \left(\alpha \cdot \dfrac{T}{2}\right)^2}$, because the (logic) equivalent torque (T_{eq}) would not have such a (mathematically) simple shape. It is on the student to derive the expression T_{eq}.

13.5 Torsion and tension (compression)

This combined loading *torsion* + *tension,* produced by normal load N and torque T, differs from the preceding *bending* + *torsion* only in the nature of the <u>normal stresses</u> which - being produced in this case by tension or compression - are <u>distributed uniformly over the cross-section of the shafts.</u>

We can readily prove that the maximally stressed fibers of the cross-section occur on the cross-section circumference that is the same type of <u>planar stress state</u> as we can see in Fig.13.4.1b. It follows from this that the *equivalent stress* for the combined loading *torsion* + *tension* has the same form as Eq.(13.4.2c), with the only difference that the bending stress

$\sigma_b = \dfrac{M}{\dfrac{\pi \cdot d^3}{32}}$ will be substituted by the tension stress $\sigma_t = \dfrac{N}{\dfrac{\pi \cdot d^2}{4}}$ which leads to the **cubic** equation
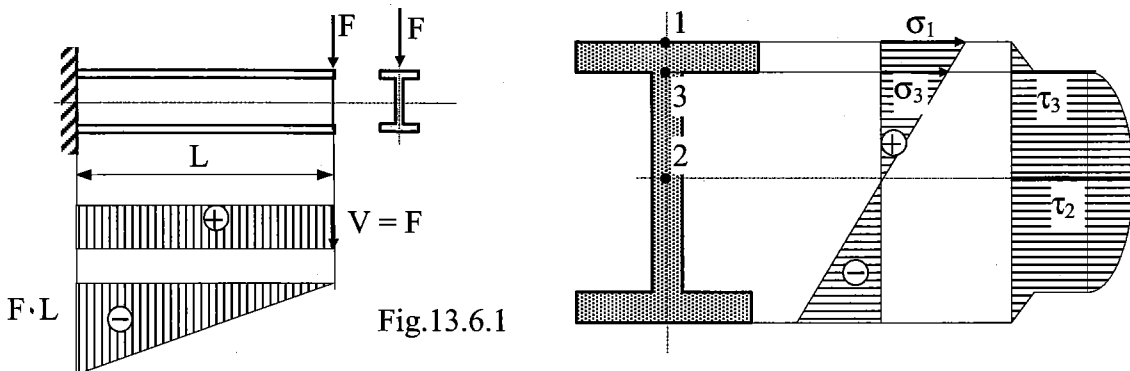
$$\sigma_{eq} = \sqrt{\left(\frac{4 \cdot N}{\pi \cdot d^2}\right)^2 + \left(\alpha \cdot \frac{16 \cdot T}{\pi \cdot d^3}\right)^2} \leq \sigma_{all} \tag{13.5.1}$$

It is clear that calculation of the shaft diameter will be a much more difficult task in this case. Therefore, the engineering approach is based on a <u>suitable estimation</u> of the diameter magnitude and subsequent verification by Eq. (13.5.1). It will help you if the estimation is based on previous separate calculations of the diameter: i) considering the member loaded <u>only in *tension*</u> by N and thus obtaining d_t ; ii) considering the member loaded <u>only in *torsion*</u> by T and thus obtaining d_T . Greater values (with an increment) then have to be verified by Eq.(13.5.1).

Conclusion: This 2D stress combination, concerning shafts, deals only with circular profiles

13.6 Bending and shear

Strictly speaking, this combined load occurs at every ordinary bending. Recalling the example in the last part of Sec.10.5.1, we observe that shearing stress is rarely taken into account when dimensioning a normally designed (not very short) beam of solid cross-section, because the shear can be neglected. When referring to <u>thin-walled</u> members, the situation may be quite different and the <u>influence of shearing stress needs to be taken into account.</u>

Fig.13.6.1

Consider a wide-flange cantilever (having second moment of area I_z and length L) subjected to a concentrated force F at its free end (Fig.13.6.1). We will observe the stress distributions over the cross-section at the fixation (where the maximum bending moment $M = F.L$ is exerted while the shear force $V = F$ is constant along the whole beam length). The stress state is there produced by: i) bending (cf. Sec.10.3); and ii) shear (cf. Sec.10.5.2). We will discover three suspicious localities, denoted 1, 2 and 3, where extreme stresses can occur, and which must obey the respective strength criteria as follows:

Loc. 1: maximum bending stress
$$\sigma_1 = \frac{F \cdot L}{I_z} \cdot \frac{h}{2} \leq \sigma_{all}$$

Loc. 2: maximum shearing stress
$$\tau_2 = \frac{F \cdot Q_2}{I_z \cdot t_w} \leq \tau_{all} = \frac{\sigma_{all}}{\alpha}; \qquad Q_2 \approx b \cdot t_f \cdot \frac{h}{2} + t_w \cdot \frac{h^2}{8}$$

Loc. 3: combination of bending + shearing stress (having a similar nature as in Secs.13.4 and 13.5)

$$\sigma_{eq;3} = \sqrt{\sigma_3{}^2 + (\alpha \cdot \tau_3)^2} \leq \sigma_{all}; \; \sigma_3 = \frac{F \cdot L}{I_z} \cdot \left(\frac{h}{2} - t_f\right); \tau_3 = \frac{F \cdot Q_3}{I_z \cdot t_w}; \qquad Q_3 \approx b \cdot t_f \cdot \frac{h}{2}$$

(when expressing the first moments of the cut areas of the cross-section with respect to $NA \equiv z$, i.e., Q_2 and Q_3, we neglected the flange thickness t_f in the algebraic sums with the cross-section height h)

Conclusion: This 2D stress combination deals mainly with short beams made of thin-walled profiles (cf. Sec.10.5.1)

13.7 Complement

There are other cases of combined stresses. One of them can be found for instance when returning to the Example 10.5.3.1, where a _thin-walled pipe with a very narrow gap_ (e.g., arisen by the weld cracking) has been studied so far only from the standpoint of shearing stress and the connected phenomenon of _shear center_ caused by ordinary bending (Fig.10.5.3.1). Now we can deal with a practical case when such a member is used as a cantilever. When studying it in detail, we will come to two types of combination depending of the load F position:

1) *a)* **shear** +*β)* **bending**+*γ)* **torsion**, when the load *F* position coincides with the vertical axis *y* (Fig.13.7.1), or at any other *F* position with the exception of that at the *shear center*;

2) *a)* **shear** +*β)* **bending**, when the load *F* goes through the *shear center* (Fig.13.7.2).

Ad 1) The combination of *a)***shear** +*β)***bending**+*γ)***torsion.**

Fig.13.7.1

R_A means the reaction of the resultant of internal shearing force $V = F$ and internal torque $T = F{\cdot}e$ overlying at the shearing center S

The torque $T_{(x)}$ needs no rule for signs
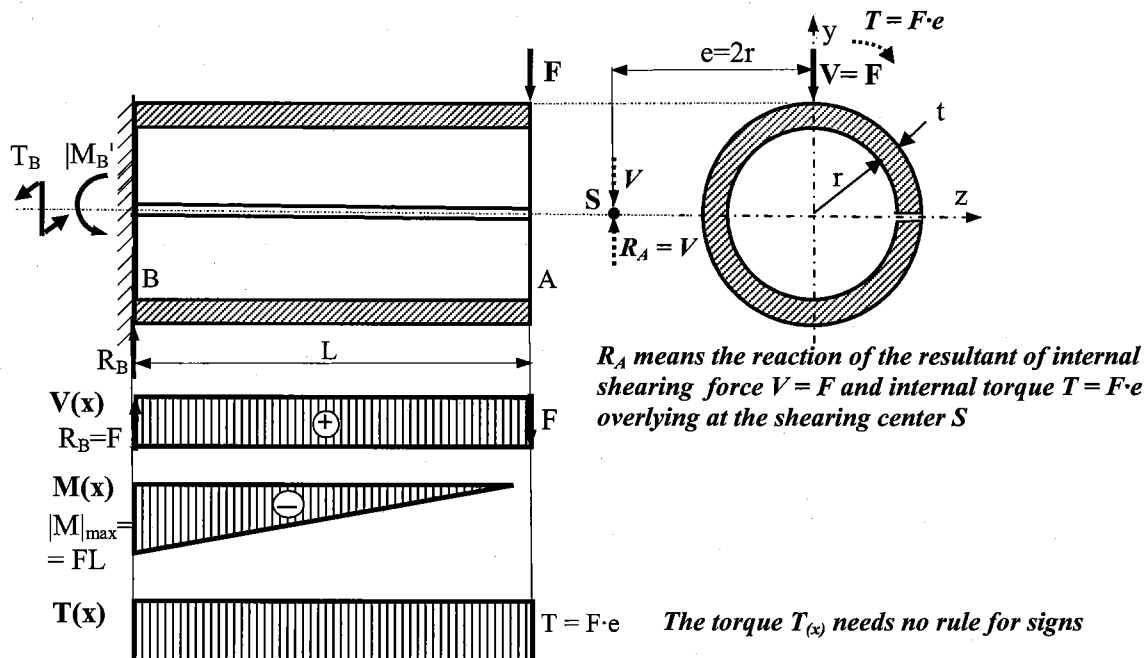
Stress distribution along the *B* cross-section (at the clamping), where the internal forces (moments) reach the maximum values:

ad *α)* Shearing force $V_B = F$:

(by *Zhurawski*) $\tau_V\left(\dfrac{\pi}{2}\right) = \dfrac{V}{\pi r t}$, cf. Sec.10.5.4.1

ad *β)* Bending moment $M_{max} = M_B = FL$:

$$\sigma_{max} = \frac{M_{max}}{Z_b} = \frac{FL}{\pi r^2 t}$$

$$\tau_V(\varphi) = \frac{V \cdot Q_z^{cut}}{I_z \cdot b} = \frac{V}{\pi r t} \cdot (1 - \cos\alpha)$$

$\tau_V(0) = 0$

$\tau_V(2\pi) = 0$

$z \equiv$ N.A.

$\tau_V(\pi) = \dfrac{2V}{\pi r t} = \tau_{Vmax}$

$\tau_V\left(\dfrac{3\pi}{2}\right) = \dfrac{V}{\pi r t}$
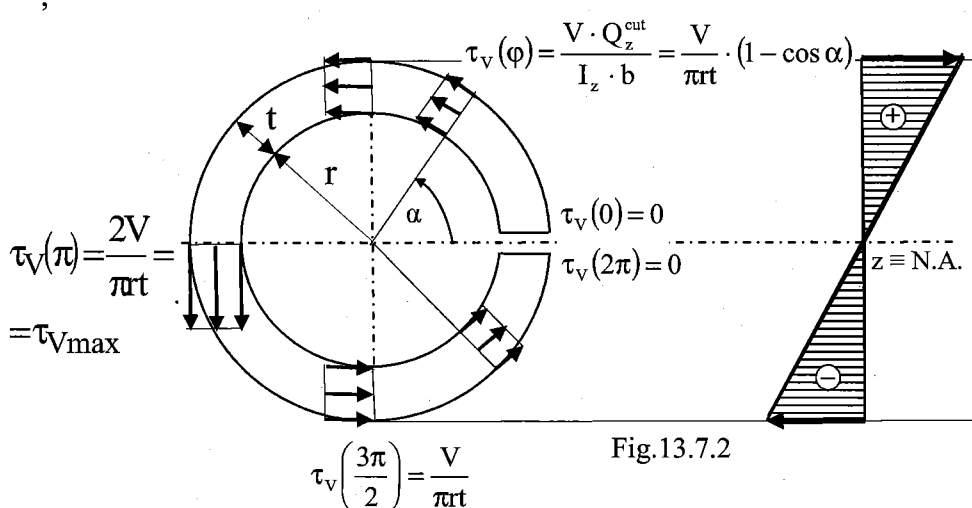
Fig.13.7.2

ad *γ) Torque T = F·2e.*

The further problem for a designer is to realize <u>what type of torsion</u> is to be applied in this case. In consequence of the gap in the originally hollow circular profile (caused, for instance, by the weld cracking), <u>this case **is not** the **torsion** of a **circular** profile</u>, which is discussed in Chap.8. The problems of **torsion of non-circular** profiles, we will discuss in the subject of *the Strength of Materials II*, in the next term. But even there, in the corresponding Chapter 4: *"Torsion of bars with non-circular profiles"*, such a problem is not completely explained. A complete solution need to analyze so called *"restrained torsion"*, which will be discussed in special advanced subjects on Theory of Elasticity in further study.
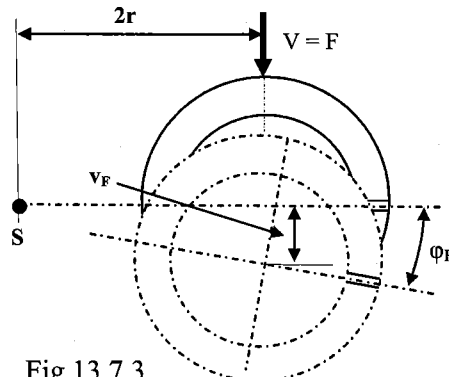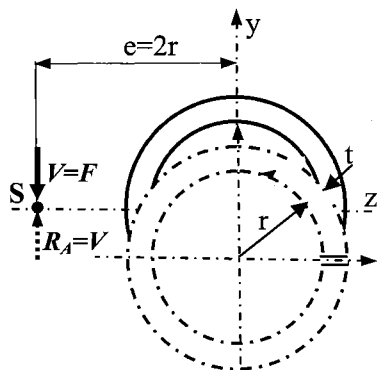

Fig.13.7.3

At the present state of knowledge, only a concept of the pipe deformation can be shown, see Fig.13.7.3.

Ad 2) The load *F* is applied at the shear center *S*, i.e., combination *a) <u>shear</u>* + *β) <u>bending</u>*

Based on Fig.13.7.2, the stress distributions of this combination are expressed as follows:

$$\sigma_b(\alpha) = \frac{M_{max}}{I_z} \cdot y = \frac{FL}{\pi r^3 t} \cdot r \cdot \sin \alpha; \quad \tau_V(\alpha) = \frac{F}{\pi r t} \cdot (1 - \cos \alpha)$$

Tresca's Strength criterion: $\sigma_{eq} = \sqrt{\sigma_b^2 + 4 \cdot \tau_V^2} \leq \sigma_{all}$

<u>Assessing $\sigma_{eq,max}$</u> (cf. Fig.13.7.2):

a) Looking for suspicious localities: for $\alpha = \pi/2$, $\sigma_{b\,max} = \frac{M_{max}}{Z_b} = \frac{FL}{\pi r^2 t}$; $\tau_V\left(\frac{\pi}{2}\right) = \frac{V}{\pi r t}$;

for $\alpha = \pi$, $\sigma = 0$; $\tau_V(\pi) = \frac{2V}{\pi r t} = \tau_{Vmax}$

b) Exact approach: $\frac{\partial \sigma_{eq}}{\partial \alpha} = \frac{\partial}{\partial \alpha}\left[\left(\frac{FL}{\pi r^3 t} \cdot r \cdot \sin \alpha\right)^2 + 4 \cdot \frac{F}{\pi r t} \cdot (1 - \cos \alpha)^2\right]^{\frac{1}{2}} = 0 \Rightarrow \alpha_{ext}$

In this way the maximum equivalent stress ($\sigma_{eq;max}$) can be assessed.

The exact approach (b) is a bit laborious, so, in practice, the tentative approach (a) is preferred.

14. Design for fatigue strength

14.1 Introduction

What is fatigue? It is the progressive failure of a part under *repeated, cyclic,* or *fluctuating* loading.

- When proper precautions against creep and corrosion are provided, a structure subjected to *steady, static load* less than the limit strength of the metal should theoretically *last for ever.*

- On the other hand, if a structure is subjected to a **cyclic, repeated, or fluctuating load,** it may fracture at a stress level *less* than that required to cause failure *under static conditions*.

- Fatigue failure starts from a single crack (or cracks at two or more locations) and propagates until ultimate failure occurs.

- The **criterion for fatigue failure** is the simultaneous action of *cyclic stress, tensile stress, and plastic strain.*

If we investigate a fracture surface due to fatigue, two zones can be observed: a *fatigue zone* and a *rupture zone* (Fig.14.1.1 shows a typical fatigue section with identifying marks):

i) The *fatigue zone* is the area of c*rack propagation* which begins with a small crack developing at a point of discontinuity in the material, e.g., a change in cross-section, a keyway, a hole, internal cracks, or even irregularities caused by machining, etc. Once a crack has developed, the stress-concentration effect becomes greater, the crack progresses more rapidly, and the stressed area decreases in size.

ii) The **rupture zone** is the area of **final failure**. It is the consequence of the gradual crack propagation bringing about an increase in stress magnitude until, finally, the remaining area fails suddenly (and whether the material is ductile or brittle, the rupture zone has a brittle character).
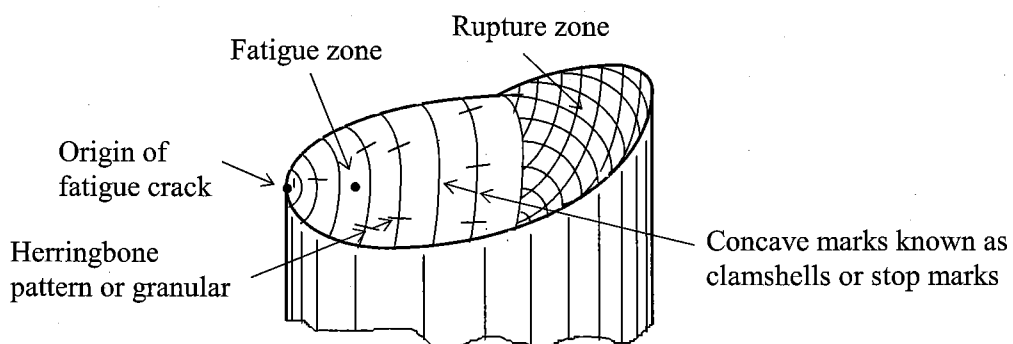

Fig.14.1.1

When machine parts fail statically, they usually develop a very large deflection, because the stress has exceeded the yield strength, and the part is replaced before fracture actually occurs. Thus many

static failures are visible, and give warning in advance. However, a fatigue failure gives no warning; it is sudden and total, and hence dangerous. It is a relatively simple matter to design against a static failure because our knowledge is quite complete. But fatigue is a much more complicated phenomenon, only partially understood, and an engineer seeking to rise to the top of the profession must acquire as much knowledge of the subject as possible. Anyone who lacks knowledge of fatigue can double or triple factors of safety and get a design that will not fail. However, such a design will not compete in today's market, and neither will the engineers who produce them.

14.2 Fatigue strength; the *S-N* diagram

To determine their strength under the *action of fatigue loads*, **specimens are subjected to repeated** or varying **forces of specified magnitudes** while the **cycles** of the stress reversals are **counted to destruction**, and the results obtained are plotted as an *S-N* (Wöhler's) diagram. To establish the fatigue strength of a material, quite a number of tests are necessary, because of the **statistical** nature of fatigue. (For the rotating-beam test, which is the simplest one, a constant bending load is applied, and the number of revolutions (stress reversals) of the beam required for failure is recorded). A typical *S-N* diagram for steel and aluminium is shown in Fig.14.2.1. The ordinate is the failure stress, expressed as a percentage of the ultimate strength S_U (limit strengths in this chapter will be denoted by S with respective subscripts) for the material, and the abscissa is the number of cycles N at which failure occurred. Note that the number of cycles is plotted on a logarithmic scale. (The chart may be plotted on semilog or log-log papers). The curve for steel becomes horizontal after manifesting a knee at about 10^7 cycles, and beyond this knee failure will not occur, no matter how great the number of cycles. The failure stress corresponding to the knee, known as the *endurance limit S_E*, is about *50%* of the *ultimate tensile strength S_U* for ordinary static loading. For nonferrous metals, such as aluminium and copper, a typical *S-N* curve shows that the stress at failure continues to decrease as the number of loading cycles is increased. For such metals, the *fatigue limit S_{Fat}* is arbitrarily defined as the stress corresponding to failure after $5x10^8$ cycles, or about *25%* of the ultimate strength.

The specimens for basic experiments are carefully polished, usually small, without imperfections (notches). Other types of experiments have been carried out with specimens: 1) of various size; 2) with various types of notches and other imperfections; 3) variously machined (varying roughness); 4) influence of technological processes (heat treating, etc.).

Since there are so many forms of structures and ways of loading them, the design of machines cannot be based on experimental investigations only. Many experiments serve for verification of engineer's computation.
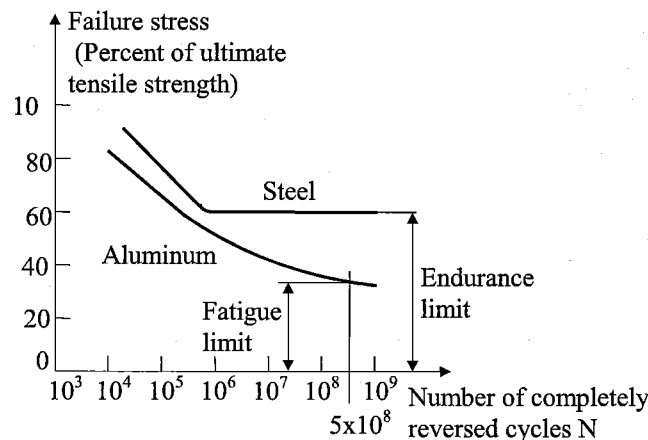
Fig.14.2.1

14.3 Endurance-limit modifying factors

It is unrealistic to expect the endurance limit of a mechanical member to match values obtained in the laboratory. We employ a variety of modifying factors, each of which is intended to account for a simple effect:

$$\sigma_E^* = k_a \cdot k_b \cdot k_c \cdot k_d \cdot k_e \cdot k_f \cdot \sigma_E \qquad (14.3.1a)$$

Czech notations:

$$\sigma_E^* = \frac{\sigma_E \cdot \eta_P \cdot \varepsilon_V}{\beta} \qquad (14.3.1b)$$

where:

σ_E^*... endurance limit of a real mechanical element; σ_E...endurance limit of a rotating specimen;

$k_a = \eta_P$ ... surface factor; $k_b = \varepsilon_V$ ... size factor; k_c... reliability factor; k_d ...temperature factor;

$k_e = \dfrac{1}{\beta}$ ... modifying factor for stress concentration; k_f... miscellaneous-effects factor.

Surface finish ($k_a = \eta_P$):

The quality of the surface finish has a great influence on fatigue life. Roughness of the surface operates as stress concentrators. **The better the material, the worse the influence of surface roughness.**

Size effects ($k_b = \varepsilon_V$):

When the volume of material subjected to a high stress is large, there is a **larger probability of failure**(interacting with a critical flaw). *Surface processing*: case hardening, surface finish, cold working, induce residual compressive stresses in an element - an effective tool for improving its fatigue life. However, these effects go to a certain surface depth only, so **the larger the size of the element, the smaller the favourable effects** of *surface processing*.

Temperature (k_c): High temperatures mobilize dislocations and reduce the fatigue resistance in many materials. There is no fatigue limit for materials operating at high temperature. This means that the S-N diagram for steels has no knee.
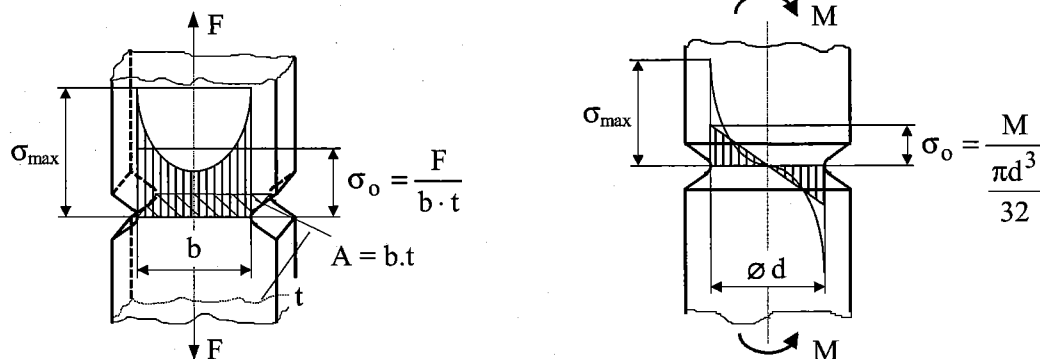
Stress - concentration effects (k_e):

Most mechanical parts have notches, grooves, holes, or other kinds of discontinuities which alter the stress distribution.

Theoretical stress concentration factors; K_t *(Czech notation:* α *)*

Stretching (Fig.14.3.1*a*) and *bending* (Fig.14.3.1*b*): $K_t = \sigma_{max} / \sigma_0$ $(\alpha = \dfrac{\sigma_{max}}{\sigma_0})$

*Torsion*: $K_{ts} = \tau_{max} / \tau_0$ $(\alpha_t = \dfrac{\tau_{max}}{\tau_0})$

a)   Fig.14.3.1   b)

K_t and K_{ts} (α and α_t) need *not* be applied to *static* stresses in <u>ductile materials</u> but *must* be used on the static stresses in <u>high-strength, low-ductility, case-hardened,</u> and/or <u>heavily cold-worked materials</u> and **mainly when parts are subjected to fatigue loading**.

However, it turns out that <u>some materials are *not very sensitive* to the existence of notches or discontinuities, and hence the *full values* of the theoretical stress concentration factors *need not be used*</u>. For these materials it is convenient to use a reduced value of K_t, which is defined as

$$K_f = \frac{\text{endurance limit of notch - free specimens}}{\text{endurance limit of notched specimens}} = \beta \qquad (14.3.2)$$

where K_f (*Czech notation* β) is the **fatigue stress-concentration factor**. To avoid a great many troublesome problems, $K_f = \beta$ is treated as a factor which reduces the strength of a member. Therefore we shall call $K_f = \beta$ the *fatigue-strength reduction factor*. This means that the modifying factor k_e of Eq.(14.3.1) and $K_f = \beta$ have the relation $k_e = 1/K_f = 1/\beta$.

Notch sensitivity q is defined by the equation: $0 \leq q = \dfrac{K_f - 1}{K_t - 1} = \dfrac{\beta - 1}{\alpha - 1} \leq 1$ (14.3.3)

(**the better the material, the greater the notch sensitivity** - in limits reaching *1*, i.e., *100%*)

From this follows the expression for K_f and its magnitude interval based on values of *q*:

$$1 \leq K_f = 1 + q(K_t - 1) \leq K_t \text{ or } 1 \leq \beta = 1 + q(\alpha - 1) \leq \alpha \qquad (14.3.4)$$

Miscellaneous - effects:

Residual stress, corrosion, frettage corrosion (this phenomenon is the result of microscopic motions of tightly fitting parts, e.g., bolted joints, bearing-race fits, wheel hubs), etc.

14.4 Fluctuating stresses

It is quite often necessary to determine the stress of parts corresponding to stress situations other than complete reversals. In design, stresses often fluctuate without passing through zero. Fig.14.4.1 illustrates some of the various stress-time relationships which may occur. The components of stress with which we must deal, some of which are shown in Fig.14.4.1a, are

σ_{max} ... maximum stress; σ_{min} ... minimum stress; σ_r... stress range;

σ_M ... limit mean stress; σ_m ... working mean stress;
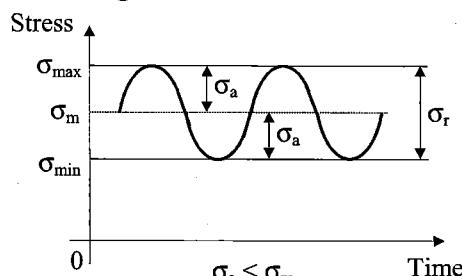
σ_A ... limit stress amplitude; σ_a... working stress amplitude

The subscripts of these components can be applied to shearing stresses as well as normal stresses. The following relations are evident from Fig.14.4.a:
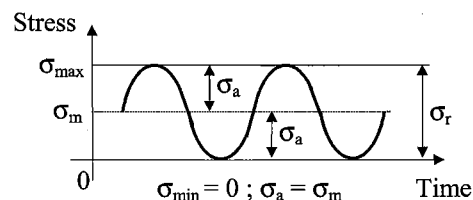
$$\sigma_m = \frac{\sigma_{max} + \sigma_{min}}{2} \quad \text{and} \quad \sigma_a = \frac{\sigma_{max} - \sigma_{min}}{2} \qquad (14.4.1a,b)$$

Although some of the stress components have been defined by using an ideal sine stress-time relation, the exact shape of the curve does not appear to be of particular significance.
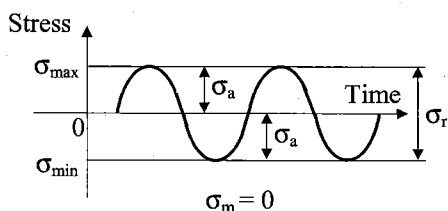
1) fluctuating stress

2) repeated stress

3) completely reversed stress

4) incompletely reversed stress
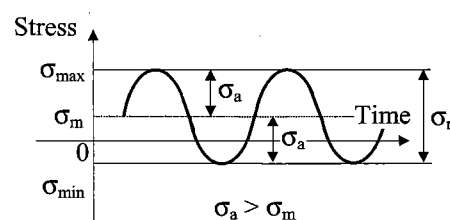
Fig.14.4.1

14.4.1 Smith's and Haigh's fatigue diagrams

Now that we have defined the various components of stress associated with a part subjected to fluctuating stress, we want to vary both the mean stress and the stress amplitude, in order to learn something about the fatigue resistance of parts when subjected to such situations. Two methods of plotting the results of such tests are in general use, and are both shown in Fig.14.4.1.1a,b, where:

$\sigma_E \equiv S_E$...endurance limit (for laboratory specimens); $\sigma_Y \equiv S_Y$... yield strength; $\sigma_U \equiv S_U$... ultimate strength; $\sigma_F \equiv S_F$...fictitious strength (= $2\sigma_U$ for structural steel). (The symbol S is often used in U.S. literature)
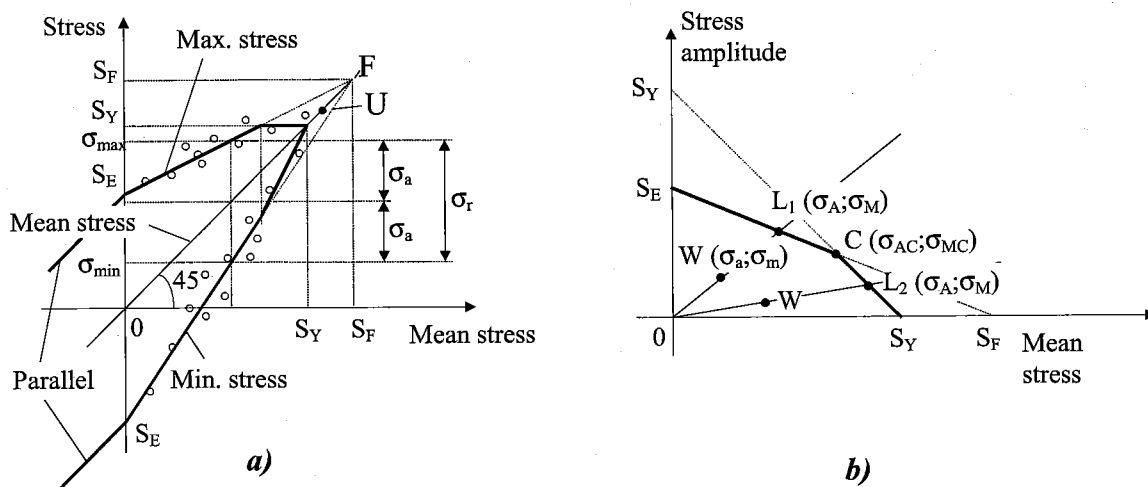

Fig.14.4.1.1

Smith's diagram of Fig.14.4.1.1a has the mean stress plotted along the abscissa, and all other components of stress plotted on the ordinate, with tension in the positive direction. The endurance limit S_E is plotted on the ordinate above and below the origin. The mean-stress line is a 45° line passing through the origin. The best average through the experimental points of failure (plotted as small circles) will be obtained by constructing curved lines from points S_E above and below the origin to point U, lying on the mean-stress line, which represents the tensile strength S_U of the part. The modified *Smith diagram* makes approximate use of tangents to the potential curved lines at $+S_E$ and $-S_E$ and hence intersecting the mean-stress line at point F, representing the fictitious strength S_F ($\approx$ $2S_U$ for structural steel) of the part. (In U.S. literature we encounter the so-called *modified Goodman diagram*, which is more conservative, because it uses straight lines outgoing from points S_E above and below the origin and intersecting the mean-stress line at point U). Note that the yield strength S_Y is also plotted on both axes, because yielding would be the criterion of failure if σ_{max} exceeded S_Y. When the mean stress is compression, failure is defined by two heavy lines originating at $+S_E$ and $-S_E$ and drawn downward and to the left. When the mean stress is tension, failure is defined by the maximum-stress line or by the yield strength as indicated by the heavy outline to the right of the ordinate.

Another fatigue diagram that we will employ frequently for design purposes is that of Fig.14.4.1.1b, called *Haigh's diagram* (in English literature called the *modified Goodman line*). Here the mean stress is also plotted on the abscissa. However, the ordinate has only the stress amplitude σ_A (σ_a) plotted along it and is limited by the endurance limit S_E. Straight lines from S_E to F (the fictitious strength S_F) on the abscissa and from S_Y on the ordinate to S_Y on the abscissa (defining tensile yielding) correspond to the part of *Smith's diagram* situated above the mean-stress line. The intersection of the two lines is the transition point between a failure by fatigue and a failure by yielding. The heavy outline therefore specifies when failure by either method will occur.

14.4.2 Safety factors for fatigue strength

When we assume proportional loading (the stress amplitude will increase proportionally to the mean stress), *Haigh's diagram* can be placed in equation forms for machine computation by writing the equations of the straight lines in intercept forms.

A) Failure by fatigue (the straight line between S_E and S_F in Fig.14.4.1.1b)

Writing the straight line equation in intercept form
$$\frac{\sigma_A}{S_E} + \frac{\sigma_M}{S_F} = 1 \qquad (14.4.2.1)$$

and defining the safety factor by

$$k = \frac{\overline{OL_1}}{\overline{OW}} = \frac{\sigma_A}{\sigma_a} = \frac{\sigma_M}{\sigma_m} \quad \Rightarrow \sigma_A = k \cdot \sigma_a; \quad \sigma_M = k \cdot \sigma_m; \qquad (14.4.2.2)$$

we obtain the following relation
$$\frac{1}{k} = \frac{\sigma_a}{S_E} + \frac{\sigma_m}{S_F} \qquad (14.4.2.3a)$$

from which we can determine the safety factor of the designed machine member.

Eq.(14.4.2.3a) will be applied for the following stress-time relations:

    1) completely reversed stress (Fig.14.4.1c); 2) incompletely reversed stress (Fig.14.4.1d);

    3) repeated stress (Fig.14.4.1b); 4) fluctuating stress (Fig.14.4.1a) with relatively **high** amplitude up to ratio σ_{AC}/σ_{MC} given by point C in *Haigh's diagram* (Fig.14.4.1.1a)

B) Failure by yielding (the straight line between S_Y and S_Y in Fig.14.4.1.1b)

Proceeding in the same way we obtain successively

$$\frac{\sigma_A}{S_Y} + \frac{\sigma_M}{S_Y} = 1; \qquad k = \frac{\overline{OL_2}}{\overline{OW}} = \frac{\sigma_A}{\sigma_a} = \frac{\sigma_M}{\sigma_m}; \qquad \frac{1}{k} = \frac{\sigma_a}{S_Y} + \frac{\sigma_m}{S_Y} \qquad (14.4.2.3b)$$

Eq.(14.4.2.3b) will be applied for fluctuating stress (Fig.14.4.1a) with relatively **low** amplitude, for ratios $< \sigma_{AC}/\sigma_{MC}$, corresponding to the right part of *Haigh's diagram* from point C in Fig.14.4.1.1b.

Note: The expression (14.4.2.3a), holding for laboratory specimens, is modified for real parts (see

Eqs. (14.3.1a,b)) as $\dfrac{1}{k} = \dfrac{\sigma_a}{S_E^*} + \dfrac{\sigma_m}{S_F}$ (or $\dfrac{1}{k} = \dfrac{\sigma_a}{\sigma_E^*} + \dfrac{\sigma_m}{\sigma_F}$) (14.4.2.3c)

14.5 Stresses due to combined loading

One of the most frequently encountered problems in design is that of a rotating shaft subjected to a constant torque and a stationary bending load. The problem is even more complicated when it is realized that the bending stresses as well as the shear stresses produced by torsion may have both mean and alternating components. In this section we shall present a method of using *Tresca's theory* or the *distortion-energy (HMH) theory* applied to fatigue to solve this problem, because all available experimental evidence shows these theories to be conservative.

To derive a safety factor for a combination of *bending* + *torsion* it is convenient to consider both loadings as completely reverse loadings with amplitudes σ_a and τ_a, respectively. Issuing from Eq.(13.4.2c), we express the fatigue limit state (considering limit amplitudes σ_A and τ_A) of the combination as

$$\sigma_{A;eq} = \sqrt{\sigma_A^2 + (\alpha \cdot \tau_A)^2} \le \sigma_E \qquad (14.5.1)$$

Introducing the endurance limit for torsion $\tau_E = \sigma_E / \alpha$ (analogously to Eqs.(8.1.3.7b,c)), based on bending, we can rewrite Eq.(14.5.1) in the form

$$\left(\dfrac{\sigma_A}{\sigma_E}\right)^2 + \left(\dfrac{\tau_A}{\tau_E}\right)^2 = 1 \qquad (14.5.2)$$

which represents an ellipse in the coordiate system σ_A and τ_A. Taking into consideration a proportional increase of both loadings, we can express the looked-for safety factor as $k = \sigma_A / \sigma_a = \tau_A / \tau_a$, and, after substitution for σ_A and τ_A into Eq.(14.5.2), we have

$$\dfrac{1}{k^2} = \left(\dfrac{\sigma_a}{\sigma_E^*}\right)^2 + \left(\dfrac{\tau_a}{\tau_E^*}\right)^2 = \dfrac{1}{k_\sigma^2} + \dfrac{1}{k_\tau^2} \qquad (14.5.3)$$

where we introduced the *endurance limit* σ_E^* (Eq.14.3.1) holding for a real part instead of σ_E for a laboratory specimen. Furthermore, in Eq.(14.5.3), we substitute the factors of safety k_σ and k_τ as if the bending and torsion took place separately.

With a certain approximation, we can apply Eq.(14.5.3) for all types of cycles (cf. Fig.14.4.1), even when considering a type of cyclic loading for bending that is different than that for torsion. In general, we will calculate k_σ and k_τ from Eqs.(14.4.2.3a,b), while taking into account the respective types of cyclic loading. For instance, when a shaft is subjected to a completely reversed bending and to a constant torque, we can calculate k_σ from Eq.(14.4.2.3a), where substituting $\sigma_m = 0$, and k_τ from Eq.(14.4.2.3b), where substituting $\tau_a = 0$.

14.6 Examples on comparing different types of cyclic modes.

A rod, with a bilateral notch, is subjected in tension with a load F. The rod dimensions can be seen in Fig.14.6.1.
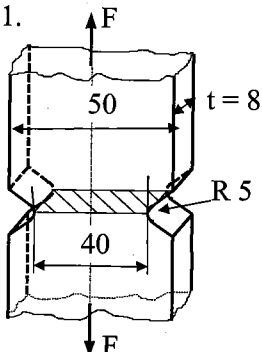
Given: material – $\sigma_{Ut} = 750$ MPa;

required factor of safety **k = 2,**

**Task:** Assess allowable load based on a type of cyclic mode:
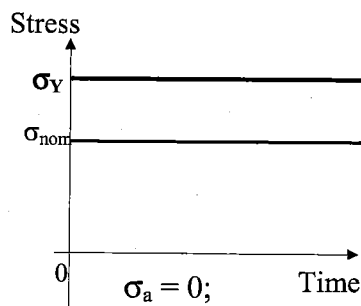
1) Static load; 2) Repeated load; 3) Completely reversed stress

Fig.14.6.1

Solution:

Ad 1) Static load
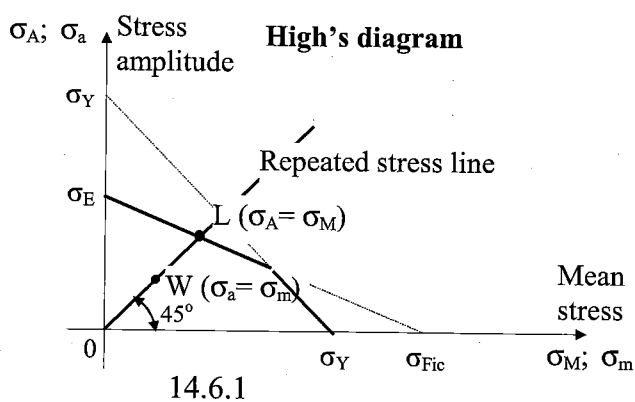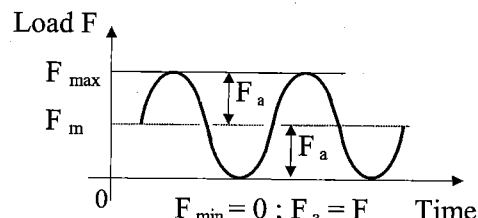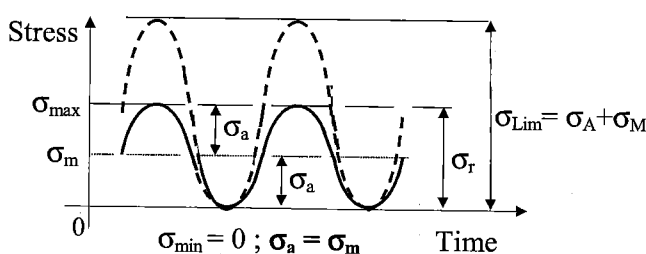
The working stress $\sigma_{nom} = \dfrac{F}{A} = \dfrac{F}{40 \cdot 8} = \dfrac{F}{320} = \sigma_w = \sigma_m$

Using Smith's diagram (Fig.14.6.2), we obtain $\sigma_Y = 450$ MPa for the given material

$$k = \frac{\sigma_Y}{\sigma_{nom}} = \frac{450}{\dfrac{F}{320}} = 2 \Rightarrow F = 72[kN] \Rightarrow \sigma_{nom} = \frac{72000}{320} = 225[MPa = N/mm^2]$$

Ad 2) Repeated load

The factor of safety: $\dfrac{1}{k} = \dfrac{\sigma_a}{\sigma_E^*} + \dfrac{\sigma_m}{\sigma_{Fict}}$ *)

The working stress:

$$\sigma_a = \sigma_m = \frac{F}{2} \cdot \frac{1}{A_{notch}} = \frac{F}{2} \cdot \frac{1}{8 \cdot 40} = \frac{F}{640}$$
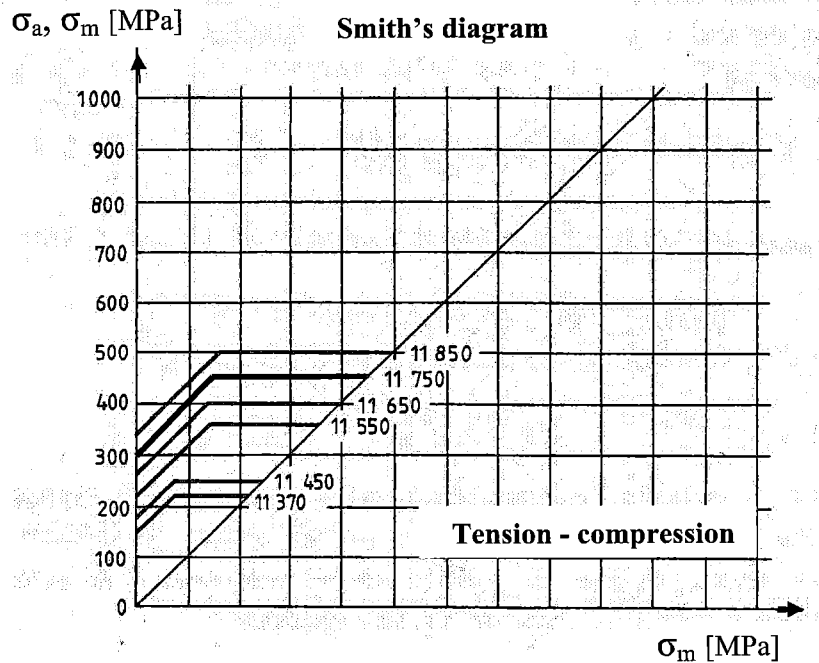
The fictitious limit: $\sigma_{Fict} \sim 2\sigma_{Ut} = 1500$ [MPa]

(this simple relation holds for structural steels)

14.6.1

The endurace limit: $\sigma_E^* = \dfrac{\sigma_E \cdot \eta_P \cdot \varepsilon_V}{\beta} = \dfrac{300 \cdot 0.92 \cdot 0.84}{2.037} = 113.8[N/mm^2]$

The parameters applied: (though older but instructive diagrams are used)

The size effect (for the given dimension $b = 40$ mm): $\varepsilon_v = 0.84$ (Fig.14.6.3)

The surface finish (for the given material $\sigma_{Ut} = 750$ MPa and *fine grinding*): $\acute{\eta}_P = 0.92$ (Fig.14.6.4)

σ_a, σ_m [MPa]   **Smith's diagram**

For the material given

($\sigma_{Ut} = 750$ MPa),

we read:

$\sigma_Y = 450$ MPa;

$\sigma_E = 300$ MPa

Fig.14.6.2

σ_m [MPa]
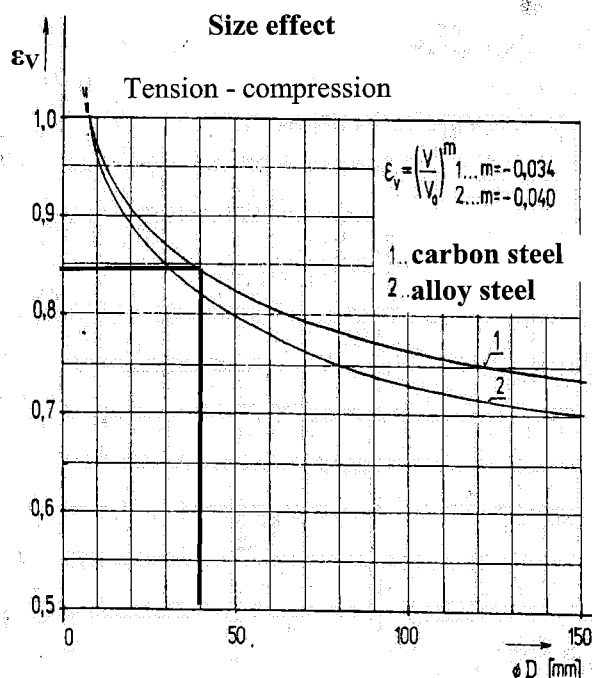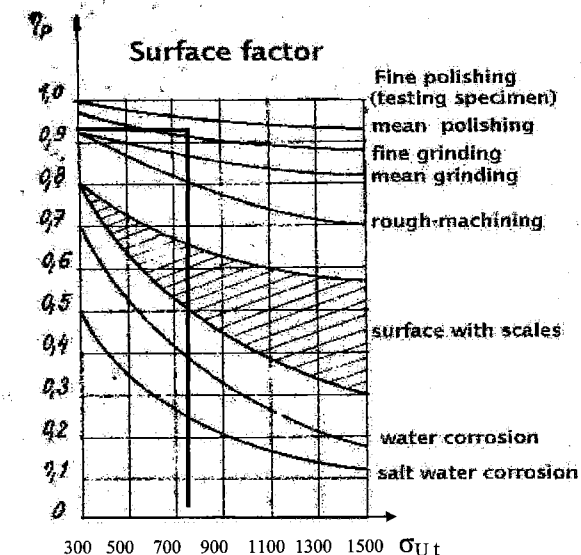
Fig.14.6.3

Fig.14.6.4

The fatigue stress-concentration factor β depends on the theoretical stress concentration factor

$\alpha = 2.28$ (see Fig.14.6.5) and the material notch sensitivity $q = 0.82$, which are found in Fig. 14.6.6

based on the given material $\sigma_{Ut} = 750$ MPa.

Theoretical stress concentration factor α for flat bars with a bilateral notch subjected to tension or bending

When comparing the bar given (Fig.14.6.5) with the model shape, we have:

$$\frac{\rho}{B-b} = \frac{5}{10} = 0.5$$

and

$$\frac{\rho}{b} = \frac{5}{40} = 0.125.$$

After conecting these two positions, we obtain:

$$\underline{\alpha = 2.28}$$

Fig. 14.6.5

Influence of the notch radius on the notch sensitivity factor

Tension - compression
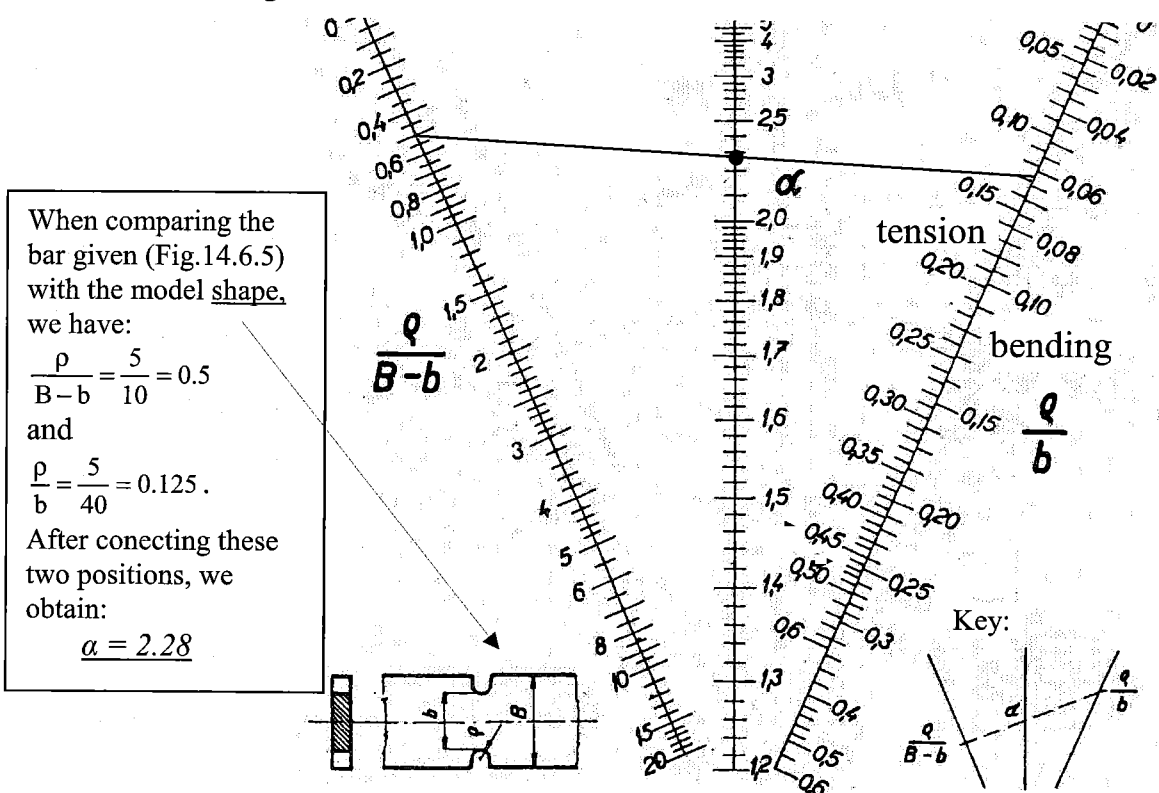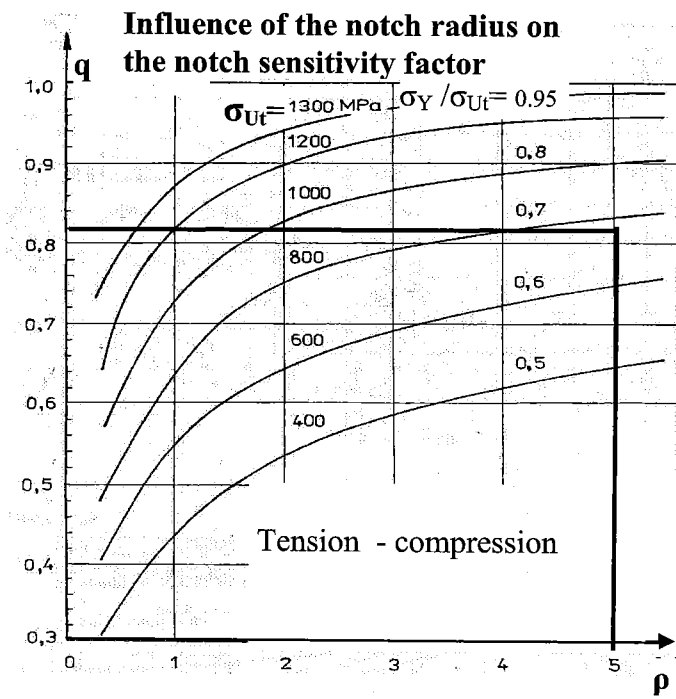
$$0 \leq q = \frac{\beta - 1}{\alpha - 1} \leq 1 \Rightarrow$$

$$\beta = q \cdot (\alpha - 1) + 1 =$$

$$= 0.81 \cdot (2.28 - 1) + 1 = 2.037$$
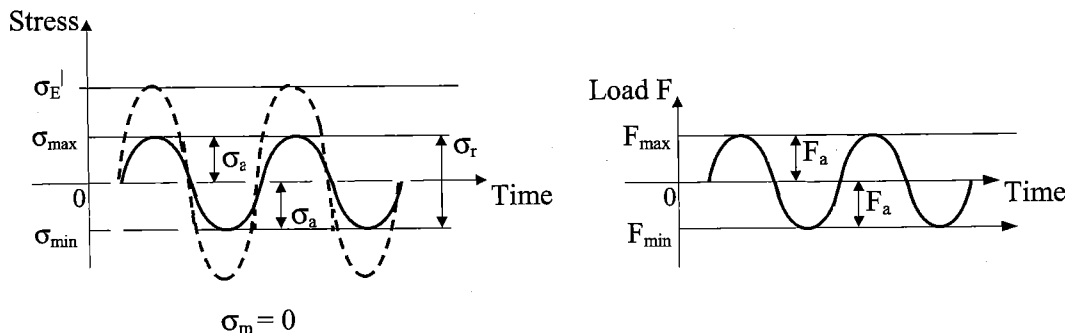
Fig.14.6.6

The allowable load F_{all} :

Using the expression *) , derived from the Haight's diagram (Fig.14.6.1], we obtain

$$\frac{1}{k} = \frac{1}{2} = \frac{\sigma_a}{\sigma_E^*} + \frac{\sigma_m}{\sigma_{Fict}} = \frac{\dfrac{F}{640}}{113.8} + \frac{\dfrac{F}{640}}{1500} = F \cdot 1.477 \cdot 10^{-5} \Rightarrow$$

$$F_{all} = \frac{1.477 \cdot 10^5}{2} = 33848[N] = 33.848[kN]$$

Ad 3) Completely reversed stress:

$$\sigma_m = 0$$

The stress amplitude: $\sigma_a = \dfrac{F_a}{A_{notch}} = \dfrac{F_a}{8 \cdot 40} = \dfrac{F_a}{320}$

The allowable load amplitude $F_{a; all}$:

$$2 = k = \frac{\sigma_E^*}{\sigma_a} = \frac{113.8}{\dfrac{F}{640}} \Rightarrow F_{a;all} = \frac{113.8 \cdot 320}{2} = 18.2[kN]$$

Conclusion:

Comparing all the three cyclic modes, we can see that the stress changing is for technical materials quite adverse process, especially when tension alternates compression (cf. the *completely reversed stress*)

15. **Thin-walled shells**

15.1 Introduction

Shells are structure elements of a planary character, i.e., one dimension - *thickness* - of which *is much smaller* (< 10x) than the other two dimensions.

Membrane stress
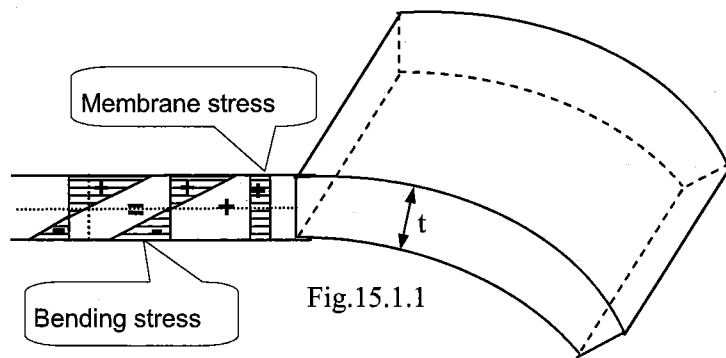
Bending stress

Fig.15.1.1

Generally, there are all the types of stresses (studied so far) exerted in the shell walls (tension-compression, shear, torsion and bending), from which two types (tension = membrane stress and bending stress) are shown in Fig.15.1.1

15.2 Membranes

In this chapter we will discuss only *thin shells (membranes) of revolution* (undergoing axi-symmetric deformation), the analysis of which is based on the consideration of axi-symmetric normal stresses **uniformly** distributed across the thickness of the shell wall. Consequently, such shells **are not able to withstand** loads producing **bending,** and both the loading forces and the reaction forces of their supports must obey this condition. We will discuss thin-walled pressure vessels, such as cylindrical, spherical, conical, and toroidal shells subjected to internal or external pressure from a gas or a liquid.

Axis of symmetry

σ_1

σ_2

σ_2

Shell element

σ_1

Parallel circle
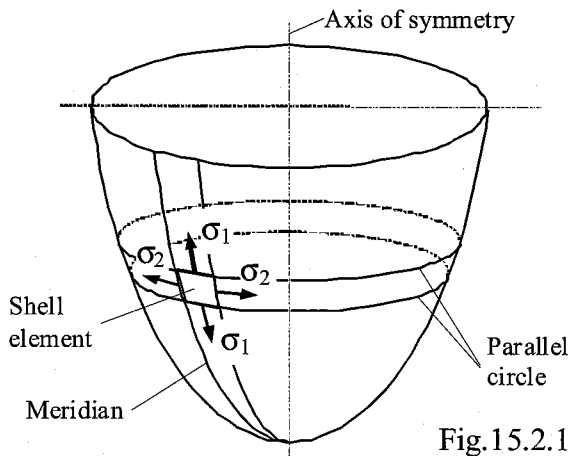
Meridian

Fig.15.2.1

The shell of revolution shown in Fig.15.2,1 is formed by rotating a plane curve (the meridian) about an axis lying in the plane of the curve. We cut an element of the membrane bounded by two closely adjacent parallel circles whose planes are normal to the vertical axis of symmetry of the shell and two closely adjacent generators, or meridians, of the shell. We use r_1 to denote the radius of curvature of the meridian (which varies along the length of the meridian), and r_2 to denote the radius of curvature of the shell surface in a direction perpendicular to the meridian (Fig.15.2.2a). The centre of curvature corresponding to r_2 must lie on the axis of symmetry, although the centre for r_1 does not (in general) lie there. An internal pressure p acting normal to the curved surface of the shell gives rise to *meridional* stresses σ_1 and *hoop* (*circumferential*) stresses σ_2 as indicated in the figure. These stresses are orthogonal to one

another and act in the plane of the shell wall. Since no shearing stresses are produced, the stresses σ_1 and σ_2 are principal stresses.
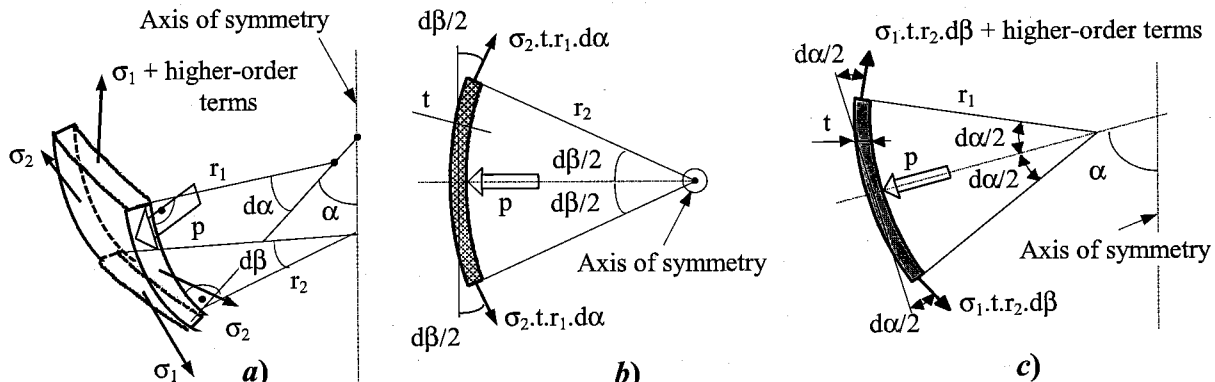

Fig.15.2.2

Fig.15.2.2*b* shows the hoop *forces* more clearly, as seen by looking along the axis of symmetry. It is evident that each of the hoop stresses σ_2 is exerted on the area $t.(r_1.d\alpha)$ and produces the force vector $\sigma_2.t.(r_1.d\alpha)$ which makes an angle $d\beta/2$ with the tangent to the element. The component of these hoop forces, $2 \cdot \sigma_2 \cdot t \cdot r_1 \cdot d\alpha \cdot \sin\dfrac{d\beta}{2}$ or, since $d\beta/2$ is small, $\sigma_2 \cdot t \cdot r_1 \cdot d\alpha \cdot d\beta$, is acting normal to the shell. Analogously, the meridional forces appear in Fig.15.2.2*c* and have a component $\sigma_1 \cdot t \cdot r_2 \cdot d\beta \cdot d\alpha$ acting normal to the shell. Pressure p acts over an area $(r_1.d\alpha).(r_2.d\beta)$, so that the equation of equilibrium in the normal direction becomes

$$\sigma_1 \cdot t \cdot r_2 \cdot d\beta \cdot d\alpha + \sigma_2 \cdot t \cdot r_1 \cdot d\alpha \cdot d\beta - p \cdot r_1 \cdot d\alpha \cdot r_2 \cdot d\beta = 0$$

After dividing this equation by $t.r_1.d\alpha.r_2.d\beta$, we obtain *Laplace's formula*

$$\frac{\sigma_1}{r_1} + \frac{\sigma_2}{r_2} = \frac{p}{t} \qquad (15.2.1)$$

This fundamental equation, called the *Laplace theorem,* applies to axi-symmetric deformations of all thin shells (membranes) of revolution.

A second equation (since there are two unknowns σ_1, σ_2) is yielded by consideration of the vertical equilibrium of the entire shell with respect to some convenient parallel circle of arbitrary position y from which we obtain the meridional stress σ_1 (Fig.15.2.3):

$$\sigma_1 \cdot 2 \cdot \pi \cdot r \cdot t \cdot \cos\alpha - Q_1 - Q_2 - Q_3 = 0 \quad \Rightarrow \quad \sigma_1 = \frac{Q_1 + Q_2 + Q_3}{2 \cdot \pi \cdot r \cdot t \cdot \cos\alpha} \qquad (15.2.2)$$
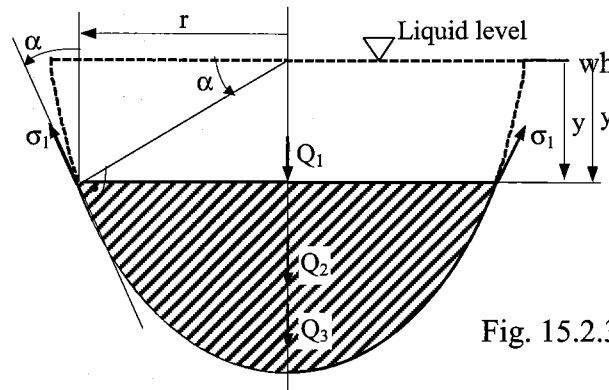
Fig. 15.2.3
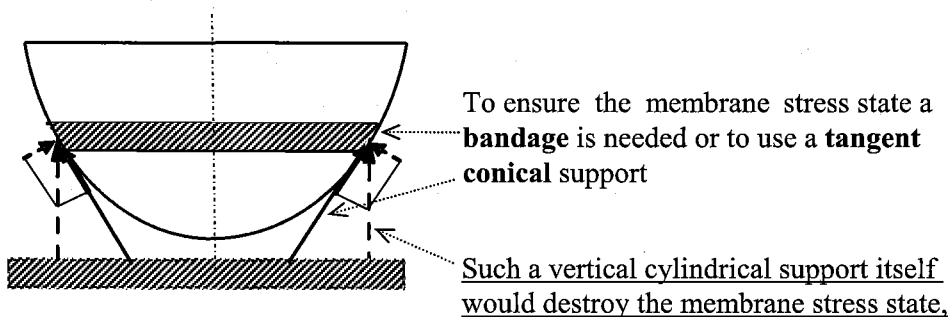
where: $2\pi \, .r.t$...the area of the circular ring (with radius r) obtained by the section of a plane (at an arbitrary ordinate y) perpendicular to the axis of the shell;

Q_1 ... the load produced by the pressurizing medium (liquid, or gas) above section y;

Q_2 ... the weight of the liquid beneath section y (for gas $Q_2 = 0$);
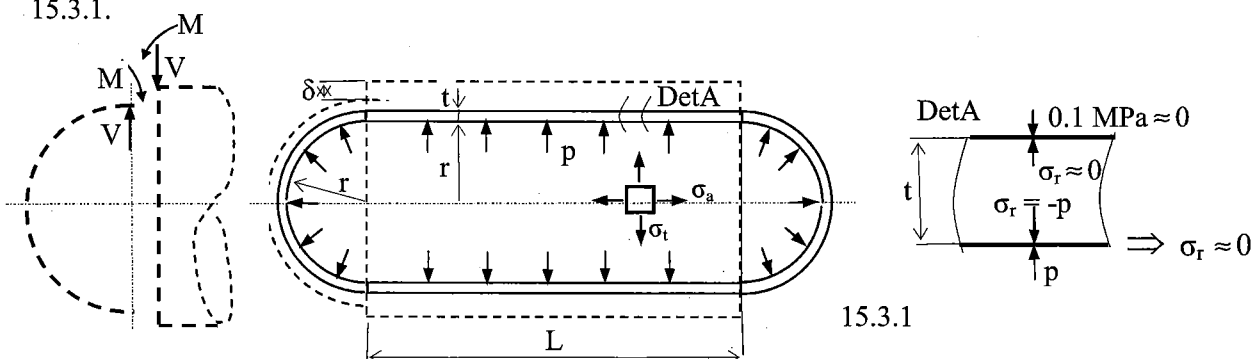
Q_3 ... the weight of the shell material beneath section y.

Note: How to support a membrane?

To ensure the membrane stress state a **bandage** is needed or to use a **tangent conical** support

Such a vertical cylindrical support itself would destroy the membrane stress state,

15.3 Pressure vessels.

Basic components of pressure vessels are thin-walled shells, i.e., membranes. Such a pressure vessel often consists of a cylindrical body closed with lids (in this case hemispherical ones), see Fig 15.3.1.

15.3.1

When studying the Laplace formulas, (15.1) and (15.2), it is clear that this problem is SD and thus the items of the general solving flow diagram, to be applied, are those of 6 – 10.

The items 6 and 7 are substituted just with the Laplace formulas:

- cylinder: $\dfrac{\sigma_1}{r_1} + \dfrac{\sigma_2}{r_2} = \dfrac{p}{t}$ (15.2.1), where $\sigma_1 = \sigma_a$, $\sigma_2 = \sigma_t$, $r_1 = \infty$. $r_2 = r$,

which yields $\sigma_t = \dfrac{p \cdot r}{t}$;

$\sigma_1 = \dfrac{Q_1 + Q_2 + Q_3}{2 \cdot \pi \cdot r \cdot t \cdot \cos\alpha}$ (15.2), where $\sigma_1 = \sigma_a$, $Q_1 = \pi \cdot r^2 \cdot p$, $Q_2 = Q_3 = 0$, $\Rightarrow \sigma_a = \dfrac{p \cdot r}{2t}$;

- hemisphere – lid: $\dfrac{\sigma_1}{r_1} + \dfrac{\sigma_2}{r_2} = \dfrac{p}{t}$, where $\sigma_1 = \sigma_2 = \sigma$, which yields $\sigma = \dfrac{p \cdot r}{2t}$

Items 8: Dimensioning (when comparing the vessel parts, the maximum stress state is that in the cylindrical one). Using *Tresca's Strength Criterion:* $\sigma_{eq} = \sigma_t - \sigma_r \approx \sigma_t = \dfrac{p \cdot r}{t} \le \sigma_{all}$,

we can assess either $p_{all} \le \dfrac{\sigma_{all} \cdot t}{r}$, or $t_{all} \ge \dfrac{p \cdot r}{\sigma_{all}}$, depending on the given parameters.

Items 9: For numerical computation only.

Items 10: We can assess the change in radii:

- cylinder: $\dfrac{\Delta r_c}{r} = \varepsilon_t = \dfrac{1}{E}[\sigma_t - \mu \cdot \sigma_a] \Rightarrow \Delta r_c = \dfrac{pr^2}{2E \cdot t}[2 - \mu]$ (when separated)

- lids: $\Delta r_L = \dfrac{pr^2}{2E \cdot t}[1 - \mu]$ (when separated)

Important remark:

The difference assessed between those two displacements is: $\delta = \Delta r_c - \Delta r_L = \dfrac{\mu p r^2}{2E \cdot t}$

This can only be reacted by the introduction of shear forces and moments as shown in Fig.(15.3.1), where V = shearing force and M = bending moment, *both per unit length*. When dealing with a **static load**, this disproportion arisen is compensated with both elastic and plastic deformations of the two parts. But a great problem could appear with a **cyclic loading, which can lead even to a low-cyclic fatigue fracture.**

15.4 Centrifuge

Another interesting problem is to assess the allowable wall thickness t_{all} of a centrifuge (Fig.15.4.1) having dimensions: $r \gg t$, material: E, σ_{all}, ρ_S (specific mass), and rotating with the angular velocity of $\omega [rad/s]$. The centrifuge contains a liquid of specific mass ρ_L.

Solution:

The centrifuge is stressed with the tangent stress $\sigma_t = \sigma_{t\omega} + \sigma_{tp}$, where:

i/ $\sigma_{t\omega} = \rho_S \cdot v^2$, i.e., the tangent stress caused by *the centrifuge shell revolution* (cf. Sec.2.11.1, *revolving ring*), when neglecting a reinforcing influence of the centrifuge lids.

$$\text{ii/ } \sigma_{tp} = \frac{p \cdot r_S}{t} = \frac{\int\limits_{r_L}^{r_S} \varpi^2 \cdot x \cdot \rho_L \cdot 1 \cdot 1 \cdot dx}{t} \cdot r_S = \frac{\rho_L \cdot \varpi^2 \cdot \left(\dfrac{r_S^2 - r_L^2}{2}\right)}{t} \cdot r_S ,$$

*i.e.,* the tangent stress caused by *the rotating liquid pressure p* (using *Laplace theorem*).
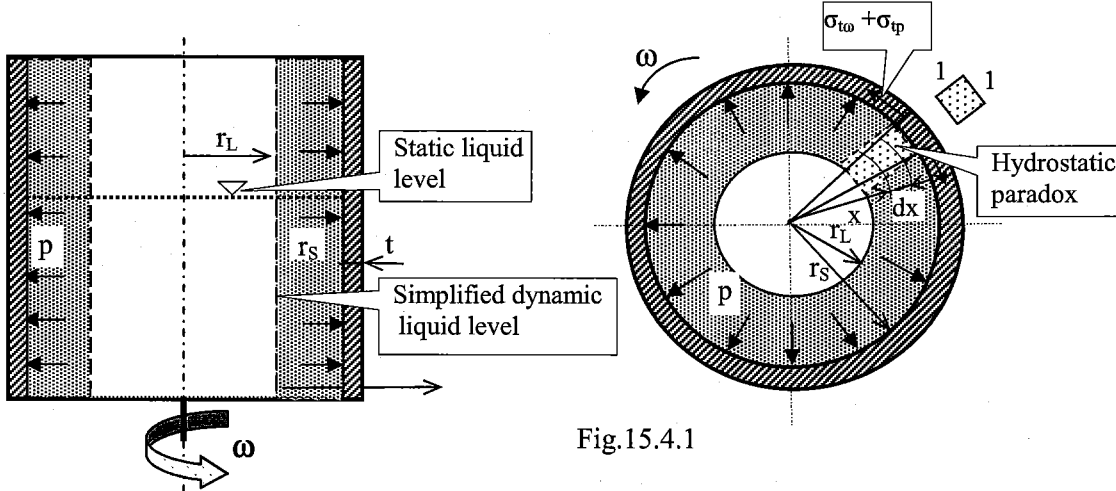
Fig.15.4.1

Note: How assess the force action of the rotating liquid?

The originally horizontal level of the liquid is gradually changed, by the rotation, into a paraboloid, which, at a high angular velocity ω, can be app. considered as a hollow cylinder (Fig.15.4.1). The centrifugal force of the liquid cylinder loads the centrifuge shell with a pressure p .The pressure p can be computed by utilizing the so called *hydrostatic paradox*:

Using the liquid elementary parallelepiped of a unit base $(dV = 1 \cdot 1 \cdot dx)$, *computing its centrifugal force, summing by integration, we obtain the liquid pressure:*

$$p = \int\limits_{r_L}^{r_S} \varpi^2 \cdot x \cdot \rho_L \cdot 1 \cdot 1 \cdot dx$$

The Tresca's strength criterion: $\sigma_{eq} = \sigma_{max} - \sigma_{min} = \sigma_t \le \sigma_{all}$, where

$$\sigma_{max} = \sigma_t = \sigma_{t\omega} + \sigma_{tp} = \rho_S \cdot (r \cdot \varpi)^2 + \frac{\rho_L \cdot \varpi^2 \cdot \left(\dfrac{r_S^2 - r_L^2}{2}\right)}{t} \cdot r_S$$

$$\sigma_{min} = \sigma_r = 0 .$$

The allowable membrane thickness t_{all} is then:

$$t_{all} = \frac{\rho_L \cdot \varpi^2 \cdot \left(\dfrac{r_S^2 - r_L^2}{2}\right) \cdot r_S}{\left[\sigma_{all} - \rho_S \cdot (r \cdot \varpi)^2\right]} \left[\frac{\dfrac{kg}{m^3} \cdot \dfrac{1}{s^2} \cdot m^3}{\dfrac{N}{m \cdot s^2}} = m\right]$$

That checking of the units is recommendable, since it helps to prove the result correctness.

References

1) Michalec, J. et al.: Strength of Materials I, [In Czech: Pružnost a pevnost I], Textbook of CTU in Prague, 1995.

2) Nash, W. A.: Strength of Materials, Schaum's Outline Series, McGraw-Hill, Inc., 1994.

3) Beer, F. P. - Johnston, E. R.: Mechanics of Materials, McGraw-Hill, Inc., 1992.

4) Hearn, E. J.: Mechanics of Materials 1, Butterworth-Heinemann, Linacre House, Jordan Hill, Oxford OX2 8 DP, A division of Reed Educational and Professional Publishing Ltd, 1997.

5) Gere, J. M. - Timoshenko, S. P.: Mechanics of Materials, PWS Publishing Company, Boston, 1997.

References

1) Michalec, J. et al.: Strength of Materials I, [In Czech: Pružnost a pevnost I], Textbook of CTU in Prague, 1995.

2) Nash, W. A.: Strength of Materials, Schaum's Outline Series, McGraw-Hill, Inc., 1994.

3) Beer, F. P. - Johnston, E. R.: Mechanics of Materials, McGraw-Hill, Inc., 1992.

4) Hearn, E. J.: Mechanics of Materials 1, Butterworth-Heinemann, Linacre House, Jordan Hill, Oxford OX2 8 DP, A division of Reed Educational and Professional Publishing Ltd, 1997.

5) Gere, J. M. - Timoshenko, S. P.: Mechanics of Materials, PWS Publishing Company, Boston, 1997.